Functional Characterization of the Nup93 Complex in Nuclear Pore Complex Assembly

Dissertation

der Mathematisch-Naturwissenschaftlichen Fakultät

der EBERHARD KARLS UNIVERSITÄT TÜBINGEN

zur Erlangung des Grades eines

Doktors der Naturwissenschaften

(Dr. rer. nat.)

vorgelegt von

Ruchika Sachdev

aus New Delhi, India

Tübingen

2013

ACKNOWLEDGEMENTS

TABLE OF CONTENTS

ABBREVIATIONS

µm	Micrometre
nm	Nanometre
A.nidulans	Aspergillus nidulans
APC	Anapahse Promoting Complex
aa	Amino acid
BAF	Barrier to auto integration factor
BSA	Bovine serum albumin
C. thermophilum	Chaetomium thermophilum
CDK1	Cyclin Dependent Kinase 1
C. elegans	Caenorhabditis elegans
D. rerio	Danio rerio
DAPI	4',6-Diamidino-2-phenyindole
DiIC18	1,1'-Dioctadecyl-3,3,3',3' tetramethylindocarbocyanine perchlorate
DNA	Deoxyribonucleic acid
E. coli	*Escherichia coli*
EDTA	1-(4-Aminobenzyl)ethylenediamine- N,N,N',N'-tetraacetic acid
EGFP	Enhanced green fluorescent protein
EM	Electron microscopy
ER	Endoplasmic reticulum
FG	Phenylalanine glycine dipeptide
GFP	Green fluorescent protein
GST	Glutathione-S-transferase
GTP	Guanosine triphosphate
GTPase	Guanosine triphosphatase
HP1	Heterochromatin Protein 1
hCG	Human chorionic gonadotropin
INM	Inner nuclear membrane
IP	Immune precipitation
IPTG	Isopropyl-β-D-thiogalactopyranoside

kDa	Kilo Dalton
LBR	Lamin B receptor
MTOC	Microtubule organizing centre
MISTIC	Membrane-integrating sequence for translation of integral membrane protein constructs
mRNA	Messenger RNA
NE	Nuclear envelope
NES	Nuclear export signal
NIMA	Never in mitosis A
Ni-NTA	Nickel-nitrilotriacetic acid
NLS	Nuclear localization signal
NPC	Nuclear pore complex
NTF-2	Nuclear transport factor 2
Nup	Nucleoporin
ONM	Outer nuclear membrane
ORF	Open reading frame
PCR	Polymerase chain reaction
PFA	Paraformaldehyde
PKC	Protein kinase C
PLK	Polo like kinase
PMSG	Pregnant mare serum gonadotropin
PNS	Peri nuclear space
PP1	Protein phosphatase 1
Ran	Ras-related nuclear protein
RanGAP	Ran GTPase activating protein
RanGEF	Ran guanine nucleotide exchange factor
RCC1	Regulator of chromatin condensation 1
RNA	Ribonucleic acid
RNAi	RNA interference
SAC	Spindle assembly checkpoint
S. cerevisiae	Saccharomyces cerevisiae
SDS-PAGE	Sodium dodecylsulfate - polyacrylamid gel

	electrophoresis
TEV	Tobacco etch virus
TM	Trans membrane
WGA	Wheat germ agglutinin
X. laevis/Xenopus	Xenopus laevis

SUMMARY

The defining attribute of the eukaryotic cell is the compartmentalization of genetic material inside the cell's nucleus. This is possible by the existence of a double lipid bilayer: the nuclear envelope (NE). This compartmentalization enables the eukaryotic cells to separate transcription and translation both spatially and temporally. The NE comprises two membranes: the outer nuclear membrane (ONM) that is continuous with the endoplasmic reticulum and the inner nuclear membrane (INM) that is characterized by a distinct protein composition and can make contact with the chromatin and the nuclear lamina. The ONM and the INM fuse to form pores where the nuclear pore complexes (NPCs) reside. NPCs act as gatekeepers of the nucleus and are involved in nucleo-cytoplasmic transport. They also act as a physical barrier thereby maintaining distinct composition of the nucleus and the cytoplasm. NPCs are proteinaceous macromolecular assemblies ranging from 40-60 Mega Daltons in size. Despite their enormous size, NPCs are composed of approx. 30 proteins referred as nucleoporins or Nups. Most nucleoporins are organized into distinct sub complexes that act as building blocks for NPC assembly. The NPC can be roughly dissected into two parts, the structural backbone of the pore that is composed of structural nucleoporins, which establish the basic scaffold of the pore and act as anchor proteins to recruit other nucleoporins. The other portion is the functional region of the pore that is composed of mainly the FG repeats containing nucleoporins that form the central channel of the pore thereby imparting functional properties like transport and exclusion competency. In animals undergoing open mitosis the NE and the NPCs are disassembled in prophase and they must reassemble from disassembled soluble pore components and membranes as the cell enters interphase to re-establish an intact nucleus.

This thesis aims to functionally characterize the role of one of the sub-complexes that is the Nup93 complex, in NPC assembly and function. Nup93 is one of the structural complexes of the NPC. It is positioned in the pore at a region where it establishes a link between membranes of the NE and the NPC. Nup93 complex is composed of five nucleoporins: Nup53, Nup93, Nup155, Nup188 and Nup205. It was previously shown in the lab that Nup93 exists as part of two distinct complexes: Nup93-Nup188 and the Nup93-Nup205. Individually neither the Nup93-Nup188 nor the Nup93-Nup205 complexes were essential for NPC assembly. We were curious to find out if both the complex together were not essential for NPC assembly, as they have been speculated to have redundant roles in the pore.

For this we took advantage of the *Xenopus laevis* egg extract system (in vitro nuclear assembly reactions) and by various cell biological and biochemical assays showed that the conserved nucleoporin Nup93 is essential for NPC/NE formation and functions. Immunodepleting Nup93 (thereby co depleting Nup205 and Nup188) lead to a block in NPC and NE formation and this was rescued by addition of the full-length recombinant Nup93. Hence Nup93 could compensate for the loss of both Nup93-Nup188 and Nup93-Nup205 complexes and thereby establishing the evidence that both major components of the Nup93 complex, Nup188 and Nup205 together are not crucial for post-mitotic NPC assembly. We also found that the C-terminus of Nup93 was sufficient and essential for formation of the structural backbone of the pore. It does so by strengthening the interaction between two major structural components of the pore Nup53 and Nup155. We believe that this is a key event in the formation of the scaffold/structural skeleton of the pore and hence in post-mitotic NPC assembly. Via the N-terminus, Nup93 recruits the Nup62 complex and other FG repeats containing nucleoporins to the pore, which form the central channel of the pore. Through the central channel of the pore nucleo-cytoplasmic transport occurs and a permeability barrier is established thereby maintaining distinct environments of the nucleus and cytosol in the cell. In this way, Nup93 connects both the structural and functional regions of the NPC and serves as a decisive and critical link between the two portions. We could also show that the middle domain of Nup93 is dispensable for NPC assembly. This study also sheds light on the order of recruitment of different nucleoporins in post-mitotic NPC assembly. It places Nup93 at a crucial and strategic position wherein it serves as a link between the structural and functional parts of the pore. Our findings also elucidated the role of different domains of Nup93 and their contribution in NPC assembly and function.

ZUSAMMENFASSUNG

Das namensgebende Charakteristikum einer eukaryontischen Zelle ist die Kompartimentierung des genetischen Materials im Zellkern. Dies wird durch die Existenz einer Lipiddoppelschicht möglich: der sogenannten Kernhülle. Die Kompartimentierung ermöglicht es, Transkription und Translation räumlich und zeitlich voneinander zu trennen. Die Kernhülle besteht aus zwei Membranen: der äußeren Kernmembran, die in das endoplasmatische Retikulum übergeht, und der inneren Kernmembran, die sich durch eine individuelle Proteinzusammensetzung auszeichnet und mit dem Chromatin und der Kernlamina interagieren kann. Die äußere und die innere Kernmembran verschmelzen miteinander, um Poren zu formen, in denen die Kernporenkomplexe eingelagert sind. Die Kernporenkomplexe fungieren als Wächter des Zellkerns und sind am Transport in und aus dem Zellkern beteiligt. Zudem bilden sie eine Diffusionsbarriere aus, wodurch die unterschiedlichen Zusammensetzungen von Zellkern und Zytoplasma gewährleistet werden. Kernporenkomplexe sind makromolekulare Proteinkomplexe mit einer Größe von 40-60 Mega Dalton. Trotz ihrer enormen Größe bestehen Kernporenkomplexe nur aus etwa 30 Proteinen, den sogenannten Nukleoporinen oder Nups. Die meisten dieser Nukleoporine bilden kleinere Untereinheiten, die als Grundbausteine für den Zusammenbau der Kernporen dienen. Die Kernporenkomplexe können grob in zwei Bereiche unterteilt werden. Das strukturelle Rückgrat der Pore besteht aus strukturellen Nukleoporinen, welche das Grundgerüst der Pore vorformen und als Ankerproteine dienen, um weitere Nukleoporine zu rekrutieren. Der andere Teil ist der funktionelle Bereich der Pore, der zumeist aus Nukleoporinen aufgebaut ist, die FG-Wiederholungen tragen und den zentralen Kanal der Pore bilden. Diese Nukleoporine vermitteln die funktionellen Eigenschaften, wie die Transportfähigkeit oder den Größenausschluss der Pore. In Lebewesen, die einer offenen Mitose unterzogen sind, werden die Kernhülle und die Kernporenkomplexe während der Prophase aufgelöst und müssen, sobald die Zelle wieder in die Interphase eintritt, aus den demontierten, löslichen Kernporenbestandteilen und aus Membranen erneut zusammengebaut werden, um wieder einen intakten Zellkern herzustellen.

Das Ziel dieser Arbeit ist es, die Funktion einer dieser Untereinheiten, nämlich des Nup93-Komplexes, im Kernporenaufbau und in der Kernpore selbst zu charakterisieren. Nup93 bildet einen der strukturellen Komplexe der Kernpore und befindet sich in dem Bereich der Pore, wo er eine Verbindung zwischen den Membranen der Kernhülle und dem Rest des Kernporenkomplexes herstellt. Der Nup93-Komplex besteht aus fünf Nukleoporinen: Nup53, Nup93, Nup155, Nup188 und Nup205. Es wurde bereits in unserem Labor gezeigt,

dass Nup93 in zwei verschiedenen Unterkomplexen vorkommt: als Nup93-Nup188 und als Nup93-Nup205. Weder der Nup93-Nup188- noch der Nup93-Nup205-Unterkomplex waren jeweils essentiell für den Kernporenzusammenbau. Wir wollten nun herauszufinden, ob auch beide Unterkomplexe zusammen nicht essentiell für den Aufbau der Kernporen sind, da vermutet wurde, dass sie redundante Funktionen in der Pore besitzen.

Hierfür nutzten wir das Eiextrakt-System aus *Xenopus Laevis* (um in vitro den Kernporenaufbau nachzustellen) und zeigten mittels verschiedener zellbiologischer und biochemischer Experimente, dass das konservierte Nukleoporin Nup93 für den Aufbau der Kernporen und der Kernhülle essentiell ist. Die Immundepletion von Nup93 (wodurch Nup205 und Nup188 mitdepletiert wurden) führte zu einem Block im Kernporen- und Kernmembranaufbau und konnte durch die Zugabe von rekombinantem Nup93 aufgehoben werden. Nup93 allein konnte somit die fehlenden Nup93-188- und Nup93-205-Unterkomplexe ersetzen. Dies belegte gleichzeitig, dass die beiden größten Bestandteile des Nup93-Komplexes, Nup188 und Nup205, auch zusammen keine wichtige Rolle für den post-mitotischen Kernporenaufbau spielen. Zudem haben wir gezeigt, dass der C-terminale Teil von Nup93 notwendig und ausreichend ist, um das strukturelle Rückgrat der Pore zu bilden, indem Nup93 die Interaktion zwischen den beiden wesentlichen strukturellen Komponenten der Pore, Nup53 und Nup155, verstärkt. Wir glauben, dass dies ein entscheidender Schritt in der Ausbildung des strukturellen Rückgrats und damit für den post-mitotischen Aufbau der Kernporen ist. Nup93 rekrutiert mit seinem N-Terminus Nup62 und weitere Nukleoporine, die FG-Wiederholungen tragen, an die Pore, die den zentralen Kanal der Pore bilden. Dieser zentrale Kanal vermittelt den Transport in und aus dem Zellkern und ist für den Größenausschluss der Kernpore verantwortlich, wodurch die verschiedenen Milieus von Zellkern und Zytosol aufrechterhalten werden. Somit verbindet Nup93 den strukturellen und den funktionellen Bereich der Kernpore und fungiert als das entscheidende Bindeglied zwischen diesen beiden Regionen in der Kernpore. Wir konnten zudem zeigen, dass die mittlere Domäne von Nup93 nicht notwendig für den Kernporenaufbau ist. Diese Arbeit gibt außerdem Aufschluss über die Reihenfolge der Rekrutierung verschiedener Nukleoporine für den post-mitotischen Kernporenaufbau. Sie zeigt die bedeutsame Rolle und Position von Nup93 in der Kernpore, wo es das Bindeglied zwischen dem funktionellen und dem strukturellen Teil der Pore darstellt. Unsere Ergebnisse erklären zudem die einzelnen Funktionen der verschiedenen Proteinabschnitte von Nup93 und ihre Bedeutung für den Aufbau und die Funktion der Kernpore.

1. INTRODUCTION

1.1. Basic architecture of the mammalian cell nucleus

Cell is the structural, functional and biological unit of all living organisms. It's an autonomous unit that can self replicate and perform specialized functions in the organism. A cell carries the heritable information. To maintain the life forms cell division occurs after the genome is duplicated leading to formation of a mother and a daughter cell. A major difference between the prokaryotic and eukaryotic cell is the existence of a membrane-enclosed organelle, nucleus surrounded by the nuclear envelope (NE) in the eukaryotic cells, which leads to compartmentalization of the genetic material. The NE demarcates the nucleus in the cell. The nuclear envelope comprises of two lipid bilayers, the outer nuclear membrane (ONM) and the inner nuclear membrane (INM). The ONM is continuous with the endoplasmic reticulum (ER) and faces the cytosolic side. ER and the ONM are believed to have a similar protein composition (for review see Mattaj, 2004). The INM on the other hand is characterized by a distinct protein composition, and faces the nucleoplasm (Senior et al., 1998 and see figure 1.1). The ONM and the INM fuse to form pores where the nuclear pore complexes (NPCs) reside, (for review see Antonin et al., 2008), which are involved in nucleo-cytoplasmic transport.

The nucleus contains the genetic material of the cell organized as linear DNA molecules, this along with histones forms chromatin. The nucleus pretty much is the "brain" of the cell as it controls the integrity of the genes and can control cellular activities by influencing gene expression. The chromatin in the cell can exist in two states, euchromatin that is less compact and houses genes that are frequently expressed by the cell. The other kind is the heterochromatin that is much more compact and harbors DNA that is not transcribed often. The heterochromatic genes are usually located at the nuclear periphery and the euchromatic genes are mostly localized in the interior of the nucleus. Thus both euchromatin and heterochromatin occupy distinct territories in the nuclear space in interphase (Lamond et al., 1998; Schardin et al., 1985; Grigoryev et al., 2006; Williams, 2003). The regions in the interphase nuclei that are devoid of chromatin contain the transcription machinery, components for processing of different kinds of RNA and other nuclear bodies for instance the PML bodies (Cremer and Cremer 2000; Williams, 2003). The nuclear interior contains many

distinct sub structures that are characterized by lacking a membrane and are known to contribute towards gene expression (for review see Dundr and Misteli, 2001). One such sub organelle is the nucleolus that synthesizes rRNA and is involved in ribosome assembly. The genes for rRNA are transcribed as precursors, which are then processed and assembled into ribosomal sub units and exported to the cytoplasm where they assist in translating the mRNA (Hernandez-Verdun et al., 2006). Other sub-nuclear structures include Cajal bodies, PML bodies, paraspeckels, speckels and PIKA (polymorphic interphase karyosomal association) (for review see Dundr and Misteli, 2001). PML bodies are mostly involved in regulating transcription. Nuclear speckles contain serine/arginine rich proteins that are involved in mRNA processing (Sanford, 2005). Cajal bodies or coiled bodies contain factors for U sn RNP assembly and PML bodies (Gall, 2000).
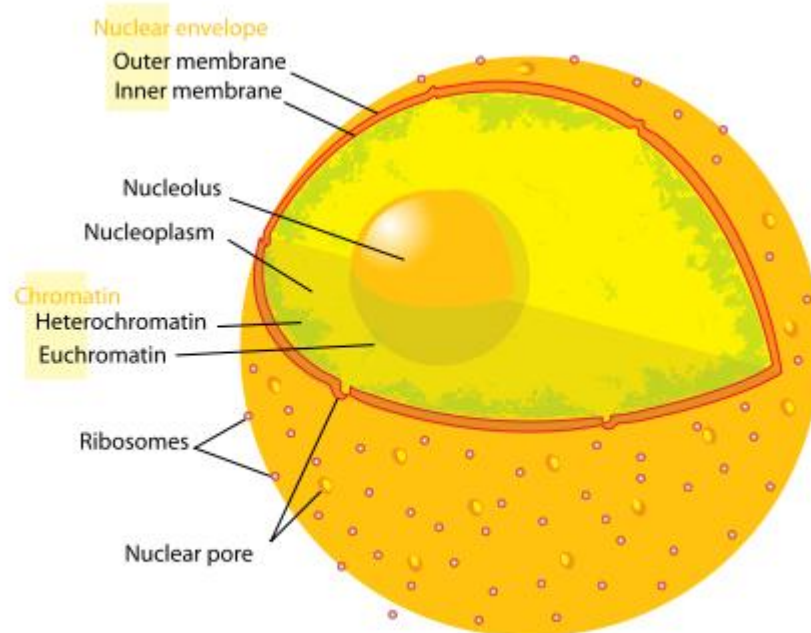
Figure 1.1: Schematic representation of the nuclear architecture of a eukaryotic cell. A nuclear envelope composed of an outer nuclear membrane (ONM) and an inner nuclear membrane (INM) that encloses the nucleus. The nuclear pores are embedded where the outer nuclear membrane (ONM) and the inner nuclear membrane (INM) fuse to form holes. The nucleoplasm consists of euchromatin (yellow) and heterochromatin (green) and nucleolus (modified from Wikipedia, courtesy Mariana Ruiz).

1.2. The nuclear envelope

The nuclear envelope is the major hallmark of a eukaryotic cell as it encloses the genetic material and hence spatially and temporally separates the nuclear activities like gene transcription, DNA replication and RNA processing from cytoplasmic processes like translation. This attribute of compartmentalizing the genetic material imparts a level of regulation to gene expression. For instance a number of extracellular signaling pathways make use of the NE as a translocation mechanism for gene activation. NE is a phospholipid bilayer comprising of an ONM that is continuous with the ER and is decorated with ribosome. The INM on the other hand is characterized by a distinct set of integral membrane proteins. The proteins present in the INM make contact with the underlying chromatin and the nuclear lamina (Holmer and Worman, 2001). Lamina is a meshwork of intermediate filaments that provide mechanical support to the nucleus. The nuclear lamina is composed of lamin proteins (Lamins A and B). The close association of nuclear lamina with the INM is mediated by the interaction of nuclear lamins with proteins present in the INM. More than eighty transmembrane proteins have found to be localized at the INM but only few of them have been characterized in detail. Some of these include LAP2, MAN1, LBR (lamin B receptor) and emerin, an INM protein, which are mutated in Emery-Dreifuss muscular dystrophy (Worman, 2005) implying the importance of INM proteins as they have been linked to various human diseases. LBR contains eight TM domains and can interact with the B type Lamins thereby linking the lamin intermediate filament network and the INM (Worman et al., 1998). LBR can also interact with the chromatin bound protein HP1 (heterochromatin protein 1) and thus organizes the heterochromatin at the nuclear periphery (Ye and Worman, 1996). Another class of INM proteins belongs to the SUN family of proteins characterized by the SUN domain. They are involved in nuclear migration and centrosome positioning. They interact with KASH proteins present in the ONM. This way they can connect the nucleus to the cytoskeleton and establish LINC (linker of nucleoskeleton and cytoskeleton) complexes (Sosa et al., 2012).

The equal distribution of genetic material is an important step in cell division. Lower eukaryotes like yeast (*S. cerevisiae*) undergo closed mitosis where the mitotic spindle can form inside the nucleus or is able to penetrate an intact NE (Heywood 1978; Ribeiro et al., 2002). Conversely in higher eukaryotes undergoing open mitosis the NE has to breakdown,

NPCs have to disassemble at the onset of mitosis to allow for the spindle machinery to access the chromatin. Consequently every dividing cell must reform the NE and NPCs to form an intact nucleus at the end of mitosis (Hetzer et al., 2005; for review see Güttinger et al., 2009).

NE remodeling is a highly dynamic process that involves a variety of molecular players. At the end of interphase / in G2, the nuclei have duplicated their DNA and NPCs and also increased the surface area of the NE. The ER network is continuous with the NE, but not enriched in NE proteins. The entry into mitosis, in prophase, is characterized by NE breakdown (NEBD) and the loss of the permeability barrier (for review see Burke and Ellenberg, 2002). Between NEBD and early anaphase, when chromosomes align at the metaphase plate and subsequently segregate, chromatin is devoid of membranes (Puhka et al., 2007; Anderson and Hetzer, 2008a). During these cell cycle stages, the majority of soluble nuclear pore proteins are distributed throughout the cytoplasm, nuclear lamina is disassembled via phosphorylation by Cdk1 {cyclin dependent kinase} (Gerace and Blobel 1980; Ottaviano and Gerace 1985) and the transmembrane NE proteins are absorbed in the mitotic ER (Ellenberg et al., 1997; Anderson and Hetzer 2007; Puhka et al., 2007). In anaphase, ER membranes begin to re-associate and enclose the decondensing chromatin (Anderson and Hetzer 2008a). Chromatin association of a subset of nucleoporins, decondensation of chromatin, and NPC assembly occurs concomitantly with formation of the NE (Anderson and Hetzer 2008c). At the end mitosis, the NE has reformed, the exclusion barrier is established and the NPCs as they form can perform the nucleo-cytoplamsic transport (Dultz et al., 2008). The NE then undergoes expansion and more structural rearrangements are required for cell cycle progression including the assembly of new NPCs. (Winey et al., 1997; D'Angelo et al., 2006). The NE formation is a highly regulated process mostly controlled by the small GTPase Ran, which plays a role in NE membrane fusion, NPC assembly and nuclear transport.
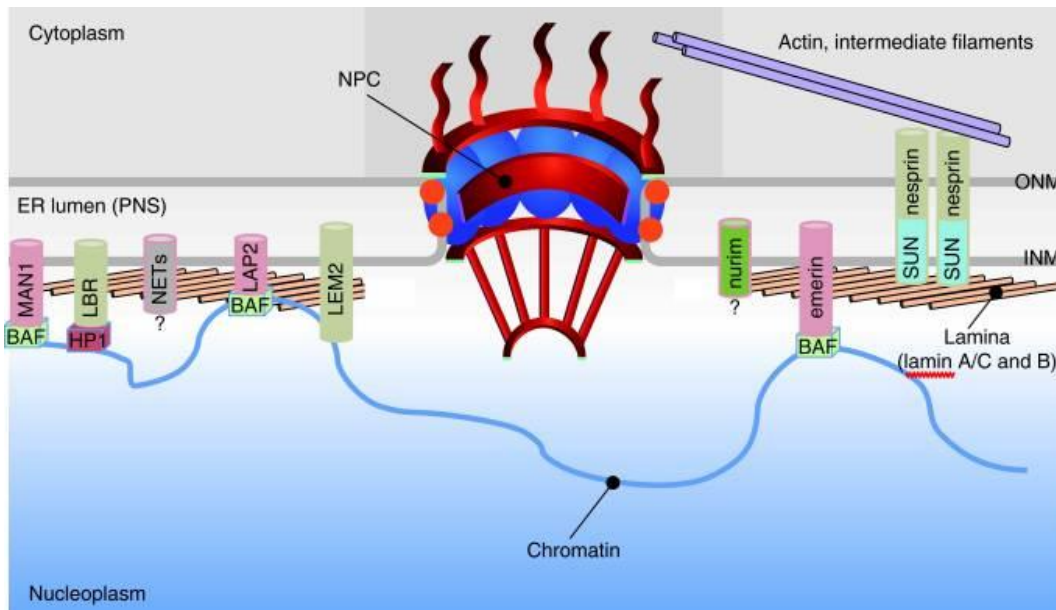
Figure 1.2: Schematic overview showing the topology of the nuclear envelope. Inner nuclear membrane and the outer nuclear membrane are separated by the endoplasmic reticulum lumen or perinuclear space (PNS). The nuclear lamina interacts with nuclear envelope proteins and chromatin. Inner nuclear membrane proteins link the nuclear envelope to chromatin and the lamina. Outer nuclear membrane proteins provide a connection from the nucleus to the cytoskeleton. Lamin B receptor interacts both with B-type lamins and chromatin-associated heterochromatin protein 1 (HP1) together with core histones. Members of the LEM (lamina-associated protein 2 [LAP2], emerin, MAN1)-domain family (pink) bind to lamins and interact with chromatin through barrier-to-autointegration factor (BAF). SUN proteins present in the inner nuclear membrane interact with nesprins (KASH: Klarsicht, ANC-1, Syne Homology domain containing proteins) in the outer nuclear membrane, forming LINC (linker of nucleoskeleton and cytoskeleton) complexes that establish connections to actin and intermediate filaments in the cytoplasm. (Adapted from Hetzer, 2010).

1.3. The nuclear pore complex

Nuclear pore complexes (NPCs) are proteinaceous macromolecular assemblies that are involved in all nucleo-cytoplasmic inside the cell. The transport of RNA, cargos, proteins etc occurs through the NPC. NPCs have an estimated mass of about 40-60 Mega Daltons in yeast and vertebrates respectively (Cronshaw et al., 2002; Rout et al., 2000 and for

review see Brohawn et al., 2008). Despite their enormous size they are composed of only approx. 30 proteins called nucleoporins or Nups. These nucleoporins are organized as distinct sub-complexes in the pore (for review see Antonin et al., 2008; D'Angelo and Hetzer, 2008). In animals undergoing open mitosis the NE and the NPCs breakdown and as the cell enters interphase, both the NE and NPCs must reform to form an intact functional nucleus. NPC assembly is a well coordinated and a highly regulated process. This study focuses on the molecular mechanisms of NPC assembly in relation to one of the sub-complex in the pore, the Nup93 sub-complex. First I will describe the basic structure, composition of the NPC and then discuss in further details about NPC assembly and regulation followed by summary of the mechanisms of nuclear transport through the pore.

1.3.1. Structural framework and composition of the nuclear pore complex

The enormous structure of the NPC is composed of approx. 30 proteins, referred as nucleoporins. Most of these proteins have been identified and are being biochemically and functionally characterized. How this massive structure is assembled with multiple copies of only 30 nucleoporins is not completely understood (for review see Antonin et al., 2008). A number of different methods and experimental systems have been utilized to study the molecular mechanisms of NPC assembly. For instance, scanning electron microscopy (Goldberg and Allen, 1993, 1996; Jarnik and Aebi, 1991; Ris, 1997; Ris and Malecki, 1993) atomic force microscopy (Rakowsk et al., 1998; Stoffler et al., 1999), cryo electron microscopy (Akey, 1989; Akey and Radermacher, 1993; Yang et al., 1998) and cryo electron tomography (Beck et al., 2004, 2007). Recently a high-resolution structure (< 6nm) of the NPC from *Dictyostelium discoideum* was solved by Beck et al., 2004, 2007) as shown in figure 1.3. Number of efforts from different labs has contributed towards solving the structure of the NPC and some of the facts that are now established are that NPCs have a 8-fold symmetry. The basic structure of the NPC can be dissected into three parts namely, the central core, the nuclear basket and the cytoplasmic filaments (see figure 1.3). The central core is made up of 8 extended filaments on the cytoplasmic and a basket like structure on the nuclear side. The attached cytoplasmic filaments are approx. 50nm in length and the nuclear basket is 100nm. The overall dimensions calculated for the NPC from *D. discoideum* is 40nm diameter at the distal nucleoplasmic ring, 125nm diameter at

the cytoplasmic face and total length being roughly 110nm. In the central pore there lies the narrowest point in the channel that is 45nm and mediates the passage of cargo complexes with diameter of about 35-40nm. Upon visualization of the luminal connector element that spans between the ONM and the INM a crucial understanding of attachment of NPCs to the NE was established. The yeast NPCs are smaller than the vertebrate NPCs and have smaller mass (approx. half that is 40 Mega Daltons).
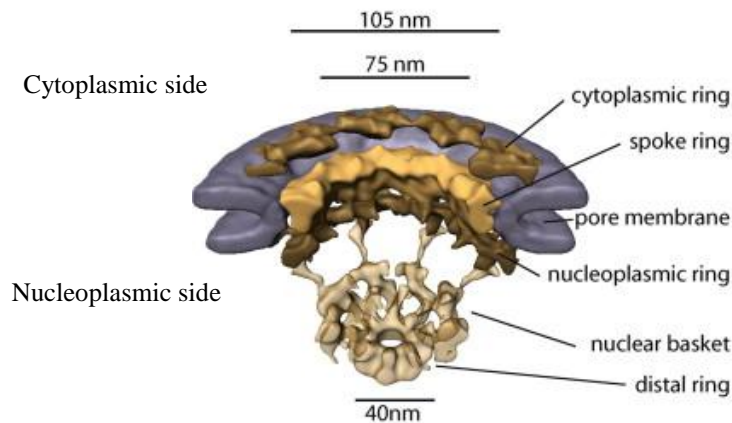
Figure 1.3: Basic structural features of the nuclear pore complex. A cut way view of the density map of the nuclear pore complex from *D. discoideum* at 5.8nm resolution obtained using cryo-elctron tomography. The spoke ring and the cytoplasmic ring of the pore are shown in yellow and brown respectively. The inner nuclear membrane and the outer nuclear membrane are represented in grey. (Modified from Beck et al., 2007).

1.3.2. Structural architecture of the nucleoporins

Structural predictions have helped group the nucleoporins into fold classes. (Berke et al., 2004; Devos et al., 2004; Devos et al., 2006; and for review see Schwartz, 2005). About 13% of the NPC is made up of the FG (phenylalanine-glycine) repeat containing nucleoporins. The FG repeat containing nucleoporins are involved in interactions with each other, which are multivalent and cohesive, and also with the transport receptors that are bound to the cargo while being transported in or out of the nucleus. FG-domains are present in about one-third of all nucleoporins. These domains are unstructured and natively unfolded. They are localized at cytoplasmic side, nuclear periphery and form a hydro gel in the central channel of the pore (Labokha et al., 2012; Fahrenkrog et al., 2004). The unfolded structure and flexibility in the FG domains contributes towards multiple and

transient contacts with various interacting partners (Denning et al., 2003). Second are the coiled-coil domains present in a number of nucleoporins and are involved in mediating protein-protein interaction (Cronshaw et al., 2002). Thirdly, the WD repeats present in a few nucleoporins are organized into beta propellers. The fourth structural feature is the presence of alpha helical repeats organized into various higher order structures in some nucleoporins. A combination of beta propellers and alpha helical domains has also been seen in a few nuclear pore proteins. For instance, members of the Nup107-160 complex contain beta propeller folds, alpha solenoids or a tandem combination of both (for review see Schwartz, 2005). See figure 1.4 below.
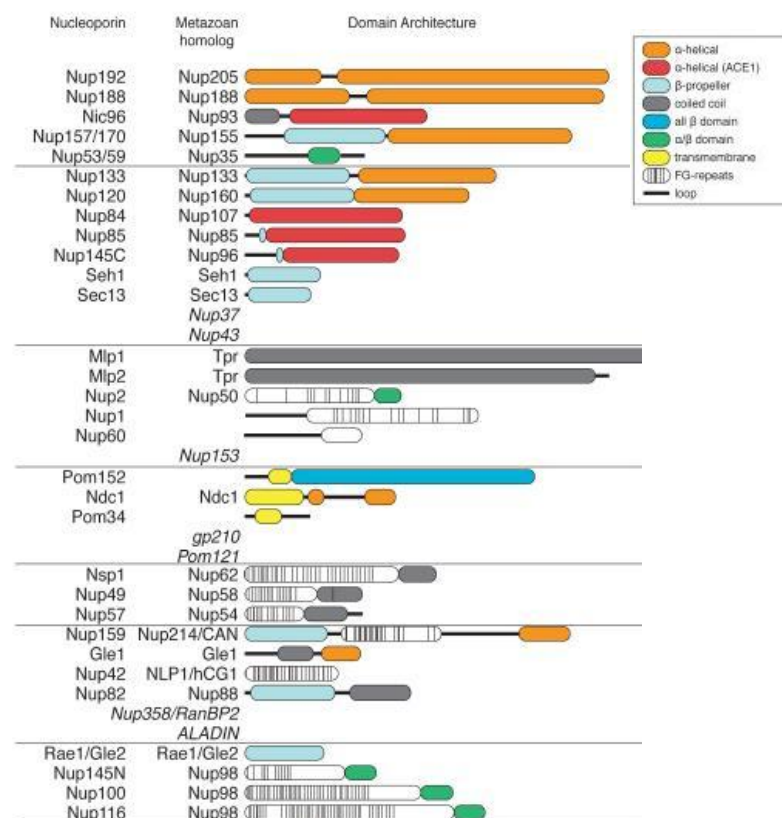
Figure 1.4: Schematic overview of structural elements present in nucleoporins. Summary of the nucleoporins that form the nuclear pore complex. The figure shows the domain architecture of nucleoporins from *S. cerevisiae* as determined by X-ray crystallography or prediction (where structural information is still lacking) modified from Brohawn et al., 2009.

1.3.3. Molecular composition of the nuclear pore complex

How the massive and enormous structure of the NPC is formed from the 30 nucleoporins is an extremely interesting problem to solve. Some of these nucleoporins can be very large in size in the range of about 360 kDa and due to the 8 fold symmetry of the pore, tend to come in copies of 8, 16, 32 or more (for review see Antonin et al., 2008). The majority of nucleoporins are organized into distinct sub-complexes both in yeast and vertebrates (Alber et al., 2007). These sub-complexes are defined biochemically and there exists a stable interaction among nucleoporins. The NPC can be roughly dissected into two parts, the structural backbone of the pore and the functional part. The structural part is composed of structural nucleoporins that form the scaffold of the pore and act as anchor proteins to recruit other nucleoporins as the pore assembles. These include Mel28-ELYS, transmembrane nucleoporins: Pom121, Ndc1, the Nup107-160 complex and members of the Nup93 complex. The functional part of the pore is formed by the FG repeat containing nucleoporins that are more flexible and line the central channel of the pore. They are responsible in imparting functional properties to the pore like transport competency and the ability to act as an exclusion barrier. The FG domains can interact with each other and also with the transport receptors bound to the cargos to allow the efficient transport of substrates. These nucleoporins are members of the Nup62 complex, Nup98 and other FG repeat containing peripheral nucleoporins.

In vertebrates the three huge complexes that build the major part of the NPC are the Nup107-160 complex, Nup93 complex and the Nup62 complex (for review see Antonin et al,. 2008). These complexes act as basic building blocks of the NPC upon which other peripheral nucleoporins are assembled from the free pool (for review see Rabut et al., 2004). The Nup107-160 complex is the best studied amongst the aforementioned sub-complexes both structurally and biochemically (Devos et al., 2004; Glavy et al., 2007; Walther et al., 2003).

The vertebrate Nup107-160 complex comprises of nine members: Nup107, Nup133, Nup160, Nup96, Nup75, Nup37, Nup43, Seh1 and the COPII protein Sec13 (coatemer like) (Loiodice et al., 2004). The homologue that exists in yeast is the Nup84 complex. The Nup84 complex can be reconstituted in vitro with these seven subunits. Using this reconstitution EM was done and a Y shaped structural complex was determined (Lutzmann

et al., 2002). This complex makes up the major part of the octagonal spoke ring complex, see figure 1.5. Sixteen copies symmetrically localize around the cytoplasmic and nuclear ring (Krull et al., 2004). It has been speculated that the yeast Nup84 complex and the vesicle coating complexes are made of beta propeller folds, alpha solenoids and share a common structure, which hints that they might have a common ancestor (Devos et al., 2004). Peripheral membrane proteins represent interesting candidates to bend the membrane. This might also hint to the fact that they share some common membrane bending functions. Nup107-160 complex is a very early player recruited in the post-mitotic NPC assembly and acts as a seeding point for pore formation (Walther et al., 2003). It is known to interact with Mel28-ELYS; a nucleoporin that binds to chromatin via it's AT hook motifs and is the starting point of pre pore formation in post-mitotic NPC assembly. There are also mitotic "tasks" that the members of the Nup107-160 perform. They have shown to be localized at the kinetochores and also are involved in spindle assembly checkpoint via interaction with MAD1 (Loiodice et al., 2004; Rodenas et al., 2012).

The NPC is anchored firmly and contacts the nuclear membrane. Three nucleoporins have been characterized that contain transmembrane (TM) regions referred to as pore membrane proteins (poms). Out of these one of the TM nucleoporin: Ndc1 is conserved. Pom152p in yeast has an equivalent homologue Gp210 in metazoans and both have one TM region. Pom34p is present only in yeast and has no structural similarity to vertebrate Pom121. Ndc1 is known to interact with Nup53 and Pom121 interacts with Nup155 potentially linking the NPC to the pore membrane (Vollmer et al., 2012; Mansfeld et al., 2006; Mitchell et al., 2010). Although individual nucleoporins show limited sequence conservation between yeast and vertebrates, the overall structure and composition of the sub-complexes is conserved during evolution.

A second major structural complex of the NPC is the Nup93 complex, which is the major focus of this study. In the pore the Nup93 complex is positioned at a region where it makes contacts with the NE proteins. In vertebrates the Nup93 complex consists of five nucleoporins: Nup53, Nup93, Nup155, Nup188 and Nup205. Both Nup53 and Nup155 are known to be indispensable for NPC assembly and function (Franz et al., 2005; Hawryluk-Gara et al., 2008; Vollmer et al., 2012). Nup53 and its yeast homologue Nup53p and Nup59p are both known to interact with the TM nucleoporins Ndc1 thereby linking NPC to the pore membrane (Mansfeld et al., 2006; Onischenko et al., 2009). Nup53 is also

known to interact with Nup155 via its C-terminus and to Nup93 via its N-terminus and similarly with the corresponding proteins in yeast linking these proteins in an interaction network (Fahrenkrog et al., 2000; Onischenko et al., 2009; Vollmer et al., 2012). Vertebrate Nup53 also associates tightly with the nuclear membranes and lamina through lamin B. Recently it was also shown that Nup53 has a direct membrane binding activity, which is necessary for NPC assembly. It has two membrane binding regions. Either one is sufficient and essential for post-mitotic NPC assembly. For interphase NPC assembly the C-terminal membrane-binding region is necessary and has membrane tubulation activities (Vollmer et al., 2012).

In *Xenopus laevis* Nup93 exists as part of two distinct complexes, one with Nup188 and one with Nup205. Individually these complexes have shown not to be essential for NPC assembly. It was shown that the Nup188-Nup93 complex regulates the targeting of integral membrane proteins to the INM. Upon depletion of Nup188-Nup93 complex from *Xenopus* egg extracts the nuclei formed there on were larger in surface area due to accelerated INM targeting of integral membrane proteins (Theerthagiri et al., 2010). Both Nup188 and Nup205 are structural nucleoporins found in the inner pore ring and have a S shape karyopherin like structure (Almacher et al., 2012). In *C. elegans* RNAi against Nup93 or Nup205 leads to embryonic lethality and smaller nuclei than in control embryos. Abnormal chromosome condensation was observed. NPCs aggregated in the NE and allowed 70 kDa dextrans to diffuse in the nuclei inspite of a closed NE and presence of NPCs. Protein import was not impaired (Galy et al., 2003). The worm arthologue of Nup188 has not been identified. In yeast the homologue of vertebrate Nup188 that is Nup188p is not essential for cell growth (Zabel et al., 1996) and its disruption leads to NE abnormalities but nuclear transport is not affected (Nehrbass et al., 1996; Zabel et al., 1996). Currently it cannot be ruled out if both Nup188 and Nup205 have other functions in vivo.

Nup93 also interacts with Nup62 and this interaction is conserved in yeast where Nic96p (the Nup93 homologue) is known to interact with Nsp1p (Nup62 homologue) (Grandi et al., 1993, 1997). This way Nup93 links the structured part of the pore to the unstructured FG repeat containing nucleoporins that form the central channel. Nup93 is an essential gene in most organisms tested implying the conservation and its importance in NPC assembly and function, for example in *D. rerio, C. elegans, S.cerevisae* and *A. nidulans* (Grandi et al., 1993; Allende et al., 1996; Galy et al., 2003; Osmani et al., 2006).

Quantification of Nup93 in NPCs of rat liver cells and of Nic96p in yeast suggested that this nucleoporin is present in more than 32-48 copies per NPC and hence is one of the most abundant nucleoporin (Rout et al., 2000; Cronshaw et al., 2002; Alber et al., 2007). Depletion of Nup93 from *Xenopus laevis* egg extracts followed by an in vitro nuclear assembly reaction resulted in nuclei with reduced NPC staining (Grandi et al., 1997) suggesting the importance of Nup93 in NPC assembly. The interaction between Nup53, Nup93 and Nup155 has also been observed by the Ed Hurt lab (Almacher et al., 2012) in thermophilic fungus *C. thermophilum*. The same study also showed that the N-terminal coiled-coil domain of Nic96p binds Nup62. Within this coiled-coil domain is a positively charged alpha helical stretch of amino acids that binds Nup205 and Nup188 at the same site. The crystal structure of Nic96p lacking the N-terminal domain has been solved (Jeudy and Schwartz, 2007; Shrader et al., 2008). The N-terminus of the protein is coiled-coil in nature and rest of the protein is mostly alpha helical. A patch of amino acids at C-terminus is predicted to take part in protein-protein interactions.

Another sub-complex that participates in forming the central channel is the Nup62 sub-complex. It is one of the first vertebrate sub-complexes to be characterized and was found to form a complex with Nup54 and Nup58 and its splice variant Nup45 (Finlay et al., 1991). This sub- complex comprises of FG repeat containing nucleoporins that line the central channel of the pore and participate in nuclear transport and formation of the permeability barrier of the pore. Recently it was shown that depletion of the Nup62 complex from *Xenopus* egg extracts followed by nuclear assembly reaction lead to formation of nuclei, which had an intact exclusion barrier and were transport competent (Hülsmann et al., 2012).

Other nucleoporins that exist, as individual proteins are the cytosolic and peripheral nucleoporins like Nup153, Nup50, TPR, Nup98, Nup88, Nup214, Nup358, Aladin, Rae1 etc. Hülasmann et al., 2012 showed that Nup98 (an FG repeat containing nucleoporin) is a major player that is part of the central channel of the pore and establishes the permeability barrier of the pore. Multivalent cohesive FG domains form the hydrogel, which acts as an exclusion barrier, and also a way to interact with transport receptors bound cargos to allow efficient transport. Post-translational modifications like glycosylations on Nup98 lead to flexibility in the FG-FG inter and intra interactions and between FG domains and the

transport receptors, which provides dynamicity in the nuclear transport process (Labokha et al., 2012).
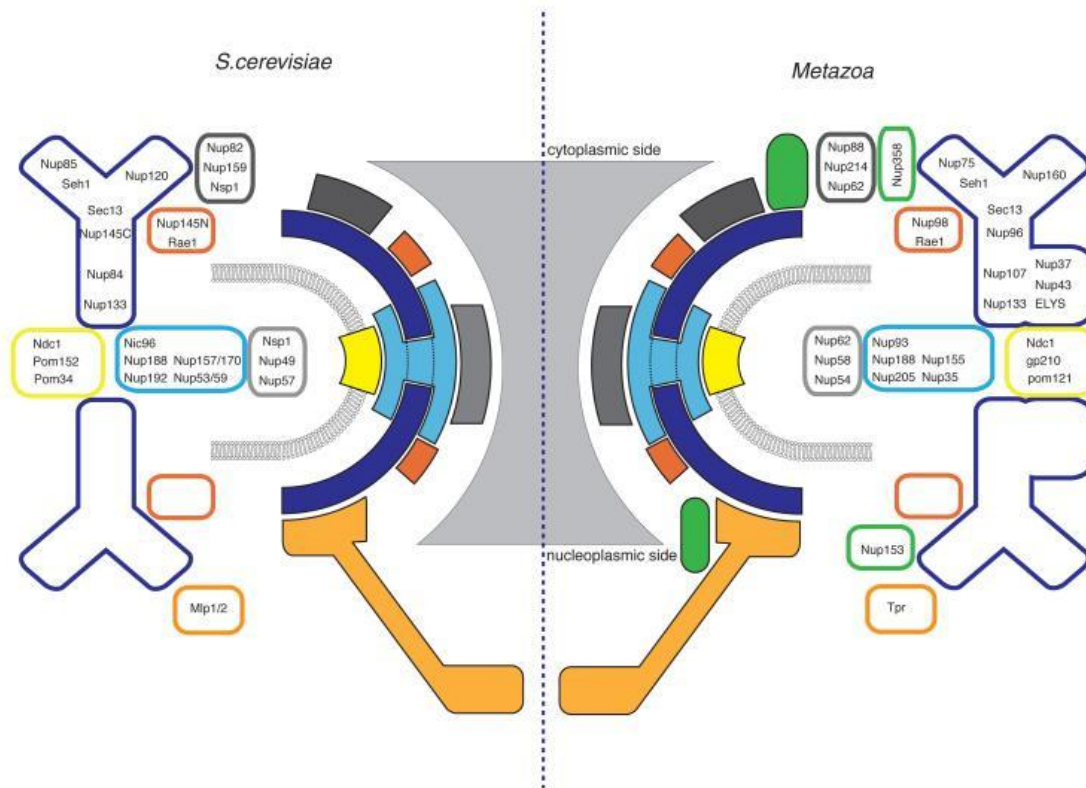
Figure 1.5: Schematic representation of the modular structure of the nuclear pore complex. The scheme shows the modular view of the vertebrate and yeast nuclear pore complex showing distinct sub-complexes that are characterized biochemically. Transmembrane nucleoporins are shown in yellow. Nup93 complex in light blue, the Nup107-160 complex as a Y shape is shown in dark blue and the Nup62 complex in grey. The nuclear envelope is shown in grey comprising of lipid and their head groups. Rest of the individual nucleoporins like Nup153, TPR, Nup98, Rae1, Nup358, Nup88, and Nup214 are also depicted in the figure. Note the critical positioning of the Nup93 complex where it contacts the nuclear envelope. Modified from Brohawn et al., 2009.

1.3.4. Nuclear pore complex assembly

In animals undergoing open mitosis, the NE and NPC disassemble at the onset of mitosis so that the spindle apparatus and the cytoplasmic microtubules can access the chromosomes. As the cell exits mitosis in telophase and prepares for entry into mitosis the NE and the NPCs must reassemble around the segregated chromatin. How the NE and NPCs reform to form an intact functional nucleus is summarized in this section. This refers to the post-mitotic NPC assembly. Also new NPCs assemble in an intact NE during cell growth in interphase or if there is a change in metabolic activity of the cell. This mechanism also implies to yeast (*S.cereviase*), which undergoes closed mitosis. The molecular mechanism of interphase NPC assembly will also be discussed briefly in this section.

1.3.4.1. Post-mitotic nuclear pore complex assembly

As the NE and NPCs breakdown the nucleoporins are dispersed in the cytoplasm either as individual proteins or as sub-complexes. At the same time the membranes are reabsorbed in the mitotic ER. Thus NPC assembly has to be coordinated with the formation of the NE. NPC assembly has been extensively studied using cell free assays like the *Xenopus leavis* egg extract system and in vitro nuclear assembly reactions done with them. Also cell culture and yeast genetics have been exploited for the same. There are two models proposed for post-mitotic NPC assembly. One is the pre pore model in which NPC assembly starts on chromatin with binding of early nucleoporins forming a pre pore after which the NE specific membranes are enriched (emanating from the mitotic ER) completing the NPC assembly with the closure of NE. In another model the post-mitotic NPC assembly occurs with the chromatin being first surrounded by membranes, and insertion of NPCs occurs via membrane fusion (for review see Rabut et al., 2004). See figure 1.6 for pictorial representation.
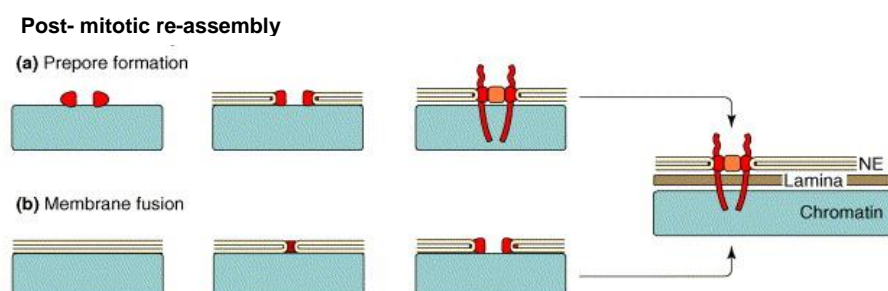
Figure 1.6: Models for post-mitotic nuclear pore complex assembly. a) shows the pre pore model where nucleoporins (shown in red/orange) bind and start the nuclear pore complex assembly on chromatin (blue) which are then surrounded by membranes from the endoplasmic reticulum (yellow) and serve as platforms for recruitment of peripheral nucleoporins. Brown color shows the nuclear lamina. b) shows the membrane fusion model wherein chromatin is surrounded by continuous double membrane into, which nuclear pore complexes are inserted by membrane fusion (adapted from Rabut et al., 2004).

Pre-pore post-mitotic nuclear pore complex assembly

The NPC assembly starts with binding of Mel28-ELYS via its DNA binding AT hook motifs to the decondensing chromatin (Rasala et al., 2006; Franz C et al., 2007). Then the Nup107-160 complex binds, which acts as a seeding point for NPC assembly. Both Mel28 and Nup107-160 complex are essential for nuclear pore formation (Sheehan et al., 1988) as their depletion leads to pore free NEs (Walther et al., 2003; Harel A et al., 2003). Then a small fraction of Nup153 and Nup50 are recruited to the assembling NPC (Dultz et al., 2008). Membranes that were dispersed in the mitotic ER then start to associate with the chromatin. As the membranes association occurs with the chromatin the tubular ER converts to sheets and starts to flatten around the decondensing chromatin. Tubular tips grow out from the mitotic ER where the NE specific membranes start to make contacts with the chromatin (Anderson et al., 2007). INM proteins of the NE have positively charged DNA binding domains that can act as initial contacts to the chromatin (Ulbert et al., 2006). Membrane flattening starts leading to expansion of the ER like network as flattened sheets on the chromatin surface. The holes or gaps are then stabilized by newly formed NPCs at sites of chromatin bound pre-pores. TM nucleoporins, which are part of the mitotic ER associate with the pre-pore on chromatin. TM nucleoporins that are enriched at this step are Pom121 and Ndc1 (Mansfeld et al., 2006; Antonin et al., 2005). Pom121 binds the Nup107-160 complex. Together they take part in the checkpoint of NE and NPC formation (Antonin et al., 2005), wherein depletion of Nup107-160 complex leads to assembly of pore free NE. Pom121 depletion on the other hand leads to a block in both NE and NPC assembly. Nup107-160 complex and Pom121 co-depletion leads to pore free NEs. Thus the Nup107-160 complex depletion in Pom121 depleted egg extracts

releases the affect of Pom121 depletion. Thus pores don't assemble which would be disastrous for the cell. The next sub-complex that steps in is Nup93 (Bodoor K et al., 1999). Nup53 binds Ndc1 and Nup155 binds Pom121, both acting as mechanisms of linking the pore membrane to soluble nucleoporins (Mitchell et al., 2011). Nup93-Nup188 and Nup93-Nup205 are recruited as separate complexes to the assembling NPC (Theerthagiri et al., 2010). Nup93 can then recruit the Nup62 complex (Dultz et al., 2008). At this point the first functional import intermediate is established. At the same time Nup98 is also recruited to the pore. Then as the last steps peripheral nucleoporins like Nup214, TPR (Hase et al., 2003), large fractions of Nup153, Nup50, and Gp210 are recruited. These nucleoporins are not essential for NPC assembly and nuclear import (Bodoor K et al., 1999; Burke and Ellenberg, 2002).

Thus post-mitotic NPC assembly is an example of a self-assembly process, which is well coordinated, regulated and occurs in a stepwise fashion. It can be summarized in four basic steps that are 1. The pre-pore formation on chromatin. 2. Membrane association. 3. NPC core component assembly. 4. Peripheral nucleoporins recruitment. Figure 1.7 shows various molecular players and structural and functional changes occurring during post-mitotic NPC assembly.

Figure 1.7: Nuclear envelope and post-mitotic nuclear pore complex assembly. a) the images show HeLa cells in which the inner nuclear membrane (INM, green), deoxyribonucleic acid (blue) and microtubules (red; stained by red fluorescent protein–alpha-tubulin) are visualized in early anaphase, late anaphase and telophase. Scale bars, 10 μm. b) Nuclear pore complex (NPC) assembly is initiated during anaphase by the recruitment of nucleoporin Nup107–160 complexes via Mel28-ELYS to chromatin, resulting in the formation of chromatin-bound pre-pores. During late anaphase, endoplasmic reticulum membrane tubules start binding to the chromatin surface. During telophase, the retraction of membrane-bending proteins (reticulons) into the peripheral endoplasmic reticulum allows the remodeling of endoplasmic reticulum, tubules to flattened membrane sheets on the chromatin surface. Binding of inner nuclear membrane proteins to deoxyribonucleic acid/chromatin supports the attachment of membrane sheets to chromatin. Nuclear pore complex formation occurs in a step-wise fashion by recruitment of further nuclear pore complex components and the nuclear envelope (NE) is sealed. Finally, transport-competent nuclear pore complexes allow for the nuclear import of lamins completing the assembly of the nuclear lamina. MTOC: microtubule-organizing centre. Adapted from Güttinger et al., 2009.

1.3.4.2. Interphase nuclear pore complex assembly

In interphase the NPCs double to prepare for new cell division. In this mode of assembly the NPCs have to assemble and insert into an intact NE. The interphase NPC assembly is not that well understood and the important molecular players and the molecular mechanism involved is also in its infancy in terms of the understanding. It's speculated that post-mitotic and interphase NPC assemblies have distinct requirements and occur via different mechanisms. Different models, which have been proposed, are a pre-pore model like the post-mitotic NPC assembly. Another is splitting and growth and third is the membrane fusion model (see figure 1.8 for representation of different models, for review see Rabut et al., 2004). Pre-pore model is not favored as it will be disastrous for the cell to locally disassemble its NE to allow for pre-pore formation and then re-growth of ER cisternae. The fusion model is a more likely scenario wherein the ONM and the INM come in close proximity and fuse to form holes where the NPCs then reside. The factors that mediate the membrane fusion are not really known. Some candidates to test in this regard

are the TM nucleoporins like Pom121 and Ndc1. It has recently been shown that Pom121 and the membrane curvature sensing domain of Nup133 (member of the Nup107-160 complex) is essential for interphase NPC assembly and none of these components was needed for post-mitotic NPC formation. Interestingly, recruitment of the Nup107-160 complex to new assembly sites in interphase does not involve Mel28-ELYS, which was shown to be specifically required for its recruitment to chromatin at the end of mitosis (Doucet et al., 2010). Also Pom121 and SUN domain proteins are essential and mediate initial steps of interphase NPC assembly (Talamas et al., 2011). It was also shown by our lab that the C-terminal membrane binding and bending domain of Nup53 is essential for interphase NPC assembly. These findings open up a plethora of questions to investigate interphase NPC assembly in further detail.
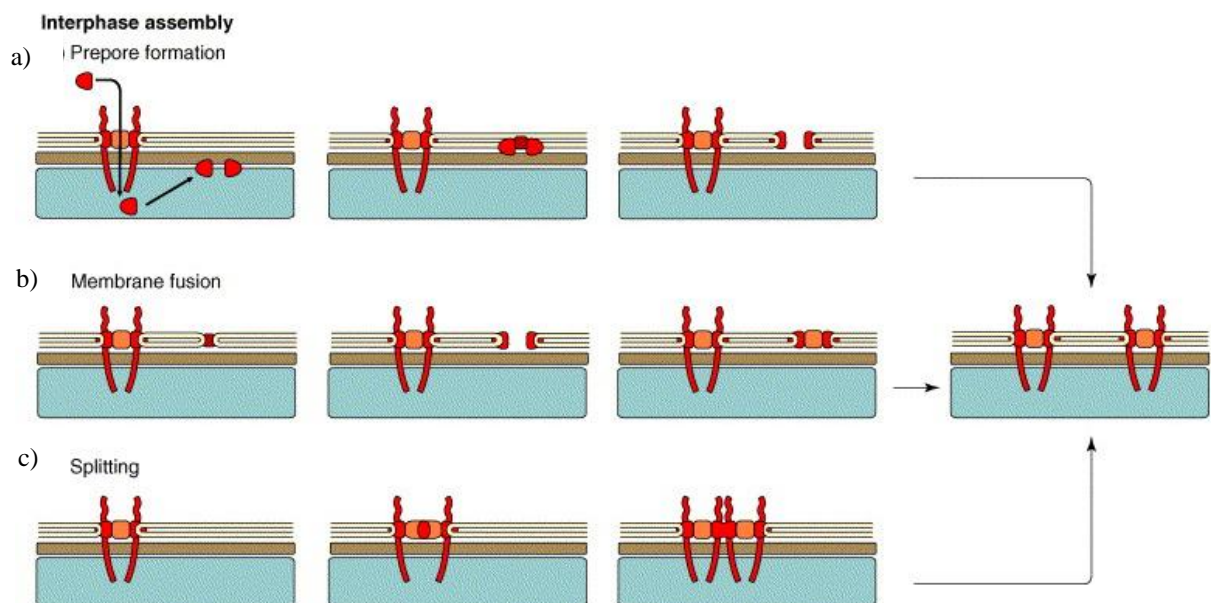
Figure 1.8: Models for nuclear pore complex assembly in interphase. a) Shows the pre-pore model where pre pore formation requires import of scaffold nucleoporins and insertion of nuclear pore complex seed into the nuclear envelope. b) Shows the membrane fusion mechanism. c) New nuclear pore complexes can form by splitting of pre existing complex. Red: nucleoporins, yellow: membranes, blue: chromatin and brown: nuclear lamina. Adapted from Rabut et al., 2004.

1.3.5. Nuclear envelope and nuclear pore complex disassembly.

In animals undergoing open mitosis the NE and the NPC have to disassemble in order to allow the spindle machinery to access the chromosomes. This occurs in late prophase. NE and NPC disassembly are regulated and coordinated processes that occur in a stepwise manner. NEBD can be dissected into various steps, NPC disassembly, depolymerization of nuclear lamina and clearance of NE membrane and INM proteins from the chromatin. NPC disassembly has shown to be simply not a reversal for NPC assembly; it rather has a distinct mechanism and takes minutes to complete. NPC disassembly starts with the dispersal of soluble nucleoporins released as stable mitotic sub-complexes or as individual nucleoporins. Upon NPC disassembly the permeability barrier of the pore is lost and intermixing of nuclear and cytosolic contents starts to occur (Terasaki M et al., 2001; Dultz et al., 2008; Katsani et al., 2008). It has been shown that the first rate-limiting step in NPC disassembly is the dispersal of the peripheral FG repeat containing nucleoporin Nup98 and this act as a rate-limiting step for NPC disassembly. It is released from the NPC via a phosphorylation dependent mechanism. Microtubule dependent tearing also assists in NEBD (Salina et al., 2002; Beaudouin et al., 2002), which leads to formation of holes on distal side of the nucleus. This also leads to mechanical shearing and stretching of nuclear lamina causing NE fenestrae. INM proteins also detach from the nuclear lamia and chromatin thereby retracting into the membrane system of the ER. Phosphorylation of nucleoporins, NE components, nuclear lamina etc is controlled and regulated by mitotic kinases like Cdk1, PLK1, PKC, NIMA etc. A number of nucleoporins, lamins and INM proteins like Nup107, Nup53, Nup98, Ndc1, Gp210 Lap2 alpha and beta and LBR are targets of the mitotic regulator kinase, Cdk1 (Favreau et al., 1996; Macaulay et al., 1995; Glavy J.S. et al., 2007; Blethrow et al., 2008; Mansfeld et al., 2006; Dechat T et al., 1998; Courvain et al., 1992). Nup98 was shown to be phosphorylated in mitosis at 13 sites by multiple kinases: PLK1, PKC, Cdk1, NIMA and this were a major trigger for NPC disassembly (Laurell et al., 2011). Figure 1.9 shows various molecular players and structural and functional changes occurring during NE/NPC disassembly.
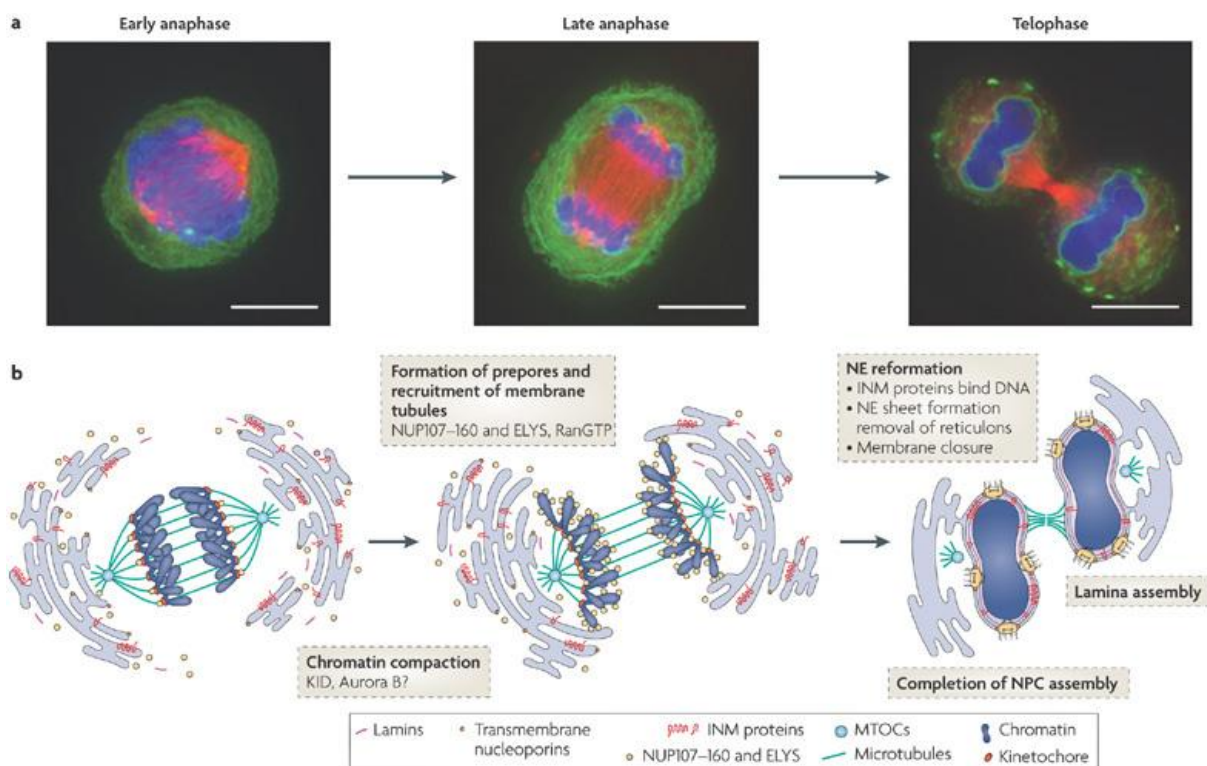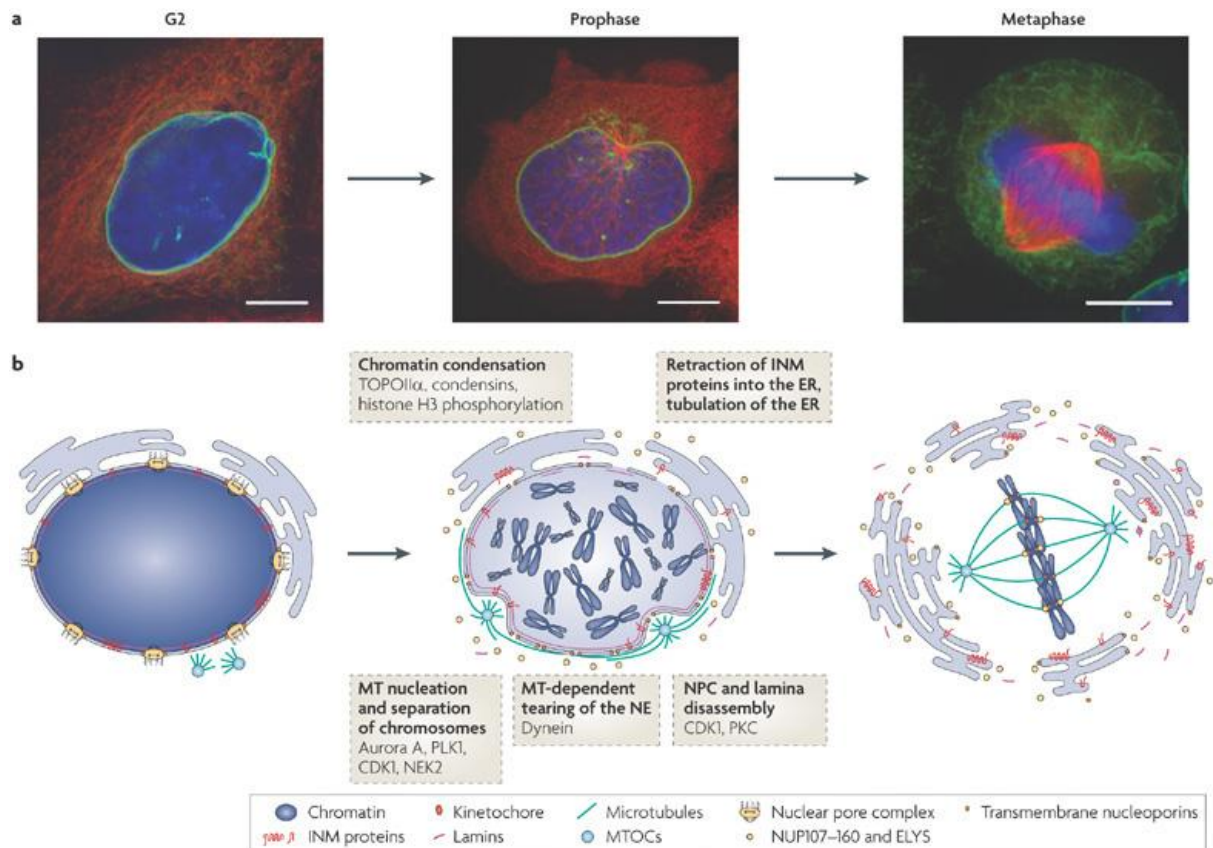
Figure 1.9: Nuclear envelope and nuclear pore complex disassembly in open mitosis. a) The images show HeLa cells in which the inner nuclear membrane (INM, green), deoxyribonucleic acid (blue) and microtubules (red; stained by red fluorescent protein–α-tubulin) are visualized in G2, prophase and metaphase. Scale bars, 10 μm. b) At the end of G2 phase, the activation of mitotic kinases, like cyclin-dependent kinase 1 (Cdk1), guides the entry into prophase, which is associated with plethora of events that include the start of chromatin condensation, formation of microtubule asters around centrosomes and centrosome separation. Microtubules that are attached to the nuclear envelope (NE) in conjunction with dynein lead to nuclear envelope invaginations around centrosomes and to the formation of holes on the opposing site of the nuclear envelope. At the same time, nuclear pore complex disassembly starts and is triggered by the phosphorylation of nucleoporins. The transition into prometaphase is marked by the loss of the nuclear envelope permeability barrier. Phosphorylation of nuclear lamins and inner nuclear membrane proteins by cyclin dependent kinase 1, protein kinase C (PKC) and probably other kinases results in lamina disassembly and allows for the retraction of nuclear envelope membranes into the endoplasmic reticulum (ER). In metaphase, most soluble components of the nuclear envelope are dispersed throughout the cytoplasm, whereas inner

nuclear membrane proteins are re-absorbed in the tubular mitotic endoplasmic reticulum. MTOC: microtubule-organizing centre; NEK2, NimA-related kinase 2; PLK1, polo-like kinase 1; TOPOIIα, topoisomerase IIα. Adapted from Güttinger et al., 2009.

1.3.6. Regulation of nuclear pore complex assembly and disassembly.

NPC assembly is regulated both spatially and temporally. It occurs in a stepwise fashion and is coordinated with chromosome segregation and NE formation. Spatial regulation of NPC assembly occurs on chromatin and aims to prevent ectopic NPC formation in the cytosol. For temporal regulation, association of nucleoporins with chromatin starts when the chromosomes begin to segregate in anaphase (Dultz et al., 2008). Chromosome segregation triggers activation of APC (anaphase promoting complex) by the SAC (spindle assembly check point), which leads to cleavage of cohesion by seperase and initiation of anaphase. APC also promotes the transition from metaphase to anaphase by inactivation of Cdk1, the mitotic master regulator kinase by degradation of cyclin. The phosphatases then become active and release phosphorylation from mitotic proteins. A number of nucleoporins are known to be phosphorylated in mitosis like Nup107, which could regulate their chromatin binding. A candidate for the phosphatase is PP1 (for review see Moorhead et al., 2007) and likely dephosphorylates the lamins and nucleoporins at the end of mitosis. The spatial regulation for NPC assembly is provided by binding of nucleoporins to the chromatin and is regulated by the GTPase Ran and its partner importin beta. Ran in its GTP form can bind importin beta and replace the binding partner of importin beta, which controls the transport through the NPC in interphase cells and at the same time NE/NPC assembly and spindle assembly in mitosis. A number of nucleoporins are known to bind importin beta like Nup107, Nup53, Nup153, Nup358 etc. (Harel et al., 2003; Walther et al., 2003). Their binding to importin beta sequesters them and NPC assembly cannot progress, as these nucleoporins cannot bind the chromatin. This inhibition is released by a high Ran GTP gradient created near chromatin by RCC1. RCC1 itself is regulated by phsophorylation and dephsophorylation, which provides another level of regulation (Hood et al., 2007; Hutchins et al., 2004; Li et al., 2004; Ramadan et al., 2007). Ran GTP binds importin beta and then the nucleoporins are free to participate in NPC assembly on the chromatin. Other factors like ubiquitination, sumolyation, relase of Aurora B kinase from chromatin can also regulate NPC assembly. Regulation of NPC disassembly also occurs

via kinases that are active in mitosis like Cdk1, PLK1, PKC etc, which phosphorylate lamins, nucleoporins, NE membrane proteins and inner nuclear membrane proteins etc. RanGTP gradient is also known to influence NPC disassembly (Mühlhäusser et al., 07).

1.3.7. Accessory roles of nuclear pore complexes (beyond nuclear transport)

NPCs are mainly involved in nucleo-cytoplasmic transport in the cell. But many new accessory roles of NPCs are emerging where they perform distinct and specialized functions. For instance, Nup133 has shown to be involved in neural stem and progenitor cell differentiation (D'Angelo et al., 2012). Recently it was shown that in post-mitotic cells the NPCS are long lived and do not turn over, which leads to the age dependent deterioration of nucleoporins. Nup93 was identified to be one such nucleoporin, which was oxidatively damaged as cells aged (D'Angelo et al., 2010). Nucleoporins are also involved in regulating gene expression, genome organization and development of organisms (Capelson et al., 2010). Nup98, Sec13 and other FG repeat containing nucleoporins are involved in active transcriptional regulation and expression of developmentally regulated genes. Number of nucleoporins like Nup98, Nup107, Nup133, and RanBP2/Nup358 are involved in spindle assembly and located on kinetochores in mitosis (Joseph J et al., 2002). They are involved in spindle assembly check point for example Nup107 in *C. elegans* has been shown to interact with MAD1 and regulate the check point (Rodenas C et al., 2012).

1.4. Nuclear Transport

The compartmentalization of the genetic material and maintaining distinct environments of the nucleus and the cytoplasm is controlled by exchange of macromolecules between the two compartments. Histones, transcription factors and nuclear proteins are imported from the cytosol where they are synthesized and mRNA, tRNA and rRNA, which are synthesized in the nucleus upon transcription, must be exported to the cytosol to perform their necessary functions. On the other hand integral membrane proteins are synthesized in the ER and must be transported from the ER to ONM and then to the INM. The transport process is directional and a regulated event in the cell and occurs with the help of transport

receptors coupled to soluble cargos that can translocate through the NPC (for review see Suntharalingim and Wente, 2003). The soluble cargos that are <40kDa (and with a diameter of 4-5 nm) in size can freely diffuse through the NPC by passive diffusion. For molecules greater than this size range an active transport mediated by the transport receptors is required. Transport receptors bound to the cargos can interact with the FG repeat containing nucleoporins present in the central channel of the NPC. Nuclear transport of proteins and RNA begins when import or export receptors binds its cargo in cytoplasm and nucleus respectively. These complexes can then pass through the pore by active transport via interactions with the FG nucleoporins and reach their destination compartment where the respective cargos are released. The best understood example is the transport mediated by the family of importins like importin beta, which requires the small GTP binding protein Ran (Kuersten et al., 2001; Weis, 2003). Ran acts as the energy generating system in the transport pathway. The function of Ran needs Ran GEF (Ran guanine nucleotide exchange factor) that helps dissociate the GDP from Ran and then bind GTP. Ran GEF (RCC1) and Ran GAP are separated in space where RCC1 binds chromatin and interacts with the histones in the nucleus. On the other hand Ran GAP, RanBP1 and RanBP2 (Ran binding proteins) are localized on the cytoplasmic side of the NE. This separation leads to a RanGTP gradient across the nucleus with its concentration being high inside the nucleus. This feature imparts directionality to the nuclear transport process. To illustrate, an adaptor molecule like importin alpha binds the NLS (nuclear localization sequences) in the cargo. NLS and also NES (nuclear export sequences) are usually a short stretch of basic amino acids that are recognized by the transport receptors. The importin alpha can then bind importin beta and this complex translocates through the NPC where a high concentration of RanGTP leads to release of the importin beta and alpha from the cargo, which is then released in the nucleus (Fried and Kutay 2003). Ran in its GTP form can bind importin beta and hence assist in the cargo release inside the nucleus. The importin beta and RanGTP then translocate from the nucleus to the cytoplasm where the RanGTP is converted to RanGDP. The binding of RanGTP stabalizes the export complexes and release of cargo occurs once the GTP is hydrolysed and the export complex is disassembled. The exportin is then recycled back to the nucleus. Importin alpha with the help of RanGTP and the export receptor CAS is assisted back to the cytoplasm. Like importin beta an export transport recptor is CRM1, which with the help of various cofactors aids in export of various cargos from the nucleus to the cytoplasm. One major class of these cargos is proteins rich in leucine as their NES. To complete the full cycle,

RanGDP is imported back into the nucleus by the nuclear transport factor 2 (NTF2, see figure 1.10, Ribbeck et al., 1998). Alternate transport routes beside the central channel of the pore have been suggested for some substrates like the peripheral hydrophilic channel on the pore.
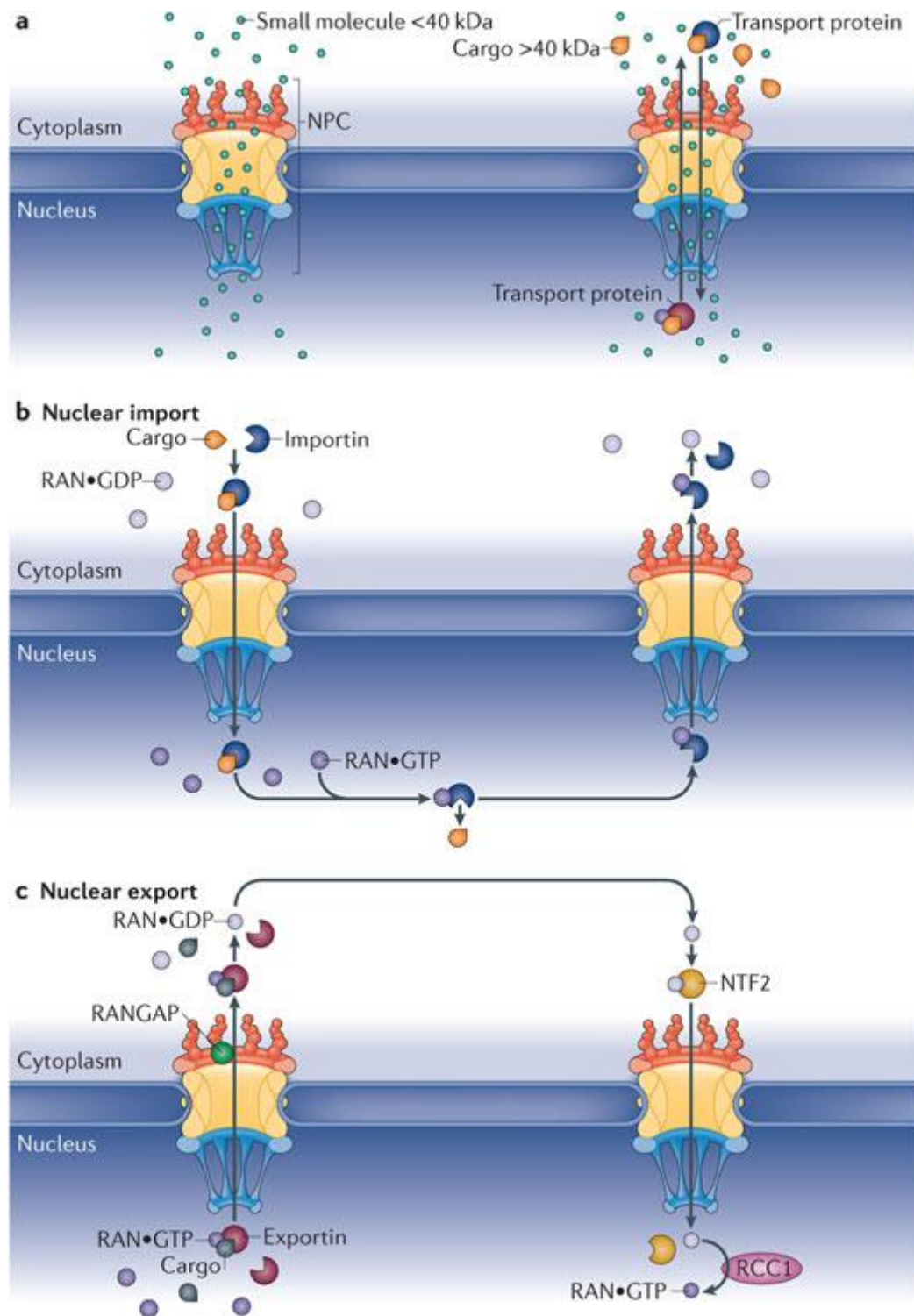
Figure 1.10: Transport of soluble cargos through the nuclear pore complex. a) Molecules smaller than 40kDa transit through the nuclear pore complex via passive diffusion. Larger cargos like mRNA and proteins bind to the nuclear transport receptors than can recognize nuclear localization sequences/nuclear export sequences. b) Nuclear import: after the binding of cargo in the cytoplasm, importins can interact with the nuclear pore complex and translocate through the central channel of the pore. Once they enter the nucleus they can bind to RanGTP that leads to cargo release. The resulting complex of importin-RanGTP translocates back to the cytoplasm. c) Nuclear export: exportins can bind the cargo and RanGTP in the nucleus and move through the nuclear pore complex to the cytoplasm. Ran GTPase activating protein (RanGAP) induces hydrolysis of GTP of Ran with the help of Ran binding protein 1 and Ran binding protein 2 at the cytoplasmic side of the nuclear envelope. RanGDP interacts with nuclear transport factor 2 (NTF-2) and translocates back to the nucleus where RCC1 can restore the RanGTP levels again to complete the transport cycle (modified from Raices et al., 2012).

1.4.1. Transport of integral membrane proteins to the inner nuclear membrane

The ER is continuous with the ONM, which is in turn continuous with the INM. The INM is characterized by a distinct protein composition and is composed of a specific set of integral membrane proteins. Thus the integral membrane protein that is synthesized in the ER need to travel to the ONM and then transported to the INM. The mechanism of this translocation is not very well understood but various models have been proposed. For example the transport to the INM could occur by a fusion between the ONM and the INM. Also budding of INM vesicles and then fusion with the ONM could establish the INM protein composition (Mettenleiter et al., 2009). Another mechanism one could envision is the diffusion of transmembrane proteins from the ONM to the NPC in the plane of the membrane (Ohba et al., 2004). Recent study from our lab showed that the nucleoporin Nup188 regulates the transport of integral membrane proteins to the INM. Upon depletion of Nup188 the nuclei grew larger in size and an accelerated targeting of INM proteins was observed. Interestingly the import of soluble cargos through the central channel was not affected. Thus this points out to the fact that the transport of soluble proteins and INM proteins probably occurs via distinct mechanisms and routes (Theerthagiri et al., 2010). Another study characterized the transport mode of the INM protein SUN2. They showed

that SUN2 contained classical NLS, which could be bound by the importin alpha and beta. SUN domain in the protein also facilitated its transport to the INM. Also arginine rich sequences in SUN2 bind COPI, which helped retrieve SUN2 from Golgi to the ER (Turgay et al., 2010; Antonin et al., 2011). Thus various mechanisms could be adopted to ensure efficient transport of the integral membrane proteins to the INM.

1.5. Experimental systems and models used to study nuclear pore complex and nuclear envelope assembly

A number of experimental systems and models have been used to study NPC and NE assembly and also translocation of molecules through the nucleus. Using cell-free extracts from eggs of *R.pipiens*, the first in vitro nuclear assembly reaction system was established (Lohka and Masui, 1983). Stockpiles of NE precursors and other nuclear proteins that permit rapid mitotic divisions upon fertilization are stored in eggs of many species. This egg extract system provides a massive amount of contents required for NE and NPC assembly, producing nuclei that can faithfully complete one or more cell division cycles in vitro. The cell cycle state of the egg extracts can be altered (interphase to mitotic and vice versa) and proteins in the extracts can be specifically depleted using antibodies allowing their functional studies and dissecting their role in NPC assembly. These advantages make the egg extracts a rich and thus a biochemically valuable source to perform in vitro nuclear assembly reactions. When sperm chromatin was incubated with egg extracts, an intact NE formed, chromatin decondensed, and DNA replication was initiated (Lohka and Masui, 1983). Cell-free extracts similarly could also be prepared from *X. laevis* eggs (Lohka and Maller, 1985) and we use these in our studies in the lab to characterize NPC assembly. *Xenopus* egg extracts can be used to make interphase or mitotic extracts to study cell cycle dependent changes. The progesterone secretion by follicle cells induces completion of meiosis I. The oocyte next enters meiosis II, which primes it for ovulation. This process can also be induced artificially by injecting female frogs with pregnant mare serum gonadotropin (PMSG). Next, the oocytes are arrested at metaphase of meiosis II, ovulate and are then ready for fertilization. Human chorionic gonadotropin (hCG) stimulates the ovulation of mature oocytes. Penetration of the egg by a sperm induces a transient cytoplasmic calcium increase, which is the trigger for release of the metaphase arrest. The

oocyte completes meiosis II, enters interphase, and starts early embryogenesis by a series of rapid mitotic cell divisions. This fertilization can be recapitulated *in vitro* by applying an electric shock or adding a calcium ionophore. In our preparation of interphase egg extracts we use calcium ionophore (A23187). This leads to release of the eggs from metaphase arrest. Egg extracts of these activated eggs will complete meiosis II and would be able to assemble the functional nucleus (Murray, 1991). These *in vitro* assembled nuclei are functional and similar to the nuclei inside the cells wherein they can perform nucleocytoplasmic transport and replicate their DNA content. (Blow and Laskey, 1986; Newmeyer et al., 1986).

Xenopus eggs can be kept arrested in metaphase II and used to generate mitotic egg extracts. In this case, the eggs are not activated by release of Calcium. Instead, EGTA (a Calcuim chelator) and phosphatase inhibitors are added to prevent dephosphorylation of cell cycle regulators. Thus the cell-free *Xenopus* egg extract system has manifold advantages and can be manipulated to dissect individual steps of complex and multi step processes. Cell lethality is not an issue in these extracts hence components can be depleted from the *Xenopus* egg extracts to understand their functional relevance through their respective phenotypes. The specificity of the observed phenotypes can also be understood by the addition of recombinant proteins to the egg extracts (Grandi et al., 1997; Harel et al., 2003; Walther et al., 2001; Walther et al., 2002; Walther et al., 2003; Antonin et al., 2005).

Synthetic lethality screens in yeast are also a valuable tool to identify essential sub complexes. (Fabre and Hurt, 1997). Genetic screens in *S cerevisiae* have been successfully employed to identify proteins involved in different transport pathways. But yeast cannot be exploited to study the proteins involved in post-mitotic NE assembly as they undergo a closed mitosis (Straube et al., 2005). In *C.elegans*, genome wide systematic RNAi knock down studies have described and grouped candidates leading to defects in pronuclear/nuclear appearance and role of nucleoporins in development can be studied. (Zipperlen et al., 2001; Colaiacovo et al., 2002; Sonnichsen et al., 2005). However, the process of NE assembly is difficult to manipulate experimentally in intact cells.

1.6. Aims of the PhD project

As part of my PhD project the aim was to functionally characterize the role of Nup93 complex in NE, as well as NPC assembly and function. I choose to study the Nup93 complex firstly because it is one of the major structural sub-complexes of the NPC. Secondly the Nup93 complex is the point of interaction of membrane proteins of the NE due to its critical positioning at the core of the NPC where the NE (pore membrane) and NPC interact. However it being such an important sub-complex in the NPC, it has not been characterized extensively. In vertebrates the Nup93 complex is composed of five nucleoporins that are: Nup205, Nup188, Nup155, Nup93 and Nup53. My focus was specifically on the role of Nup93 in NPC assembly and function. Previously in the lab it was shown that Nup93 is part of two distinct complexes: Nup93-205 and Nup93-188 (Theerthagiri et al., 2010). Immunodepletion experiments were done to deplete the Nup93-188 complex from *Xenopus laevis* egg extracts using anti Nup188 antibody. No block in NE or NPC assembly was observed and most of the NPC functions were normal. In another experiment the Nup93-205 complex was immunodepleted from *Xenopus laevis* egg extracts using anti Nup205 antibody. As before no block in NE and NPC assembly was observed and all of the NPC functions were intact (Theerthagiri et al., 2010). I wanted to know what the consequences are if both the Nup93-188 and Nup93-205 complexes are depleted together. Then I wanted to check for NE, NPC assembly and functions. I was curious to know whether Nup188 and Nup205 together are not essential for NPC assembly and if they have redundant functions in the pore.

To answer these questions we raised antibody against the common protein of the two complexes that is Nup93. The idea was to immunodeplete Nup93, Nup188 and Nup205 together from the egg extracts using anti Nup93 antibody and then use these extracts for in vitro nuclear assembly reactions to study NE, NPC assembly and functions. The nuclei would be analyzed using various biochemical, cell biological and microscopic assays to elucidate the role of these nucleoporins in NPC assembly, function and nucleocytoplasmic transport. We also planned to add back recombinant Nup93 to the nuclei assembled with Nup93 depleted extracts and see if Nup93 itself is essential and sufficient to rescue NE and NPC assembly and whether or not it can compensate for the loss of Nup188 and Nup205 from the pore. This would also explain if Nup188 and Nup205 together are essential in NPC assembly and function. If it turns out that Nup93 is essential for NPC assembly we

would go into more detail to analyze different domains of Nup93 and dissect their contribution in NPC assembly and function.

2. RESULTS

Contributions

The experiments shown in the results section are performed by me. The designing and data analysis of the experiments was done together with Dr. Wolfram Antonin. Cornelia Sieverding helped with the cloning of the DNA constructs used in this study. Matthias Flötenmeyer assisted me with the electron microscopy experiments.

2.1. The C-terminal domain of Nup93 is essential for assembly of the structural backbone of the nuclear pore complexes.

2.1.1. Generating the tools.

Nup93 being a common nucleoporin found between both the Nup93-205 and Nup93-188 complexes we decided to immunodeplete Nup93 from *Xenopus laevis* egg extracts and perform in vitro nuclear assembly reactions to study the role of Nup93, Nup188 and Nup205 in NPC assembly and function. For this we raised antibody against Nup93. We used an N- terminal fragment of Nup93 (aa 1-230). The protein was expressed and purified from *E.coli* and the polyclonal antibody was generated in rabbits. The antiserum was tested for the recognition of Nup93 in *Xenopus laevis* egg extracts (cytosol) by western blot. Nup93 antiserum successfully detected the *Xenopus leavis* Nup93. A double band was observed: one at 93kDa and another at 95kDa as shown in fig. 2.1. The slower migrating band was a cross reactivity with another protein in the *Xenopus laevis* egg cytosol as this band was lost when we did an immune precipitation (IP) of Nup93 or upon depletion of Nup93 from the extracts. For the detection of Nup188 and Nup205 our lab already had working antibodies.
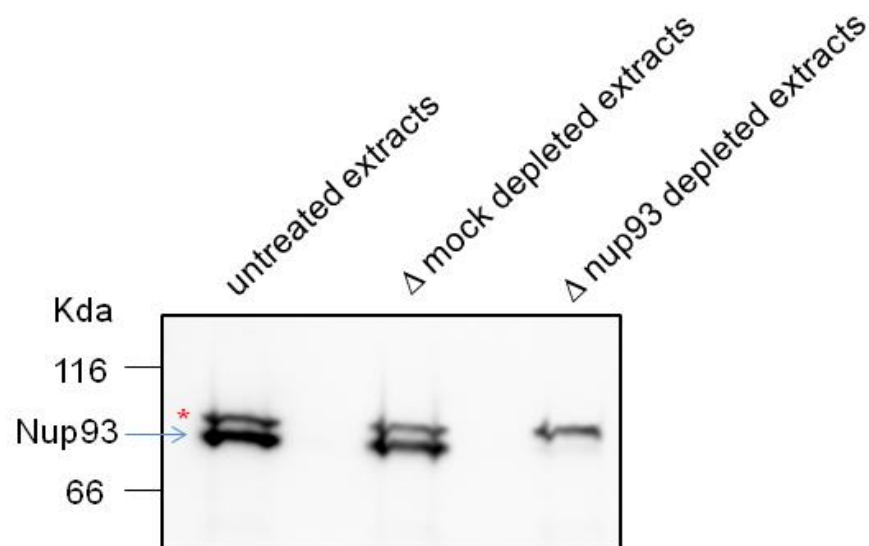
Figure 2.1: The Nup93 antibody recognizes the Xenopus laevis Nup93. Western blot analysis of untreated, mock depleted and Nup93 depleted extracts respectively. The Nup93 antibody recognized a slightly lower migrating cross reactivity (* asterisks), which was not

immunodepleted from *Xenopus laevis* egg extracts upon Nup93 depletion although we observed a double band in the mock depleted and untreated extracts. This showed that the other band was cross-reactive and the Nup93 band was specifically lost upon Nup93 immunodepletion from the egg extracts. On the left the kDa refers to the low molecular weight marker bands.

2.1.2. Nup93 is efficiently depleted from *Xenopus laevis* egg cytosol.

It was previously shown in our lab that Nup93 is part of two distinct complexes: Nup93-205 and Nup93-188 (Theerthagiri et al., 2010) and that none of the complexes individually are essential for NE and NPC formation. In order to elucidate the functional significance of these two complexes I decided to deplete both the complexes together by immunodepleting Nup93 from *Xenopus leavis* egg cytosol. The eggs from *Xenopus laevis* are known to be a storehouse of disassembled NE components and nuclear proteins (Murray, 1991; New Meyer et al., 1991). The eggs contained the cytosol, which is highly active in nature and hence can give rise to a large number of functional nuclei. Thus to immunodeplete all of the specific proteins from the cytosol one requires stringent depletion conditions (that is high amount of antibodies) due to large quantity of nucleoporins. Due to this we could not deplete Nup188 and Nup205 together using a combination of anti Nup188 and anti Nup205 antibodies. This would be technically very challenging and require four rounds of immunodepletion after which the harshly treated extracts would fail to assemble proper nuclei even in the case of a mock depletion. To surmount this constraint we generated antibodies against Nup93, which is a common member between of two complexes. We purified a large quantity of Nup93 antibody by affinity purification and then covalently coupled it to protein A sepharose beads. Before using the beads for the depletion of Nup93 from the egg cytosol the beads were blocked with bovine serum albumin (BSA) to prevent the binding of non-specific proteins from the egg extracts. The cytosol was then incubated with protein A sepharose beads that were coupled to Nup93 antibody for two rounds to efficiently immunodeplete Nup93, Nup188 and Nup205. The ratio of bead: cytosol was 1:1.2. In case of mock depletion the cytosol was incubated (two rounds) with protein A sepharose beads coupled to rabbit IgG in the same ratio as for Nup93 depletion. We were able to efficiently immunodeplete Nup93 from *Xenopus laevis* egg extracts as shown in the western blot in fig. 2.2 (please note that the slower migrating band (*) is cross reactivity). The mock depletion showed normal levels of Nup93 comparable to the untreated extracts

(see the start lane in fig 2.2). The interacting partners of Nup93, Nup205 and Nup188, were both efficiently co depleted. The levels of other nucleoporins that are members of the Nup93 complex, Nup53 and Nup155, were not altered upon Nup93 depletion. We also checked for the specificity of depletion for Nup93 by inspecting the levels of nucleoporins, which belong to different, unrelated complexes like Nup62, Nup98 and Nup160 by western blot. Their levels were not changed upon Nup93 depletion (levels are comparable to mock and untreated extracts: fig.2.2). Hence we could specifically and efficiently immunodeplete Nup93, Nup188 and Nup205 from *Xenopus laevis* egg extracts using anti Nup93 antibody.
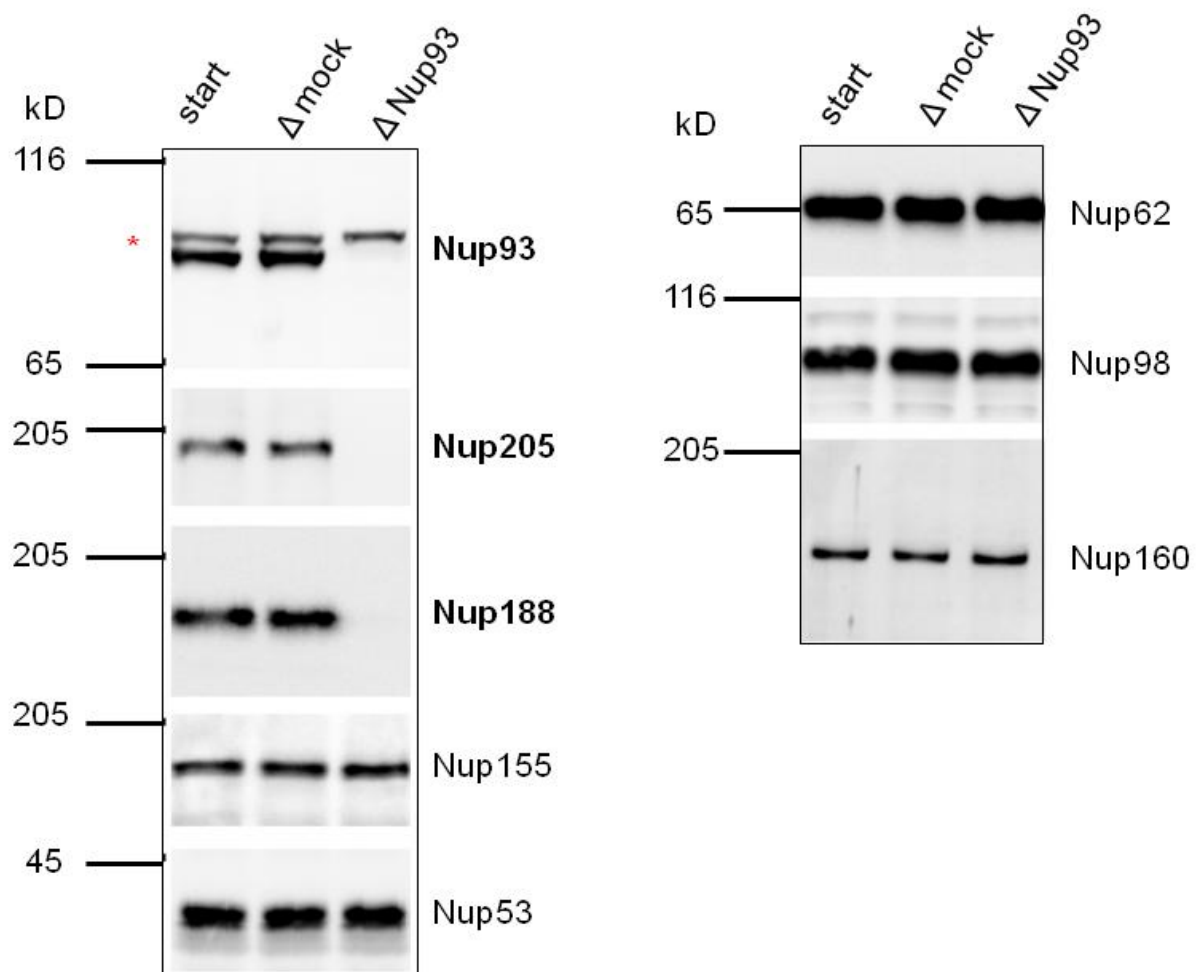
Figure 2.2: Nup93 is efficiently depleted from Xenopus laevis egg extracts. Western blot analysis of untreated, mock and Nup93 depleted (Δ Nup93) extracts respectively. As shown before the Nup93 antibody recognized a slightly lower migrating cross reactivity by western blotting (* asterisk), which was not depleted. The western blot showed that Nup93 was efficiently immunodepleted from the egg extracts. The interacting partners of Nup93 that is Nup188 and Nup205 were also efficiently co-depleted as seen by their absence in

ΔNup93 lane in the western blot. Levels of other members of the Nup93 complex, Nup155 and Nup53, were not affected upon Nup93 depletion. The levels of unrelated nucleoporins like Nup62, Nup98 and Nup160 were also not altered upon Nup93 depletion as seen by the equal band intensity for these nucleoporins in all the lanes as depicted in the western blot.

2.1.3. Nup93 is essential for NE formation.

Next we were interested to find out the consequences of Nup93 depletion on NE assembly. For this both the mock and Nup93 depleted extracts were immediately used to perform in vitro nuclear assembly reactions as freezing of extracts leads to a drop in activity of the proteins present in them. Using the power of *Xenopus leavis* egg extracts system functional nuclei can be assembled in vitro by incubating the extracts with DNA (in our case sperm DNA) and membranes (both from *Xenopus laevis*). This reaction was done for 90 minutes using both Nup93 depleted and mock depleted extracts. In case of the nuclei assembled using mock depleted egg extracts we observed a normal NE formation (red staining of membranes by DilC18 dye). The membrane showed a smooth staining and the NE was closed (fig. 2.3A). On the other hand in case of nuclei assembled using Nup93 depleted extracts we observed a block in NE formation wherein the membrane vesicles were docked on to the chromatin (DAPI-blue) but they did not fuse to form a closed NE. Also in the mock depleted nuclei the chromatin decondensed over time but in case of Nup93 depleted nuclei the chromatin did not fully decondense (fig. 2.3A). Grandi et al., 1997, also observed this phenotype. Such phenotype has also been shown for other nucleoporins essential for NE and NPC formation (Franz et al., 2005; Hawryluk-Gara et al., 2008) where discontinuous membrane staining is observed if there is a block in NE formation. We also quantified the nuclei showing a closed NE assembled with either mock or Nup93 depleted extracts (fig. 2.3B). As shown approx. 90% of the nuclei assembled with mock depleted extracts had a closed NE as opposed to roughly 5% or so in the case of nuclei assembled using Nup93 depleted extracts which is represented in the bar graph below.

(A)

(B)
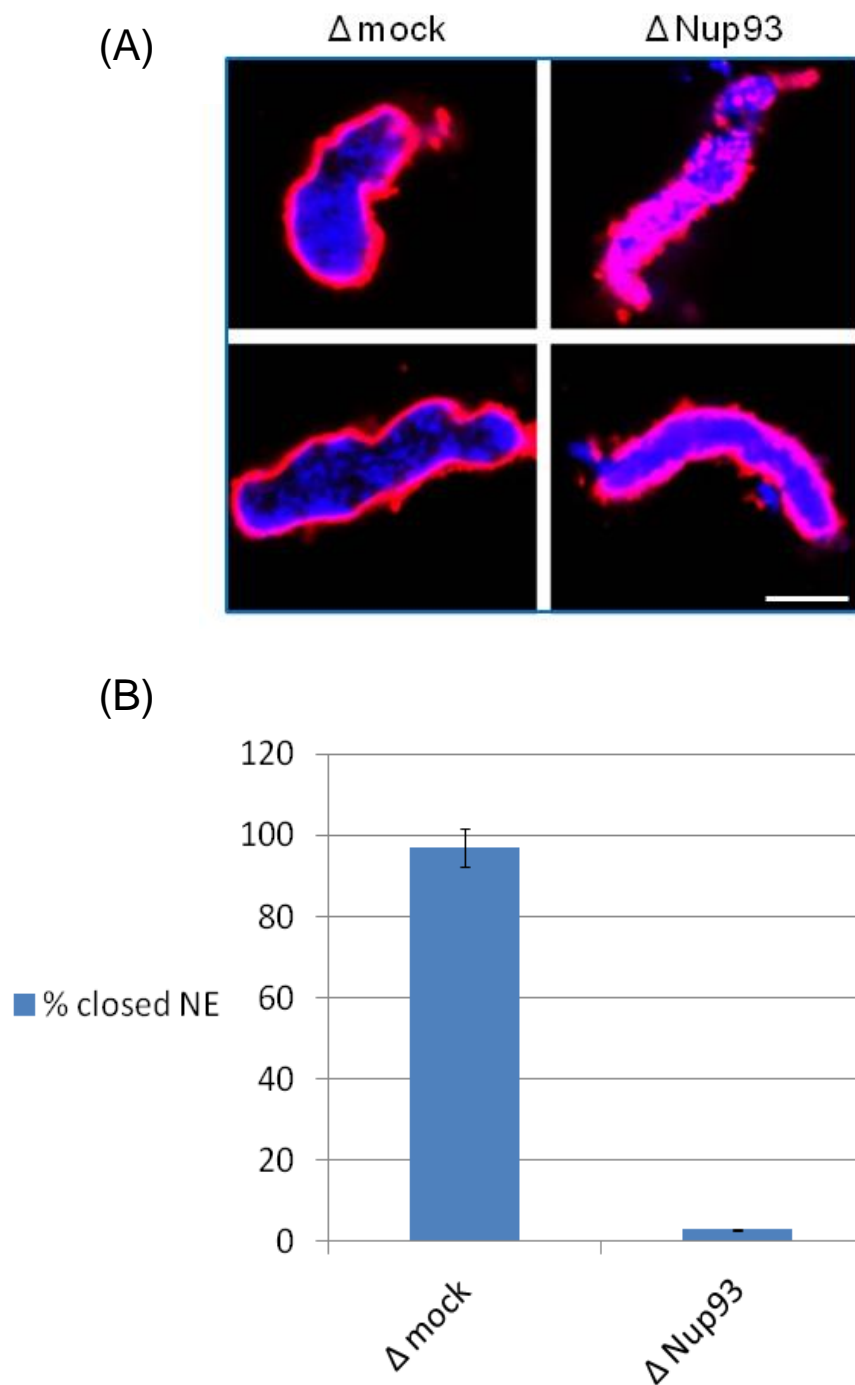
Figure 2.3: Nup93 is essential for nuclear envelope assembly. (A) Nuclei were assembled in vitro using mock and Nup93 depleted extracts for 90 minutes. The nuclei were fixed with 2% paraformaldehyde (PFA) + 0.5% glutaraldehyde. Chromatin was stained using DAPI (4'6-diamidino-2-phenylindole-Blue) and membrane staining was done using the red dye DilC18. As shown, the mock depleted nuclei had a closed and a smooth nuclear envelope (NE) as opposed to a block observed in NE formation upon Nup93 depletion (discontinuous membrane staining). Bar: 10µm. (B) The number of nuclei or chromatin substrates were quantified for the NE assembly reactions done in (A). For one condition

more than 100 randomly chosen chromatin substrates or nuclei were counted. An average of three independent experiments was calculated as shown in the bar graph. The error bars represent the total variation observed. The counting of closed NE was based on the DilC18 membrane staining.

2.1.4. Add back of full-length recombinant Nup93 can rescue the block in NE assembly.

As mentioned before depletion of Nup93 from *Xenopus laevis* egg extracts lead to a block in NE formation, however this phenotype observed could be due to two courses of events. (a) a direct result of Nup93 depletion or (b) as a result of co depletion of the interacting partners of Nup93, Nup205 and Nup188. To discriminate between these two situations we performed add back experiments using recombinant Nup93. To start with we used the full-length recombinant protein (aa 1-820) that was expressed and purified from *E.coli*. The full-length Nup93 was added back at approx. endogenous levels to Nup93 depleted extracts as detected by the western blot (see lane Nup93 add back in fig. 2.4A). To see if the full-length recombinant Nup93 added back could rescue the block in NE formation, we did in vitro nuclear assembly reactions with mock depleted, Nup93 depleted and Nup93 depleted extracts supplemented with full-length Nup93 as described before. The Nup93 was added back to Nup93 depleted extracts at the very beginning of nuclear assembly reactions and incubated with sperm chromatin and DilC18 labeled membranes for 90 mins. In case of nuclei assembled with mock depleted extracts the NE formation was normal as seen by a closed NE and smooth membrane staining. The chromatin also decondensed over the reaction time. As observed before in case of nuclei assembled with Nup93 depleted extracts the NE formation was blocked. When full-length recombinant Nup93 was added back we observed formation of a closed NE, as detected by the smooth membrane staining (red DilC18 staining) and decondensed chromatin (blue DAPI staining in fig. 2.4B). Hence in this case the membranes docked on to the chromatin and fused to form a smooth and closed NE. By this we concluded that the full-length Nup93 that was added back to Nup93 depleted extracts could rescue the block in NE formation (fig. 24B). It is interesting to note that the nuclei formed upon re -addition of full-length recombinant Nup93 are larger in size as compared to nuclei assembled using mock depleted extracts or Nup93 depleted nuclei. We also quantified the nuclei having a closed NE (inferred from DilC18 membrane

stain) in all the aforementioned situations as shown in the bar graph in fig. 2.4C, which fits to our observations explained above.

(A)

(B)

(C)
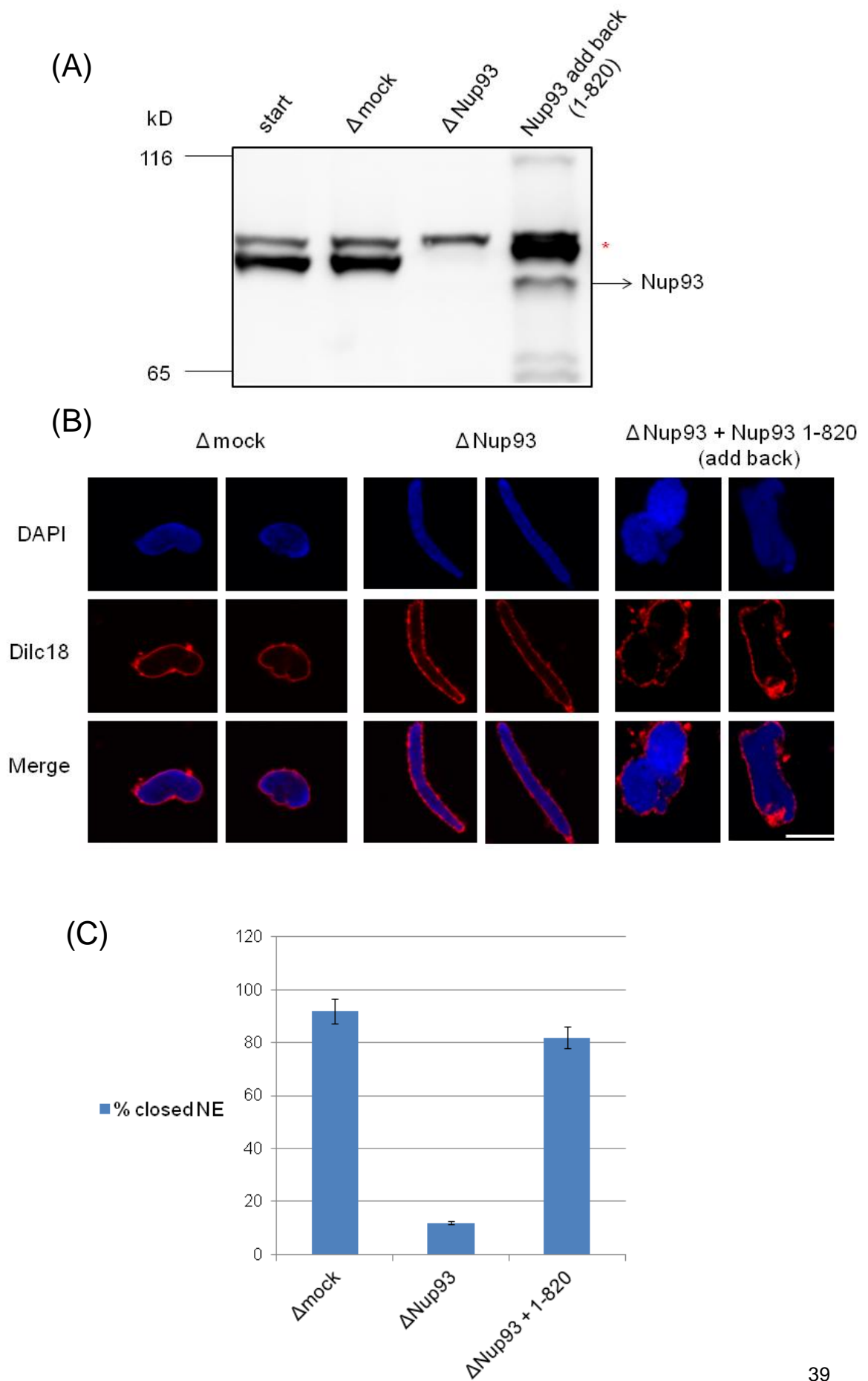
Figure 2.4: Add back of full-length recombinant Nup93 can rescue the block in nuclear envelope formation. (A) Western blot analysis of untreated, mock, Nup93 depleted and Nup93 depleted (supplemented with full-length recombinant Nup93) extracts that is referred as add back. The Nup93 was efficiently depleted from the egg extracts. The recombinant Nup93 was added back at endogenous levels to Nup93 depleted extracts. Please note that the recombinant Nup93 protein migrates little slowly than the endogenous Nup93 probably due to post-translational modifications that were missing when the recombinant protein was expressed and purified from E.coli. The western blot shown here is part of the same figure 2.2 (A). (B) Nuclei were assembled in vitro using mock, Nup93 depleted and Nup93 depleted (supplemented with the addition of recombinant full-length Nup93) extracts for 90 minutes. The nuclei were fixed with 2% PFA +0.5% glutaraldehyde. DNA was stained using DAPI and membranes were visualized using the red dye DilC18. As shown in the figure nuclei assembled using mock depleted extracts had a closed NE. Nuclei assembled using Nup93 depleted extracts had a block in NE formation. When the full-length recombinant Nup93 was added, the nuclei could rescue the block in NE assembly as seen by a smooth, continuous DilC18 membrane staining. Bar: 10μm. (C) The number of nuclei having a closed NE under all conditions (mock, Nup93 and Nup93 depleted extracts (supplemented with the full-length Nup93) were quantified. For each sample more than 100 randomly chosen substrates or nuclei were counted. An average of three independent experiments was calculated as shown in the bar diagram. The error bars represent the total variation observed. The counting was based on the judgment of a closed NE observed by the staining of the membrane dye DilC18.

2.1.5. Nup93 is essential for NPC assembly.

The next question that we asked was whether Nup93 is essential for NPC formation? To monitor NPC assembly we used an antibody called mab414 which is a commonly used mouse monoclonal antibody that recognizes four different FG repeat containing nucleoporins that localize to different regions of the pore and hence it is widely used as a marker for NPCs. As before we did in vitro nuclear assembly reactions with mock depleted, Nup93 depleted and Nup93 depleted extracts that were supplemented with full-length recombinant Nup93. The nuclei that were formed after 90 minutes were further processed for immunoflorescence (IF) with mab414 antibody to check for NPC assembly

or with Nup93 antibody to check the efficiency of Nup93 depletion and to check for the localization of the full-length Nup93 that was added back. As seen in fig. 2.5 in case of nuclei assembled with mock depleted extracts we observed a rim staining for mab414 showing normal NPC formation. The same rim staining was observed with anti Nup93 antibody suggesting that the endogenous Nup93 gets incorporated into the assembling NPCs. In case of nuclei assembled with Nup93 depleted extracts, no specific rim staining was observed for mab414. We observed no staining for Nup93 in these nuclei proving that Nup93 was efficiently depleted from extracts. Similar reduction of mab414 staining has been seen in HeLa cells upon RNAi of Nup93 (Krull et al., 2004). In case of nuclei assembled with Nup93 depleted extracts supplemented with added back full length recombinant Nup93 we observed a smooth nuclear rim staining for mab414 suggesting that NPC assembly is rescued upon re- addition of Nup93 and that Nup93 is essential for NPC assembly. We also observed Nup93 staining at the nuclear rim supporting the fact that the Nup93 that was added back is functional and can faithfully integrate into the assembling NPC.

Taken all together with the data we had so far we concluded that Nup93 was essential for NE and NPC formation at the end of mitosis.
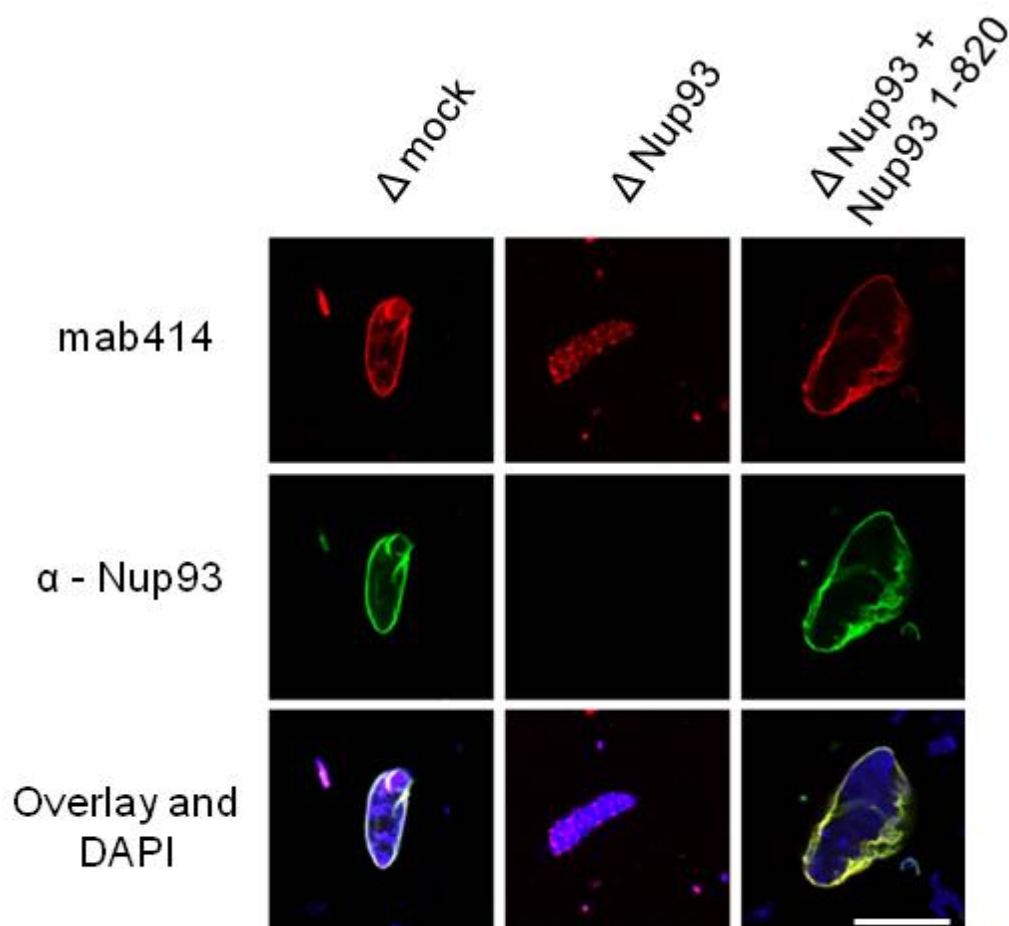
Figure 2.5: Nup93 is essential for nuclear pore complex assembly. Nuclei were assembled using mock depleted, Nup93 depleted and Nup93 depleted (supplemented with full length recombinant Nup93) extracts for 90 minutes. The nuclei were fixed with 4% PFA and analyzed with Nup93 antibody (green) and mab414 antibody (red), which recognizes FG repeat containing nucleoporins. The chromatin was stained using DAPI (blue). Scale bar: 10μm. As shown, in the nuclei where Nup93 was depleted, we observed no staining for Nup93 and a faint chromatin staining for mab414 suggesting that Nup93 depletion was efficient and lead to a block in NPC assembly. Upon addition of full-length recombinant Nup93 we observed a rim staining for both Nup93 and mab414, suggesting that the addition of full-length recombinant Nup93 rescued the block NPC assembly and the Nup93 added back could faithfully integrate into the assembling NPCs. Note the differences observed in the chromatin decondensation observed via DAPI staining.

2.1.6. Nup205 and Nup188 together are not essential for NE and NPC assembly.

We then wanted to check for Nup188 and Nup205 in different depletion and add back scenarios using IF. As explained before we assembled nuclei in vitro with mock depleted, Nup93 depleted and Nup93 depleted extracts supplemented with full-length recombinant Nup93. In case of nuclei assembled with mock depleted extracts we observed a nuclear rim staining for both Nup205 and Nup188 suggesting that the endogenous proteins were integrated into the assembling NPCs. In case of nuclei assembled with Nup93 depleted extracts we observed no staining for Nup205 and Nup188 suggesting that both the nucleoporins were efficiently codepleted from the extracts upon Nup93 depletion. In case of nuclei assembled with Nup93 depleted extracts that were supplemented with full length added back Nup93 we observed no staining for both Nup205 and Nup188 but as before we did observe a nuclear rim staining for mab414 and Nup93 (fig.2.6). Hence the rescue of Nup93 depletion phenotype upon addition of recombinant Nup93 could not be assigned to the residual levels of Nup205 and/or Nup188 that might be left over in the extracts upon Nup93 depletion. If that was the case then recombinant Nup93 added back could have formed a complex with residual Nup188 and/or Nup205, which would have shown a staining in IF. Hence Nup205 and Nup188 together are not essential for NE and NPC formation. On the other hand Nup93 was crucial for both NE and NPC assembly. It was indeed surprising that NE and NPC assembly could occur normally in the absence of two

major components of the Nup93 sub-complex, Nup205 and Nup188. In fact Nup93 alone was essential and sufficient to compensate for the loss of Nup93-205 and Nup93-188 complexes.
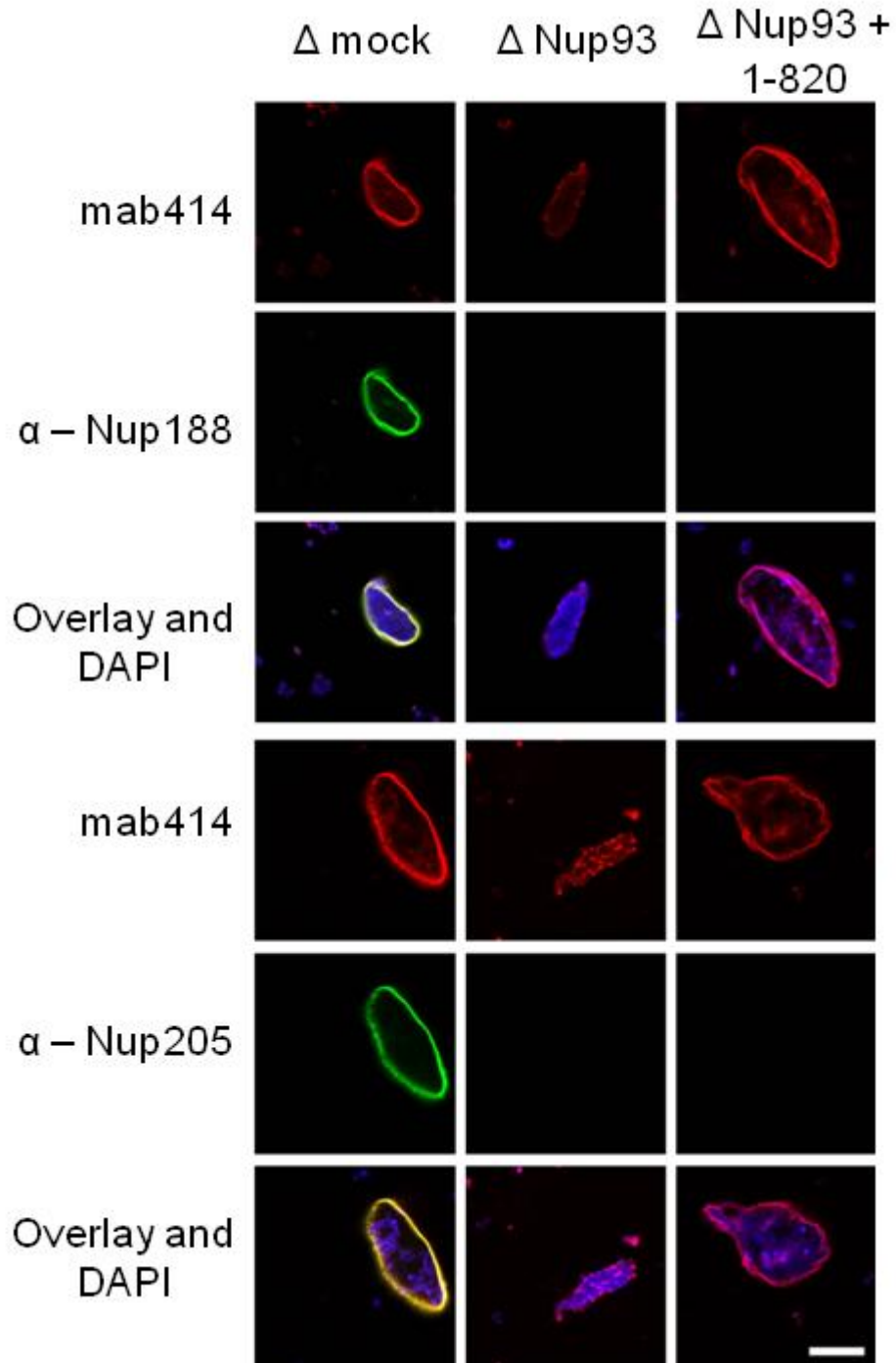
Figure 2.6: Nup205 and Nup188 are together not essential for nuclear pore complex assembly. Nuclei were assembled using mock depleted, Nup93 depleted and Nup93 depleted (supplemented with full-length Nup93: add back) extracts for 90 minutes. The nuclei were then fixed with 4% PFA and analyzed with Nup188 and Nup205 antibody

(both green) and mab414 antibody (red). Mab414 recognizes a set of FG repeat containing nucleoporins. Chromatin was stained using DAPI (blue). Scale bar: 10µm. This is the same experiment and part of figure 2.5. As shown in the ΔNup93 panel both Nup188 and Nup205 are efficiently depleted as seen by absence of staining as oppose to mock depleted nuclei where we observe a rim staining for both mab414 and Nup188/Nup205. Hence both Nup188 and Nup205 were not essential for NPC assembly as add back of Nup93 alone restores NPC formation (see mab414 red staining).

2.1.7. Transmission electron micrographs (TEM) reveal a closed NE in nuclei assembled using add back of the full-length recombinant Nup93.

To confirm that the re-addition of Nup93 (full length recombinant protein) to Nup93 depleted extracts lead to the formation of nuclei with a closed NE we did transmission electron microscopy (TEM) on these nuclei. Shown in fig. 2.7 is the TEM view of nuclei that were assembled with mock depleted, Nup93 depleted and Nup93 depleted extracts supplemented with full length Nup93 to compare the morphology of the nuclei assembled using differently treated extracts. In case of the mock sample we observed a closed NE. In the nuclei where Nup93 was depleted NE formation was blocked hence we observed a NE that was not closed. But in case of nuclei where the full length recombinant Nup93 was added back a closed NE was observed and the block in NE formation was rescued supporting the view that Nup93 is essential for formation of a closed NE at the end of mitosis. As before we observed that the size of nuclei where full length Nup93 was added back was much larger than nuclei assembled using mock or Nup93 depleted extracts.
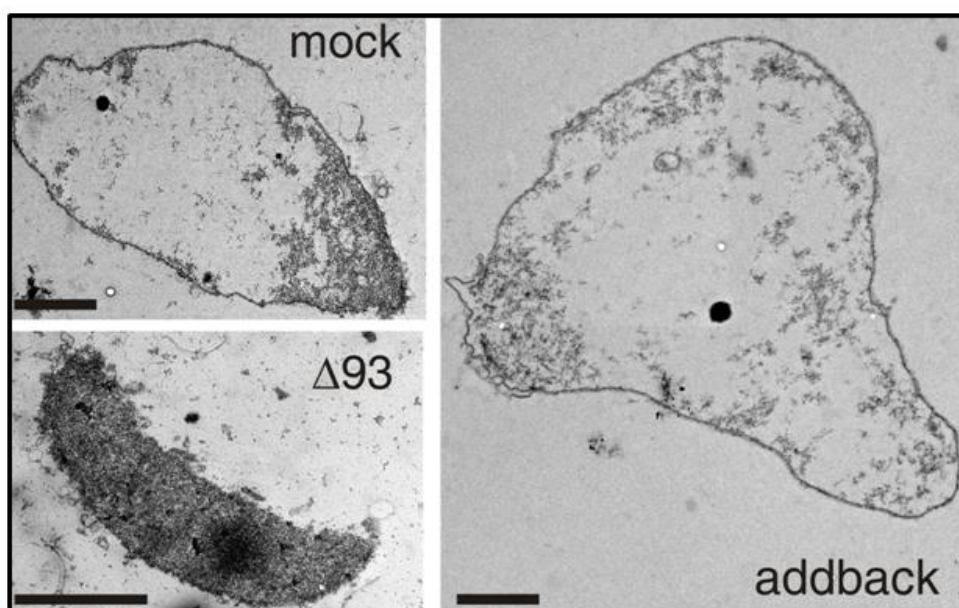
Figure 2.7: Nuclear envelope formation is restored upon re-addition of full-length recombinant Nup93 as visualized by transmission electron microscopy. Transmission electron micrographs of nuclei assembled using mock depleted, Nup93 depleted and Nup93 depleted (supplemented with full-length Nup93) extracts was done after the nuclei were assembled for 90 minutes and fixed as before. We observed a closed NE in nuclei assembled using mock depleted extracts. Upon depletion of Nup93 the nuclei no longer had a closed NE as seen by TEM. This was rescued with the addition of full-length Nup93 as we observed a closed NE. Bar: 2μm.

2.1.8. Composition of nuclei assembled without Nup205 and Nup188 (in the presence of full-length recombinant Nup93)

Surprisingly, the two major components of the Nup93 complex (Nup205 and Nup188) were found not to be essential for NE and NPC assembly. We were curious to know the composition of the nuclei assembled with added back full length Nup93 in the absence of Nup205 and Nup188. Hence we did in vitro nuclear assembly reactions with mock depleted, Nup93 depleted or Nup93 depleted extracts that were supplemented with recombinant full length Nup93 as before. The nuclei were assembled for 90 minutes and processed further for IF.

First we checked for the localization of the structural nucleoporins in the NPC (Fig. 2.8A). For instance Mel-28 which is am early player in NPC assembly (Rasala et al., 2006; Franz C et al., 2007) was found to be present at the nuclear rim in mock depleted, Nup93 depleted and in nuclei assembled with Nup93 depleted extracts supplemented with full length Nup93 add back situation. Similar staining pattern was observed for Nup107, which belongs to the Nup107-160 complex that is a structural sub-complex involved in early steps of NPC formation (Walther et al., 2003; Harel et al., 2003). We also checked for the localization of other members of the Nup93 complex, Nup53 and Nup155. For both the nucleoporins we observed a nuclear rim staining in case of nuclei assembled with mock depleted extracts. In case of nuclei assembled with Nup93 depleted extracts the staining intensity was reduced in comparison to mock (see section 3.1.4. in discussion). When the full-length recombinant Nup93 was added back to these nuclei we observed a normal bright and smooth nuclear rim staining for both Nup53 and Nup155.

Next we checked for the TM nucleoporins Gp210 and Pom121 (Fig. 2.8B). Pom121 is a transmembrane nucleoporin that is recruited early in NPC assembly unlike Gp210, which

comes much later (Antonin et al., 2005). In case of mock depleted nuclei we observed a smooth rim staining for both Pom121 and Gp210. Interestingly in case of nuclei where the Nup93 had been depleted we observed a punctate staining pattern for both the TM nucleoporins Gp210 and Pom121 (a sign of unclosed NE). When full-length recombinant Nup93 was added back into the system the phenotype was reversed i.e. we observed a smooth and continuous nuclear rim staining for Gp210 and Pom121, which was also a sign of NE closure upon addition of full length Nup93.

Localization of cytoplasmic and peripheral nucleoporins was also checked by IF. As shown in fig.2.8C, the peripheral nucleoporin Nup153 showed a normal nuclear rim staining in the mock depleted nuclei. In case of Nup93 depleted nuclei we also observed Nup153 at the nuclear rim and in nuclei that were assembled with Nup93 depleted extracts supplemented with full length Nup93, Nup153 showed a bright nuclear rim staining like other nucleoporins which suggests that the NPC assembly is rescued and nucleoporins are recruited in a coordinated fashion upon addition of Nup93. The staining observed for Nup153 in Nup93 depleted nuclei was because a fraction of Nup153 is known to interact with the Nup107-160 sub-complex (Vasu et al., 2001) and the Nup107-160 complex is recruited to the assembling pore earlier than Nup93 (E. Dultz et al., 2008). Similar staining pattern was observed for Nup98. For the cytoplasmic nucleoporins Nup88 we observed a normal recruitment at the nuclear rim in case of mock depleted nuclei. In the nuclei where Nup93 was depleted we observed no staining for Nup88. When the full length Nup93 was added back the Nup88 showed a bright and smooth nuclear rim staining.

46

(B)

Transmembrane nucleoporins
- α-pom121
- α-gp210

(C)

cytoplasmic and peripheral nucleoporins
- α - Nup153
- α – Nup88
- α – Nup98
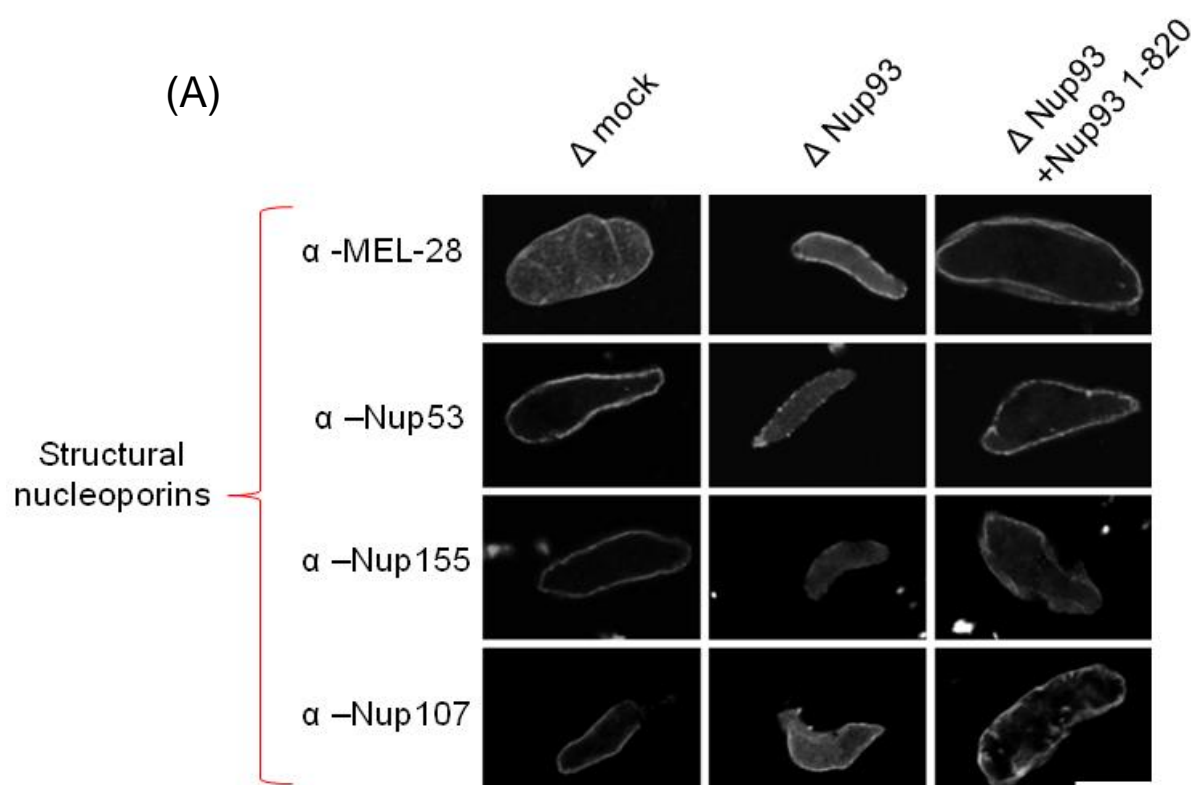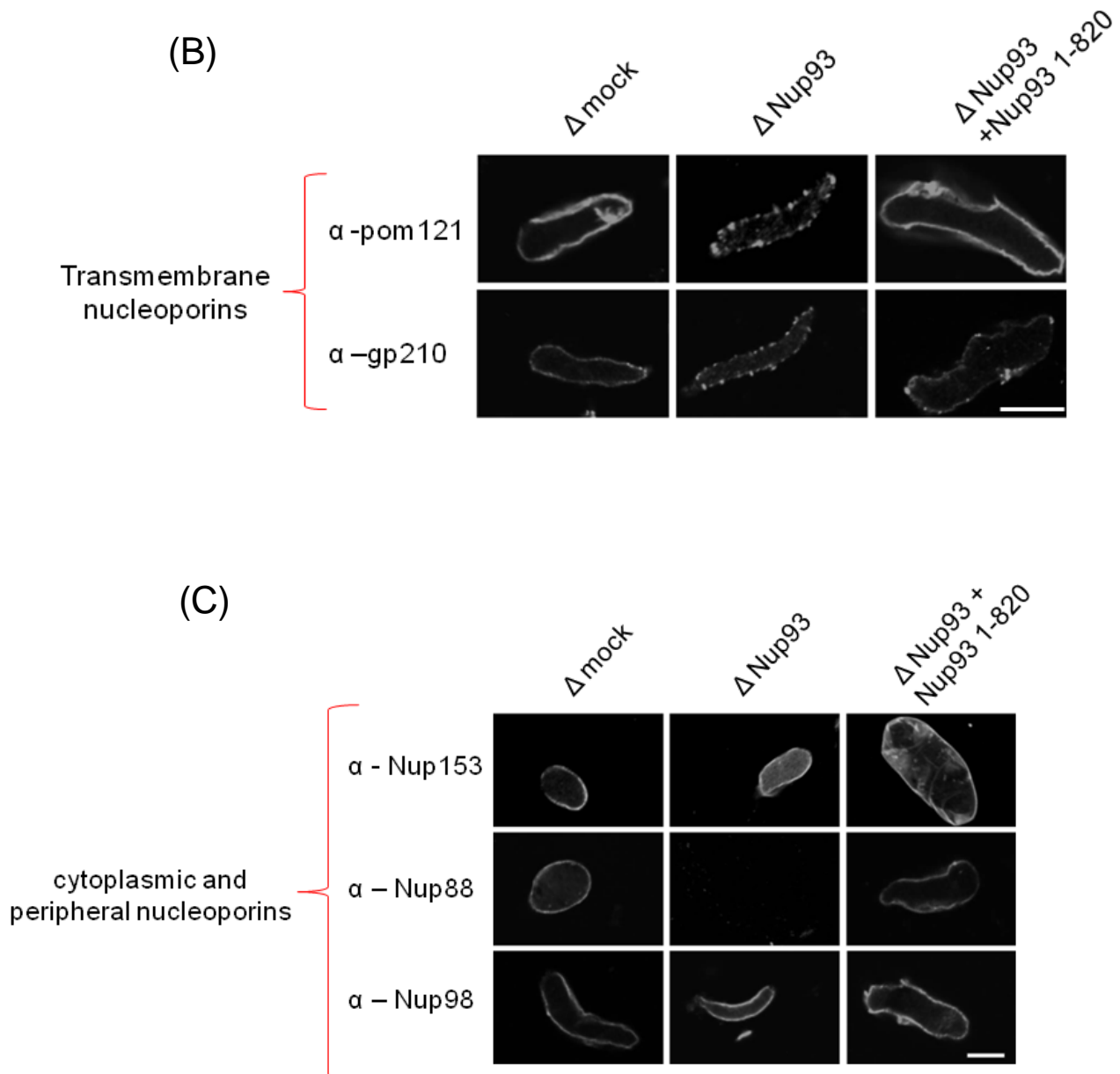
Figure 2.8: Nuclear pore complex composition of nuclei formed in the absence of Nup205 and Nup188. Nuclei were assembled using mock depleted, Nup93 depleted and Nup93 depleted (supplemented with recombinant full-length Nup93) extracts for 90 minutes. The nuclei were fixed with 4% PFA. Immunoflorescence (IF) was done on these nuclei using antibodies against: (A) Structural nuceloproins: MEL-28, Nup53, Nup155 and Nup107. (B) Transmembrane nucleoporins: Pom121 and Gp210. (C) Cytoplasmic and peripheral nucleoporins: Nup153, Nup98 and Nup88. The antibody staining was visualized by confocal microscopy. Bar: 10µm. All the nuclei shown in the figure2.8 (A, B and C) are

part of one experiment. It's divided into parts to get a clear view of different kinds of nucleoporins present in different regions of the NPC.

2.1.9. The C-terminal domain of Nup93 is essential and sufficient for NE assembly.

We obtained a surprising yet an interesting result that both Nup205 and Nup188 were not essential for NPC assembly. Nup93 on the other hand was indispensable for both NE and NPC formation. We then decided to go into more detail to investigate the role of Nup93 in NE and NPC formation. We wanted to elucidate the function of different regions of Nup93 and how they actually contributed to NE, NPC assembly and function? Shown in fig. 2.9A is the domain organization of *Xenopus laevis* Nup93. The N-terminal half of vertebrate Nup93 and its yeast homologue Nic96p are both known to form coiled - coil domain (Grandi et al., 1995 and 1997). The rest of the protein is mainly an elongated alpha helical structure (Jeudy and Schwartz, 2007; Schrader et al., 2008). In yeast (*Saccharomyces cerevisiae*) the protein is divided into an N-terminal coiled-coil domain, (aa 1-175 of *Xenopus laevis* Nup93), the middle part (aa 197-583 in *Saccharomyces cerevisiae* corresponding to aa 183-579 in *Xenopus laevis*) and a C-terminal domain (aa 617-839 in *Saccharomyces cerevisiae* which correspond to aa 608-820 in *Xenopus laevis*). The N-terminal coiled coil domain of vertebrate Nup93 and yeast Nic96p are both known to interact with Nup62 and Nsp1p respectively (Grandi et al., 1995, and 1997). Nup62 is a member of the Nup62 complex and is a FG repeat containing nucleoporin that is part of the central channel of the NPC and imparts functional properties to the pore like transport competency and to function as an exclusion barrier.

To elucidate the functions of different domains of Nup93 we cloned different fragments of Nup93 in the pet28stev vector. (FL: aa 1-820, N: aa 1-175, M: aa 183-579, C: aa 608-820, N+M: aa 1-579 and M+C: aa 183-820) as shown in fig. 2.9A. We then expressed and purified these proteins from *E.coli*.

We used the above-mentioned Nup93 constructs for the in vitro nuclear assembly reaction. As before, we assembled nuclei with mock depleted, Nup93 depleted and Nup93 depleted (supplemented with aforementioned fragments of Nup93) extracts. The nuclei were assembled for 90 minutes and chromatin was stained with DAPI. DilC18 was used as a membrane dye. As observed before the full-length protein could rescue the block in NE assembly. The N- terminus, M domain and the N+M domain could not rescue the block in

NE formation as we observed a punctate membrane staining; unclosed NE and chromatin did not decondense. On the other hand if C-terminal domain of Nup93 was part of the protein construct (FL: aa 1-820 or M+C: aa 183-820) we observed a closed NE formation and the block in NE assembly was rescued. In fact surprisingly only the C-terminal domain itself (aa 608-820) was sufficient to rescue the block in NE assembly as seen by a smooth nuclear envelope membrane staining wherein the membranes were docked on to the chromatin and then eventually fused to form a closed NE (fig. 2.9B). Thus we could conclude that the C-terminal domain of Nup93 was essential and sufficient for NE formation and could make up for the loss of the endogenous Nup93 in this regard.

We also quantified the nuclei having a closed NE, which were assembled with different fragments of Nup93 as shown in the bar graph in fig. 2.9C.
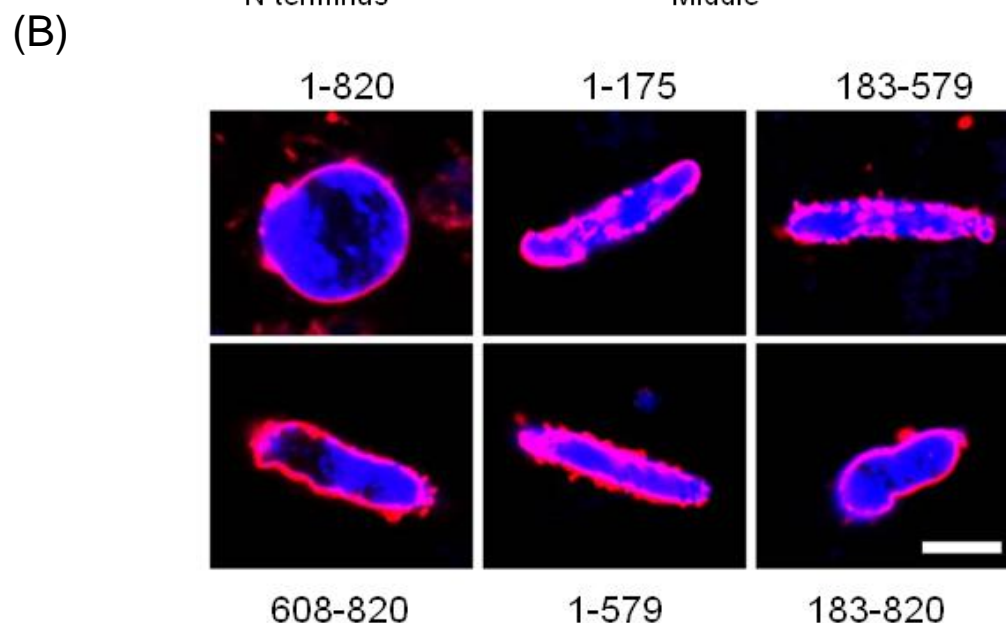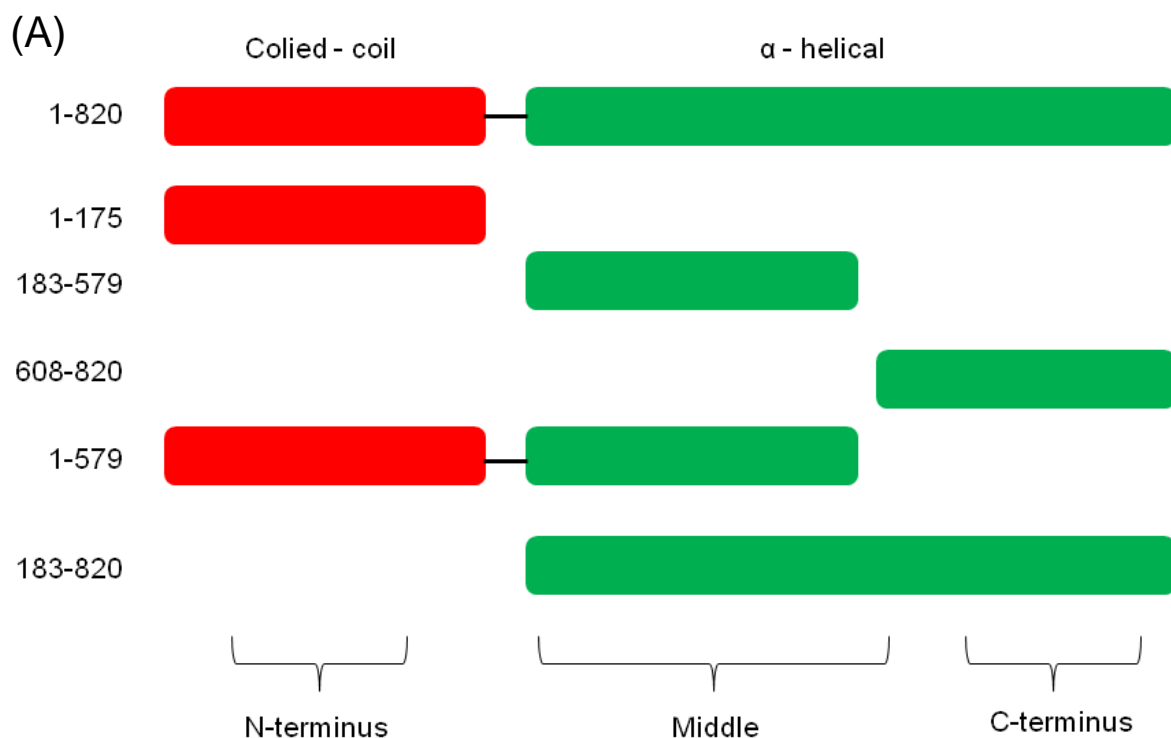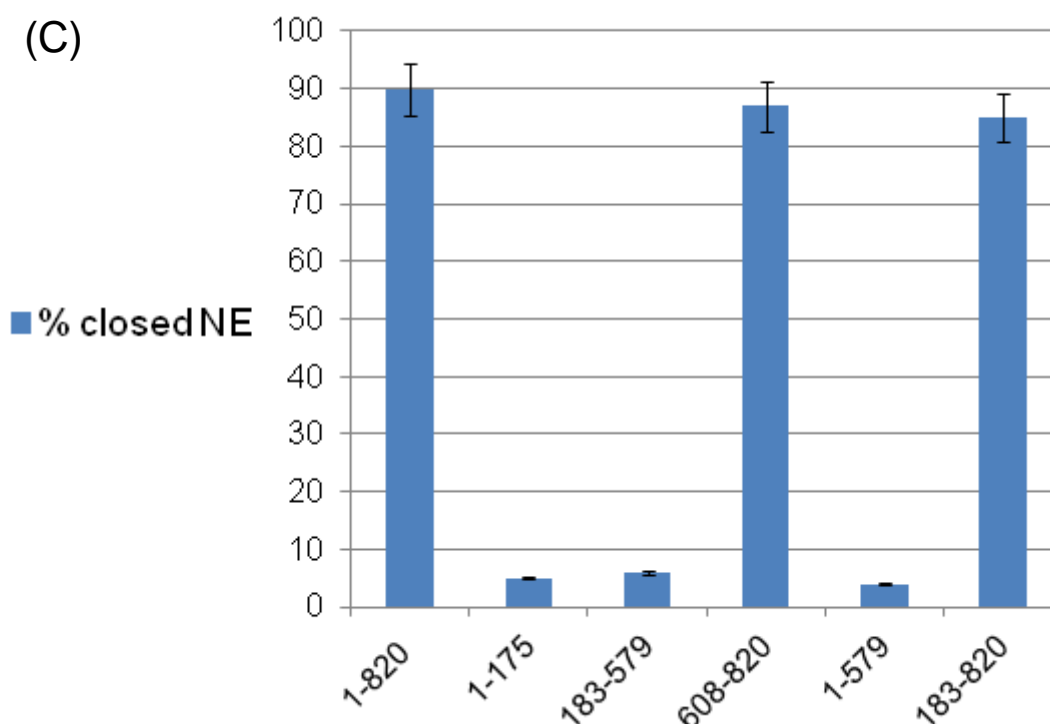
Figure 2.9: The C- terminal domain of Nup93 is sufficient and essential for nuclear envelope assembly. (A) Shows the schematic representation of the domain organization of *Xenopus laevis* Nup93. These fragments were used for in vitro nuclear assembly reactions. The protein can be divided into N, middle and C-terminal domains. The N-terminal domain is coiled-coil in nature as shown in red. The rest of the protein is mostly alpha helical in nature as show in green. The numbers shown indicate the amino acid of the corresponding fragments of *Xenopus leavis* Nup93. (B) Nuclei were assembled using Nup93 depleted extracts supplemented with add back of different fragments of Nup93. For instance full-length Nup93 (aa 1-820), N-terminal (aa 1-175), middle domain (aa 183-579), C-terminal domain (aa 608-820), N+M (aa 1-579) and M+C (aa 183-820). The nuclei were assembled for 90 minutes and then fixed with 2% PFA +0.5% glutaraldehyde. The chromatin was stained with DAPI (blue) and membranes using the red dye DilC18. The nuclei were visualized using confocal microscopy. Only when the C-terminal domain was part of the Nup93 construct (aa 183-820 or aa 608-820) we observed a closed NE. Bar: 20μm. aa refers to amino acid. (C) Nuclei having a closed NE was counted based on the visual DilC18 membrane staining for the nuclei assembled in (B). More than 100 randomly chosen chromatin substrates were counted per reaction/per experiment. The average of three independent experiments is shown and the error bars represent the total variation observed in the three individual experiments.

2.1.10. The C-terminal domain of Nup93 is sufficient for the closure of the nuclear envelope.

To strengthen the fact that the C-terminal 200 amino acids of Nup93 is able to compensate for the loss of the full length Nup93 in regard of a closed NE we decided to have a look at the transmission electron micrographic view of these nuclei to better observe their morphology. As shown in fig. 2.10 the nuclei assembled with Nup93 depleted extracts that were supplemented with the C-terminus of Nup93 all had a closed NE.
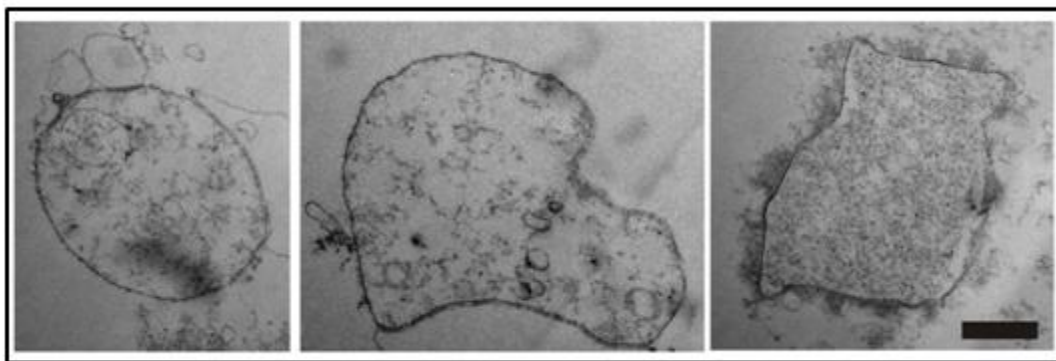
Figure 2.10: Transmission electron micrographic view of nuclei assembled with C-terminus of Nup93. Nuclei were assembled using Nup93 depleted extracts that were supplemented with the C-terminus of Nup93 (aa 608-820) for 90 minutes. The nuclei were then fixed and analyzed by TEM. The figure shows the transmission electron microscopic view of these nuclei and depicts a closed NE formation upon addition of C-terminus of Nup93 to the nuclear assembly reaction. Bar: 2µm.

2.1.11. Composition of nuclei assembled with the C-terminus of Nup93.

Once we knew that only the C-terminal (aa 608-820) domain of Nup93 was sufficient for the closure of the NE we decided to analyze the composition of these nuclei in detail. For this we did IF on nuclei assembled with mock depleted extracts, Nup93 depleted extracts and Nup93 depleted extracts supplemented with the full length Nup93 or only the C-terminus of Nup93.

Mel28, an early player in NPC assembly (Franz C et al., 2007; Rasala et al., 2006) showed a normal recruitment at the nuclear rim in all cases (fig. 2.11A). Its incorporation in the NPC was not influenced by the presence or absence of Nup93 (full length or any other

fragment of Nup93) as it is the starting point of post mitotic NPC assembly and Nup93 is recruited later on. A similar phenotype was observed for Nup107, which is recruited to the assembling NPC after Mel28 and before Nup93 (E. Dultz et al., 2008; Franz et al., 2007). In case of Nup53 and Nup155 which are members of the Nup93 complex the brighter smooth nuclear rim staining in case of nuclei assembled with the C-terminus of Nup93 in comparison to the nuclei assembled with Nup93 depleted extracts should be noted. As before in case of mock depleted nuclei and in nuclei where full length Nup93 was added back we observed a normal nuclear rim staining for both Nup53 and Nup155 suggesting a faithful incorporation of both the nucleoporins in the assembling NPCs.

We also checked the staining and localization for the TM nucleoporin Pom121 (fig. 2.11B). In the case of nuclei assembled with mock depleted extracts we observed a normal nuclear rim staining of Pom121. In case of nuclei assembled using Nup93 depleted extracts as before we observed a punctate staining for Pom121. When the nuclei were assembled with the full length add back of recombinant Nup93 a smooth nuclear rim staining was observed for Pom121. A similar phenotype was observed for Pom121 when the nuclei were assembled with only the C-terminus of Nup93. Please note the difference in staining pattern observed for Pom121 in nuclei where Nup93 was depleted and nuclei assembled using Nup93 depleted extracts supplemented with C-terminus of Nup93 (punctuate and smooth staining respectively).

For the peripheral nucleoporin (Nup153 and Nup98) in case of nuclei assembled using mock depleted, Nup93 depleted and Nup93 depleted (supplemented with full length Nup93) extracts we observed the same staining pattern as before (fig. 2.11C, compare to fig. 2.8C). In case of nuclei assembled with Nup93 depleted extracts supplemented with the C-terminus of Nup93 we observed a normal smooth nuclear rim staining for both Nup153 and Nup98. For the cytoplasmic nucleoporin Nup88 we observed no staining when nuclei were assembled only with the C-terminus of Nup93. In case of nuclei assembled using mock depleted, Nup93 depleted and Nup93 depleted (supplemented with add back of the full length recombinant Nup93) extracts the phenotype of Nup88 was same as observed before (fig. 2.8C).
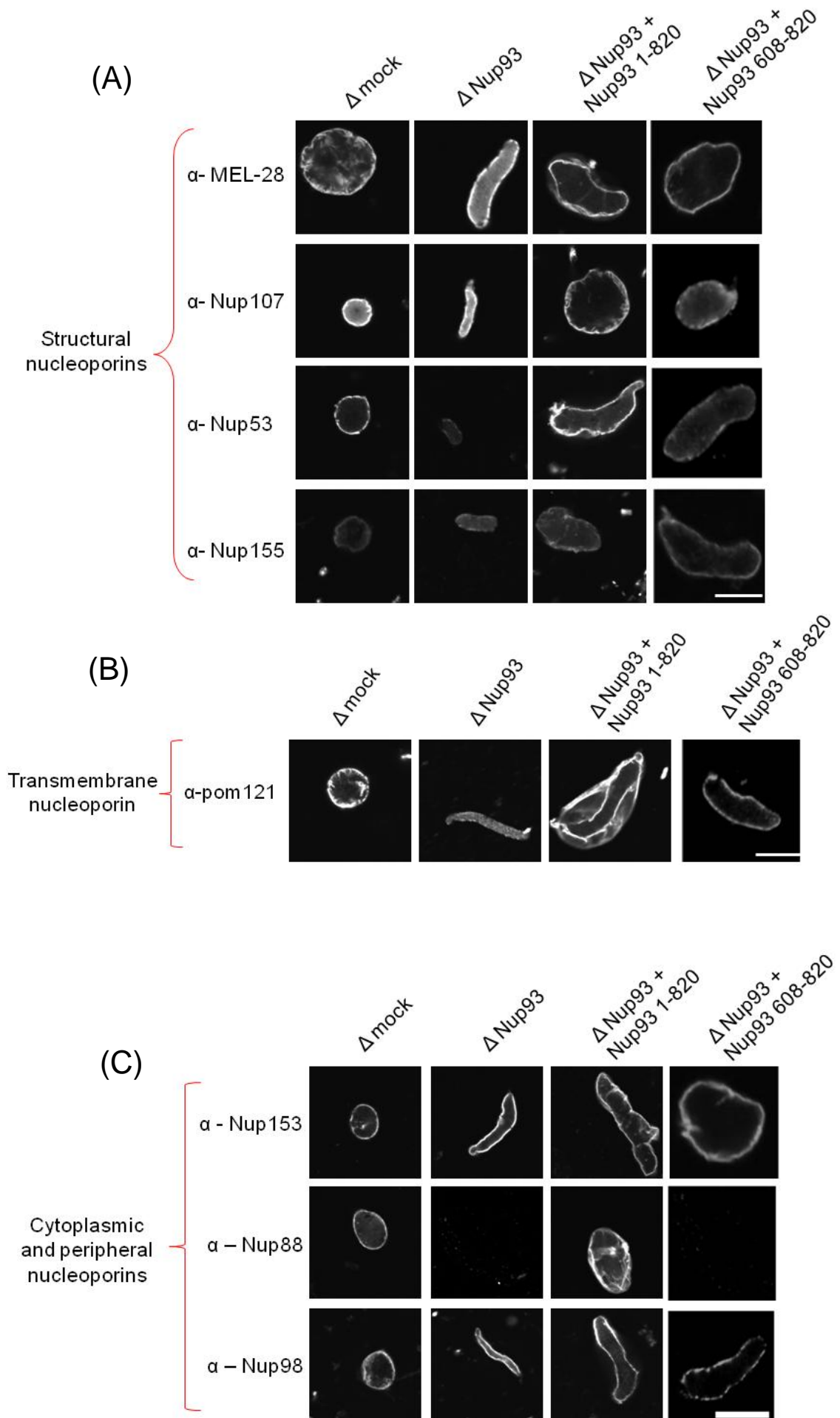
Figure 2.11: Composition of nuclei assembled with the C-terminus of Nup93. Nuclei were assembled using mock depleted, Nup93 depleted and Nup93 depleted (supplemented with either the full-length Nup93 or C-terminus of Nup93; aa 1-820 and aa 608-820 respectively) extracts for 90 minutes. The nuclei were then fixed with 4% PFA and stained with the respective antibodies. The nuclei were imaged using a confocal microscope. Bar: 10µm. (A) Structural nucleoporins: Nup107, MEL-28, Nup53 and Nup155. Please note the increase in staining intensity of Nup53 and Nup155 in the nuclei that were assembled with the C-terminus of Nup93 as compared to nuclei where Nup93 was depleted. (B) Transmembrane nucleoporins: Pom121. Note the smooth staining observed for Pom121 in nuclei assembled with the C-terminus of Nup93 and full-length Nup93 as oppose to punctuate staining in Nup93 depleted nuclei. (C) Cytoplasmic and peripheral nucleoporins: Nup153, Nup98 and Nup88. All these immunoflorescence for different nucleoporins are part of the same experiment. They have been divided for the sake of clarity in visualization of different kind of nucleoporins.

2.1.12. Recruitment of the Nup62 complex at the assembling NPCs is mediated by the N-terminus of Nup93.

The nuclear pore complex can be dissected in two ways: the structural backbone of the pore and the functional part. The structural backbone is composed of Mel-28, Nup107-160 complex, TM nucleoporins, and Nup93 complex. These complexes are composed of structural nucleoporins that form the scaffold core backbone of the NPC (Vasu et al., 2001 and 2003; Rasala et al., 2006; Walther et al., 2003; Franz C et al., 2007; Harel et al., 2003 and Antonin et al., 2005). On the other hand the nucleoporins that form the central channel of the pore imparts functional properties to the NPC like transport competency and ability to act as an exclusion barrier. These proteins mostly consist of unstructured FG repeat containing nucleoporin for instance the members of the Nup62 complex (Fukuhara T et al., 2006).

As mentioned before it's known in literature that Nup93 and its yeast homologue Nic96p can interact with Nup62 and Nsp1p respectively (Grandi et al., 1995 and 1997). Specifically the N- terminal coiled- coil domain of Nup93 binds Nup62 as shown in the cartoon (fig. 2.12A). Hence we questioned for the nuclei assembled only with the C-terminus of Nup93 the functional nature of these pores and thus decided to analyze these nuclei in more detail. In these nuclei the N-terminus of Nup93 was missing because of

which Nup62 complex could not be recruited to the assembling NPC. Nevertheless we knew that in the nuclei that were assembled with only the C-terminus of Nup93 had a closed NE. To unravel the mechanism of this interesting observation we first decided to check for the presence or absence of FG repeat containing nucleoporin (using mab414 antibody) and for members of the Nup62 complex using antibodies specific for its members by IF. As shown in fig. 2.12B for mab414 staining: in case of nuclei assembled with mock depleted extracts we observed a smooth nuclear rim staining for mab414 suggesting that the FG repeat containing nucleoporins (Nup62, Nup153, Nup214 and Nup358) recognized by the mab414 antibody were recruited to the assembling NPCs normally. In case of nuclei assembled with Nup93 depleted extracts we observed a very faint or negligible staining for mab414 as NPC assembly is blocked upon Nup93 depletion and FG repeat containing nucleoporins are not recruited to the assembling pore. In case of nuclei assembled with Nup93 depleted extracts supplemented with full length recombinant Nup93 we observed a normal smooth nuclear rim staining for mab414 likewise as the mock depleted nuclei suggesting that the NPC assembly was restored upon re addition of the full- length Nup93 and the FG repeat containing nucleoporins were recruited to the assembling NPCs in a normal fashion. When the nuclei were assembled with Nup93 depleted extracts supplemented with the C-terminus of Nup93 we observed a fainter nuclear staining of mab414 as compared to mock depleted nuclei or if the full length Nup93 was added back. The same was observed for the nuclei, which were assembled with M+C fragment of Nup93 (aa 183-820). The weak mab414 staining observed could be attributed to the presence of Nup153 at the pore as a fraction of Nup153 is known to interact with Nup107-160 sub-complex which is an early player in NPC assembly and is recruited to the assembling pore before the Nup93 complex (Vasu et al., 2001; E. Dultz et al., 2008).

Although one of the nucleoporins that mab414 antibody recognizes is indeed Nup62 we nevertheless wanted to specifically check for Nup62 and its complex members to not get any misleading information about the specific nucleoporins and avoid any interference in staining for instance from Nup153. First we checked for Nup62 that is known to interact with the N- terminal half of Nup93 using an affinity purified Nup62 antibody. In case of mock depleted nuclei we observed a smooth nuclear rim staining for Nup62. In case of nuclei assembled with Nup93 depleted extracts we observed absolutely no staining of Nup62. It's noteworthy that the absence of nuclear rim staining for Nup62 was not due to the fact that Nup62 was co depleted upon Nup93 depletion; in fact its levels were not

altered upon Nup93 depletion (see fig. 2.2). Nup62 although present at normal levels in the Nup93 depleted extracts, which were comparable to mock depleted extracts could not be recruited to the assembling pore due to absence of its anchor protein that is Nup93, which had been depleted from the extracts. In case of nuclei assembled with Nup93 depleted extracts supplemented with the add back of full length recombinant Nup93 we observed a normal smooth nuclear rim staining for Nup62 like in the case of mock depleted nuclei. Hence when Nup93 was added back in the system, NPC assembly was restored, Nup93 was recruited to the assembling NPC (fig. 2.5) and the full-length protein could thereby recruit Nup62 from the *Xenopus laevis* egg extracts to the pore. In case of nuclei assembled with Nup93 depleted extracts supplemented with either the C- terminus (aa 608-820) of Nup93 or the fragment comprising the M+C-terminal domain (aa 183-820) of Nup93 we observed no staining of Nup62. This could be explained by the fact that in this situation although these domains of Nup93 are enough to support NE formation (see fig. 2.9B) but as the N-terminal half of Nup93 was missing, it could not therefore bind and recruit Nup62 to the assembling NPC. To be sure that this staining pattern observed was not only valid for Nup62, we also checked for Nup58, which is another member of the Nup62 complex. We observed exactly the same phenotype for Nup58 as well (fig. 2.12). Thus a major component of the NPC that is the Nup62 complex was missing from the assembling NPC when the nuclei were assembled with only the C-terminus (aa 608-820) or M+C (aa 183-820) terminus of Nup93.

Thus by the results so far we concluded that the C-terminus of Nup93 can support the formation of NE (fig. 2.9B) and formation of the structural backbone of the NPC (fig. 2.10A) but these nuclei were missing the Nup62 complex which is composed of unstructured FG repeat containing nucleoporins and thereby responsible for the formation of the central channel of the NPC which imparts functionality to the pore for instance to conduct transport and behave as an exclusion barrier. Henceforth we decided to check for the functionality of the nuclei that had been assembled with the C-terminus of Nup93.
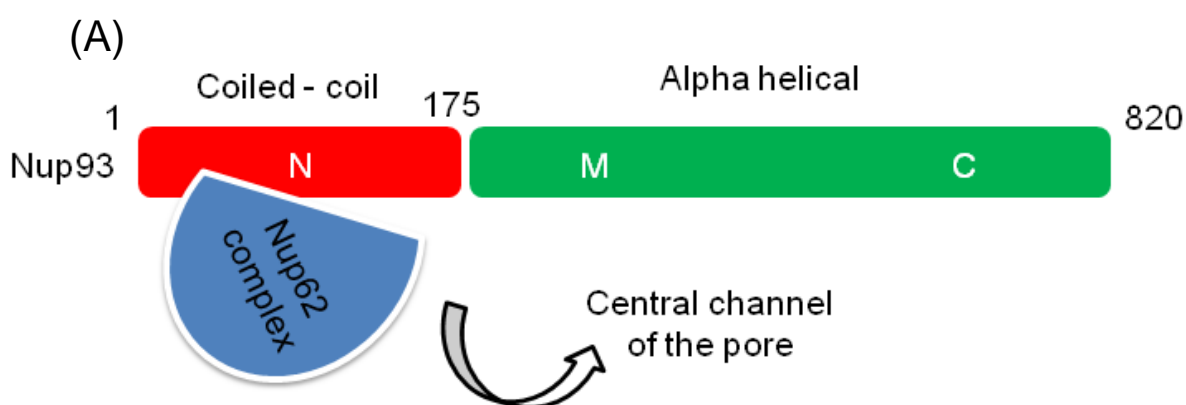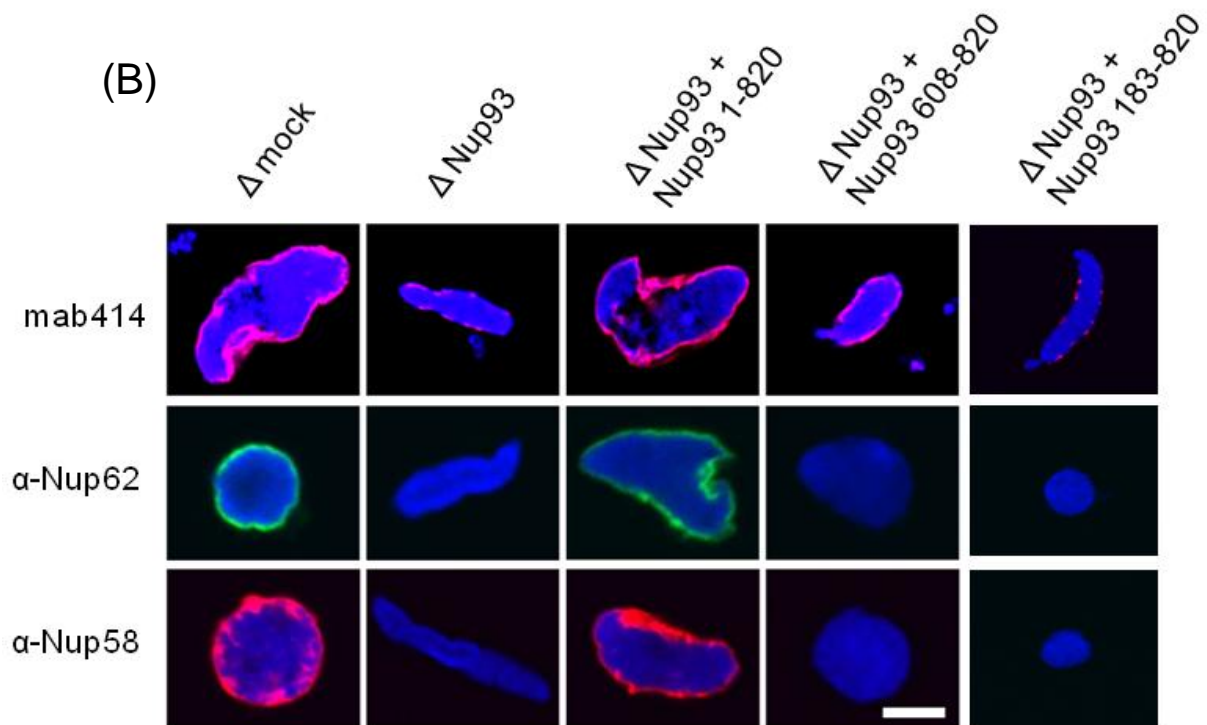
Figure 2.12: The N-terminus of Nup93 recruits the Nup62 complex to the assembling pore. (A) The cartoon depicts the interaction between *Xenopus laevis* Nup93 and the Nup62 complex. The N-terminus coiled-coil region of Nup93 (aa 1-175) is known to interact with the Nup62 complex. Nup62 complex is part of the central channel of the NPC that is involved in transport and exclusion competency of the pore. The N-terminus coiled-coil region of Nup93 is shown in red and rest of the protein that is mainly alpha helical in nature is shown in green. The numbers represent the corresponding amino acids in *Xenopus laevis* Nup93. (B) Nuclei were assembled using mock depleted, Nup93 depleted and Nup93 depleted [supplemented with full length (aa 1-820), C-terminus (aa 608-820) or middle +C-terminus (aa 183-820) of Nup93] extracts for 90 minutes. The nuclei were then fixed with 4% PFA and immuno florescence was done using mab414 antibody (red upper panel), Nup62 antibody (green middle panel) and Nup58 antibody (red bottom panel). The chromatin was stained with DAPI (blue). Overlay images with the corresponding antibody and DAPI are shown. The nuclei were imaged using confocal microscopy. Scale bar: 10μm.

2.1.13. The N-terminus of Nup93 is essential for the formation of import-competent nuclei.

One of the major functions of the NPC is to act as the gatekeeper of the cell and mediate the nucleocytoplasmic transport of protein, RNA and various other molecules. The Nup62 complex plays a major role in imparting this property to the NPC. The unstructured FG repeat containing nucleoporins which are part of the Nup62 complex form the central channel of the pore through which the import and export of substances is possible. We decided to analyze the transport competency for the nuclei assembled with either full length (aa 1-820) or different fragments of Nup93. Specifically we were curious to see whether the nuclei that have only the C-terminus (aa 608-820) of Nup93 can import substrates inside their nuclei as in this situation Nup62 was not recruited to the NPC due to the absence of its anchoring protein: the N-terminus of Nup93 (fig. 2.12). To test this we did in vitro nuclear assembly with Nup93 depleted extracts supplemented with different fragments of Nup93 and added an EGFP (enhanced green florescent protein) fused to a nuclear import substrate. In case of nuclei assembled with mock depleted extracts the import substrate was localized and enriched in the nucleoplasm (green EGFP signal). The same was observed when the nuclei were assembled with Nup93 depleted extracts supplemented with full-length recombinant Nup93, suggesting that these nuclei were import competent. In case of nuclei assembled with extracts that were either supplemented with only the C-terminus of Nup93 (aa 608-820) or with the M+C- terminus (aa 183-820) the import substrate did not enrich in the nucleoplasm. We observed a very faint or almost negligible nuclear staining and hence these nuclei were not import competent (fig. 2.13A). With the above-mentioned observations we concluded that the N- terminus of Nup93 was essential for the formation of import competent nuclei. We also quantified the number of nuclei that were competent for import based on the EGFP staining. The graph was in accordance with the above-described results (fig. 2.13B).

(A)

(B)

Figure 2.13: The N-terminus of Nup93 is essential for formation of import competent nuclei. (A) Nuclei were assembled using mock depleted, Nup93 depleted and Nup93

depleted [supplemented with full-length Nup93 (aa 1-820), C-terminus of Nup93 (aa 608-820) and the middle + C-terminus of Nup93 (aa 183-820)] extracts. After 50 minutes of the in vitro nuclear assembly reaction an enhanced green florescent protein (EGFP) - fused nuclear import substrate was added. After 2 hours the nuclei were isolated, fixed with 4% PFA+0.5% glutaraldehyde and analyzed immediately with confocal microscopy to check for import of the substrate. The membrane staining was visualized by DilC18 dye (red). Bar: 20µm. The EGFP signal (green) seen inside the nuclei corresponded to the efficiency of the import substrate. The faint green signal observed with the C-terminus or the M+C-terminus of Nup93 was background staining. (B) Shows the quantification of the nuclear import for all conditions tested in (A). More than 100 randomly chosen chromatin substrates were counted per reaction per experiment based on the EGFP signal inside the nucleus, which is denoted as import competent nuclei. The average of three independent experiments is shown and the error bars represent the total variation.

2.1.14. The N-terminus of Nup93 is required for the formation of exclusion-competent nuclei.

NPCs act as highly selective gates in the cell by restricting the nucleocytoplasmic flux of most macromolecules but allowing an efficient facilitated passage of cargo complexes bound to the transport receptors. Thus the NPC acts like an exclusion barrier or has sieve like properties that helps maintain distinct environments of the cytoplasm and the nucleus by restricting the passage of molecules. Substances >30 kDa or larger than 2.5nm in radii are excluded from the nucleus (Mohr et al., 2009) and can be trans-located only by signal-mediated transport. This function of the NPC is imparted by the central channel of the pore, which is composed of highly cohesive FG repeat containing nucleoporins that keep the NPC barrier intact. One of the major complexes in the NPC that does this job is the Nup62 complex, which is composed of unstructured FG repeat containing nucleoporins, which build up the central hydrophobic channel of the pore and hence establish the diffusion barrier within the NPC. One of the major roles of the structural or the scaffold nucleoporins is to anchor NPC components that are involved in establishing the nuclear permeability barrier (Alber et al., 2007; Frosst et al., 2002; Grandi et al., 1997). We decided to test whether the permeability barrier was intact in the nuclei that had been assembled with different fragments of Nup93 wherein in some cases Nup62 complex members were either recruited or not to the assembling NPC.

Defects in the NE integrity or the permeability of the NPC can be tested by fluorescently labeled dextrans with defined molecular weights. If the permeability barrier of the NPC is perturbed then a 70 kDa dextran molecule can freely diffuse into the nucleus, as the pores are leaky in nature whereas perturbations of the NE are required for 500 kDa dextrans to enter the nucleus (Gary et al., 2003). To test the intactness of the permeability barrier of the NPCs we did in vitro nuclear assembly reactions with Nup93 depleted extracts that were supplemented with different fragments of Nup93 and then added fluorescently labeled 70kDa dextrans and imaged the nuclei on the confocal microscope. In case of nuclei assembled with mock depleted extracts the 70kDa dextran molecules were excluded (fig. 2.14A: as seen by a dark black nucleus with bright florescence of the 70kDa dextran molecules seen outside the nucleus). In case of nuclei where Nup93 was depleted, the 70kDa dextran molecules were not excluded as seen by bright florescence in and out of the nucleus (fig 2.14A). This is due to the fact that NPC formation was blocked due to which the central channel of the pore was not formed and the permeability barrier of the pore could not be established thus the dextran molecules could freely diffuse across the nucleus. In case of nuclei that were assembled with Nup93 depleted extracts supplemented with the recombinant full-length Nup93, they excluded the 70kDa dextran molecules (fig. 2.14A) as now the NPC formation was restored and the full length added back Nup93 could recruit the Nup62 complex which forms the central channel of the pore and hence establish the permeability barrier of the NPC thereby excluding 70kDa sized dextrans. On the other hand if only the C-terminus (aa 608-820) or M+C-terminus (aa 183-820) of Nup93 was part of the pore the nuclei could not exclude 70kDa dextrans anymore (fig. 2.14A) as observed by the bright florescence of dextran molecules in and out of the nucleus. This is explained by the fact that the pores formed in this situation were leaky in nature. Although the nuclei assembled with these fragments (C or M+C) of Nup93 had a closed NE, and structural nucleoporins were present at the pore but the central channel could not be formed due to the absence of recruitment of the Nup62 complex as the N-terminus of Nup93 was missing in the pores. Due to the lack of the FG repeat containing nucleoporins at the pore the permeability barrier could not be established hence leading to leaky pores. Please note that the diffusion of 70kDa dextrans is not due to the perturbation of the NE integrity as the NE in the above mentioned case was closed its rather the leakiness of the pores due to the absence of central channel formation. We also counted the nuclei based on exclusion of the 70kDa dextran molecules in all the above-mentioned situations. The quantification is shown in the bar graph in fig. 2.14B.

Thus all together the results so far suggested that the different domains of Nup93 contributed to different functions of the NPC. The N-terminal coiled coil domain recruited the Nup62 complex to the assembling NPC that forms the central channel of the pore. This hydrophobic central channel is composed of unstructured cohesive FG repeat containing nucleoporins that impart functional properties to the pore like transport competency and formation of a permeability barrier. The C-terminal domain on the other hand does not recruit the Nup62 complex and cannot support the formation of a transport and exclusion competent nucleus but it is essential and sufficient for the formation of a closed NE and the structural backbone of the pore (partially assembled NPCs).
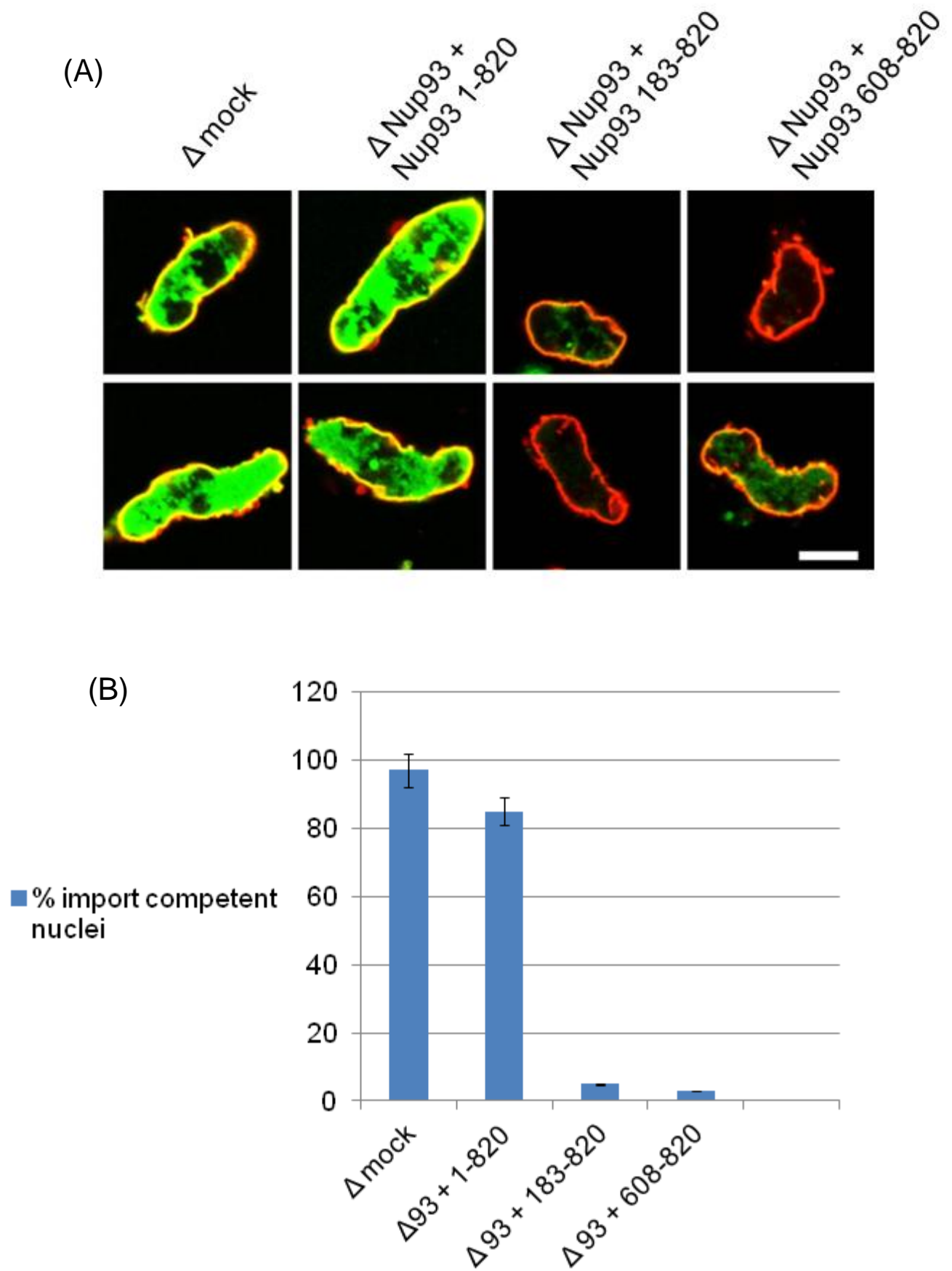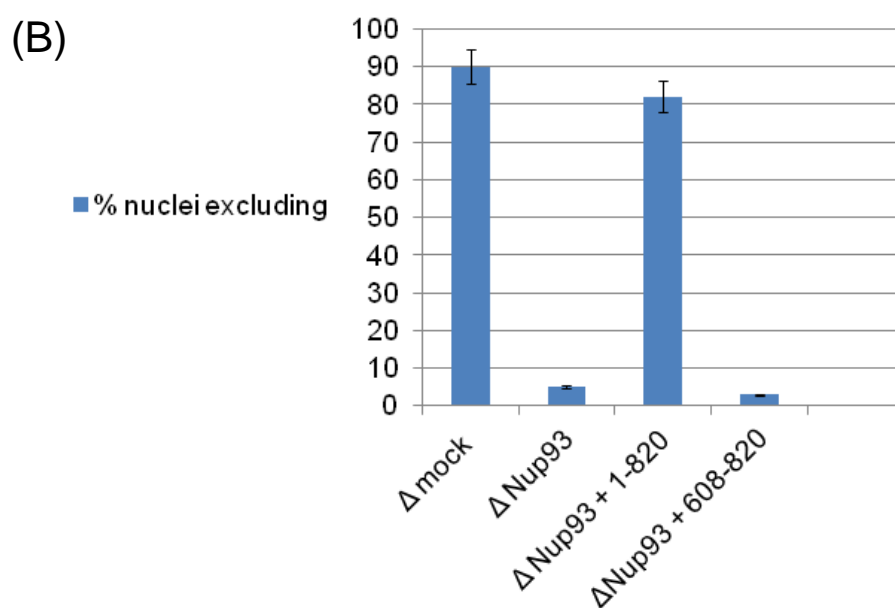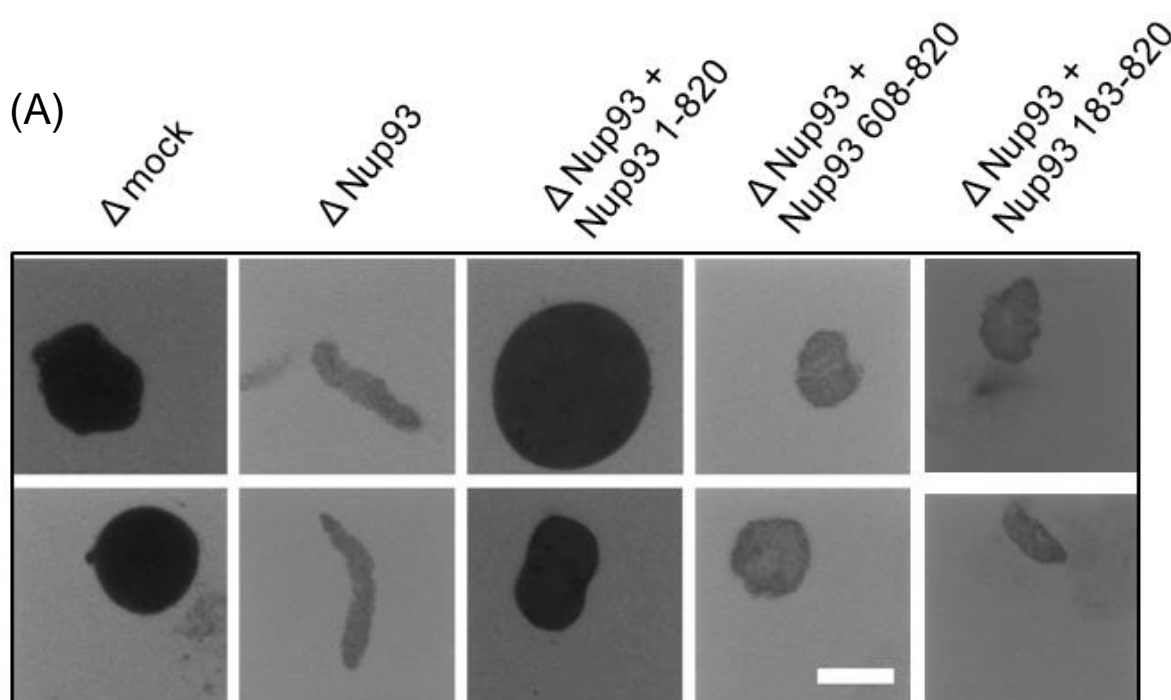
Figure 2.14: The N-terminus of Nup93 is required for formation of exclusion competent nuclei. (A) Nuclei were assembled using mock depleted, Nup93 depleted and Nup93 depleted [supplemented with full-length Nup93 (aa 1-820), C-terminus of Nup93 (aa 608-820) and the middle + C-terminus of Nup93 (aa 183-820)] extracts for 90 minutes. After which fluorescein labeled 70Kda dextran was added and incubated for 15 minutes at room temperature (25ºC). The nuclei were fixed temporarily with squash fix. DNA was stained using DAPI to identify nuclei in the respective samples. The samples were then immediately imaged using confocal microscopy. The dark black hole represents that the 70Kda dextran molecules were excluded whereas if the dextran molecules were included we observed a fluorescent staining both in and out of the nucleus as the dextrans could freely diffuse. Representative images of the 70Kda dextran staining are shown here. Scale bar: 10µm. (B) The nuclei excluding the 70Kda dextran molecules were counted. Two experiments were done and in each 40 nuclei per reaction were counted for exclusion. The quantification is shown in the bar graph above. The error bars represent the total variation observed.

2.1.15. The middle domain of Nup93 is dispensable for NPC formation.

From our data so far we had a thorough and extensive idea about the varied functions of different domains of Nup93. The N-terminus coiled-coil domain of Nup93 recruited the Nup62 complex to the assembling NPC, which is a major component, involved in the formation of the central channel of the pore. The central channel that mostly consists of the cohesive FG containing nucleoporins imparts functional properties to the pore like ability to transport various molecules and act as an exclusion barrier to maintain distinct environments of the nucleus and the cytoplasm. The C-terminus of Nup93 on the other hand was involved in the formation of the structural backbone of the pore and was essential and sufficient for NE assembly.

We were then curious to know the role of the middle domain of Nup93 in NE /NPC assembly and function. We therefore designed a fusion construct comprising the N and the C-terminus of Nup93 (deletion of middle domain) whether it could substitute for the full length endogenous Nup93 as individually both the N and the C termini had specific roles that could support NE, NPC assembly and all the tested functions of the pore as explained above.

To study this we designed a fusion construct of the N and the C-terminus of Nup93 (fig. 2.15A). The construct was a fusion between aa 1-175 and aa 608-820. We also included a linker of about 8 amino acids: GGSGSGGS between the N and C-terminal domains to ensure flexibility in the protein. We cloned this construct in the pet28stev vector. We then expressed and purified the protein from *E.coli* and eventually had the protein tag free to be used in the in vitro nuclear assembly reactions.

We tested the fusion protein (N+C-terminus of Nup93) in the nuclear assembly reactions. We immunodepleted Nup93 from *Xenopus laevis* egg cytosol and added back either the full-length or different fragments of Nup93 including the fusion (N+C: aa 1-175+608-820) construct to check for NE assembly (fig. 2.15B). In case of untreated extracts we observed a closed NE, smooth membrane staining and fully decondensed chromatin. In case of nuclei assembled with mock depleted extracts we also observed a closed NE and decondensed chromatin after 90 minutes of the nuclear assembly reaction. When the nuclei were assembled using Nup93 depleted extracts we observed a block in NE formation as seen before (fig. 2.3A). Nuclei that were assembled with Nup93 depleted extracts supplemented with the full-length Nup93 a closed NE, decondensed chromatin was observed. The nuclei were also bigger in size as compared to mock or Nup93 depleted nuclei (see discussion section 3.12). In case of nuclei assembled where the C-terminus of Nup93 replaced the endogenous Nup93, as before we observed a closed NE formation. In case of nuclei assembled with Nup93 depleted extracts supplemented with the fusion construct (N+C-terminus) of Nup93 we observed a closed NE with smooth membrane staining. The chromatin was also decondensed (fig. 2.15B). The nuclei were smaller in comparison to nuclei assembled with add back of the full-length recombinant Nup93. This showed that the middle domain of Nup93 was dispensable for NE assembly, which also supports our previous observations that the C-terminus of Nup93 alone was sufficient and essential for NE formation. It also reassured us that the fusion construct generated was indeed functional as it could support the NE assembly in the egg extract system.

We also counted the nuclei that had a closed NE in all situations tested for NE assembly. The quantification of the same is shown as a bar graph in fig. 2.15C, which correlated to the above-mentioned observations.

Next, we wanted to know if the fusion protein (N+C-terminus of Nup93) would be able to compensate for the endogenous full-length Nup93 and support NPC assembly, especially recruiting the Nup62 complex. We immunodepleted Nup93 from the egg extracts, added back different fragments of Nup93 and analyzed NPC formation. We assembled the nuclei

for 90 minutes and stained them with mab414 antibody using IF. As mentioned before mab414 is an antibody that recognizes a set of FG repeat containing nucleoporins and by its staining pattern we can know if NPCs are formed properly. In case of nuclei that were assembled with untreated extracts we observed a normal smooth nuclear rim staining for mab414. The same phenotype was observed when nuclei were assembled using mock depleted extracts. In case of nuclei that were assembled using Nup93 depleted extracts we observed no staining for mab414 indicating that formation of NPC containing the Nup62 complex was blocked. When the full length recombinant Nup93 was added back to Nup93 depleted extracts the nuclei formed henceforth showed a normal, bright nuclear rim staining for mab414. If only the C- terminus of Nup93 was added back we observed a partial faint staining of mab414 in those nuclei. When the nuclei were assembled with the fusion protein (N+C-terminus of Nup93) we observed a bright nuclear rim staining for mab414 (fig. 2.16). Thus the fusion construct could even rescue the block in the assembling NPC containing the Nup62 complex like the full length Nup93. Hence the middle domain was not essential for assembling pores at the end of mitosis. This was an intriguing result and hence we decided to go into more detail to check for the recruitment of Nup62 complex members in these nuclei. Although mab414 is a mouse monoclonal specific antibody and gives a good staining pattern for the NPC assembly we nevertheless wanted to check for Nup62 and Nup58 (members of the Nup62 complex) with antibodies specific for these nucleoporins. These antibodies were polyclonal and generated in house in rabbits.

For both Nup62 and Nup58 we observed the same staining pattern. In case of untreated extracts the nuclei showed a normal, smooth nuclear rim staining for both the nucleoporins. The same was observed in the nuclei that were assembled using mock depleted extracts. When the nuclei were assembled with Nup93 depleted extracts we observed a faint background staining (this is due to some level of non specific binding of the antibody). The absence or negligible background staining of Nup62 and Nup58 in this situation suggested that the proteins are not recruited to the assembling NPC. This was because Nup93 was absent from these nuclei hence no pores were assembled and Nup62 complex could not be recruited to the pore. (Please note that the levels of Nup62 and Nup58 are not altered upon Nup93 depletion (fig. 2.2) in comparison to mock depleted extracts but they just could not be recruited to the pore due to the absence of its anchor protein that is Nup93) When the full-length Nup93 was added back to Nup93 depleted extracts and then the nuclei assembled, the NPC assembly was rescued and both Nup62

and Nup58 were recruited to the pore via the N-terminus of Nup93, which was now part of the assembling NPC. This is illustrated in fig. 2.17 by a smooth nuclear rim specific staining for both Nup62 and Nup58 (also see fig. 2.13). In case of nuclei assembled with the C-terminus of Nup93 we again did not observe a specific nuclear rim recruitment of Nup62 and Nup58 as the N-terminus of Nup93 was missing. The staining observed in fig. 2.17 was a background non-specific. Please note in fig. 2.13 we used an affinity purified antibody for both Nup62 and Nup58, which gave a more specific staining. When the nuclei were assembled using Nup93 depleted extracts supplemented with the fusion protein (N+C-terminus: aa 1-175 + 608-820 of Nup93) we observed a smooth nuclear rim specific staining for both Nup62 and Nup58. Thus in the absence of the middle domain of Nup93 the Nup62 complex could be recruited to the assembling pore precisely. The middle domain of Nup93 was not required for NE and NPC assembly. Also it was not necessary to recruit the Nup62 complex to the NPC that is involved in central channel formation. Nevertheless we could not rule out other functions that the middle domain of Nup93 might have in relation to the NPCs. More light will be shed on this in the discussion section 3.1.5.

(C)
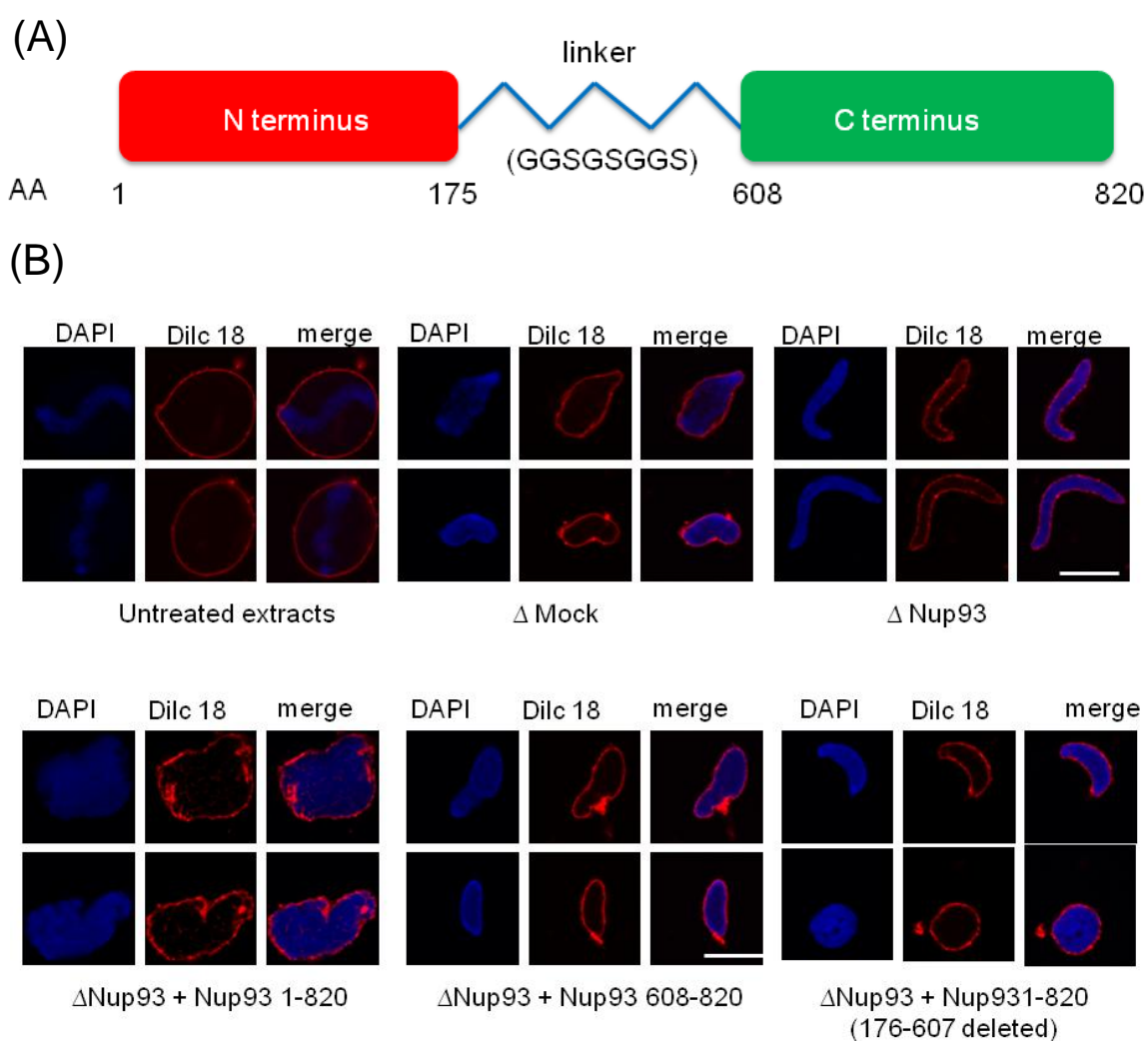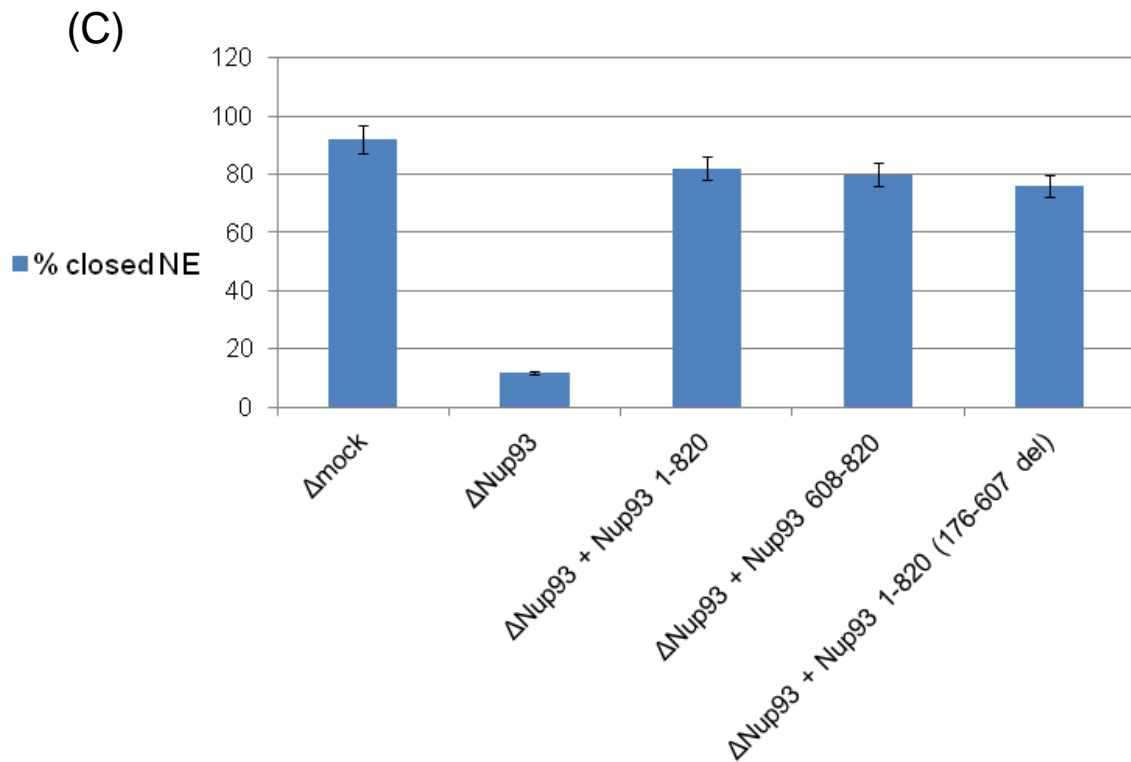
Figure 2.15: The middle domain of Nup93 is dispensable for nuclear envelope formation. (A) Schematic representation of the design of the fusion construct for *Xenopus laevis* Nup93. The construct shows the fusion between the N-terminal coiled-coil domain of Nup93 (aa 1-175) and the C-terminal domain of Nup93 (aa 608-820). A linker of 8 amino acids was inserted between the N and the C-terminal domain. The numbers correspond to the amino acids of *Xenopus laevis* Nup93. G: glycine, S: seriene, red: N-terminus of Nup93, Green: alpha helical C-terminal domain of Nup93. aa 176-607 was deleted. (B) Nuclei were assembled using untreated, mock depleted, Nup93 depleted and Nup93 depleted [supplemented with full-length Nup93 (aa 1-820), C-terminus of Nup93 (aa 608-820) and the fusion construct lacking the middle domain of Nup93] extracts for 90 minutes. Nuclei were then fixed with 2% PFA+0.5% glutaraldehyde. Chromatin was stained with DAPI (blue) and membranes were visualized by the red DilC18 dye to check for the formation of a closed NE. Scale bar: 10µm. (C) Nuclei having a closed NE was counted. More than 100 randomly chosen chromatin substrates per reaction were checked for the closed NE. Average of three independent experiments is shown in the bar graph. The error bars show the total variation observed, which shows that the middle domain was

not essential for NE formation as in the presence of the fusion construct of Nup93 (ΔM domain) the nuclei could assemble and showed a closed NE.
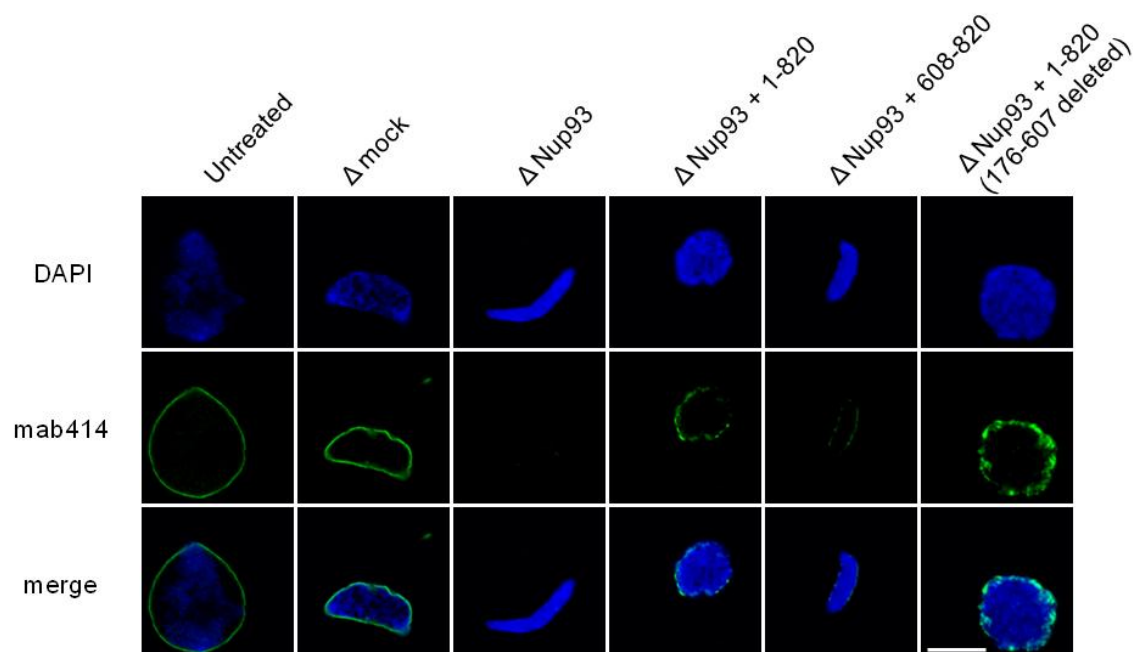
Figure 2.16: The middle domain of Nup93 is dispensable for nuclear pore complex formation. Nuclei were assembled using untreated, mock depleted, Nup93 depleted and Nup93 depleted [supplemented with full-length Nup93 (aa 1-820), C-terminus of Nup93 (aa 608-820) and the fusion construct lacking the middle domain of Nup93] extracts for 90 minutes. The nuclei were then fixed with 4% PFA and immunoflorescence was done using mab414 antibody (green, middle panel) and chromatin was stained using DAPI (blue, upper panel). The overlay is shown in the bottom panel. The nuclei were imaged using confocal microscopy. Bar: 10μm.
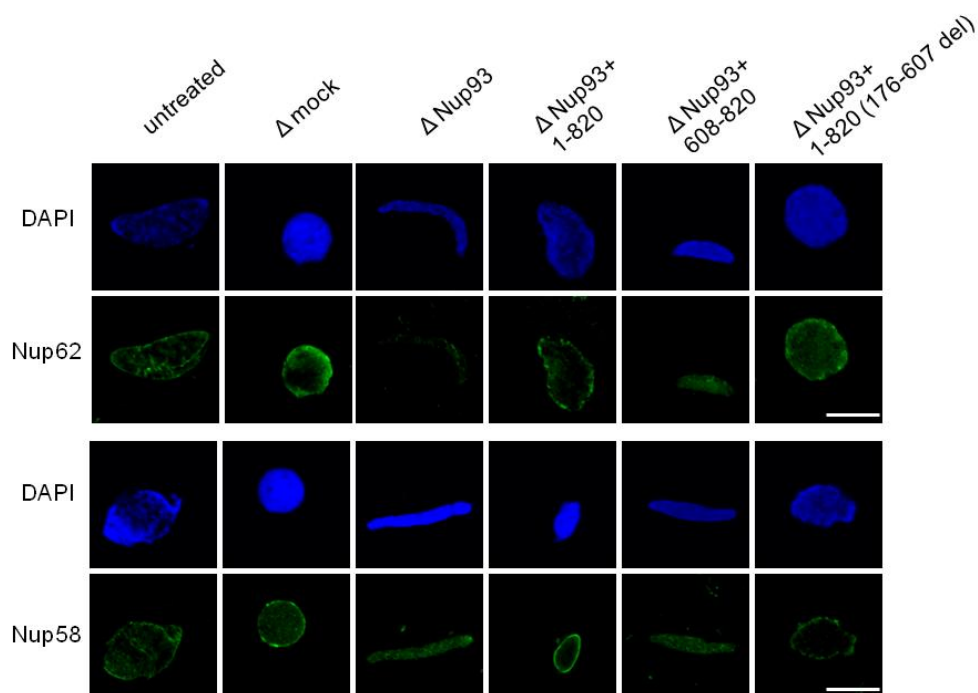
Figure 2.17: The middle domain of Nup93 is not essential for recruitment of the Nup62 complex to the assembling pore. Nuclei were assembled using untreated, mock depleted, Nup93 depleted and Nup93 depleted [supplemented with full-length Nup93 (aa 1-820), C-terminus of Nup93 (aa 608-820) and the fusion construct lacking the middle domain of Nup93] extracts for 90 minutes. The nuclei were then fixed with 4% PFA and immunoflorescence was done using antibodies against Nup62 (upper half, green) and Nup58 (lower half, green). Chromatin was stained using DAPI (blue). The nuclei were imaged using confocal microscopy. Bar: 10μm.

2.1.16. The C-terminus of Nup93 strengthens the Nup53-Nup155 interaction.

We were curious to know how the C-terminus of Nup93 might be contributing towards formation of a closed NE and to the formation of the structural backbone of the pore. Nucleoporin interactions are known to be essential for NPC assembly and can contribute in a number of ways to NPC formation and function (Vollmer et al., 2012; Hawryluk-Gara et al., 2008; Amlacher et al., 2011; Fahrenkrog et al., 2000). To address this question we went back to literature to see what is known about the interaction network of Nup93 in relation to the structural nucleoporins, which are part of the Nup93 complex. Nup53 for instance (member of the Nup93 complex) is known to interact with Nup93 via its N-terminal region (Fahrenkrog et al., 2000; Hawryluk-Gara et al., 2008; Amlacher et al., 2011; Vollmer et al., 2012 and our unpublished results). The interaction between Nup53-Nup93 is indeed essential for NPC assembly. Nup53 also interacts with Nup155 another member of the Nup93 complex via its C- terminus (Fahrenkrog et al., 2000; Hawryluk-Gara et al., 2008; Amlacher et al., 2011; Vollmer et al., 2102 and our unpublished results). Both Nup53 and Nup155 are essential for NPC formation and probably also the interaction between these nucleoporins (Vollmer et al., 2012; Hawryluk-Gara et al., 2008). These interactions result in an interaction network between Nup53-Nup93 and Nup155 (Onischenko et al., 2009; Amlacher et al., 2011). We were inquisitive to know whether the C-terminal domain of Nup93 (aa 608-820) has some sought of an effect or contribution to these interactions, which might play a role in establishing the structural backbone of the pore.

Previous experiments using immune precipitations from egg extracts done in our lab did not point out to a noticeable interaction between Nup93, Nup53 and Nup155. (Unpublished data and see fig. 1a in Theerthagiri et al., 2010)

This time we used GST pull down assays with full length GST Nup53 as bait and pulled out Nup155 from *Xenopus laevis* egg extracts. We observed a weak interaction between Nup53 and Nup155 (fig. 2.18). This interaction was strengthened when Nup93 C-terminus (aa 608-820) was present in the reaction. We expressed the C-terminal domain of Nup93 as a SUMO construct to allow for its detection in the western blot with anti SUMO antibody as shown in fig 2.17. We did not observe any strengthening of the interaction between Nup53 and Nup155 if the middle domain (aa 183-579) of Nup93 was part of the reaction. If the GST pull down was done using C-terminal fragment of Nup93 (aa 608-820) we did not observe its interaction with Nup155 (data not shown). As a negative control on the bait side we used GST Gp210 (nucleoplasmic domain) protein, which showed no interaction with Nup155. This did not change if Nup93 fragments (C: aa 608-820 or M: aa 183-579) were part of the reaction when Gp210 was used as bait. To be sure that the interaction and its strengthening are specific to Nup53-Nup155 we also probed the blots for other unrelated nucleoporins for example Nup98, Nup153 and observed no interaction with either GST Gp210 or GST Nup53 that were used as baits. Thus Nup53 formed a complex and an interaction network with Nup155 and Nup93. The Ed Hurt lab had also observed a similar complex formation recently where they showed these interactions in the fungus *Chaetomium thermophilum* (Amlacher et al., 2011). By this GST pull down assay and the nuclear assembly data we concluded that the C-terminus of Nup93 (aa 608-820) was indeed playing a crucial role in NPC assembly. It was essential and sufficient for NE formation. It strengthened the Nup53-Nup155 interaction and thereby contributed to the formation and stabilization of the structural backbone of the NPC.
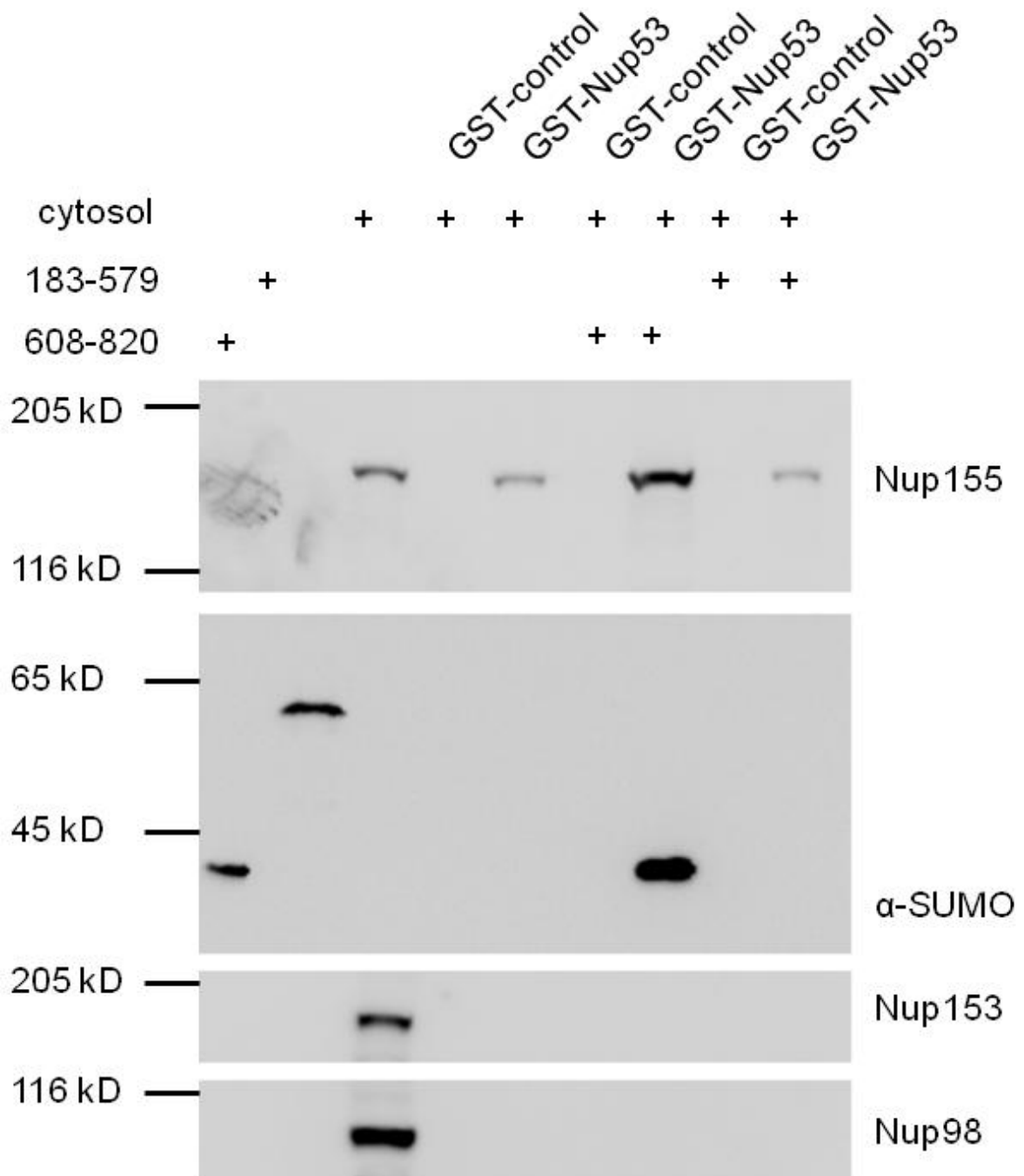
Figure 2.18: The C-terminus of Nup93 strengthens the Nup53-Nup155 interaction in Xenopus laevis egg extracts. GST pull down experiment was done using GST full-length Nup53 or GST Gp210 (nucleoplasmic domain) as baits. The GST proteins were coupled to GSH sepharose beads, blocked with BSA and incubated with the *Xenopus laevis* interphasic egg extract cytosol in the presence or absence of SUMO fused Nup93 protein fragments (middle domain of Nup93 (aa 183-579) or the C-terminus of Nup93 (aa 608-820). The eluates from the GST pull down experiment were analyzed using western blot

with antibodies against SUMO for detection of the different fragments of Nup93 or against Nup155, Nup153 and Nup98 to detect the corresponding proteins. In the western blot shown the first three lanes on the left hand side are inputs wherein 5% of the input of the SUMO recombinant Nup93 fragments and 2% of cytosol (egg extracts) were loaded. As shown we observed a binding of Nup155 to Nup53 bait but not to Gp210 (negative control). This interaction was strengthened when Nup93 C-terminal domain (aa 608-820) was part of the reaction and not when the middle domain of Nup93 (aa 183-579) was. We did not pull out unrelated nucleoporins from the egg extracts like Nup153 or Nup98, which showed that the interactions observed were specific in nature.

2.1.17. In vitro trimeric complex between Nup53-Nup93-Nup155 is important for formation of the structural backbone of the NPC.

We also wanted to confirm the trimeric complex between Nup53-Nup155-Nup93 in an in vitro, pure system using all recombinant proteins. This would help us to know how specific the interactions were amongst the proteins and the fact that these interactions were direct and not influenced by other factors that might be present in the *Xenopus laevis* egg extracts. To do this we generated bacterial lysate that expressed full-length Nup155 with NusA as a solubility tag. The C-terminus of Nup93 (aa 608-820) was expressed and purified from *E.coli*. We incubated the bait GST Nup53 with Nup155 bacterial lysate in the absence or presence of the C-terminus of Nup93. In the absence of Nup93 C-terminus we detected an interaction between Nup53 and Nup155 and this interaction was strengthened when the C-terminus of Nup93 was part of the reaction (fig. 2.19). As a negative control we used GST as bait. We did not detect its interaction with Nup155 with or without the C-terminus of Nup93. Thus our data suggested that the C-terminus of Nup93 (aa 608-820) was sufficient to bind Nup53, which in turn strengthened and stabilized the interaction between Nup53 and Nup155. This interplay of interactions amongst the members of the Nup93 complex was essential and promoted the formation of the structural backbone of the NPCs. This held true both in *Xenopus laevis* egg extracts and also the GST pull down experiment was done in a pure recombinant system.

All together with the cell biological and biochemical experiments done so far we concluded that Nup93 plays manifold roles in NE/NPC assembly and function. The N-terminus for instance recruits the central channel forming complex: Nup62 complex, which is in turn required for formation of an exclusion and transport competent nuclei. The C-

terminus on the other hand is involved in NE formation plays a crucial role in the formation of structural backbone of the pore. It does so by promoting the interaction between the central constituents of the scaffold of the NPC: that is Nup53 and Nup155. The middle domain is dispensable for NE and NPC assembly but nevertheless we cannot rule out if it has an additional function (for details see section 3.1.5. in discussion). Thus Nup93 forms a link between the structural backbone and the functional central channel of the NPC. It is indeed surprising and interesting that both Nup188 and Nup205 together are not essential for NE and NPC assembly.
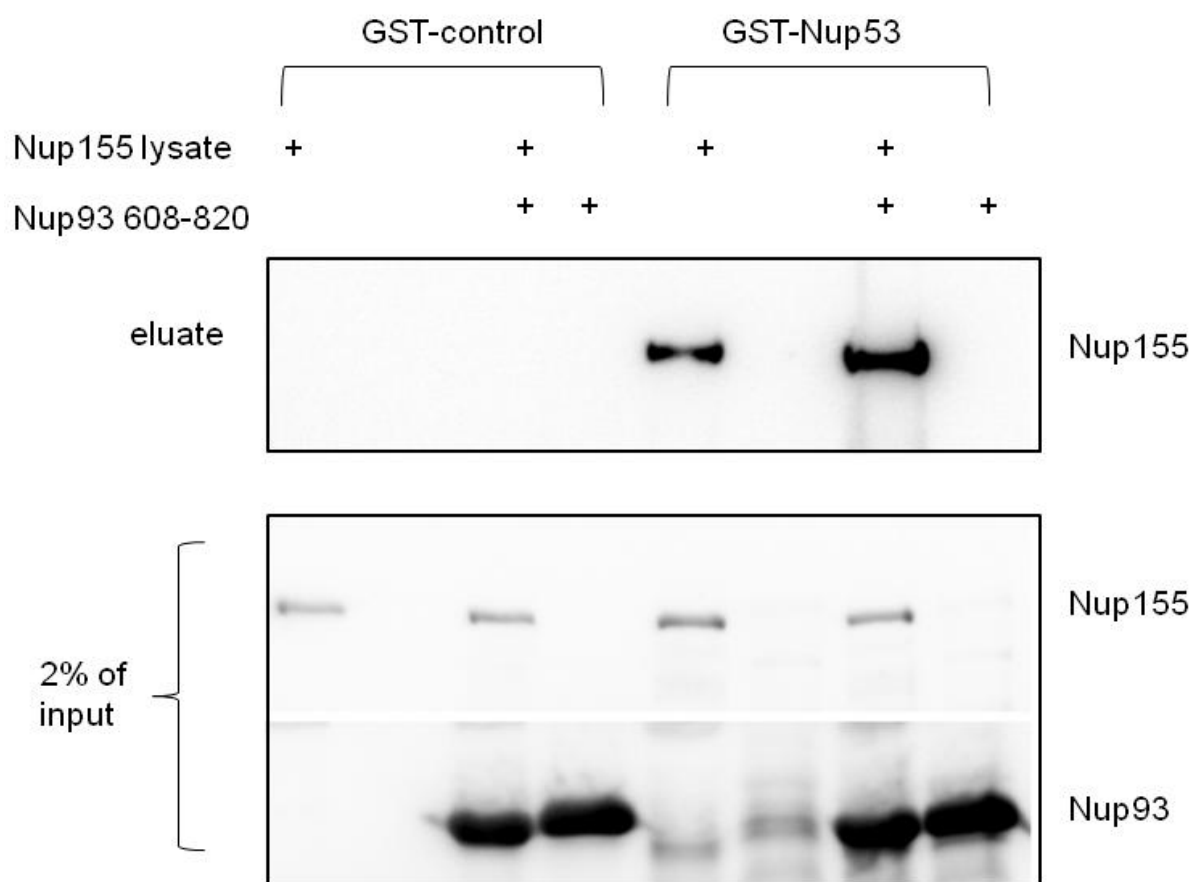
Figure 2.19: Nup53-Nup155 interaction is stabilized by the Nup93 C-terminus in vitro. GST pull down experiment was done using either GST alone or GST full-length recombinant Nup53 as baits. The GST proteins were expressed and purified from E.coli and coupled to GSH sepharose beads. The beads were then blocked with BSA and then incubated with bacterial lysate expressing NusA fused *Xenopus laevis* Nup155 in the presence or absence of the protein fragment that is the C-terminus of Nup93 (aa 608-820).

Input and eluates were analysed by western blot using anti-His$_6$ antibodies to detect the GST baits and Nup155. Due to the removal of the His$_6$ tag from the Nup93 protein fragments used during the TEV protease digest we could not detect it in the elution but we did see the protein in the input using the His$_6$ antibody (elution was done by TEV protease). We detected the binding of Nup53 with Nup155, which was strengthened in the presence of the C-terminus of Nup93. We did not observe any binding to GST (negative control) alone. All the proteins and lysates used were recombinant and hence show direct interaction and complex formation between Nup93-Nup53 and Nup155 in vitro.

2.2. Regulation of the cell cycle dependent interaction between Nup53 and the Nup93-205 complex.

The nuclear envelope (NE) and the nuclear pore complex (NPC) are both dynamic in nature during the course of the cell cycle. At the onset of mitosis the NE and the NPCs break down and this process has to be reversed at the end of mitosis. The assembly and disassembly of NPCs occurs in a coordinated fashion. For instance interactions between nucleoporins (Nups) have to be regulated throughout the cell cycle to achieve a regulated NE/NPC assembly and disassembly. When the NPCs disassemble the soluble Nups are dispersed throughout the cytoplasm. During this course of events interactions between Nups have to be disrupted (Kutay and Hetzer, 2008; Antonin et al., 2008; Güttinger et al., 2009).

Many Nups are post translationally modified during the cell cycle. For example phosphorylation of Nups and lamins is a major trigger for NPC breakdown (Laurell et al., 2011; D' Angelo and Hetzer, 2008). A major kinase involved in this process is the Cdk1/cdc2. A number of Nups like Nup98, Gp210, members of the Nup93 complex like Nup53, Nup107-160 complex members are known targets of cdk1 (Lusk et al., 2007; Favreau et al., 1996). Not only phosphorylation but also other posttranslational modifications like ubiquitination, and sumolytion etc might also regulate the interactions between Nups. Nucleoporins interactions or interactions between nups and chromatin can also be regulated by transport receptors like importin beta along with the Ran GTP cycle. To achieve this dynamicity in the NPC the Nup-Nup interactions have to break and reform, which is regulated precisely during the cell cycle by various posttranslational modifications and transport, factors.

As explained in section 2.1, the interplay of interactions among the members of the Nup93 complex plays a crucial role in NPC assembly and function. We were curious to know if some of these interactions occur in a cell cycle dependent fashion. If so it will be interesting to understand the regulation of this cell cycle dependency and the importance of these interactions in NPC assembly/ disassembly and function. One such interaction we choose to study is between Nup53 and the Nup93-205 complex.

2.2.1. Nup53 interacts with the Nup93-205 complex in a cell cycle dependent fashion.

To check for the interaction between Nup53 and the Nup93-205 complex during the cell cycle, we decided to approach this by performing a GST pull down experiment. The idea was to make interphasic or post mitotic extracts (where the *Xenopus laevis* eggs have been activated by calcium based ionophore to enter into interphase) and mitotic extracts (prepared by adding calcium chelators and active cyclin B) and use these extracts as a source of the Nup93-205 complex. For this we used the full length Nup53 as bait and as a negative control we used GST Gp210 (nucleoplasmic domain) as bait. The GST proteins used as baits were coupled to glutathione sepharose beads and blocked with BSA to prevent non-specific binding of proteins from the extracts. The glutathione sepharose coupled to either GST Nup53 or GST Gp210 was then incubated with either mitotic or interphasic extracts, to pull out the Nup93-Nup205 complex. The beads were also incubated with buffer alone (PBS) alone to check for non-specific binding on the beads. Then the beads were washed and the eluted samples were run on an SDS- PAGE gel. The gels were further processed for western blotting to probe for the interacting partners with Nup53. As shown in fig.2.20 we probed for Nup205, Nup93, Nup188 and Nup98 in the start material (egg extracts) that is mitotic and interphasic extracts. We loaded 2% of the input on the gel. We observed that when GST Nup53 was used as bait we could pull out both Nup93 and Nup205 from interphasic but not from mitotic extracts. Both Nup93 and Nup205 are known to form a complex in interphasic and mitotic extracts (Theerthagiri et al., 2010). We detected no interaction with Nup188, which suggested that Nup53 binds to the Nup93-205 complex but not to the Nup93-188 complex. To be sure that the interaction between Nup53 and the Nup93-205 complex was specific we also probed for Nup98: an unrelated Nup. We did not observe any interaction between Nup53 and Nup98. We also did not observe any non-specific nup binding to beads (gsh sepharose coupled to GST nup53 or GST Gp210) incubated with buffer alone. When GST Gp210 was used as bait we did not observe any binding of Nup93, Nup205, Nup188 or Nup98. Thus we concluded that the binding of Nup53 to the Nup93-205 complex was specific. This interaction occurred only in interphase and not in mitosis and hence it was a cell cycle dependent interaction. This was a very exciting result for us and we thus decided to follow this up and understand how this interaction is regulated and what its role in NPC assembly and function is. It suggested to us that Nup53 binds to the Nup93-205 complex in interpahse,

which aids in NPC assembly. On the other hand the loss of Nup53 and Nup93-205 interaction in mitosis could be crucial for NPC disassembly.
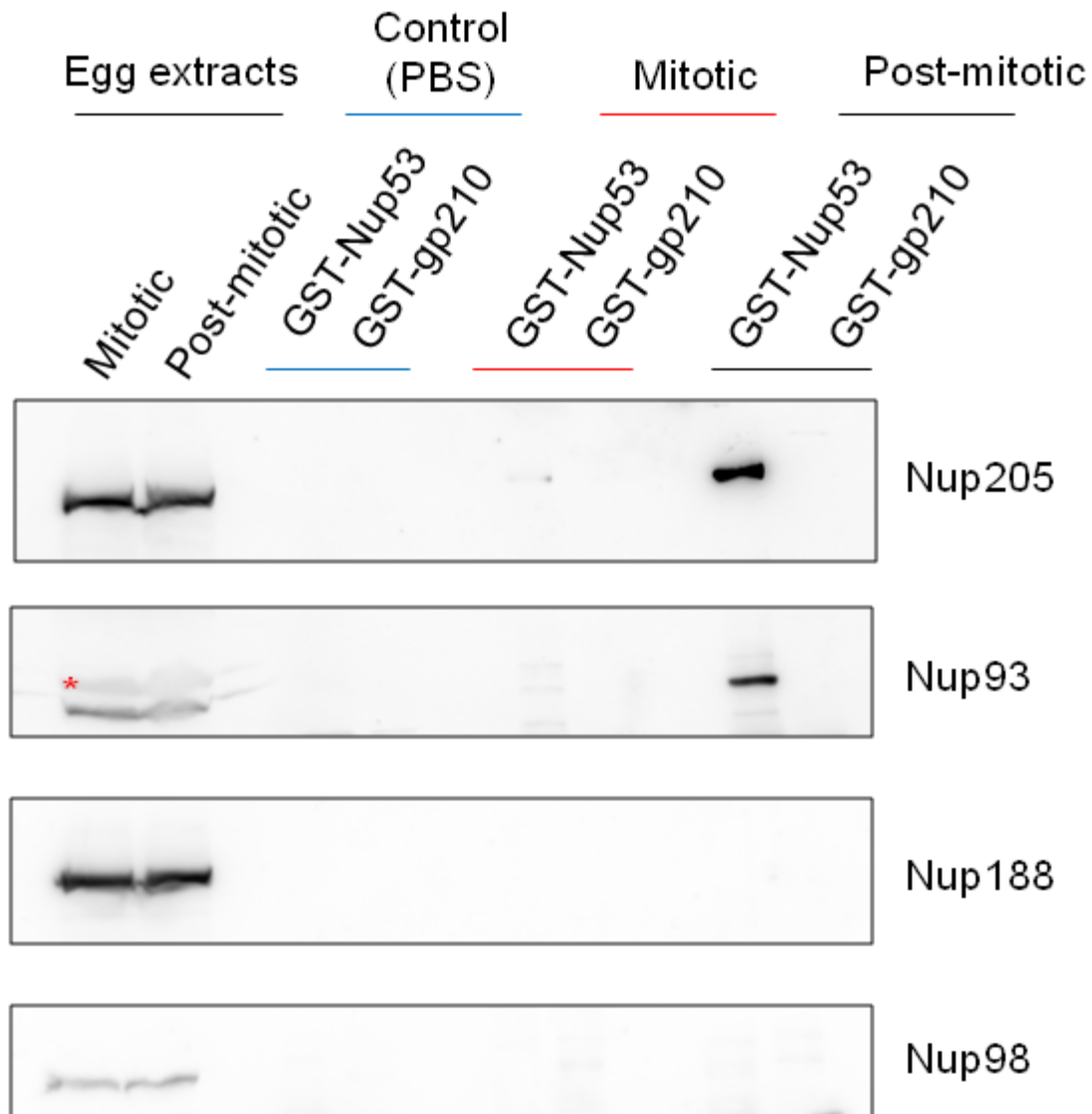
Figure 2.20: Nup53 interacts with the Nup93-205 complex in a cell cycle dependent fashion. GST pull down was done using full-length GST Nup53 or GST Gp210 (nucleoplasmic domain) as baits that were expressed and purified from E.coli. The GST proteins were coupled to GSH sepharose beads and pre blocked with BSA. The beads were then incubated with mitotic or interphasic (post mitotic) extracts or with buffer alone (1X PBS) as indicated in the figure. The eluates from the GST pull down were analysed by western blotting using antibodies against Nup205, Nup93, Nup188 and Nup98. As shown both Nup93 and Nup205 bind to Nup53 in post-mitotic but not in mitotic extracts. On the left hand side of the western blot the first two lanes is 2% input (starting material: mitotic

and post mitotic extracts), which shows the levels of Nup93, Nup188, Nup205 and Nup98 in the start material. We did not observe any binding to GST Gp210, which acts as a negative control. Also we did not observe binding of Nup188 and Nup98 to GST Nup53 suggesting the specificity of the interactions observed.

2.2.2. Transport receptors like importin beta do not regulate the interaction between Nup53 and the Nup93-205 complex.

Next we wanted to understand how the cell cycle dependent interaction between Nup53 and the Nup93-205 complex is regulated? Transport receptors like importin beta are known to regulate interaction between Nups during the cell cycle. Importin beta for instance is known to bind a number of Nups during mitosis like Mel28 (Asaf Rotem et al., 2009), Nup53 (Corine K. Lau et al., 2009) etc. The binding of Nups to importin beta sequesters these Nups during mitosis and at the end of mitosis concomitant with the post mitotic NPC assembly this interaction is lost. The loss of this interaction is mediated by the high concentration of Ran GTP near the chromatin due to the presence of active RCC1, which regulates the GTP/GDP cycle of Ran. Due to high concentration of Ran GTP in the vicinity of the decondesing chromatin the Nups are released from importin beta as Ran binds to it (D' Angelo and Hetzer, 2008). These Nups are now available for post mitotic NPC assembly. Based on this existing knowledge we hypothesized that transport receptors like importin beta could regulate the interaction between Nup53 and the Nup93-205 complex. The idea was that in mitosis importin beta would bind Nup53 hence Nup53 could no longer bind the Nup93-205 compelx. This would be reversed in interphase wherein importin beta will dissociate from Nup53 and then it could bind the Nup93-205 complex as illustrated in fig.2.21. To know if this hypothesis held true we did a GST pull down experiment as before but this time in the presence of RanQ69L. RanQ69L is a constitutive active mutant of Ran that cannot efficiently hydrolyze GTP and is insensitive to the action of Ran-GAP (Klebe C et al., 1995). If our hypothesis was valid then the RanQ69L can bind importin beta permanently in the extracts and hence Nup53 would be free to bind the Nup93-205 complex even in mitosis. So to confirm this we made interphasic and mitotic extracts and did the GST pull down experiment as before +/- RanQ69L. We used GST Nup53 as bait to pull out Nup93 and Nup205 from extracts. As described in section 2.2.1. we blocked the beads (glutathione sepharose beads coupled to the full length Nup53) first with BSA and then incubated with them with either interphasic or mitotic extracts +/-

RanQ69L. The beads were then washed and eluted samples were further processed for western blotting in order to probe for Nup205 and importin beta. The start (2% of input of egg extracts: mitotic and interphasic +/- RanQ69L) was also loaded on the gel to check for Nup205 and importin beta. As shown in fig.2.21 we observed the binding of Nup205 to Nup53in interphasic extracts (+RanQ69L) as before. In case of mitotic extracts where no RanQ69L was added we did not see any interaction between Nup53 and Nup205 as expected. When RanQ69L was added to mitotic extracts we still did not observe any binding between Nup53 and Nup205. The same binding pattern was observed for Nup93 (data not shown). The RanQ69L added was indeed functional, as we did not observe any interaction between Nup53 and importin beta in both interphasic and mitotic extracts (+ RanQ69L). The RanQ69L permanently sequestered the importin beta, which could not henceforth bind Nup53. On the other hand we did detect binding of Nup53 and importin beta when RanQ69L was not added (faint band, fig.2.21). Hence from this data we concluded that although Nup53 does bind to importin beta in mitosis it does not regulate the interaction between Nup53 and the Nup93-205 complex during the cell cycle.
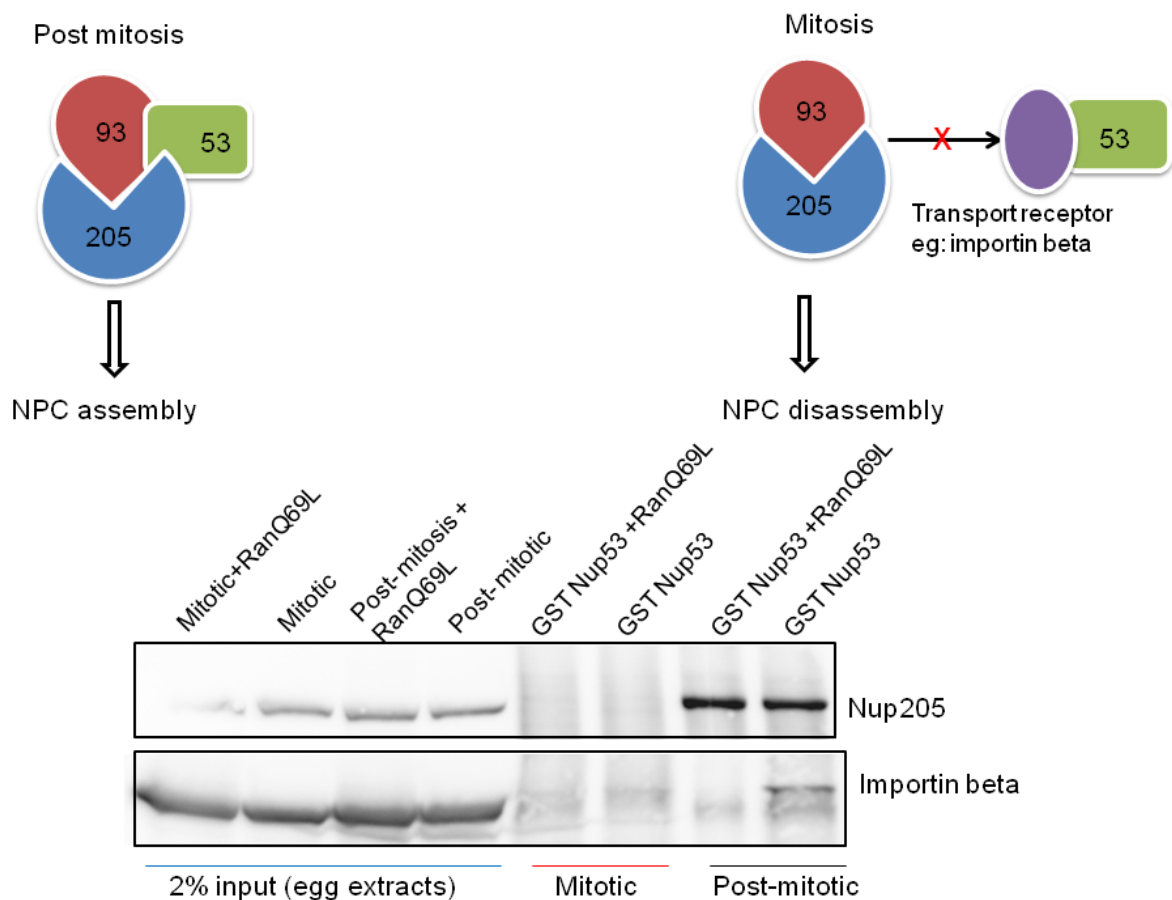
Figure 2.21: Transport receptors do not regulate the cell cycle dependent interaction between Nup93-205 complex and Nup53. GST pull down experiment was done using full-

length GST Nup53 as bait, which was expressed and purified from E.coli. The GST Nup53 was coupled to GSH sepharose beads and blocked with BSA. The beads were then incubated with either mitotic or post mitotic extracts +/- RanQ69L where indicated. The eluates were analysed by western blotting using antibodies against Nup205 and importin beta. On the left hand side of the western blot the first four lanes show the levels of Nup205 and importin beta in the start material (2% input: post mitotic and mitotic egg extracts +- RanQ69L). As shown the addition of RanQ69L to either mitotic or post mitotic extracts did not change or abolish the binding of Nup53 to Nup205 as they still interact with each other in post mitotic but not in mitotic extracts (+/- RanQ69L). Same binding pattern was observed for Nup93 binding to Nup53. The cartoon in the top panel depicts the hypothesis of the experiment wherein transport receptors like importin beta (purple) could regulate the cell cycle dependent interaction between Nup53 and Nup93-205 complex. But this does not hold true based on the result obtained by the GST pull down experiment shown below it.

2.2.3. Mapping the binding region of the Nup93-205 complex on Nup53.

We were also interested in mapping the minimal binding region of the Nup93-205 complex on Nup53. This would make our studies easier as expressing the full-length protein was difficult due to degradation problems. It would also be important for our future experiments as we can do further analysis with the minimal fragment of Nup53. This narrowing down will also helps us to design the mutants of Nup53 which do not bind or bind constitutively to the Nup93-205 complex and test these mutants in the NPC assembly reaction. Thus we decided to map the binding region of the Nup93-205 complex on *Xenopus laevis* Nup53. In order to this we generated many GST truncations of Nup53, which would be used as bait protein. With the fragments generated we covered the entire length of Nup53. We also generated very short fragments in order to really map the minimal binding region. Some of the constructs tested are shown in fig.2.22. To start with we cloned larger fragments of Nup53 into pet28e vector (GST tag). The protein was expressed and purified from *E.coli*. The GST Nup53 was coupled to glutathione sepharose beads and beads were blocked with BSA to prevent any non-specific binding from the extracts. The beads coupled to different Nup53 fragments were incubated with interphase egg extracts to check for Nup93-205 binding. The beads were washed and the eluted samples were further processed for western blotting to check for Nup93 and Nup205

binding. The beads as before were also incubated with buffer alone to check non- specific binding to beads itself. Nup53 has a RRM (RNA recognition motif) domain (in *Xenopus laevis*: aa 162-242) (Handa et al., 2006). Previous GST-pull down experiments done in our lab had shown that the C- terminal region of Nup53 does not bind the Nup93-205 complex. Thus we cloned several truncations within the large N-terminal region of Nup53 and expressed them as GST fusion proteins to use as baits. We also wanted to know if the RRM domain is essential for binding to the Nup93-205 complex. The truncations were generated within GST Nup53 aa 1-267. As shown in fig. 2.22 we observed no binding of both Nup205 and Nup93 with the GST Nup53 fragments: aa 78-136, 130-267, 78-166, 162-267 (RRM domain), 93-267 and 52-136. We did observe a faint binding with GST Nup53 aa 1-77 and a strong binding with Nup53 aa 1-166. The binding to Nup205 was highly strengthened (in comparison to the start: interphase extracts) if the RRM domain was part of the GST Nup53 fragment used (see the Nup205 binding in the lane aa 1-267 Nup53). The negative control on the bait side (GST) showed no binding to the Nup93-205 complex. The beads showed no non-specific binding as seen by the blot of buffer control. Thus by the above mentioned GST pull down experiments we concluded that the minimal binding region of the Nup93-205 complex lies in the N-terminus (approx. aa 1-77). Although this is sufficient to bind Nup93-205 complex but the binding is strengthened if the RRM domain is part of the construct (Nup53 aa 1-267). The RRM domain itself (Nup53 aa 162-267) showed no binding to the Nup93-205 complex as it was missing the N-terminal half of Nup53, which was crucial for the binding.

Fig.2.23 summarizes the results from the various GST pull down experiments done to map the binding region of Nup93-205 complex on *Xenopus laevis* Nup53. The summary shows that the N-terminal half of Nup53 was necessary to bind Nup93 and Nup205. The RRM domain of Nup53 was important to achieve a strong binding to Nup93-205 complex. The C-terminal domain of Nup53 did not contribute to the Nup93-205 complex binding.
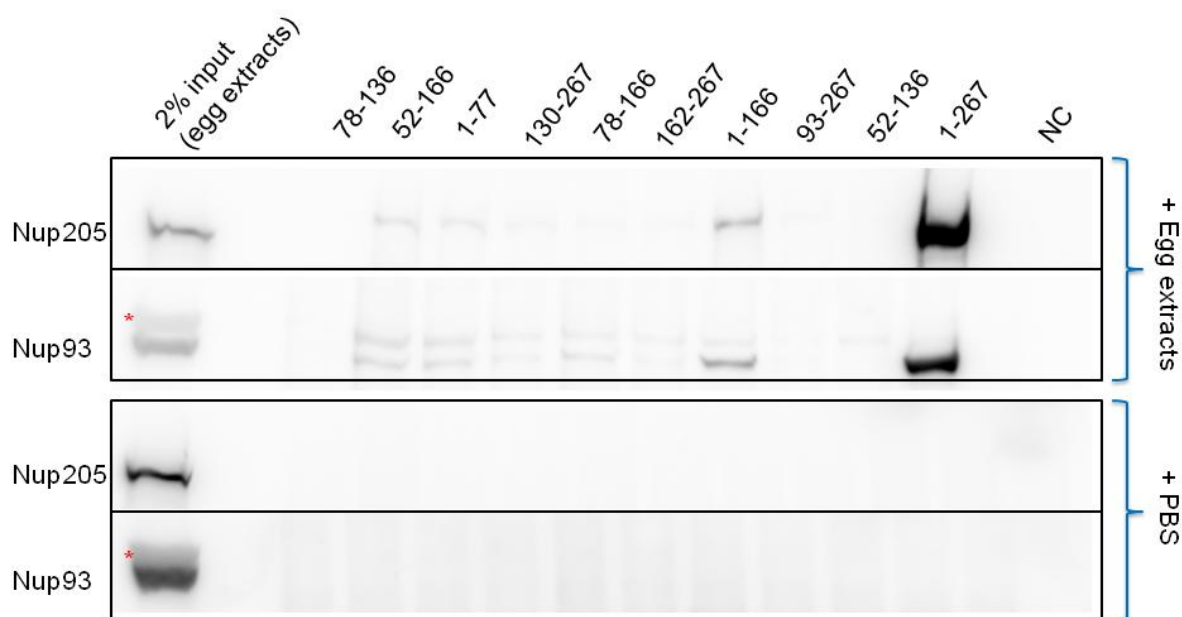
NC: GST protein
Numbers correspond to GST Nup53 constructs used

Figure 2.22: Nup93-205 complex binds at the N-terminus of Xenopus laevis Nup53.
GST pull down was done using different fragments of *Xenopus leavis* GST Nup53 or GST alone as baits. The baits were expressed and purified from E.coli. The proteins were then coupled to GSH sepharose beads and blocked with BSA. The beads were incubated with interphase egg extracts or with buffer alone (1X PBS) where indicated. The numbers indicate the amino acids of the GST Nup53 constructs used. NC: refers to negative control. The eluates were analyzed by western blotting using antibodies against Nup205 and Nup93. On the left hand side of the western blot the first lane represents 2% input (start material that is interphase egg extracts), which shows the levels of Nup205 and Nup93 in the start material. * Asterisk refers to the cross reactivity detected by the Nup93 antibody. As shown in the western blot we observed a binding to Nup205 when GST Nup53 aa 1-166 was used as bait. We also observed a faint binding to GST Nup53 aa 1-77. No binding was observed to Nup205 when various N-terminal truncations of Nup53 were used (aa 78-136, aa 130-267, aa 78-166, aa 162-267 {RRM domain}, aa 93-267 and aa 52-136). We observed a very strong and enriched binding to Nup205 when the N-terminus + RRM domain were used as bait. (GST Nup53 aa 1-267) No binding was observed when GST was used as bait (NC: negative control). Also no non-specific binding was observed when the GST proteins were incubated with buffer alone (1X PBS). The same binding pattern was observed for Nup93 in all the GST pull downs done. Thus from the GST-pull down experiment shown above we could conclude that Nup93-205 complex binds on the N-

terminal region of *Xenopus laevis* Nup53 and this interaction is strengthened in the presence of the RRM domain of Nup53.
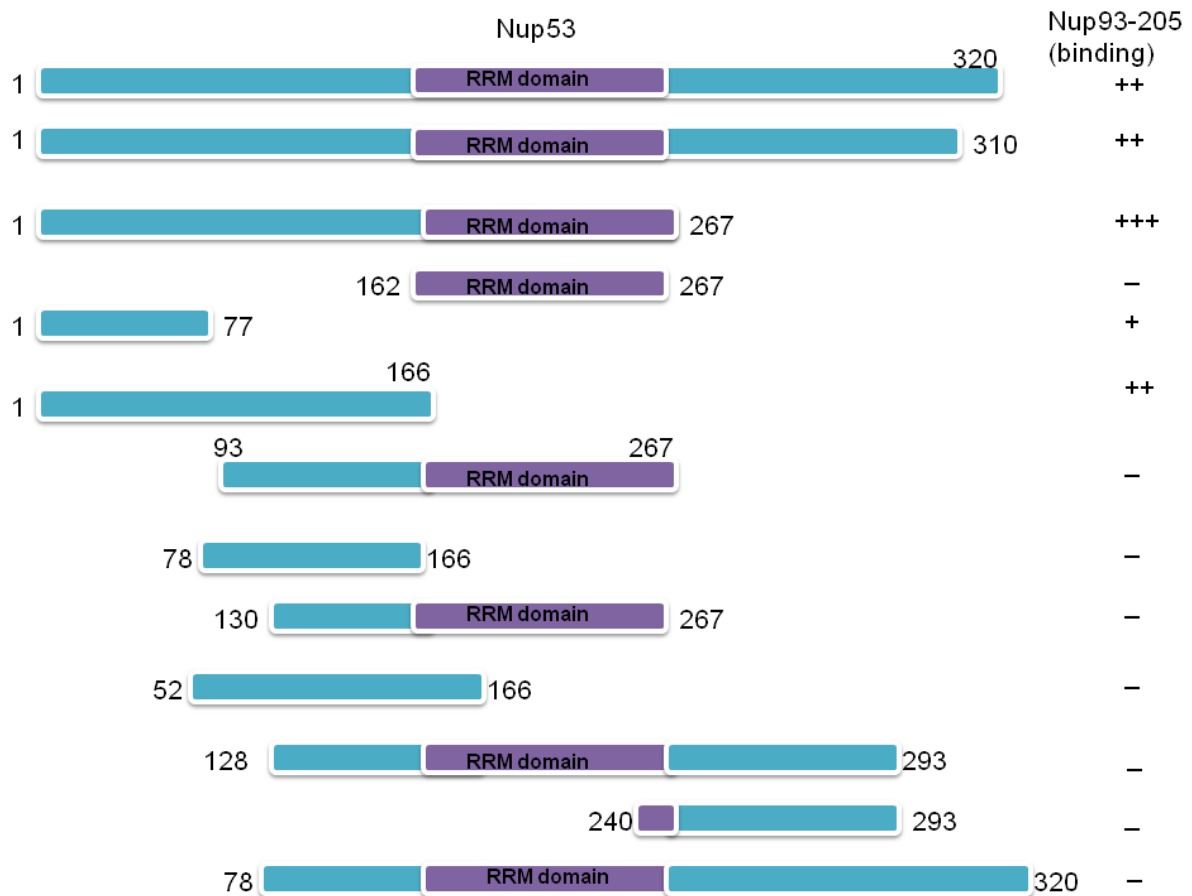
Figure 2.23: Summary of the mapping of the binding region of the Nup93-205 complex on Nup53. The cartoon shows the schematic representation of the constructs used (GST Nup53) and their binding to Nup93-205 complex. The numbers correspond to the amino acids of *Xenopus laevis* Nup53. The RRM domain is shown in purple and rest of the protein in green. The more the number of + means stronger the binding observed.

2.2.4. *Xenopus laevis* Nup53 is phosphorylated during the cell cycle.

We were very excited to investigate what kind of post translational modification might occur on Nup53 during mitosis and how it could regulate its binding to the Nup93-205 complex? Nup53 is also termed as a mitotic phosphoprotein of about 44kda (Stukenberg et al., 1997). So first we checked for phosphorylation of Nup53. For this we used phosphate-affinity manganese phos-tag SDS-PAGE that detects mobility shift of phosphoproteins. The basic principle of these gels is that they are prepared normally like acrylamide gels but with the addition of manganese phostag, which binds to polyacrylamide. The manganese

phostag can capture the phosphor monoester dianion R-OPO2$^-$ and shows preferential trapping of phosphorylated proteins, which is because of separation of the phosphoproteins from their non phosphorylated counter parts (Kinoshita et al., 2009 and fig.2.25 A). Thus we can see a clear shift in a phosphorylated protein as oppose to the non-phosphorylated version. Keeping this in mind we probed for Nup53 using anti Nup53 antibody on a western blot where we loaded mitotic and interphasic extracts (fig.2.25B). Indeed, Nup53 migrated slowly (as seen by the shift) in mitotic extracts as compared to the interphasic extracts (also see Vollmer et al., 2012). To be sure that difference in migration was specific to Nup53 we immune precipitated the endogenous Nup53 from the mitotic and interphasic extracts. As shown in fig. 2.25B we observed a dramatic shift of Nup53 in mitotic extracts as compared to interphasic extracts. This is a more significant shift than what we observed in the case of next gel (fig.2.24). Also it's worth noticing that even in the interphasic extracts the Nup53 that was immune precipitated ran at a higher molecular weight than expected (35kda). This might be because Nup53 was also phosphorylated in interphase but hyper phosphorylated in mitosis. This migration pattern was specific to Nup53 as in the IP done with control rabbit IgG antibodies we did not observe a band for Nup53 in either mitotic or interphasic extracts. Henceforth we concluded that Nup53 was modified during the cell cycle. More precisely phosphorylation could be a major kind of posttranslational modification occurring on Nup53 in both mitosis and interpahse as observed by a dramatic migration pattern in the phostag gels, which specifically detect the mobility shift in phopho proteins. Based on this we hypothesized that Nup53 was phosphorylated during mitosis, which disrupts its interaction with the Nup93-205 complex and this could be a trigger for NPC disassembly. At the end of mitosis (or in interphase) Nup53 might be dephosphorylated and hence could bind the Nup93-205 complex and aid in NPC assembly.

High resolution SDS PAGE – NEXT GEL
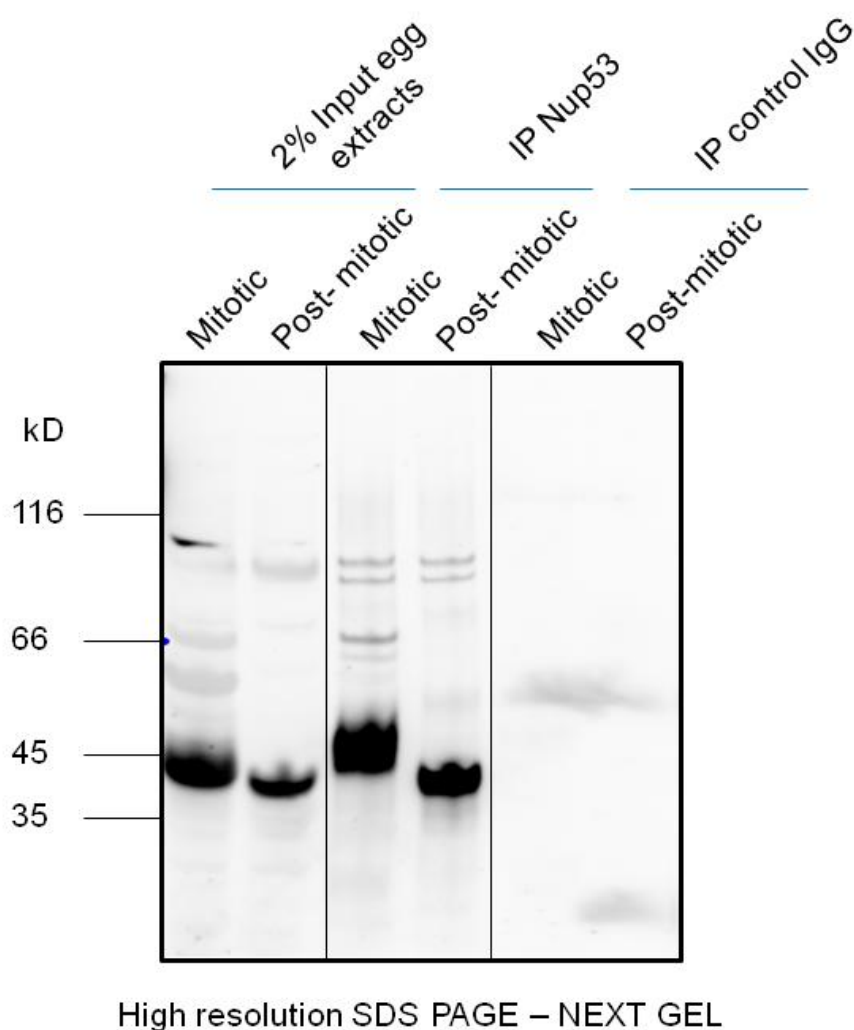
Figure 2.24: Xenopus laevis Nup53 is post-translationally modified during the cell cycle.
Xenopus laevis Nup53 was immune precipitated (IP) from both mitotic and post-mitotic (or interphasic) egg extracts using anti Nup53 antibody. As control we used rabbit IgG's. The eluates were analyzed on a western blot using antibodies against Nup53. We used NEXT-gel (high resolution SDS PAGE gel) for analysis of the eluates. On the left hand side of the blot the first two lanes represent input (2% egg extracts) that is start material and show Nup53 in both mitotic and post mitotic extracts. Note the slightly slower migrating Nup53 in mitotic extracts. The Nup53 that was immune precipitated from the mitotic extracts ran slowly as compared to the Nup53 that was immune precipitated from post mitotic extracts as seen by the different migrating pattern. We did not observe any non-specific Nup53 immune precipitated when control rabbit IgG were used as antibodies. This hinted towards a post-translational modification occurring on Nup53 in mitosis.

(A) Basic principle of the Phos-tag gels

(a)

(b)
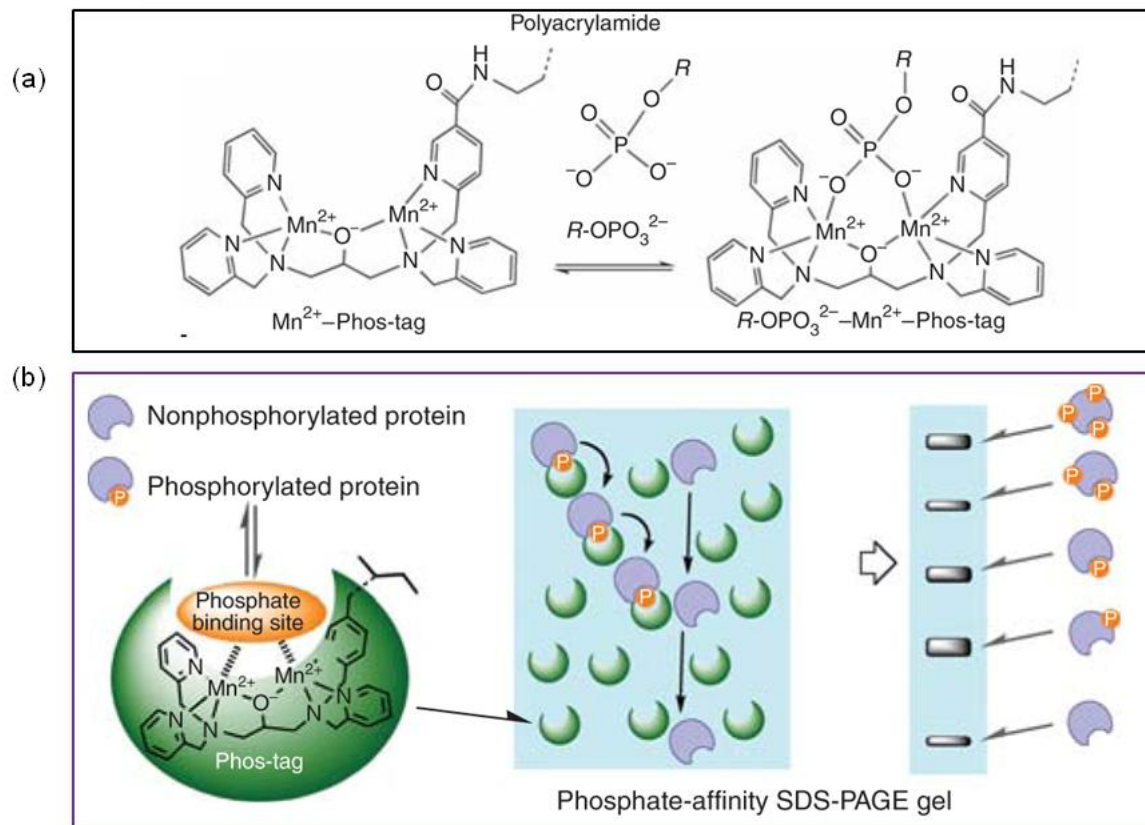
Kinoshita et; al Nature protocols, 2009

(B)
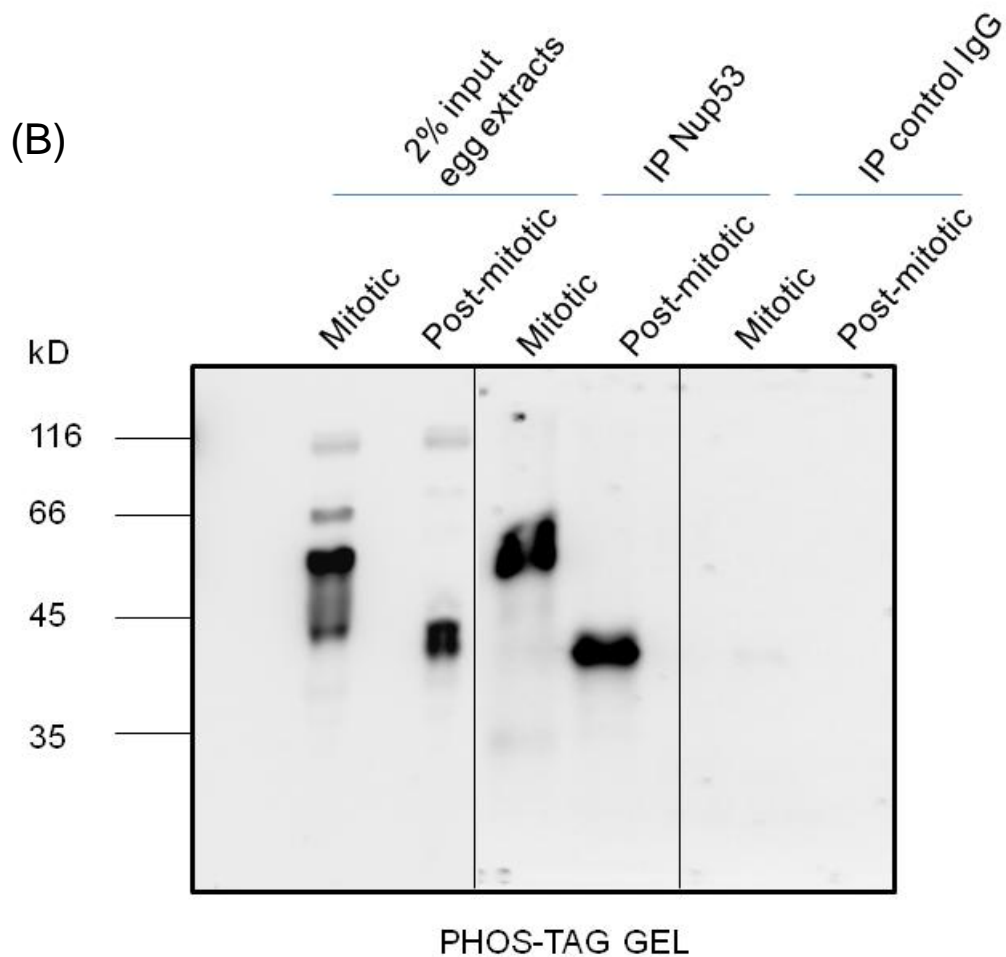
PHOS-TAG GEL

Figure 2.25: Xenopus laevis Nup53 undergoes phosphorylation during the course of the cell cycle. (A) Basic principle of a phostag-gel: The manganese ions bind the phostag compound and form a complex of R-OPO$_3$$^{2-}$Mn^{+2}-phostag (see the chemical reaction showing the complex formation {a}). The cartoon is shown in {b} where the phospho protein bound to manganese phostag runs slower than its non-phosphorylated counterpart and can be detected on the SDS PAGE as a slower migrating protein as it runs at a higher molecular weight. The more the number of phosphorylations the slower the protein would run on the gel. (B) IP of Nup53 was done from mitotic and post-mitotic (or interphasic) egg extracts using anti Nup53 antibody. As a control we used rabbit IgG's antibodies for the IP. As shown we observed a dramatic shift of Nup53 in mitotic and post-mitotic extracts. The mitotic Nup53 ran slowly and at a higher molecular weight as compared to interphasic (post-mitotic) Nup53. Please note that the interphasic Nup53 (or post-mitotic) also ran at a higher molecular weight than expected (35Kda). We observed no non-specific IP product when we used rabbit IgG's. The left hand side of the western blot (first two lanes) shows the input (2% of mitotic and post mitotic egg extracts) was loaded where we also observed a difference in migration pattern of mitotic and interphasic Nup53.

2.2.5. Phosphorylation of Nup53 during the cell cycle is reversed by the addition of Lambda phosphatase.

To be sure that phosphorylation is a major posttranslational modification occurring on Nup53 during the cell cycle we decided to test this by adding Lambda phosphatase in the system. For this both the mitotic and interphasic extracts were diluted in phosphatase buffer and incubated where indicated with Lambda phosphatase (fig.2.26) Samples were analyzed by a 12% SDS-PAGE and western blotting was done using anti Nup53 antibody. As shown in fig. 2.26 we observed that when the phophatase was added to the mitotic extracts, Nup53 no longer migrated slowly as compared to mitotic extracts without the phosphatase addition. Thus the lambda phosphatase reversed the phosphorylation of Nup53 in mitosis. In case of post mitotic /interphasic extracts when the phosphatase was added we also observed a shift in the migration of Nup53 as compared to interphasic extracts without phosphatase addition. This indicated that Nup53 was phosphorylated throughout the cell cycle but hyper phosphorylated in mitosis. This could be a way to

regulate the cell cycle dependent interaction between Nup53 and the Nup93-205 complex (also see Vollmer et al., 2012).
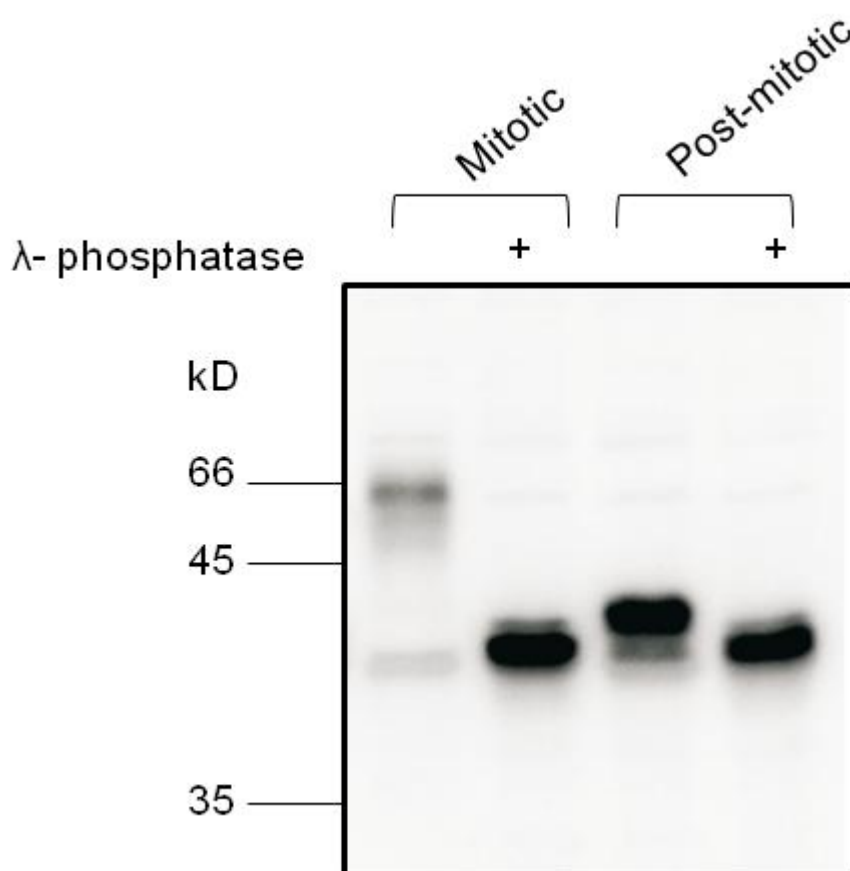
Figure 2.26: Nup53 is hyper phosphorylated during mitosis. 4 μl of mitotic (CSF arrested) or interphasic Xenopus egg extracts were diluted in 100 μl of phosphatase buffer (NEB) and incubated where indicated with 400 U lamda-phosphatase for 30 min at 30°C. Samples were analyzed by 12% SDS-PAGE and Western blotting using the *Xenopus* Nup53 antibody. Please note the different shifting of mitotic and interphasic Nup53 after phosphatase treatment indicating that Nup53 is a phosphoprotein throughout the cell cycle but hyperphosphorylated during mitosis.

2.2.6. Phosphorylation sites on Nup53 obtained by mass spectrometric analysis.

As our main goal was to find out the regulation of the cell cycle dependent interaction between Nup53 and the Nup93-205 complex, we wanted to hence know the specific amino acids that were phosphorylated on Nup53 in mitosis. With this information in hand we could design phospho mimicking and non mimicking mutants of Nup53 and test their

binding to the Nup93-205 complex in *Xenopus laevis* egg extracts. Eventually we would also test these mutants in NPC assembly and function. To do this we did an IP of the endogenous Nup53 from both mitotic and interphasic extracts. We performed this using anti Nup53 antibody coupled to protein A sepharose beads. Proteins eluted after IP were run on an SDS-PAGE gel. Gel sections from 35-45 kda were excised and the proteins were in gel digested by trypsin. Mass spectrometric analysis was done with the resulting peptide mixtures. For now is intriguing to see the table in fig.2.27 where the mitotic specific phosphoryltion sites are indicated in red. The amino acids: S94, T100, T288 and S291 were found to be specifically phosphorylated in mitosis. The table shows the mass spectrometric analysis of *Xenopus laevis* Nup53 peptides carrying the mitotic specific phosphorylation. We identified a number of mitotic specific phosphorylation sites on Nup53. A number of these were consensus sites for the kinase cdk1. This fits to the literature wherein Nup53 is known to be a target of cdk1 in both yeast and humans (Lusk et al., 2007; Blethrow et al., 2008). Interestingly for us the N terminal region of Nup53 that binds the Nup93-205 complex (see fig.2.23) contains two amino acids that were differentially phosphorylated in mitosis: S94 and T100. These were phosphorylated by cdk1 (also show in vitro in Vollmer et al., 2012) as they possess a consensus site for cdk1 (Blethrow et al., 2008). The consensus sequence for the phosphorylation site in the amino acid sequence of a CDK substrate is [S/T*]PX[K/R], where S/T* is the phosphorylated serine or threonine, P is proline, X is any amino acid, K is lysine, and R is arginine (Morgan David O. , 2007). This was very exciting for us as now we could design the phospho mimicking (S94ET100E) and the phospho non-mimicking (S94AT100A) mutants of Nup53 and test their binding to the Nup93-205 complex in the egg extracts. This would tell us if the mitotic specific phosphorylation on Nup53 could regulate its cell cycle dependent interaction with the Nup93-205 complex.

phosphopeptide	amino acid
PSAGAQFLPGFLLGDIPTPV**T**PQPR	T46
SPLH**S**GG**S**PPQPVLPTHK	S60, S64, S67
SPLHSGG**S**PPQPVLPTHK	S67
SIYDDVA**S**PGLGSTPR	S94
SIYDDVA**S**PGLGS**T**PR	S94, T100
MASFSVLHTPLSGAIPS**S**PAVFSPATIGQSR	S124
MASFSVLHTPLSGAIPSSPAVF**S**PATIGQSR	S131
V**S**TPSVSSVFTPPVK	S249
VS**T**PSVSSVFTPPVK	T250
VSTP**S**VSSVFTPPVK	S252
VSTP**S**VSSVF**T**PPVK	S252, T258
VSTPSVSSVF**T**PPVK	T258
SIRTPTQSVGTPR	S263
SIR**T**PTQSVGTPR	T266
SIRTPTQ**S**VGTPR	S270
TPTQSVG**T**PR	T273
TPTSADYQVVSDKPAPR	T288
TPT**S**ADYQVVSDKPAPR	T288, S291

Figure 2.27: Peptide with phospho sites identified in Xenopus laevis Nup53 by Mass spectrometric analysis. Shows the phospho sites mapped in *Xenopus laevis* Nup53 after the mass spectrometric analysis of IP of mitotic and interphasic Nup53. All the phospho sites identified are shown in red and the mitotic specific phospho sites we found were: S94, T100, S291 and T288. These were not identified in interphasic Nup53.

2.2.7. Cell cycle dependent phosphorylation of Nup53 does not regulate its interaction with the Nup93-205 complex.

Once we knew that there were amino acids in the N-terminal region of Nup53 (S94, T100) that were specifically phosphorylated in mitosis, we wanted to use this information to test for the cell cycle dependent interaction of Nup53 and the Nup93-205 complex.

For this we did in vitro mutagenesis and designed phospho mimicking and phospho non-mimicking mutants of Nup53 that are GST Nup53 1-267 S94ET100E and GST Nup53 1-267 S94AT100A respectively. We used the fragment of Nup53 aa 1-267 as this showed the strongest binding to both Nup93 and Nup205 (fig.2.22). The idea was to mimic the phosphorylated state of Nup53 (using the S94ET100E) mutant and first test it's binding in interphase extracts. If mitotic specific phosphorylation on these amino acids disrupts the interaction between Nup53 and the Nup93-205 complex in mitotic extracts then using the phospho mimicking mutants should also disrupt the interaction between Nup53 and the

Nup93-205 complex in interphase. To investigate this hypothesis we cloned these mutants and the wild type Nup53 as GST constructs. The proteins were expressed and purified from *E.coli* in order to be used as baits. We did a GST pull down experiment using interphasic extracts as a source of the Nup93-205 complex using Nup53 wild type and mutants as baits. As a negative control we used GST bait. The eluted samples were run on an SDS PAGE gel and processed further for western blotting. The blot was probed for Nup205, Nup93 and Nup98 (to check for specificity of the interaction). As shown in fig. 2.28 the wild type protein (GST Nup53 aa 1-267) showed a strong binding to Nup93 and Nup205. The phospho non-mimicking mutant (GST Nup53 1-267 S94AT100A) also showed a normal binding to the Nup93-205 complex and as expected behaved like the wild type Nup53. The phospho mimicking mutant (GST Nup53 aa 1-267 S94ET100E) also bound equally well to both Nup93 and Nup205. This was indeed surprising, as mimicking the phosphorylation state of Nup53 had no effect on binding to both Nup93 and Nup205. Thus we concluded that the cell cycle dependent interaction between Nup53 and the Nup93-205 complex is not regulated by the mitotic specific phosphorylation of Nup53. It could be that there are other factors or posttranslational modification on Nup93/Nup205 that might regulate this interaction. It could also be that we might have missed some sights via mass spectrometric analysis that might regulate the binding of Nup53 to the Nup93-205 complex. This will be further investigated in our laboratory.

As mentioned before the RRM domain of Nup53 significantly increased it's binding to the Nup93-205 complex (fig.2.22) we wanted to test this further. It is known that the RRM domain forms dimmers both in vitro and vivo (Handa et al., 2006; Vollmer et al., 2012). The dimerisation of the RRM domain is essential for the membrane binding activity of Nup53, which in turn is essential for the NPC assembly and function (Vollmer at al., 2012). We wanted to check if the dimerisation of the RRM domain of Nup53 contributes to its interaction with the Nup93-205 complex. To test this we cloned the RRM dimerisation mutant (GST Nup53 aa 1-267 F172EW203E), which leads to the formation of monomeric Nup53 (Vollmer et al., 2012). The protein was expressed and purified from *E.coli* and used as bait in the GST pull down experiment. We used interphasic extracts as a source of Nup93 and Nup205. As shown in fig.2.28 we observed a decrease in binding to both Nup93 and Nup205 if the RRM dimerisation mutant of Nup53 was used as bait as compared to wild type Nup53 (GST Nup53 aa 1-267). The drop in binding was quantified and it was roughly a 50% decrease. Thus we concluded that that the dimerisation of Nup53 contributed to its binding with Nup93-205 complex. We also observed that the dimeric

form of Nup53 also was crucial to its interaction with Nup155 (data not shown but see Vollmer et al., 2012).
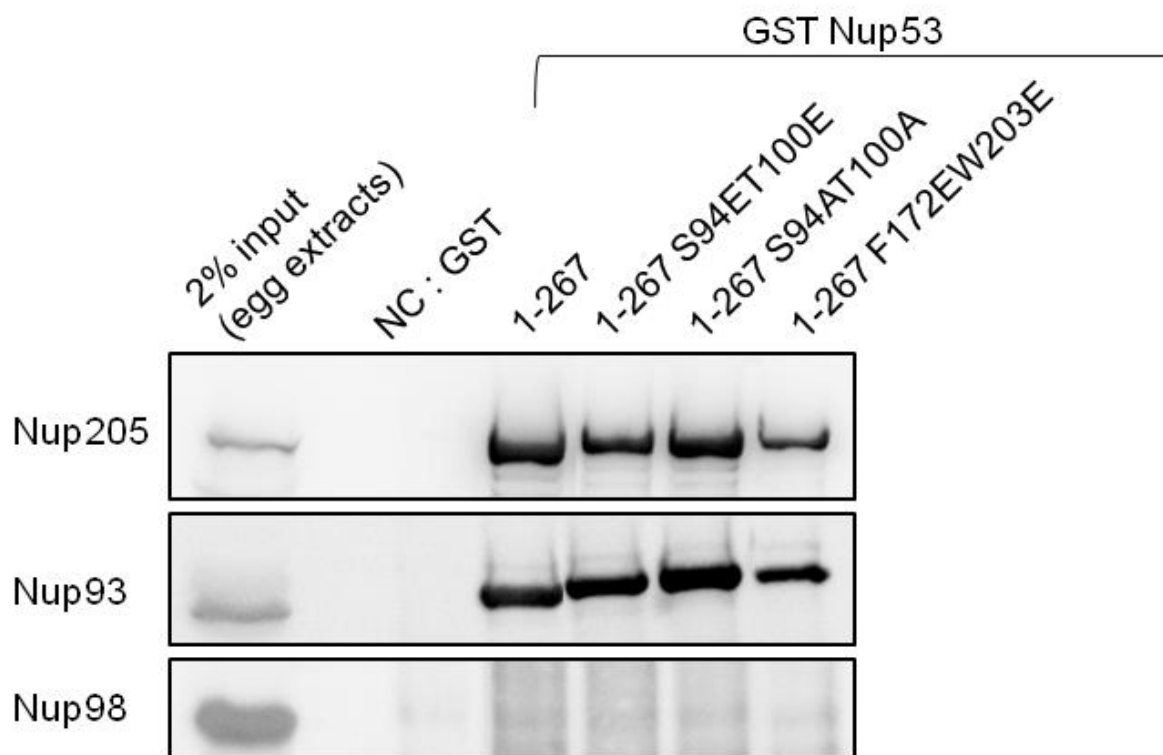
Figure 2.28: Mitotic specific N-terminal phosphorylation of Nup53 does not regulate its cell cycle dependent interaction with Nup93-205 complex. GST pull down was done using GST Nup53 (aa 1-267, different mutations and GST alone) as baits. The proteins were expressed and purified from E.coli and then coupled to GSH sepharose beads. The beads were blocked with BSA and then incubated with *Xenopus laevis* interphasic egg extracts. The eluates were analyzed by western blotting using antibodies against Nup93, Nup205 and Nup98. We tested wild type Nup53 (aa 1-267), phospho mimicking (aa 1-267 S94ET100E) and phospho non-mimicking (aa 1-267 S94AT100A) and the RRM dimer mutants (aa 1-267 F172EW203E) as baits for binding to Nup93 and Nup205. As shown we still observed a binding to Nup93 and Nup205 with phospho mimicking mutant of Nup53 (aa 1-267 S94ET100E) as compared to the wild type protein (aa 1-267). Phospho non-mimicking mutant (aa 1-267 S94AT100A) as expected also showed binding to Nup93 and Nup205. Interestingly the RRM dimer mutant (GST Nup53 aa 1-267 F172EW203E) showed a reduced binding to both Nup93 and Nup205. Negative control that is GST bait alone showed no binding to Nup93 and Nup205. On the left hand side 2% of input

(interphasic egg extracts) was loaded to see the levels of Nup93, Nup205 and Nup98. The binding observed of Nup53 to Nup93-205 complex was specific, as we did not see any binding of Nup98 when GST alone or GST Nup53 constructs were used as baits.

3. DISCUSSION

3.1. The C-terminal domain of Nup93 is essential for assembly of the structural backbone of the nuclear pore complexes.

3.1.1. Nup93 is essential for nuclear envelope and nuclear pore complex assembly (a feature conserved during evolution).

Nup93 is essential for NE and NPC formation as shown in our system using *Xenopus laevis* egg extracts. On depleting Nup93 from the egg extracts it led to block in NE/NPC assembly and most functions of the pore were compromised. This effect could be rescued by the addition of full-length recombinant Nup93. Nup93 has also been shown to be essential in yeast wherein a thermosensitive Nic96p (Nup93 homologue) at restrictive temperature leads to a decrease in NPC density (Grandi et al., 1993 and Zabel et al., 1996). Also RNAi of Nup93 in HeLa cells leads to a decrease in intensity of mab414, an antibody that recognizes FG repeat containing nucleoporins and is a widely used as an NPC marker (Krull et al., 2004). It has also been shown previously that immunodepletion of Nup93 from *Xenopus laevis* egg extracts followed by in vitro nuclear assembly reaction leads to a decrease in NPC staining (Grandi et al., 1997). But the function of Nup93 and the phenotypes observed were not clearly understood hence we wanted to explore in more detail the role of Nup93 in NPC assembly and function. It was indefinite if the decrease in NPC density and other effects observed upon depletion of Nup93 were due to Nup93 itself or because of co depletion of its interacting partners that are Nup188 and Nup205. To get a clearer picture about this we did depletion and add back experiments of Nup93 in the *Xenopus* in vitro nuclear assembly system to understand the role of Nup93 apart from the Nup93-188 and Nup93-205 complexes. The feature of Nup93 being essential for nuclear pore formation is conserved during evolution. For instance Nup93 has found to be essential in *C.elegans, Danio rerio, S.cerevisiae and A.nidulans* (Grandi et al., 1993; Allende et al., 1996; Galy et al., 2003 and Osmani et al., 2006).

3.1.2. Nup188 and Nup205 are together not essential for NPC assembly.

Theerthagiri et al., 2010 showed that Nup93-188 complex is not essential for NPC assembly. The same was observed for Nup93-205 complex. We wanted to test if both Nup188 and Nup205 together were not essential for NPC assembly and if both Nup188 and Nup205 have redundant functions at the pore. It was also shown in this study that there is a 5-10% of free pool of Nup93 existing, which might have functions beyond the Nup93-188 and the Nup93-205 complexes. So we wanted to know how the free pool of Nup93 contributes to NPC assembly and function. Also one could imagine a scenario where one complex can compensate for the loss of another from the pore (Nup93-188 and/or Nup93-205 complex). To get an insight into the answers of the above-mentioned questions we depleted Nup93 from the egg extracts using anti Nup93 antibody and observed a block in NE and NPC formation. The block in NPC assembly and function was rescued by the addition of the full length Nup93 (that is in the absence of both Nup188 and Nup205 as they are co depleted upon Nup93 depletion). Hence we concluded that Nup188 and Nup205 together are not essential for NPC assembly and most functions like transport and exclusion competency. This was indeed surprising that two structural nucleoporins and members of the Nup93 complex are not essential for NPC formation even though they are part of the structural scaffold of the pore and take part in inner pore ring formation (Alber et al., 2007 and Amlacher et al., 2011). One could imagine that as the nucleoporins evolved duplication events might have occurred and caused redundancies in NPC components (Stavru et al., 2006). Extensive redundancies have been seen in protein-protein interaction within the NPCs. But we can't exclude if there are other functions, which might be affected by co depletion of Nup188 and Nup205 in vivo that we cannot detect in our in vitro *Xenopus* nuclear assembly system. For instance it is worth mentioning that in the nuclei where Nup93 was depleted and the full-length recombinant protein was added back the block in NE and NPC formation was rescued and the pores were transport and exclusion competent. But these nuclei as shown are much larger in surface area compared to mock depleted or Nup93 depleted nuclei or in nuclei where the endogenous Nup93 is replaced by the C- terminus of Nup93 (aa 608-820) {see figure 2.4A and 2.9B}. This phenotype is due to the absence of Nup188 from the pore. As the NPC assembly progresses the NE undergoes expansion and nuclear growth proceeds further as the pores start to import proteins and other molecules. As shown in Theerthagiri et al., 2010 that when Nup93-188 complex is depleted form the egg extracts, the nuclei assembled there after show an accelerated targeting of integral membrane proteins to the inner nuclear

membrane. Transfer of membrane components can be rate limiting for nuclear growth and not only increase in NPC numbers. The primary effect is NE expansion which leads to an accelerated import of membrane proteins and thereby an increase in overall nuclear size. The secondary effect of this is the increase in NPC number, which then further augments the nuclear growth effect. Thus Nup93-188 complex restricts the passage of membrane proteins from the outer nuclear membrane to the inner nuclear membrane and hence acts as an important factor in establishing these two membrane sub-compartments of the NE (Antonin et al., 2011). This is the reason we observed much larger sized nuclei when we added back the full-length Nup93 in the nuclear assembly reaction to Nup93 depleted extracts (absence of Nup188). Interestingly the nuclei did not grow larger in comparison to mock depleted nuclei when the endogenous Nup93 was replaced by the add-back of the C-terminus of Nup93 (aa 608-820) even though in this situation the Nup188 was absent in the extracts as Nup93 was depleted. The accelerated targeting of integral membrane proteins to the inner nuclear membrane was still occurring but nuclear import of soluble cargos did not occur, as the central channel was not formed. Thus further augmentation of the nuclear growth could not occur leading and the nuclei hence formed were not large in size as was the case with addition of full-length Nup93 as explained above. This also points out to the fact that there might be distinct mechanisms of inner nuclear membrane protein and soluble cargo import (Antonin et al., 2011).

3.1.3. The N-terminus of Nup93 is essential for recruiting the Nup62 complex to the assembling NPC.

Based on our immunoflorescence experiments we observed that if the endogenous Nup93 is replaced by the add-back of the C-terminal domain (aa 608-820) or middle + C-terminal domain (aa 183-820) of Nup93, the Nup62 complex could not be recruited at the pore but the add-back of the full-length Nup93 could recruit the Nup62 complex (see figure 2.12B). Thus the N-terminal coiled-coil region of Nup93 acts as an anchor protein to recruit the Nup62 complex at the pore. The binding of the N terminus of Nup93 to Nup62 complex has already been reported in literature. This has also been observed in yeast where Nic96 (homologue of Nup93) was shown to bind to Nsp1p (homologue of Nup62) and its involvement in nuclear transport has been studied (Grandi et al., 1995). It was also shown at genetic and biochemical level that Nsp1p, Nup49p, Nup57p and Nic96p form a complex, which also fits with our data that is the N terminus of Nup93, is essential to recruit the Nup62 complex to the pore. Nup62 complex consists of FG repeat containing

nucleoporins that contribute to the formation of the central channel of the pore. Even other cytoplasmic and peripheral FG containing nucleoporins are responsible for establishment of the central channel of the pore and thereby imparting functional properties to the NPC like transport and exclusion competency. One such nucleoporin is Nup98, which contributes majorly in imparting the aforementioned properties to the pore (Laurell et al., 2011 and Hülsmann et al., 2012). The formation of the central channel (mainly established by the cohesive nature of the FG containing nucleoporins) of the pore is a very important step in NPC formation as this leads to the nucleo-cytoplasmic transport and establishment of a permeability barrier thereby maintaining distinct environments of the nucleus and the cytoplasm. We checked for these functions of the pore under various conditions tested in our Xenopus system and nuclear assembly reaction by substituting the endogenous Nup93 with different fragments of the recombinant protein. Nuclei where the C terminus or the middle + C terminus of Nup93 were added back we did not observe the import of the EGFP fused nuclear substrate. But the full-length Nup93 add- back did support an efficient nuclear import of the substrate tested. The lack of import upon addition of only the C terminus of Nup93 or the middle + C terminus of Nup93 was due to lack of formation of the central channel of the pore as FG containing nucleoporins like Nup62 and probably a major fraction of Nup98 is not recruited to the pore. Recently a study from the Ed Hurt lab (Almacher et al., 2011) showed that the coiled-coil region of Nup93 {in fungi *C. thermophilus*) interacts with the Nup62 complex. Within the coiled-coil region of Nup93 is an alpha helical basic stretch of amino acids that binds the Nup188 and Nup205 (referred as Nup192). Nup62 is recruited synergistically by interaction with the coiled-coil domain of Nic96p and by interaction with Nup188 and Nup192. Deletion of alpha helix (Nup188 and Nup192 interacting site) in Nic96p leads to a mild growth defect. Whereas deletion of coiled-coil region of Nic96p (Nup62 binding region) lead to severely retarded cell growth. Deletion of alpha helix and the coiled-coil domain together leads to a very slow growth phenotype. This deletion experiments suggested that Nup62 is recruited to the NPCs by a direct and more important interaction to Nic96p and may be an indirect interaction via Nup188p and Nup192p. This also correlates with the add back experiments we did where the N terminus of Nup93 is sufficient and essential to recruit the Nup62 complex to the assembling pore and this can occur without Nup188 and Nup205. Direct binding of Nup93 is required for Nup62 complex recruitment, which along with other FG containing nucleoporins forms the central channel and thereby making the pores transport competent.

Another functional property imparted by the central channel is the establishment of permeability barrier of the pore which helps maintaining distinct environments of the nucleus and the cytoplasm by excluding molecules >30kDa/ 2.5nm in radii to freely diffuse across the nuclei. We checked for this function using the dextran exclusion assays wherein if pores are leaky in nature (not an intact permeability barrier) they would allow the 70Kda dextrans to pass through but the NE integrity has to be lost for 500Kda dextrans to enter the nucleus. In Nup93 depleted nuclei both 70 and 500Kda dextrans were included in the nucleus due to absence of an intact NE and NPC formation. When the full-length Nup93 was added back to Nup93 depleted extracts, the nuclei formed there on excluded both the 70kDa and 500 kDa dextran molecules as now both NE and NPC assembly were restored. When the endogenous Nup93 was replaced by add back of the C terminus of Nup93 (aa 608-820) the 70 kDa dextrans were included in the nucleus but not the 500 kDa dextrans. This was because in the nuclei assembled using C terminus of Nup93 the central channel was not formed as the FG containing nucleoporins (Nup62 complex and probably a large fraction of Nup98) was not recruited to the pore and an intact permeability barrier could not be established. As the NE was still closed in this situation thus the 500 kDa dextrans were excluded (data not shown). This supports the fact that the C terminus of Nup93 is essential and sufficient for NE formation and the N terminus of Nup93 acts as an anchor to recruit the Nup62 complex and via this probably also other FG repeat containing nucleoporins leading to formation of the central channel and hence import and exclusion competent NPCs.

Another aspect worth discussing is what actually forms the central channel of the pore and establishes the transport and exclusion competent nuclear pores. Recruitment of the Nup62 complex to the NPC is indeed affected when its anchor protein Nup93 (N terminus coiled-coil region) is missing. But the defects observed in terms of transport and exclusion competency of the pore cannot be directly linked to absence of the Nup62 complex at the pore as recently Hülsmann et al., 2012 showed that the Nup62 complex can be depleted from *Xenopus laevis* egg extracts and the nuclei assembled have an intact permeability barrier and are transport competent. They showed that the main component that forms the permeability barrier of the pore is the FG repeat containing nucleoporins Nup98. The multivalent cohesion between FG repeats is required which leads to formation of barrier that is formed by a sieve-like FG hydrogel (also see Laurell et al., 2011 and Labokha et al., 2012). In our system, we see a Nup98 staining at the pore in Nup93 depleted nuclei or in nuclei assembled using the C terminus of Nup93 (see figure 2.11C). This probably is an

early fraction of Nup98 that is recruited to the pore via the Nup107-160 complex in post-mitotic NPC assembly. A major fraction of Nup98 is recruited at later steps in NPC assembly. So it could very well be that due to the absence of Nup93 particularly the N terminus coiled-coil domain we do see transport and exclusion related defects in the pore but this affect can be due to lack of a major fraction of Nup98 at the pore. This can also be associated with the recruitment of the Nup62 complex or other nucleoporins in the central channel as we still do not understand how Nup98 is really anchored in the NPC. One could imagine that upon Nup93 depletion we do miss some anchor proteins in the pore which are needed to recruit Nup98 and hence establish the central channel and a transport and exclusion competent NPC. The molecular mechanism of this needs further investigation.

3.1.4. The C-terminal domain of Nup93 is essential and sufficient for assembly of the structural backbone of the NPC.

We observed that the C-terminal domain of Nup93 was essential and sufficient for the formation of a closed NE. This also explains the smoothening in staining of the transmembrane nucleoporins Pom121 at the nuclear rim in the nuclei that were assembled using the C terminus of Nup93 (see figure 2.11B) as oppose to nuclei where Nup93 was depleted and showed a punctate staining for Pom121 and Gp210. The addition of the C terminus of Nup93 could not restore the NPC functions like transport and exclusion competency due to lack of formation of the central channel. Along these lines the C terminus of Nup93 could not recruit the Nup62 complex to the pore as well. In fact the C terminus of Nup93 played a crucial role in stabilizing the Nup53-Nup155 interaction as seen in the GST- pull down experiments (see figure 2.18 and 2.19). This interplay of interactions can be imagined as a key event in the formation of the structural backbone/scaffold of the pore. It is surprising that in yeast the C terminus of Nup93 is considered not to play a crucial role in NPC formation and function as deletion of the last 30 amino acids of Nic96p is still functional for nuclear pore formation (Grandi et al., 1995 and Schrader et al., 2008). They hypothesized a redundant function of the C terminus of Nic96p and the C terminus of Nsp1p but this is not the case in our *Xenopus* in vitro nuclear assembly system where the C terminus of Nup93 plays an important role in formation of the structural backbone of the pore. The crystal structure of Nic96p shows an extreme C-terminal conserved surface patch (P2) that might be involved in protein-protein interaction (Jeudy and Schwartz, 2007) Our data supports this view C-terminus of Nup93 interacts directly with Nup53 and stabilizes its interaction with Nup155. Also it was shown in yeast

that the N terminus of Nic96p can substitute for the endogenous protein and can integrate into the NPCs, which does not hold true in our vertebrate *Xenopus* system. It could be that in yeast different regions of Nic96p and Nup53p might be involved in interactions. Due to high sequence conservation of Nup93 across the eukaryotes the overall structure of yeast and vertebrate Nup93 is similar (Jeudy and Schwartz, 2007) but Nup93 has a smaller dipole moment than Nic96p so there might be a yeast specific particularity (Schrader et al., 2008). The differences observed in the importance of the C- terminal domain of yeast and vertebrate Nup93 (in *Xenopus laevis* system) and the fact that in yeast the N-terminal domain can substitute for the loss of the endogenous Nic96p might reflect different NPC assembly modes adopted in yeast vs. the vertebrate systems. Yeast undergoes closed mitosis where NPCs are assembled into an intact NE. In metazoans post mitotic NPC assembly occurs on the chromatin surface concomitant with the formation of a closed NE (Antonin, 2008; Kutay and Hetzer, 2008). The post-mitotic NPC assembly is recapitulated in the *Xenopus laevis* egg extract system (in vitro nuclear assembly reactions) and might have unique and distinct requirements of nucleoporin interactions. In nuclei where Nup93 was depleted we did observe a staining of both Nup53 and Nup155 on the chromatin but at reduced levels. When the C-terminus of Nup93 was added both Nup53 and Nup155 showed a bright nuclear rim staining (see figure 2.11A). We now understand why we observed this difference. GST-pull down experiments point to a strengthening of Nup53-Nup155 interaction in the presence of the C terminus of Nup93 most likely by inducing a conformational change in Nup53. This leads to formation of "minimal" pores that have a structural backbone and the basic scaffold but no central channel and hence are transport and exclusion incompetent. It's known that Nup53 and Nup155 are both individually essential for NE and NPC assembly and function (Hawryluk-Gara et al., 2008; Franz et al., 2005; Mitchell et al., 2010 and Vollmer et al., 2012). Both Nup53 and Nup155 comprise the central components of the structural backbone of the pore (Alber et al., 2007). Nup155 has shown to be essential in *C.elegans* andcruicial for NPC assembly in vitro (Franz et al., 2005). Nup155 is recruited at the time of NE sealing and might participate in the NE assembly checkpoint. Nup53 is also essential for NE and NPC formation (Hawryluk-Gara et al., 2008). Establishing and stabilizing the interaction between Nup53 and Nup155 might be a key event in formation of the structural backbone of the NPC as pointed out by our results. Keeping this in mind our results contradict slightly with the study done by Hawryluk-Gara et al., 2008 where they used a fragment of Nup53 (aa 167-300: binds Nup155), which can rescue the block in NPC assembly observed upon Nup53 depletion.

This region of Nup53 does not bind Nup93 (Vollmer et al., 2012 and our own unpublished data) and we know from our results that the interaction between Nup53 and Nup93 is essential for NPC assembly (also see Vollmer et al., 2012). We know that the C-terminal domain of Nup93 binds to Nup53 and stabilizes the Nup155-Nup53 interaction, which is important for NPC assembly. Also in Vollmer et al., 2012 a construct of Nup53 that lacks the Nup93 binding region cannot rescue the block in NPC formation that occurs upon Nup53 depletion. The fragment of Nup53 used by Hawryluk-Gara et al., 2008 also lacks the membrane binding regions of Nup53, a property necessary for NPC assembly as shown by Vollmer et al., 2012. This discrepancy observed could be due to the difference in the depletion efficiency of Nup53 as we noticed that a fraction of floated membrane preparation contained Nup53, which we avoided in our in vitro nuclear assembly reactions. Thus the Nup53-Nup155 an interaction seems to be an essential step in NPC assembly but requires more careful analysis and further experiments. Studies from other labs have also observed an interaction between Nup53, Nup155 and Nup93. For example in Almacher et al., 2011 mapping of Nup155, Nup93, and Nup205 binding on Nup53 has been done. In Busayavalasa et al., 2012 a direct binding of Nup155 with Nup53 and Nup155 and Nup93 was shown. Although we did not see a direct binding of Nup155 and Nup93 in our GST-pull down assays but rather Nup93 binds directly to Nup53 and in turn stabilizes its interaction with Nup155.

3.1.5. The middle domain of Nup93 is dispensable for NPC assembly.

We observed that the fusion construct of Nup93 (N + C-terminal domains) lacking the middle domain could rescue the block in NE and NPC assembly observed upon Nup93 depletion. We also noticed a bright nuclear rim staining by mab414 antibody and recruitment of Nup62 complex at the pore when the nuclei were assembled using this fusion construct (ΔM). Thus the middle domain of Nup93 is dispensable for NE, NPC formation and for recruitment of the Nup62 complex. Having said that we still do not understand the function of the middle domain of Nup93, which will be an interesting aspect to explore further. It could be involved in interaction with other nucleoporins or transport functions of the pore for instance import of specific cargo proteins like INM proteins as in these nuclei where endogenous Nup93 is replaced by the fusion construct of Nup93 (N+C, ΔM), they still lack Nup188 which is involved in regulating the targeting of integral membrane proteins to the inner nuclear membrane. It could also be involved in maintenance of the permeability barrier of the pore or might have a role in interphase NPC

assembly. It will be exciting to test these hypotheses and it could be that the deletion of the middle domain of Nup93 might show a phenotype in vivo, which is not obvious in our *Xenopus* in vitro nuclear assembly system. In the near future we would also like to confirm our observations regarding the middle domain of Nup93 in yeast and see if this feature is conserved.

3.1.6. Kinetic analysis of the order of nucleoporin recruitment in post-mitotic NPC assembly.

Based on experiments of depletion and add back of nucleoporins using the *Xenopus* system, other labs and data from our lab are now beginning to unravel the kinetics of post-mitotic NPC assembly. It is a step wise, well-coordinated and regulated process. In organisms undergoing open mitosis the NE and the NPC disassembles in prophase and in telophase the

NPC and the NE have to reform to form the intact nucleus. When the NPC disassembles the nucleoporins either as individual proteins or as sub complexes are dispersed in the cytoplasm and membrane components are reabsorbed in the endoplasmic reticulum (ER). Post-mitotic NPC has to assemble from these soluble nucleoporins and starts with the chromatin binding of Mel28-ELYS, which then recruits the Nup107-160 complex. This complex is recruited as a whole and acts as the seeding point of NPC formation (also small fraction of Nup98, Nup153 and Nup50 are recruited to the chromatin). Membranes then associate with chromatin and enrichment of NE and NPC specific membranes like Pom121 and Ndc1 occurs (Dultz et al., 2008). Then the Nup93 complex is recruited to the pore as individual components or as sub complexes. The members of the Nup93 complex come as functional units and individual components come separately making it interesting to study the kinetics of these nucleoporins based on depletion and add back experiments in our *Xenopus* in vitro nuclear assembly system in a time dependent manner. Nup53 is the first member of the Nup93 complex that is recruited to the pore most likely via Ndc1. The next member of the Nup93 complex that is recruited to the pore is Nup155, which binds Pom121. This forms a link of soluble nucleoporins to the pore membrane. Nup53 depletion blocks the recruitment of Nup93 and Nup155 on chromatin (Vollmer et al., 2012) but upon Nup93 depletion Nup53 and Nup155 are recruited on to the chromatin but at reduced levels as seen in our results (see figure 2.11A). With this logic the next player is Nup93 (as Nup93-188 and Nup93-205 complex, also some fraction as free Nup93). Nup53 precedes Nup93 recruitment as Nup53 is required for binding to Nup93 at the end of mitosis, a

hypothesis that is consistent with the yeast NPC assembly model (Rexach, 2009). Then the Nup62 complex binds via the N terminus of Nup93 to the assembling pore. First functional import intermediates are seen after Nup93 binds the Nup62 complex (Dultz et al., 2008). As the next steps cytoplasmic, peripheral nucleoporins and other FG repeat containing nucleoporins (large fraction of Nup153, Nup50, Nup98, Rae1, and Nup214 etc) are recruited to the pore, which leads to formation of a central channel and a fully functional NPC that is transport and exclusion competent. Thus Nup93 acts as a link between the structural and functional central channel of the pore. Thus immunodepletion and add back experiments done on nucleoporins in the in vitro nuclear assembly system (using *Xenopus laevis* egg extracts) act as a good tool to dissect the recruitment of nucleoporins at the pore as we could show for the members of the Nup93 complex (see figure 3.1).

Fully functional NPC

105
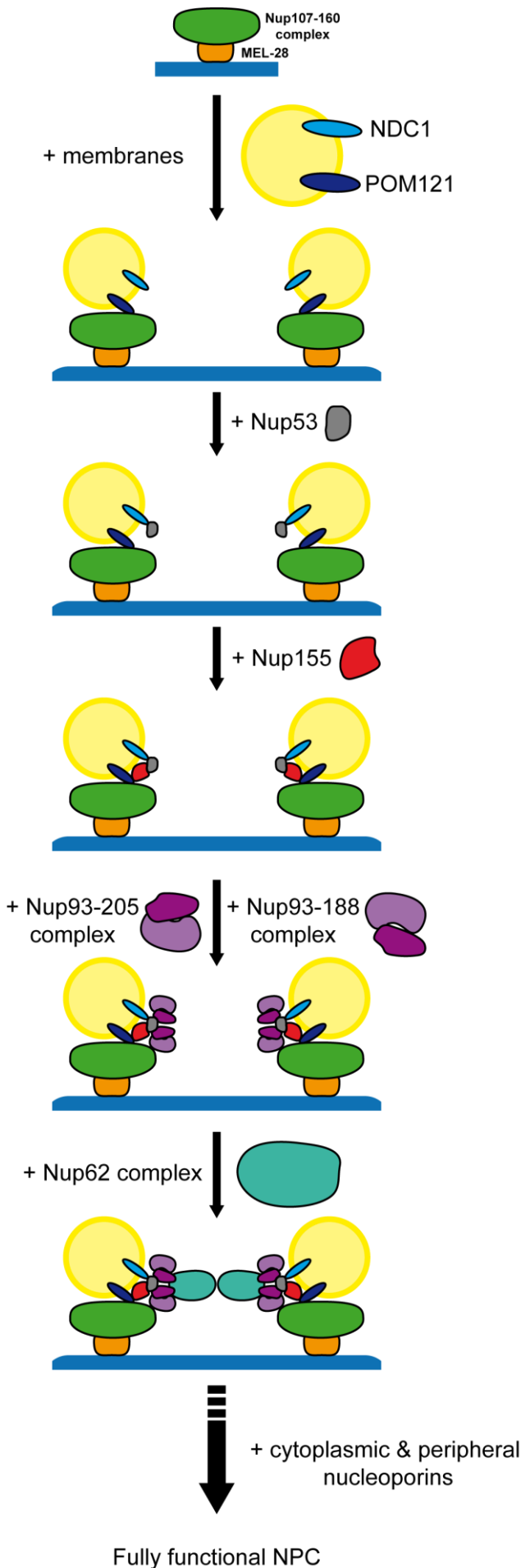
Figure 3.1: Kinetic analysis of steps involved in post-mitotic NPC assembly. The figure depicts the order of nucleoporin recruitment in post-mitotic NPC assembly based on depletion and add-back experiments and IF on nucleoporins. The post-mitotic NPC assembly starts on chromatin (blue) by binding of Mel28-ELYS (orange) via it's AT hook DNA binding motifs as the very early first step. Mel28-ELYS then recruits the Nup107-160 complex (green). Simultaneously membrane vesicles (yellow) for instance containing the transmembrane nucleoporins Ndc1 (light blue) and Pom121 (dark blue) are recruited to the assembling pore via interaction with Nup107-160 complex members or by binding to the decondensing chromatin. These transmembrane nucleoporins link the soluble nucleoporins to the pore membrane. Nup53 (gray) is the next nucleoporin recruited by binding to Ndc1 and then comes Nup155 (red), which binds to Pom121 and at the same time can interact with Nup53 present at the pore. Then the recruitment of Nup93 (deep purple) occurs as Nup93-205 (light purple) and Nup93-188 (light purple) complex. Nup93 can interact with Nup53, which in turn strengthens the Nup53-Nup155 interaction stabilizing the structural backbone of the pore. The Nup62 complex (turquoise) is then recruited and is anchored via the N terminus of Nup93 to the pore.

3.1.7. Model summarizing the role of Nup93 in post-mitotic NPC assembly and function. *{Nup93 acts as a link between the structural backbone of the pore and the functional central channel of the NPC}*

Based on our findings we depict the role of Nup93 in post-mitotic NPC assembly and function in the form of a model as we envision it. The post-mitotic NPC assembly starts on chromatin with the binding of Mel28, which then recruits the Nup107-160 complex. Transmembrane nucleoporins like Pom121 and Ndc1 then bind to the assembling pore. Nup53 is recruited to the pore probably via Ndc1 and Nup155 binds to Pom121, linking the soluble nucleoporins to the pore membrane. If the full-length Nup93 (aa 1-820) is present in the nuclear assembly reaction it binds to Nup53 at the pore and stabilizes the Nup53-Nup155 interaction. This is a major contribution towards the formation of the structural backbone of the pore. The full-length Nup93, via its N terminus coiled-coil region recruits the Nup62 complex, which might then also recruit cytoplasmic, peripheral and other FG repeat containing nucleoporins like Nup98. This leads to the formation of the central channel of the pore composed mainly of multivalent cohesive FG repeat containing nucleoporins. The central channel imparts functional properties to the pore like nucleo-

cytoplasmic transport competency and the ability to act as an exclusion barrier thereby maintaining distinct environments of the nucleus and the cytoplasm. Surprisingly the aforementioned NPC assembly and functions can occur without the presence of both Nup188 and Nup205 in the NPC as seen in our Nup93 depletion and add back experiments (for example full-length recombinant Nup93 add back). This scenario is depicted on the left hand side in figure 3.2.

On the other hand if the C-terminal of Nup93 (aa 608-820) is part of the nuclear assembly reaction it is recruited to the assembling NPC via Nup53, which precedes Nup93 recruitment (Nup53 binds to Ndc1). Binding of the C terminus of Nup93 leads to the strengthening of the Nup53-Nup155 interaction. This we think is a key event in the formation and stabilization of the structural backbone of the NPC. But the Nup62 complex cannot be recruited to the NPC if only the C terminus of Nup93 is present at the pore as the N-terminal coiled-coil domain of Nup93 that interacts with the Nup62 complex is missing. Thereby other cytoplasmic, peripheral and FG repeat containing nucleoporins are most likely also not recruited to the pore. Due to this a functional central channel cannot be established leading to formation of transport and exclusion incompetent pores. But minimal pores are established that have a structural backbone, that is structural nucleoporins like Mel28, Nup107-160 complex, Nup53, Nup155 and Nup93 (C terminus) are present at pore that can form the scaffold. This scenario is depicted on the right hand side in figure 3.2. The structural nucleoporins act mostly as anchor proteins to recruit other nucleoporins (functional), which leads to formation of the central channel. The structural nucleoporins are less dynamic in nature and hence form the stable backbone of the pore whereas the FG containing nucleoporins are dynamic and establish the central channel of the pore thereby imparting functionality like transport and exclusion competency.

Thus Nup93 forms a link between the structural skeleton of the pore (via its C terminus stabilizing the Nup53-Nup155 interaction) and the functional central channel of the pore (via its N terminus recruiting the Nup62 complex and probably other FG containing nucleoporins). Nup93 can thus connect both structural and functional portions of the pore and is a key player in the ordered post-mitotic NE/NPC assembly.

Assembling NPC (post mitotic)
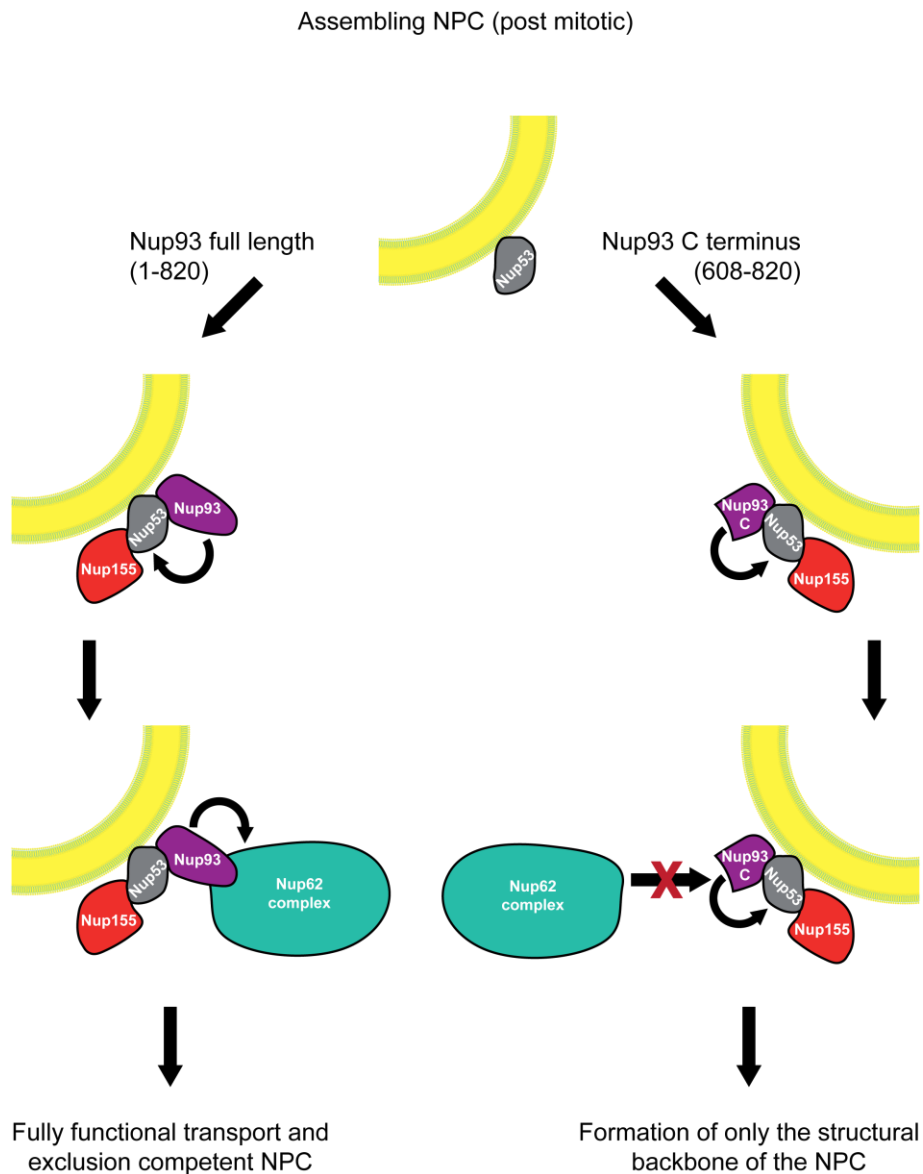
Figure 3.2: Model for Nup93 function in post-mitotic NPC assembly. The figure depicts a cartoon to illustrate the role of Nup93 in post-mitotic NPC assembly and function. As the NPC is assembling Nup53 (gray) is recruited to the pore via Ndc1at the membrane (yellow). In one scenario shown on the left hand side, the full-length Nup93 (purple) is recruited to the pore, which interacts with Nup53 (gray) and in turn stabilizes the Nup53-Nup155 interaction (red). The full-length Nup93 (via its N-terminal coiled-coil region) recruits the Nup62 complex (turquoise) to the assembling NPC, which leads to the formation of the central channel and thereby an exclusion and transport competent pore. On the right hand side another scenario is depicted wherein the endogenous Nup93 is replaced by the C-terminal domain (last 200 amino acids) of Nup93. In this situation the C-

terminus of Nup93 can still interact with Nup53 and stabilize the Nup53-Nup155 interaction (stability of structural backbone of the pore). But the C terminus of Nup93 cannot recruit the Nup62 complex hence only the structural backbone of the pore is formed. Note that for the sake of simplicity the transmembrane nucleoporins and the Nup107-160 complex are not shown in the figure although are data do indicate that they are present in both the assembly lines shown above. INM: inner nuclear membrane and ONM: outer nuclear membrane. Numbers correspond to the amino acids in *Xenopus laevis* Nup93.

3.2. Regulation of the cell cycle dependent interaction between Nup53 and the Nup93-205 complex.

3.2.1. Nup53 interacts with the Nup93-205 complex in a cell cycle dependent fashion.

By GST-pull down assays using *Xenopus laevis* egg extracts we found that Nup53 interacts with the Nup93-205 complex in a cell cycle dependent fashion (interacts in interphase and not in mitosis). This interaction could be regulated during the cell cycle to coordinate NPC assembly and disassembly. In animals undergoing open mitosis the NE and the NPC disassemble at the onset of mitosis (prophase) and at the end of mitosis (telophase) the NE and the NPC have to reassemble as the cell enters interpahse. A number of nucleoporin-nucleoporin interactions have to break and reform as part of the dynamicity observed in the NE and NPC throughout the cell cycle. The Nup53 and the Nup93-205 interaction that occurs in interphase and not in mitosis is one such example. We believe that when the NPCs have to disassemble (in mitosis) the interaction between Nup53 and the Nup93-205 complex has to break, which might lead to structural instability in the inner ring of the pore and facilitate the process of NPC disassembly. On the other hand in interphase, Nup53 interacts with the Nup93-205 complex, which might aid in NPC assembly process and stabilize the structural scaffold of the pore. But the interaction between Nup53 and Nup93-205 complex is not a key point and probably not essential for NPC assembly as we know that pores can assemble and function in the absence of the Nup93-205 complex (Theerthagiri et al., 2010).

During nuclear envelope breakdown (NEBD) and NPC disassembly a major trigger is the phosphorylation of nucleoporins by mitotic kinases like Cdk1. A number of nucleoporins are known to be phosphorylated in a cell cycle dependent fashion for instance Nup53p, members of the Nup107-160 complex and Nup98 etc. The mitotic kinases that have nucleoporins as their substartes are Cdk1, NIMA family kinases, PLK1 etc. For instance it was shown for Nup98 that it is phosphorylated at multiple sites during mitosis by the above mentioned kinases and this act as a trigger and a rate limiting step in NEBD and NPC disassembly, which ultimately leads to loss of the permeability barrier of the pore (Laurell et al., 2011 and Güttinger et al., 2009). We believe that mitotic specific phosphorylation of Nup53 and its cell cycle dependent interaction with the Nup93-205 complex could also be involved in NEBD and NPC disassembly. As shown in figure 2.20

when the GST-pull down assay was done using Nup53 as bait, we could pull out the Nup93-205 complex from the interphasic egg extracts but not from mitotic extracts. But we did not pull down Nup188. This suggested that the interaction of the Nup93-205 complex with Nup53 is most likely via Nup205 and not via Nup93. But the direct binding of Nup205 to Nup53 could be tested further, which is currently ongoing in the lab.

3.2.2. The Nup93-205 complex binds at the N terminus of Nup53 and the RRM domain (dimeric form) of Nup53 strengthens this interaction.

Using various truncations of Nup53 as bait in the GST-pull down assays with interphase egg extracts we found that the minimal binding region on Nup53 that binds the Nup93-205 complex lays in the N terminus of Nup53. We also showed that the dimerization of Nup53 via its RRM domain strengthens this interaction (GST Nup53 aa 1-267, see figure 2.22 and figure 2.28). It was shown by Handa et al., 2006 that the RRM domain of vertebrate Nup53 forms homodimers in crystal and solution most likely by the FG hydrophobic interactions. The same has also been confirmed by results from our lab (Vollmer et al., 2012). The highly conserved portions in the RRM domain are beta sheet surface and these regions are likely to contribute to protein-protein interactions which fits with our observations as the monomeric version of Nup53 (GST Nup53 aa 1-267 F172EW203E) reduces its binding to the Nup93-205 complex (see figure 2.28). We also observed that the dimerization mutant of Nup53 alters its binding to Nup155 and also the membrane binding activity of Nup53 (essential for NPC assembly) is dependent on the dimerization of the protein (Vollmer et al., 2012). Thus most likely a conformational change occurs on Nup53 due to the dimerization of the RRM domain, which regulates its interaction with the Nup93-205 complex as seen in our GST-pull down assays.

Our results of the mapping of the interaction site of the Nup93-205 complex on Nup53 support the findings known in literature. In Hawryluk-Gara et al., 2008 they also observed that Nup93 binds on the N-terminal site of human Nup53 and the RRM domain is essential for the same. They did not observe Nup93 binding to Nup53 (aa 1-83), in our case we observed a weak binding (aa 1-77 in *Xenopus* Nup53) to both Nup93 and Nup205. RRM domain alone in their study and also in our GST-pulls down assays (GST Nup53 aa 162-267) did not bind the Nup93-205 complex. Thus we concluded that the minimal region on *Xenopus laevis* Nup53 that binds the Nup93-205 complex lies in the extreme N terminus and the RRM domain strengthens this interaction (via dimerization of Nup53). It was shown by Almacher et al., 2011 that the N terminus of CtNup53 (aa 30-70 in fungi *C.*

thermophilus) was sufficient to bind CtNup192 {Nup205} and CtNic96 {Nup93}. Both Nup192 and Nic96 compete for the same binding site on Nup53. Surprisingly the RRM domain of CtNup53 did not have a positive influence on the binding of Nup192 or Nic96 but in our system we do see a strengthening of the Nup93-205 complex interaction with Nup53 if the RRM domain (dimeric version) was used as bait in our GST-pull down assays.

3.2.3. Nup53 is phosphorylated during the cell cycle and hyper-phosphorylated during mitosis.

Based on our immuneprecipitation (IP) of Nup53 from mitotic and interphasic *Xenopus laevis* egg extracts we observed that Nup53 is phosphorylated during the cell cycle. In the phostag gels the interpahse Nup53 runs at a higher molecular weight than expected (35 kDa). As phostag gels detect the shift and migration pattern specifically of the phosphorylated proteins, it suggested that Nup53 is also phosphorylated during interphase but hyper phosphorylated during mitotsis. This was because the mitotic Nup53 showed a bigger shift than interphasic Nup53 (see figure 2.25A and B). We confirmed this observation with the addition of lambda phosphatase (see figure 2.26) where addition of the phosphatase led to a shift in the mitotic and even interphasic Nup53. We observed the same when the phosphorylation sites in Nup53 were analyzed by mass spectrometric analysis. Although Nup53 was phosphorylated during interphase but it was hyper phosphorylated in mitosis. We were able to find mitotic specific phosphorylation sites on Nup53 in our mass spectrometric analysis (see figure 2.28). A subset of the phospho sites were consensus sequence for Cdk1 for instance in the N terminus of Nup53: amino acids: S94 and T100. Cdk1 can phosphorylate these amino acids of Nup53 in vitro as shown in Vollmer et al., 2012. We also found mitotic specific phosphorylation sites in the C terminus of Nup53, which might regulate its interaction with the transmembrane nucleoporin Ndc1. This fits to the literature as well wherein Nup53 is a mitotic phospho protein of 44 kDa and a known target of Cdk1 and Hrr25p as seen in yeast and humans (Stukenberg et al., 1997; Lusk et al., 2007 and Blethrow et al., 2008). Cdk1 is a major regulator of the eukaryotic cell cycle, as Cdk1-cyclinB phosphorylates a number of nucleoporins in mitosis (cell cycle dependent fashion), which can influence their interaction with other nucleoporins and aid in the release of peripheral nucleoporins and other sub complexes from the NPC (Joseph S. Glavy et al., 2007). Similarly the

transmembrane nucleoporin Gp210 was also shown to be exclusively phosphorylated in mitosis (Favreau et al., 1996).

3.2.4. Mitotic specific phosphorylation of Nup53 does not regulate its cell cycle dependent interaction with the Nup93-205 complex.

The phospho mimicking mutants of GST Nup53 tested in the GST-pull down experiment (GST Nup53 aa 1-267 S94ET100E) did not affect its binding to the Nup93-205 complex in interphase suggesting that the mitotic specific phosphorylation sites on Nup53 do not regulate its cell cycle dependent interaction with the Nup93-205 complex (see figure 2.28). There can be many reasons for this like other phosphorylation sites on Nup53, or other post translational modifications on Nup53 like ubiquitination, sumo modifications etc that can regulate its interaction with the Nup93-205 complex, which we did not detect in our mass spectrometric analysis. Even post-translational modification on Nup93 or on Nup205 (a more likely scenario) could be another level of regulation for interaction with Nup53. There of course can be unknown factors that might bind Nup53 or Nup93-205 complex and regulate this interaction.

It was indeed surprising that transport factors like importin beta that bind Nup53 in mitosis did not regulate its cell cycle dependent interaction with the Nup93-205 complex. It's known that in mitosis when NPCs are disassembled importin beta and transportin bind to several nucleoporins and sequester them. As the cell exits mitosis concomitant with the NPC re-assembly a high concentration of RanGTP is generated near the decondensing chromatin by RCC1, which leads to the release of importin beta from the nucleoporins. The importin beta binds RanGTP and the nucleoporins are free to participate in NPC assembly. This has been shown for Mel28-ELYS, Nup107-160 complex and Nup53 (Lau et al., 2009). Thus we speculated importins to be a regulatory factor for the cell cycle dependent interaction between Nup53 and the Nup93-205 complex but this was not the case as confirmed with our GST-pull down assays done in the presence of RanQ69L (see figure 2.21). The phosphorylated Nup53 in mitosis could also perform certain mitotic "tasks" like participation in kinetochore or spindle assembly checkpoint etc, which will be exciting to explore.

In summary our results from this study show that Nup53 interacts with the Nup93-205 complex in a cell cycle dependent fashion. We found that Nup53 is a phospho protein during the cell cycle that is hyper phosphorylated during mitosis. The mitotic specific phosphorylation of Nup53 or the transport receptors like importin beta do not regulate its

cell cycle dependent interaction with the Nup93-205 complex. We also mapped the minimal region on Nup53 (N terminus) that binds the Nup93-205 complex and showed that the dimerization of Nup53 via its RRM domain contributes positively to the same.

4. MATERIALS AND METHODS

4.1 Materials

4.1.1. Chemicals used

Rotiphores® gel 30 37.5:1	Carl Roth, Germany
Agarose	Invitrogen, Germany
Ammonium chloride	Carl Roth, Germany
Ammonium sulfate	Merk, Germany
BCATM Protein Assay Kit	Thermo Scientific, USA
Bovine serum albumin (BSA)	Calbiochem, Germany
4',6-Diamidino 2-phenyindole (DAPI)	Roche, Germany
1,1'-Dioctadecyl-3,3,3',3' tetramethylindocarbocyanine perchlorate (DiIC18)	Invitrogen, Germany
1,4-Dithio L-threitol (DTT)	Carl Roth, Germany
Ethanol	Carl Roth, Germany
Ethylenediamine-N,N,N',N'-tetraacetic acid (EDTA)	Merk, Germany
Glutaraldehyde (50% aqueous solution)	Sigma-Aldrich, Germany
Glutathione Sepharose 4 Fast Flow	GE Healthcare, Sweden
Glycerol (87% aqueous solution)	Sigma-Aldrich, Germany
Glycine	Carl Roth, Germany
Glycogen (source: oyster)	Sigma-Aldrich, Germany
GSH sepharose beads	GE heatlh care, Sweden
4-(2-Hydroxyethyl)piperazine-1-ethansulfonic acid (HEPES)	Carl Roth, Germany
Imidazole	Carl Roth, Germany
Immersion oil	Olympus, Japan
Kanamycin	Carl Roth, Germany
Lambda phosphatase	New England Biolabs
Magnesium chloride	J.T.Baker, Netherlands
Milk powder	Applichem, Germany
Next gel	Amresco, Solon

Paraformaldehyde	ACROS organics, Belgium
Phenylmethylsulfonyl fluoride (PMSF)	Carl Roth, Germany
Phostag	Alpha labs, UK
Poly-L-Lysine solution	Sigma-Aldrich, Germany
Protein A Sepharose TM CL-4B	GE Healthcare, Sweden
QIAquick® PCR Purification Kit	Qiagen, Germany
QIAquick Gel Extraction Kit	Qiagen, Germany
Restriction enzymes	NEB or Fermentas, Germany
Sodium chloride	Merk, Germany
Sodium dodecylsulfate	Carl Roth, Germany
Sucrose	Carl Roth, Germany
N,N,N′,N′-Tetramethylethylenediamine (TEMED)	Carl Roth, Germany
Thrombin	ICN biomedicals, USA
Tris(hydroxymethyl)amino methane (Tris)	Carl Roth, Germany
Tween®-20	Carl Roth, Germany
Vectashield® mounting medium H-1000	Vector Laboratories, USA
Western LightningTM Chemiluminiscence reagent	PerkinElmer, USA
Fluorescently labeled dextrans	Invitrogen, Germany
Detergents	Calbiochem, Germany
Lipids	Avanti polar lipids
Sodium acetate	Merk, Germany
Sodium carbonate	Merk, Germany
Cysteine	Calbiochem, Germany
Ni-NTA agarose	Qiagen, Germany
Serva unstained SDS-PAGE protein marker	Serva, Germany
Complete™ Protease Inhibitor Cocktail Tablet, EDTA-free	Roche, Germany

4.1.2. Buffers and solutions commonly used

All solutions were prepared with double de-ionized or distilled water. The solutions were sterile filtered and stored at room temperature unless otherwise indicated in braces.

30% Sucrose (4ºC)	30% (w/v) sucrose in PBS
Dejellying buffer (4 °C)	2% cysteine (w/v) in 0.25x MMR adjusted to pH 7.8 with 5M NaOH.
50X Energy mix (-20 °C)	100 mM Creatine phosphate, 5 mM GTP, 5 mM ATP, 0.5 mg/ml Creatin kinase
20X MMR	100 mM NaCl, 10 mM MgCl2, 20 mM CaCl2, 1 mM EDTA, 50 mM Hepes, pH 8.0
Ni-elution buffer	20mM TRIS pH7.4, 500mM NaCl, 400mM Imidazole, 10% (v/v) Glycerol.
Ni-wash buffer	20mM TRIS pH7.4, 500mM NaCl, 8mM Imidazole.
10X PBS (phosphate buffered saline)	130 mM NaCl, 100 mM Na2HPO4, pH 7.4
Resolving gel (8%) (modified accordingly for the other percentages)	375 mM Tris pH 8.8, 8% (w/v) acrylamide/bisacrylamide, 0.1 % (w/v) SDS.
S250 (4 °C)	250mM Sucrose, 50mM KCl, 2.5mM MgCl2, 10mM Hepes pH 7.5
SDS sample buffer (6x)	0.6% (w/v) Bromophenol blue, 12% (w/v) SDS, 60% (v/v) glycerol, 300 mM Tris, pH 6.8
Stacking gel (3%)	125 mM Tris, pH 6.8, 3% (w/v) acrylamide/bisacrylamide, 0.1 % (w/v) SDS.
Vikifix	80mM Pipes pH 6.8, 1mM MgCl2, 150mM sucrose, 2% PFA
Western blotting buffer	25mM Tris base, 92 mM Glycine

4.1.3. Materials commonly used

1.5 ml, 2 ml reaction tubes	Sarstedt, Germany
24-well plates	Greiner Bio-One, Germany
Bottle top filters, 0.22 μm pore size	Millipore, Germany
Filter paper	Whatman, England
General glass ware	Schott, Germany
MoBiCol columns	MoBiTec, Germany
SDS-PAGE Minigel system	Biorad, Germany
Ultracentrifuge tubes	Beckman, Germany
Coverslips (12 mm diameter)	Marienfeld, Germany
Microscope slides	Marienfeld, Germany
SDS-PAGE Miniprotean system	Biorad, Germany
Powerpac HC	Biorad, Germany
Syringes (Omnifix)	Braun, Germany
Diagnostic slides (3 well)	Menzel, Germany

4.1.4 Instruments commonly used

Heraeus® Multifuge® 1L-R	Thermo (USA)
Eppendorf® centrifuge 5415 R	Eppendorf (Germany)
OptimaTM L-60 Ultracentrifuge	Beckman (USA)
Rotor SW40 TI	Beckman (USA)
Rotor SW55 TI	Beckman (USA)
OptimaTM TLX Ultracentrifuge	Beckman (USA)
Sorvall Evolution RC	Thermo (USA)

4.1.5. Vectors/Plasmids generated

pET28sTEV

Generated by Dr. Wolfram Antonin. Derived from pET28s by insertion of AseI-NdeI digested SUMO fragment into NdeI site. Contains an N terminal His_6 tag, followed by thrombin site, a SUMO tag and a TEV cleavage site, use to clone with N terminal His_6 tag.
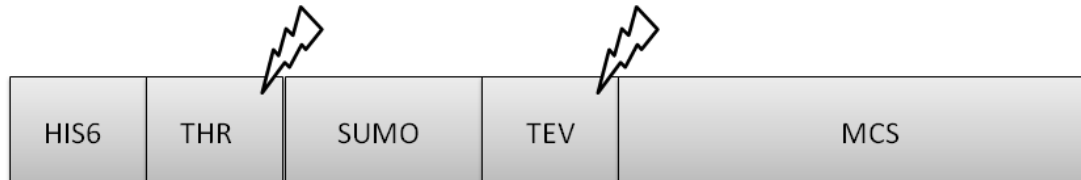
pET28e

Generated by Dr. Wolfram Antonin. Derived from pET28a by insertion of VspI-NdeI digested GST fragment into NdeI site. Contains an N terminal His_6 tag, followed by a thrombin site, GST tag and a TEV cleavage site, use to clone with N terminal His_6 tag.
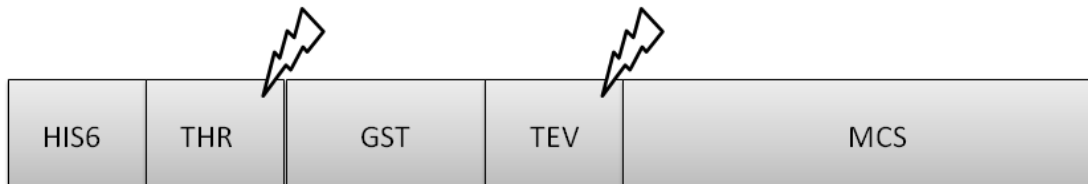
pET28n

Generated by Dr. Wolfram Antonin. Derived from pET28a by insertion of VspI-NdeI digested NusA fragment into NdeI site. Contains an N terminal His_6 tag, followed by a thrombin cleavage site, a NusA domain and a second thrombin cleavage site, use to clone with N terminal His_6 tag.
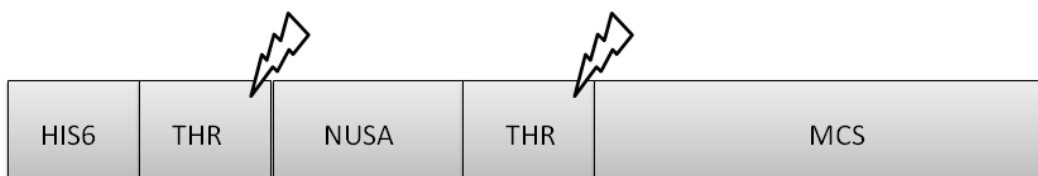
pEGFP-TEV-NPM2

Generated by Dr. Wolfram Antonin. A full length nucleoplasmin (NPM2), an importin α/β dependent nuclear import substrate, was fused to an N-terminal EGFP fragment and a TEV protease cleavage site are cloned into a modified pET28a vector allowing purification via a C-terminal His$_6$ tag.
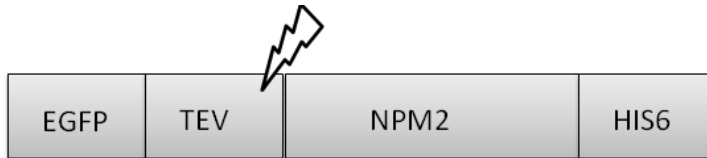
pNusA-TEV

Generated by Dr. Wolfram Antonin. TEV protease was fused with NusA (a solubility tag for protein expression) are cloned into a modified pET28a vector allowing purification via a C-terminal His$_6$ tag.

pQE32

Contains a His$_6$ tag and is ampicllin resistant. This was used for cloning of RanQ69L. This was purchased from Qiagen.

p Xenopus Nup93

Generated by Dr. Wolfram Antonin. Expression constructs for full-length *Xenopus* Nup93 and fragments were generated from a synthetic DNA, which was codon optimized according to E.coli (Geneart, Regensburg, Germany) and cloned into a modified pET28a vector (EMD) with a yeast SUMO (SMT3) as solubility tag, followed by a recognition site for the TEV (tobacco etch virus) protease upstream of the Nup93 fragments.

p Xenopus Nup53

Generated by Dr. Wolfram Antonin. Constructs for full-length *Xenopus* Nup53 and fragments, were generated from a synthetic DNA codon optimized for usage in E.coli

(Geneart, Regensburg, Germany) and cloned into a modified pET28a vector with a yeast SUMO tag followed by a TEV site upstream of the Nup53 fragments.

p Xenopus Nup155

Generated by Dr. Wolfram Antonin. Constructs for full-length *Xenopus* Nup155 and fragments, were generated from a synthetic DNA (Geneart, Regensburg, Germany) and cloned into a modified pET28a vector with a NusA tag followed by a Thrombin site upstream of the Nup155 fragments.

4.1.6. Antibodies

4.1.6.1. Primary antibodies used

Anti-Nup93 antibody

A N-terminal fragment of *Xenopus laevis* Nup93 (aa 1-230) was cloned into pET28a vector and expressed as a His_6 tagged fusion protein in BL21(DE3) as described previously (Franz C et al., 2007).
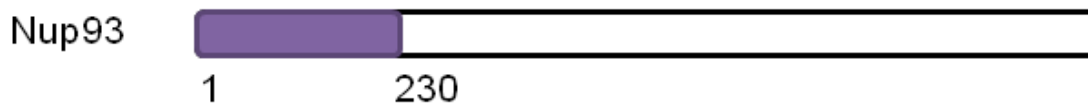
Anti-Nup188 antibody

A fragment of *Xenopus laevis* Nup188 corresponding to 1573-1731 aa of the mouse sequence were expressed as GST fusion proteins in BL21 (DE3) and purified using Glutathione Sepharose beads. The protein was purified and dialyzed against PBS and injected into rabbits for antibody production. Following is the cartoon showing the antibody recognition region in the context of the full-length protein.

Anti-Nup205 antibody

A N-terminal fragment of *Xenopus laevis* Nup205 (aa 1-283) was fused to NusA as a solubility tag, cloned into pET28a vector and expressed as a His_6 tagged fusion protein in BL21(DE3). The protein was purified and dialyzed against PBS and injected into rabbits for antibody production. Following is the cartoon showing the antibody recognition region in the context of the full-length protein.

Nup205
1   283

Anti-Nup53 antibody

A fragment of *Xenopus laevis* Nup53 (aa 78-310) was fused to NusA as a solubility tag, cloned into pET28a vector and expressed as a His$_6$ tagged fusion protein in BL21(DE3). The protein was purified and dialyzed against PBS and injected into rabbits for antibody production. Following is the cartoon showing the antibody recognition region in the context of the full-length protein.

Nup53
78   310
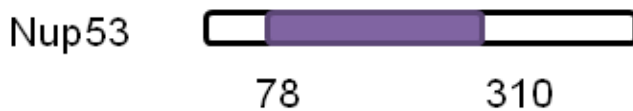
Anti-Nup155 antibody

A N-terminal fragment of *Xenopus laevis* Nup155 (aa 1-1389) was cloned into pET28a vector and expressed as a His$_6$ tagged fusion protein in BL21(DE3) as described previously (Franz C et al., 2005). The protein was purified and dialyzed against PBS and injected into rabbits for antibody production. Following is the cartoon showing the antibody recognition region in the context of the full-length protein.

Nup155
1   1389

Anti-Nup98 antibody

A fragment of *Xenopus laevis* Nup98 corresponding to 1-185 aa were expressed as GST fusion proteins in BL21 (DE3) and purified using Glutathione Sepharose beads (GE-Healthcare). The protein was purified and dialyzed against PBS and injected into rabbits for antibody production. Following is the cartoon showing the antibody recognition region in the context of the full-length protein.

Nup98
1   185
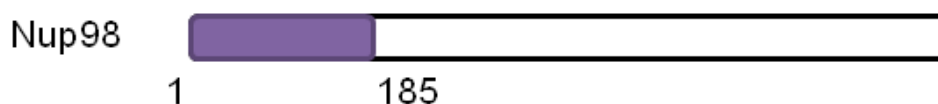
Anti-Nup160 antibody

A fragment of *Xenopus laevis* Nup160 (aa 1-414) was cloned into pET28a vector and expressed as a His6 tagged fusion protein in BL21(DE3) as described previously (Franz C

et al., 2007). The protein was purified and dialyzed against PBS and injected into rabbits for antibody production. Following is the cartoon showing the antibody recognition region in the context of the full-length protein.
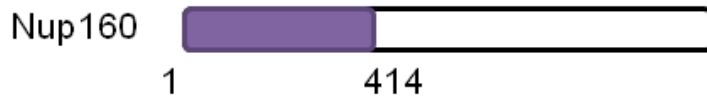
Anti-Nup107 antibody

A fragment of *Xenopus laevis* Nup107 (aa 1-164) was cloned into pET28a vector and expressed as a His_6 tagged fusion protein in BL21(DE3) as described previously (Franz C et al., 2007). The protein was purified and dialyzed against PBS and injected into rabbits for antibody production. Following is the cartoon showing the antibody recognition region in the context of the full-length protein.
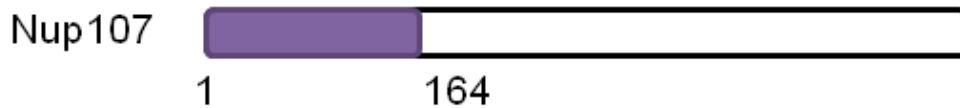
Anti-Mel-28 antibody

A fragment of *Xenopus laevis* MEL-28 (aa 2290-2408) was cloned into pET28a vector and expressed as a His_6 tagged fusion protein in BL21(DE3) as described previously (Franz C et al., 2007). The protein was purified and dialyzed against PBS and injected into rabbits for antibody production. Following is the cartoon showing the antibody recognition region in the context of the full-length protein.
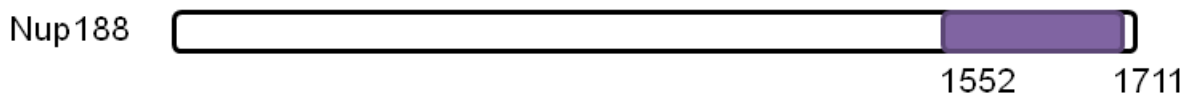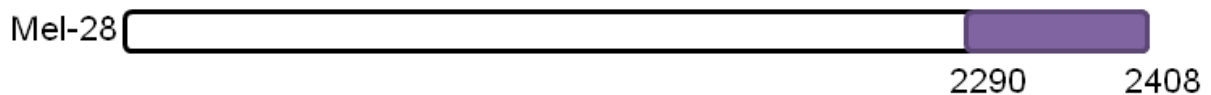

Anti-Nup58 antibody

A fragment of *Xenopus laevis* Nup58 (aa 1-546) was cloned into pET28a vector and expressed as a His_6 tagged fusion protein in BL21(DE3) 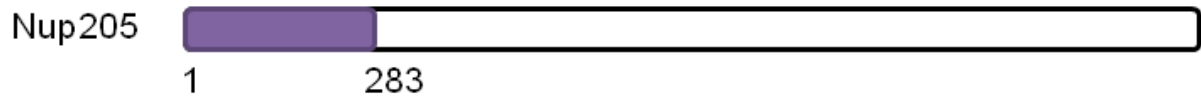as described previously (Franz C et al., 2007). The protein was purified and dialyzed against PBS and injected into rabbits for antibody production. Following is the cartoon showing the antibody recognition region in the context of the full-length protein.

Anti-Nup153 antibody

For details see Walther et al., 2001.

Anti-Pom121 antibody

The full length *Xenopus laevis* Pom121 (aa 1-1050) was cloned into pET28x MISTIC vector and expressed as a His_6 tagged fusion protein in BL21 (DE3). SDS elution from the magnetic his beads were done and protein was dialyzed against PBS and injected into rabbits for antibody production. Following is the cartoon showing the antibody recognition region in the context of the full-length protein.


Anti-Gp210 antibody

For details see Antonin et al., 2005.

Anti-Nup62 antibody

The polyclonal anti-Nup62 antibody raised in rabbits was provided to us by Birthe Fahrenkog (Universite Libre de, Bruxelles, Belgium). Also see Schwarz-Herion et al., 2007.

Anti-Nup88 antibody

The anti-Nup88 antibody (mouse monoclonal) used was a commercial antibody purchased from BD Biosciences (San Diego, California)

Anti-SUMO antibody

The anti-yeast SUMO antibody: SMT3 was purchased from Acris (Herford, Germany)

Anti-His antibody

The anti-His6 antibody (mouse monoclonal) was purchased from Roche.

mAb414:

Mouse monoclonal antibody was obtained from BabCO (Richmond, USA).

4.1.6.2. Secondary antibodies

Alexa Fluor 488 goat α-rabbit IgG, Cy3 goat α-rabbit IgG were bought from Invitrogen. Anti-rabbit IgG linked horseradish peroxidase and anti-mouse IgG linked horseradish peroxidase from goat (Calbiochem, Germany). The Cy3 and alexa 488 antibodies were used in 1:2000 dilutions. The anti rabbit and anti mouse IgG linked horseradish peroxidase were used in 1: 5000 dilutions.

4.2 Methods

4.2.1. Molecular cloning and Microbiological methods used.

4.2.1.1. PCR (Polymerase chain reaction)

PCR reactions to generate DNA fragments for sub cloning were done in a total reaction volume of 50 μl containing: 1 ng of DNA template, 2 mM of dNTP mix, forward and reverse primers at 0.5 μM each, 10x KOD reaction buffer and KOD Polymerase (1 μl). A typical PCR thermocycle was 30 cycles. DNA strands were separated for 30 sec at 95 °C in the first cycle and in all subsequent cycles. For next 5 cycles, annealing temperature of the primers was set at 54 °C for 30 sec. Elongation of the product by KOD polymerase occurred at 75 °C for 1 min per 2.5 kilobase templates. Then for the next 25 cycles, the annealing temperature of the primers was set at 58 °C for 30 sec and the elongation was done as before. The final extension step of a PCR cycle was continued for 5 min. All PCR reactions were carried out in a DNA Engine® Thermal cycler (MJ Research). After ensuring the correct fragment size on an agarose gel, the amplified PCR product was either purified with a PCR purification kit (Qiagen), or completely loaded it on an agarose gel and purified by gel extraction kit (Qiagen) following the manufacturer's instructions.

4.2.1.2. Competent cell preparation

The cell strain: BL21 (DE3) were grown overnight on LB-Plate. A single colony was inoculated in 100 ml LB medium and grown at 37 °C for overnight. 10 ml of the overnight culture was inoculated into two 500 ml LB medium separately with antibiotics. The cells were grown at 37°C until OD reached 600nm. The flasks were chilled on ice water for 10 min. Then the culture was spun at 4000 rpm for 10 min at 4 °C in pre-cooled Sorvall

Evolution RC centrifuge. The pellet was carefully resuspended in ice-cold 100 ml CaCl2 (50 mM) and kept in ice for 20 min. Then this suspension was spun at 4000 rpm for 10 min at 4 °C in pre-cooled Sorvall Evolution RC centrifuge. The pellet was resuspended in 16 ml ice cold CaCl2 (50 mM) and 15% glycerol. The cells were then aliquoted into 50μls, snap frozen in liquid nitrogen and stored at -80 °C.

4.2.1.3. Transformation of the engineered vector (DNA clone) into chemically competent cells

Transformation of E.coli CaCl2 competent cells was done by gently mixing 50 μl of cells with plasmid DNA (10 ng – 1 μg). After incubating for 20 min on ice, the bacteria were heat-shocked for 30 sec at 42 °C in a water bath, cooled for 2 min on ice and 500 μl LB medium (without any antibiotic) was added. Bacteria were incubated for 30 minutes at 37 °C with shaking at 1000rpm to allow the expression of antibiotic resistance and were plated out on LB agar containing supplemented with containing 25μg/ml kanamycin. The plates were finally incubated overnight at 37 °C.

4.2.1.4. DNA preparation from E.coli cells

DNA preparation was done using QIAPrep (Qiagen) kits following the manufacturer's instructions.

4.2.2. Commonly used Biochemical methods

4.2.2.1. Expression and purification of Nup93, Nup53 full length protein and fragments

The cell strain: BL21 (DE3) were grown overnight on LB-Plate containing the necessary antibiotics. A single colony was inoculated in 50 ml LB medium containing antibiotics and grown at 37 °C for overnight. 10 ml of the overnight culture was inoculated into two 500 ml LB medium (supplemented with 1/50 50X 5052, 1/1000 1M MgSO4, 1/20 20X NPS and with antibiotics). The cells were grown at 37°C until OD reached 1.5. The cultures were then shifted to the respective expression temperature (expression by auto induction) and grown overnight. Next morning the bacteria were harvested (checked OD: minimum 5) at 4000rpm for 5 minutes in the Sorvall Evolution RC centrifuge. The cell pellet was

then resuspended in 25ml ice-cold nickel wash buffer and volume was filled up to 200ml with the buffer. Also at this point we added 2ml of 0.2M PMSF. The emulsiflex was equilibrated with the wash buffer and the bacteria were then lysed. After this we added 1mM $MgCl_2$, 400µl of 10mg/ml DnaseI in PBS, 2ml 0.2M PMSF and incubated on ice for 10 minutes. This suspension was then spun for 15 minutes at 12000 rpm in cold SLA 1500 rotor. The supernatant was filtered through cheesecloth and Ni-NTA-Agarose beads (1ml 50% slurry/liter culture) was added and incubated (rotated) for 2 hours in the cold (4ºC). This was then applied to the column and washed with 200ml wash buffer. The elution was done by addition of Nickel elution buffer (4ml/liter culture) and vortexed for 2 minutes. To the eluate 1mMDTT and 1mM EDTA was added. For GST tagged proteins the protein concentration was calculated with BCA and the protein was snap frozen in liquid nitrogen and stored in minus 80ºC. Composition of additives used: 5052: (0.5% glycerol, 0.05% glucose, 0.2% alpha lactose). 20X NPS: 100mM PO_4, 25mM SO_4, 50mM NH_4, 100mM Na, 50mM K)

For SUMO tagged constructs (Nup93 fragments): The eluate was cleaved using TEV protease to get rid of the SUMO and the His6 tag. (1mg/ml TEV: use 1:10) while dialyzing the protein against the Ni-wash buffer overnight at 4ºC. After this we did a second Ni-NTA bead incubation (1ml 50% slurry/ml of the protein) for 2 hours and the unbound material (untagged final protein of our interest) was collected and then dialyzed against S250. The final protein concentration was calculated with BCA after, which the protein was snap frozen in liquid nitrogen and stored in minus 80ºC.

4.2.2.2. Generation of bacterial lysate expressing *Xenopus laevis* Nup155

The cell strain: BL21 (DE3) were grown overnight on LB-Plate containing the necessary antibiotics. A single colony was inoculated in 50 ml LB medium containing antibiotics and grown at 37 °C for overnight. 500µl ml of the overnight culture was inoculated into 50 ml LB medium (supplemented with 1/50 5052, 1/1000 MgSO4, 1/20 NPS and with antibiotics). The cells were grown at 37°C until OD reached 1.5. The cultures were then shifted to the respective expression temperature (expression by auto induction) and grown overnight. Next morning the bacteria were harvested (checked OD: minimum 5) at 4000rpm for 10 minutes in the Multifuge at 4ºC. The cell pellet was then resuspended in 10ml ice-cold l buffer (20mM Tris and 50mM NaCl, pH: 7.5). Also at this point we added 0.2M PMSF. The emulsiflex was equilibrated with the tris buffer and the bacteria were

then lysed. After this we added 1mM MgCl2, 400µl of 10mg/ml DnaseI in PBS, 2ml 0.2M PMSF and incubated on ice for 10 minutes. This suspension was then spun for 15 minutes at 12000 rpm in cold SLA 1500 rotor. The supernatant was filtered through cheesecloth and the lysate obtained was aliquoted and stored in minus 20ºC.

4.4.2.3. Purification of RanQ69L

The cell strain: BL21 (pREP4) were grown overnight on LB-plate containing 50µg/ml ampicillin. A single colony was inoculated in 50 ml LB medium containing antibiotics and grown at 37 °C for overnight. 10 ml of the overnight culture was inoculated into two 500 ml LB medium with ampicillin (50µg/ml). The cells were grown at 37°C until OD reached 0.4, then the culture was shifted to the 25ºC and grown till OD reached 0.8. Then induction was done using 0.2mM IPTG for 3hours at 25ºC. The bacteria were harvested at 4000rpm for 5 minutes in the Sorvall Evolution RC centrifuge. The cell pellet was resusupended in buffer (PBS, 150mM NaCl, 8mM imidazole, 2mM MgCl2 and 10% glycerol: pH 7.4 (total volume 200ml/liter culture). Also at this point we added 0.2M PMSF. The emulsiflex was equilibrated with the wash buffer and the bacteria were then lysed. After this we added 1mM MgCl2, 400µl of 10mg/ml DnaseI in PBS, 2ml 0.2M PMSF and incubated on ice for 10 minutes. This suspension was then spun for 15 minutes at 12000 rpm in cold SLA 1500 rotor. The supernatant was filtered through cheesecloth and 1.2ml Talon beads (50% slurry/liter culture) were added for 2 hours, rotating at 4ºC. This was then applied to column and washed with 200ml wash buffer (composition mentioned above). Stepwise elution of 500µl each was done using elution buffer (PBS, 150mM NaCl, 300mM imidazole, 2mM MgCl2, 10% glycerol, pH 7.4). The three most concentrated fractions were pooled and dialyzed against PBS, 2mM MgCl2 and 10% glycerol. To perform nucleotide exchange 3mM EDTA and 1mM GTP was added and incubated 2hours on ice. 3mM MgCl2 was added and the samples were dialyzed against PBS, 2mM MgCl2 and 10% glycerol. The final protein concentration was calculated with BCA after, which the protein was snap frozen in liquid nitrogen and stored in minus 80ºC.

4.2.2.4. Purification of proteins by size exclusion chromatography

Further purification of EGFP-TEV-NPM2 fusion was done by size exclusion chromatography on a Sepharose 200 column (GE-Healthcare).

4.2.2.5. Sodium dodecyl sulfate polyacrylamide gel, Phostag gel, Next gel electrophoresis and Western blotting

SDS-PAGE was performed as described earlier (Laemmli, 1970) on 8% or 12% gels. For Western blotting, the proteins were transferred to a Nitrocellulose membrane (Whatman, Germany) after SDS-PAGE. The membrane was then probed with rabbit polyclonal antibodies or mouse monoclonal antibodies to detect respective proteins. Anti-rabbit or anti-mouse IgG antibodies linked horseradish peroxidase from goat (Amersham Bioscience) was used to detect the antibody that is bound to the corresponding protein of interest

For Phostag gels: the main procedure was same as SDS PAGE electrophoresis. But while preparing the gel we added 5mmol/L phostag and 10mmol/L MnCl2. Before transfer the gel was incubated for 10 minutes first with transfer buffer with 1mM EDTA and then without EDTA. Rest of the procedure for western blotting was same as before.

For Next gels: we used the kit instructions for 15% gels (2.5-100Kda range). 10ml next gel solution was mixed with 6μl TEMED and 60μL APS, mixed and poured on to the glass plates (no need of stacking gel). The gel was run at 150V with the running buffer provided in the kit. The transfer and the western blotting procedure was the same as before.

4.2.2.6. Determination of protein concentration

The protein concentration of a solution was determined using BCATM Protein Assay Kit (Pierce) following manufacturer's instructions.

4.2.2.7. Generating polyclonal antibody generation in rabbits

All antigens used for rabbit immunization were recombinant proteins, purified either under native conditions or from inclusion bodies from E.coli. One milliliter antigen solution (0.5mg/ml) was mixed well with 1ml freud complete adjuvant in syringes and connector till it was highly viscous. For the initial immunizations four subcutaneous injection (23G x 1¼ needle) and two intramuscular injections (20G x 1½ needle) of the viscous mixture were given per rabbit. After the primary immunization, rabbits were boosted three times with first two boosts in a 14-day rhythm and the third after 28 days of the second boost. For the first boost, a mixture of 1 ml antigen solution (0.2mg/ml) with Freud incomplete adjuvant and for the second and third boost, 1 ml antigen solution (0.1mg/ml) with Freud incomplete adjuvant was injected. Rabbit's blood was then coagulated then it was spun down at 4000 rpm for 30 min in a Heraeus Multifuge 1L-R, the serum was collected, snap frozen in liquid Nitrogen and stored at -80 °C.

4.2.2.8. Affinity purification of antibodies

For affinity purification of antibodies from serum, an antigen column was first prepared. For this, the antigen for the specific antibody was expressed and purified in bacteria. The purified proteins were then dialyzed against buffer: 20mM HEPES, 500mM NaCl pH7.4. One ml of 100 % Affigel resin (BioRad, Affigel 10 for neutral, basic proteins and Affigel 15 for acidic proteins) was washed with ice-cold water. The resin then was incubated with 30 mg of the dialyzed protein (antigen) and incubated for 4 hrs at 4 °C with rotation. The supernatant was recovered and the efficiency of binding was calculated by measuring the protein concentration (should be 10% of the starting concentration). The reaction was stopped by the addition of 3 ml 1 M ethanolamine pH 8 for 1 hr at 4 °C (this leads to quenching of non-reacted active sites on the resin). Washing was done sequentially with 100mM NaHCO3 pH 8.3, 500mM NaCl and 100mM Sodium acetate pH 4.2; 500mM NaCl twice. The antigen resin was washed with 200mM glycine pH 2.3, 150mM NaCl to remove unbound material. Then the resin was washed with PBS for 3-4 times. 10 ml of the respective serum was incubated with the resin over night at 4 °C. The resin was washed 3 times with PBS containing 0.1% Tween 20 followed by extensive washing with ice cold PBS. The resin was transferred into a column and washed with PBS. Antibodies were eluted 3 times (low pH elution) with 1ml 200mM glycine pH 2.7, 150mM NaCl and 5 times 1ml 200mM glycine pH 2.2, 150mM NaCl. The eluted antibodies were neutralized with a small amount of 1.5M TRIS pH 8.8 and checked the pH using pH strips. The affinity purified antibodies were immediately dialyzed against ice cold PBS.

4.2.2.9. Preparation of antibody beads

To the 4 ml of 1mg/ml affinity purified antibody 1 ml of 50% protein A sepharose was added and incubated over night on a rotating wheel at 4 °C. For control beads rabbit IgGs were incubated with protein A sepharose in the same concentration. The beads were washed twice with coupling buffer (200mM NaHCO3, 100mM NaCl pH 9.3) and crosslinked twice for 20 min with 10mM DMP in coupling buffer and in between the beads were washed with coupling buffer once. The crosslinked beads were washed once with 0.1M ethanolamine pH 8.2 and incubated in 0.1 M ethanolamine for 1 hr in room temperature. The beads were washed twice with 100mM Sodium acetate, 500mM NaCl

pH4.2 and then washed twice with 100mM NaHCO3, 500mM NaCl, and pH 8.3. This consecutive washing step was repeated 4 times, finally washed with PBS and blocked with 3% BSA in PBS. We stored the beads in 3% BSA with addition of 0.5% azide and 0.2mM PMSF at 4ºC.

4.2.2.10. GST pull down assay using recombinant proteins and bacterial lysate (in vitro)

For bacterial lysate pull down experiments, full-length *Xenopus* Nup155 was cloned into a modified pET28a vector containing an N-terminal NusA solubility tag and a His6 tag at the C terminus. In a total volume of 800 μl, 2 μM GST or GST-Nup53 was incubated with 500 μl of lysates from bacteria expressing Nup155 or from untransformed bacteria (competitive lysate) and with or without addition of 10 μM recombinant Nup93 (C terminus: aa 608–820). After 1 h of incubation, 50 μl of 50% slurry of GSH–Sepharose (GE Healthcare) was added, and the sample was further incubated for 1 h with rotation. After six washes with 20 mM Tris and 50 mM NaCl, pH 7.4, the samples were eluted by cleavage using 30 μl of TEV protease (0.5 mg/ml) for 1 h at 25ºC shaking at 400rpm and analyzed by SDS–PAGE and Western blotting.

4.2.3. Biochemical experiments with the *Xenopus laevis* egg extract system

4.2.3.1. Preparation of *Xenopus laevis* egg extracts

Female *X. laevis* frogs were primed by injection with pregnant mare serum gonadotropin (PMSG) and about after 4-14 days ovulation of mature eggs was stimulated by injection of human chorionic gonadotropin (hCG) (0.5 ml of 2000 U/ml water). The frogs were transferred into boxes containing the buffer MMR and kept in dark for approx. 16 hrs at 18 °C. Eggs laid in MMR buffer were collected damaged eggs (mostly white) were discarded and only good quality eggs were sorted, pooled and washed extensively in MMR. The jelly coat of the eggs was removed by incubation with freshly prepared 0.25x MMR supplemented with 2% cystein, and the eggs closely packed together (~7 min). The collected eggs were arrested in metaphase of meiosis II. Following dejellynation, exposure to air was avoided since the eggs were very fragile and are prone to lysis easily after removal of the jelly coat. Eggs were released from cell cycle arrest at metaphase of meiosis

II by addition of the calcium ionophore A23187 (8 μl (2mg/ml in ethanol) per 100 ml MMR) that mimics fertilization. Animal cap contraction was visible after 10 min, as judged by an upturn of the vegetal, black pole. Activation was stopped after 10 min by thorough washing with cold MMR buffer, which removed the ionophore. Eggs were incubated at room temperature (25ºC) for 20 min and subsequently washed twice with ice-cold S250 buffer. Damaged eggs were removed with a pasteur pipette and the remaining eggs were transferred with a cut plastic pasteur pipette to SW55 plastic centrifuge tubes and centrifuged in low speed centrifugation for 1 min at 800 rpm (Heraeus, Multifuge 1L-R). The eggs were packed, removed additional buffer and centrifuged for 20 min 15000 rpm at 4 °C in an OptimaTM L-60 Ultracentrifuge with a SW55Ti rotor. The tubes were pierced with a syringe and nuclear material, organelles and glycogen were removed, leaving lipids, yolk and pigment behind and supplemented with 1 mM DTT, 44 μg/ml cycloheximide (inhibitor of protein synthesis), 5 μg/ml cytochalasin B (inhibitor of actin polymerization), and 10μL/ml of 1x Complete TM EDTA-free Protease Inhibitor Cocktail. This 'low speed extract' was centrifuged for 40 min at 45000 rpm at 4 °C to separate soluble and lipid components. The cytosolic phase was collected by a syringe, diluted with 0.3 fold 50mM KCl, 2.5mM MgCl2, 10mM Hepes pH 7.5 and spun again at the same centrifugation settings. The cytosolic phase 'high speed extract' (cytosolic components) were collected with a syringe, snap frozen and stored in liquid nitrogen.

For mitotic *Xenopus* egg extracts: After the dejellyniation and extensive washing with MMR eggs were rinsed carefully with XB buffer (2M sucrose, 10mM HEPES, 20x XB salts at pH 7.7). Then the eggs were washed carefully with XB-CSF buffer (in XB buffer added 1mM MgCl2, 1mM EGTA). Damaged eggs were removed with a pasteur pipette and the remaining eggs were transferred with a cut plastic pasteur pipette to SW55 plastic centrifuge tubes and centrifuged in low speed centrifugation for 1 min at 800 rpm (Heraeus, Multifuge 1L-R). The eggs were packed in SW55 tubes (pre containing 1 mM DTT, 5 μg/ml cytochalasin B (inhibitor of actin polymerization), and 1x Complete TM EDTA-free Protease Inhibitor Cocktail), removed additional buffer and centrifuged for 15 min 15000 rpm at 4 °C in a OptimaTM L-60 Ultracentrifuge with a SW55Ti rotor. The tubes were pierced with a syringe and nuclear material, organelles and glycogen were removed, leaving lipids, yolk and pigment behind and supplemented with 5 μg/ml cytochalasin B (inhibitor of actin polymerization), and 10μL/ml of 1x Complete TM EDTA-free Protease Inhibitor Cocktail and 1mM DTT. The extracts were aliquoted and snap frozen in liquid nitrogen. 20X XB salts contains: 2M KCl, 2mM CaCl2, 20mM

MgCl2 and XB buffer (1L) composition is: 50ml 20X XB salts, 10mM HEPES pH7.7 and 50mM sucrose.

4.2.3.2. Preparation of the total membrane fraction from *Xenopus laevis* egg extracts

For preparation of total membranes, the membrane fraction was diluted in 10 volumes S250 buffer, 1 mM DTT and 10μL/ml of 1X Complete TM EDTA-free Protease Inhibitor Cocktail. The membranes were homogenized in a dounce homogenizer. The suspension was then placed on top of 1ml S500 (500mM sucrose, 50mM KCl, 2.5mM $MgCl_2$, 10mM hepes, pH 7.5), 1mM DTT and 1X Complete TM EDTA-free Protease Inhibitor Cocktail in SW40 tubes, spun in SW40 rotor for 20min at 11000 rpm at 4 °C. The pellets obtained thereafter were resuspended in S250, 1mM DTT and 10μL/ml of 1x Complete TM EDTA-free Protease Inhibitor Cocktail to 20% volume of the cytosol. Then the total membrane fraction was aliquoted and snap frozen in liquid nitrogen and stored in the same.

4.2.3.3. Preparation of the floated membranes from *Xenopus laevis* egg extracts

For preparation of floated membranes the membranes were removed on top of the mitochondria and pigments. This membrane fraction is mixed with 4 volumes of S2100 (with 1 mM DTT, 10μL/ml of 1X Complete TM EDTA-free Protease Inhibitor Cocktail and homogenized two times using a 30 ml dounce homogenizer. 5 ml of this membrane suspension was added into a Beckman centrifuge tube suitable for SW40Ti rotor and overlaid with 1.4 ml S1400, S1300, S1100, S900, S700 cushion and on top of the gradient we added 0.2ml S250 buffer. Membranes were floated for 4 h at 38000 rpm at 4 °C. The upper 3 membrane fractions were isolated and diluted with 3 volumes of S250, 1 mM DTT and 1X Complete TM EDTA-free protease inhibitor cocktail. This mixture is then pelleted in an OptimaTM TLX Ultracentrifuge in TLA100.4 at 100000 rpm for half an hour. The pellet was resuspended in S250, 1 mM DTT and 1X Complete TM EDTA-free protease inhibitor cocktail to bring the volume to 50% of the cytosol. Then the floated membrane fraction was aliquoted and snap frozen in liquid nitrogen and stored in the same. S2100: 2100mM sucrose, 50mM KCl, 2.5mM $MgCl_2$, 10mM Hepes pH 7.5. For S1400: mix 6.2ml S2100 and 3.8ml S250. For S1300: mix 5.7ml S2100 and 4.3ml S250. For S1100: mix 4.6ml S2100 and 5.2ml S250. For S900: mix 3.5ml S2100 and 6.5ml S250. For S700: mix 2.45ml S2100 and 7.55ml S250.

4.2.3.4. Immunodepletion of nucleoporins from the *Xenopus laevis* interphasic egg extracts

The blocked antibody beads (as explained in section 4.2.2.9) were taken and washed twice with S250 (equilibration) and incubated with freshly prepared cytosol (4.2.3.1) in the following ratio (Nup93 − 1:1.2: beads to the extracts) and respective amount of control antibody beads {rabbit IgGs} for 20 min at 4 °C under rotation. Two rounds of the depletion were done. The repetition of the depletion step was done on fresh, pre blocked antibody beads. Depleted cytosol was recovered and immediately used for *in vitro* nuclear assembly reactions.

4.2.3.5. *In vitro* nuclear assembly reactions

For a typical nuclear assembly reaction, 0.3-0.5 µl sperm chromatin (3000 sperm heads/µl) was incubated for 10 min at 20 °C in 20 µl cytosol (obtained from extracts: for instance Nup93 depleted extracts). To start the NE assembly reaction, 2 µl floated membranes (either with DiIC18 or unlabelled floated membranes (IF 1-3) for immunofluorescence or transmission electron microscopy), 0.5 µl 50x energy mix and 0.5 µl glycogen (20 mg/ml) were added. The reaction continued till 90 minutes at 20º C and was further processed with immunofluorescence or checked for NE staining etc.

4.2.3.6. Immunofluorescence of *in vitro* reconstituted nuclei

The nuclei obtained after the completion of the NE assembly reaction were fixed in 0.5 ml 4% PFA in PBS and incubated for 20 min on ice. Cover slips (round, 12 mm in diameter) were coated with poly-L lysine solution for 5 min at RT. Poly-L-lysine solution was removed and cover slips dried and transferred to scintillation vials. Fixed NE assembly reactions were applied to 0.8 ml 30% sucrose in S250 buffer. The reaction was spun through the cushion onto the lysine coated cover slips at 3500 rpm for 15 min (4 °C) in a Heraeus Multifuge 1L-R. Cover slips were lifted off from the tube by puncturing the vials from the bottom with a syringe needle and then removed carefully with the forceps. Immunofluorescence was done in a 24-well plate. The fixative was quenched with 50 mM NH$_4$Cl in 70% PBS for 10 min at RT (approx. 25ºC). Blocking solution that is 3% BSA in 0.1% Triton-X100 in 70% PBS and was applied to the cover slips for 30 min at RT. Antibodies was diluted in the blocking solution. Primary antibodies were incubated with the nuclei on the cover slips for 2 hrs in a humid chamber followed by 3 washes with 0.1%

Triton-X100 in 70% PBS. Secondary antibodies coupled to fluorophors (Alexa Fluor®
488/Cy3 goat anti-mouse/rabbit IgG were diluted 1:2000 in blocking solution and applied
for 1 hr. After labeling with secondary antibodies, cover slips were washed 3 times with
0.1% Triton-X100 in 70% PBS and with 70% PBS alone. DAPI (1 mg/ml) was diluted
1:1000 in PBS to stain the DNA and reactions on cover slips were stained for 10 min at
RT. After two additional washes with PBS and water, cover slips were removed from
water and remaining liquid was removed by drying them on the whattman paper. Samples
were mounted on a drop of Vectarshield® mounting media on glass slides. Liquid was
removed from the rim of the cover slips with a tissue and the preparation was sealed with
nail polish to fix the coverslips. The nuclei were imaged using confocal microscopy. A
modified protocol was used when membranes were to be stained that is fixing was done
with Vikifix with 0.5% glutaraldehyde yielded better conservation of nuclear membranes
due to the presence of glutaraldehyde.

4.2.3.7. Immunoprecipitation of nucleoporins done using on *Xenopus leavis* egg extracts

Egg cytosol (interphasic or mitotic) was diluted 1:1 with PBS supplemented with
Complete TM EDTA free protease inhibitor cocktail and spun for 30 min at 100000 rpm in
a TLA100.4 rotor 50 µl antiserum were added to 300 µl cytosol after centrifugation and
incubated for 2 h at 4 °C with rotation. 60 µl Protein A sepharose (50% slurry) was added
and incubated for 1 hr. Beads were spun down, supernatant removed and the resin was
washed 5 times with 500 mM NaCl in PBS and next 5 times with PBS or 8-10 times with
PBS alone. Bound proteins were eluted with 40 µl 1x SDS-sample buffer (hot)
supplemented with 100 mM DTT. 10 µl of the eluates were loaded onto 8%/12%
polyacrylamide gels and analyzed by Western blots with corresponding antibodies. For
mitotic extracts we used low speed extracts.

4.2.3.8 Immune precipitation of mitotic and interphasic Nup53 from *Xenopus laevis* egg extracts followed by mass spectrometric analysis

2 ml interphasic or post mitotic (Hartl et al, 1994) or (CSF arrested) mitotic (Murray,
1991) *Xenopus* egg extracts were diluted with 1.2 ml wash buffer (10 mM HEPES, 50 mM
KCl, 2.5 mM MgCl2 pH 7.4), cleared by centrifugation for 10 min at 100,000 rpm in a
TLA110 rotor and incubated with 50 µl 50% slurry of protein A Sepharose (GE
Healthcare), to which affinity purified Nup53 antibodies were bound and crosslinked with

10 mM dimethylpimelimidate (DMP: Pierce). After 1h incubation the sepharose was washed 10 times with wash buffer (PBS). Proteins were eluted with SDS sample buffer (without DTT) and separated by SDS-PAGE. Gel sections from 30-45 kDa were excised and proteins were in-gel digested by trypsin. The resulting peptide mixtures were measured on an LTQ-Orbitrap XL and processed by Max Quant software as described (Borchert et al, 2010). Multistage activation was enabled in all MS measurements.

4.2.3.9. GST pull down assays using *Xenopus laevis* egg extracts

Full-length *Xenopus* Nup53 or the nucleoplasmic domain of Gp210 was expressed as GST fusion proteins followed by a recognition site for thrombin protease and purified via an N-terminal His_6 tag as described. In a 800-μl total volume, 2 μM of the respective bait proteins were incubated with interphasic *Xenopus* egg extracts (diluted 1:1 with 10 mM HEPES, 50 mM KCl, 2.5 mM $MgCl_2$, pH 7.5, and cleared by centrifugation for 20 min at 100,000 rpm in a TLA110 rotor [Beckman Coulter, Brea, CA]) with and without addition of 5 μM SUMO-tagged Nup93 (M+C terminal domains aa 183–582) or Nup93 (C terminal domain: aa 608–820). After 2 h, 50 μl of 50% slurry GSH–Sepharose (GE Healthcare, Piscataway, NJ) was added and the sample incubated for another 90 min. Six washes were done with PBS the samples were eluted by cleavage with thrombin (0.1 mg/ml) for 1 h at 25ºC with shaking at 400 rpm and analyzed by SDS–PAGE and Western blotting.

For the GST pull downs done using Nup53 as bait to pull out the Nup93-205 from the extracts (interphasic or mitotic) the main principle followed was the same except a few changes, namely: the GSH sepharose beads were pre coupled with GST Nup53 and blocked with 5% BSA in PBS. The extracts were then incubated with the beads for 2 hours. Elution was done using TEV protease as the GST Nup53 baits had a TEV cleavage site inserted. Rest of the protocol was the same as above.

4.2.3.10. Size exclusion assay (using florescent labeled dextrans)

The nuclei were assembled until 90 min with unlabelled floated membranes. For the immunodepletion of Nup93, mock depletion or add back with different fragments of Nup93 the nuclei were incubated with 30μg/ml of fluorescein labeled 70kDa Dextrans. The dextrans were incubated for 10 min and immediately analyzed using the confocal microscope.

4.2.3.11. Nuclear import assays with nuclei assembled in vitro using *Xenopus laevis* egg extracts

To test importin α/β and transportin dependent nuclear import function, a full length NPM2 (Nucleoplasmin) was fused to EGFP followed by a TEV protease recognition site and cloned into a modified pET28a vector allowing the purification via C-terminal His_6 tag. After Ni-NTA purification, both the substrates were purified size exclusion chromatography on a Sepharose 200 column (GE-Healthcare). Nuclei were assembled on a 50 µl, as the volume ratio described previously (Franz C et al., 2005). The nuclear assembly was allowed until 50 min after the addition of membranes then, 1 µg of the respective reporters was added. After 90 minutes the nuclei were fixed and analyzed using confocal microscope to check the localization of the EGFP tagged nuclear import substrate.

4.2.3.12 Electron microscopy (EM) of nuclear assembly reactions

After the fixation of the nuclei (with 1ml vikifix (80mM pipes pH, 6.8, 1mM $MgCl_2$, 150mM sucrose and 2% PFA)+ 0.5% glutaraldehyde for 30 minutes on ice) obtained using in vitro nuclear assembly reaction the nuclei were spun through 0.8ml 30% sucrose solution in PBS cushion on poly-L lysine coated coverslips for 15 minutes at 3500 rpm in the multifuge. Coverslips were then washed with 1X fix buffer (25mM HEPES pH7.5, 25mM PIPES, 1mM EGTA, 50mM KCl, 2mM MgAc and 5% sucrose) and then fixed with 1% glutaraldehyde in fix buffer on ice for 1 hour. Post-fixing was done using 2.5% glutaraldehyde in fix buffer for 2 hours on ice. The samples were then processed by the EM facility wherein $OsO4$ treatment was done followed by embedding. Then washing was done with ice-cold 100mM cacodylate buffer pH 7.2. Then incubation with 1% $OsO4$ and 1.5% K-feerocyanide in 100mM cacodylate buffer was done for 40 minutes on ice. This was followed by En bloc staining with 0.5% uranyl-acetate followed by dehydration and resin treatment and imaging was then done with the transmission electron microscope.

4.2.4. Light microscopy

The samples from the various assays as explained above were recorded using Olympus FV1000 confocal microscope with 405-, 488- and 559-nm laser lines and a 60x NA 1.35 oil immersion objective lens using the Olympus Fluoview software. Bleed through between the channels was avoided by scanning different channels sequentially in the

Fluoview. The physical measurements of the samples were done using the Fluoview. All the images were processed using ImageJ (NIH, Bethesda, USA) and Adobe® Photoshop® CS4.

Name of the antibody	Dilution used for western blot	Dilution used for IF
Nup93 antibody (K232)	1:1000	1:100
Nup188 antibody (K165)	1:1000	1:100
Nup205 antibody (K205)	1:1000	1:100
Nup53 antibody (K213)	1:1000	1:100
Nup155 antibody (D3Z)	1:1000	1:100
Nup98 antibody (EWD6)	1:1000	1:100
Nup160 antibody (EWD7)	1:1000	1:100
Nup107 antibody (G023)	1:1000	1:100
Mel-28 antibody (K256)	1:1000	1:100
Nup58 antibody (K147)	1:1000	1:100
Nup153 antibody (IP84)	1:2000	1:100
Pom121 antibody (K189)		1:100
Gp210 antibody (CVK9)		1:100
Importin beta antibody (K169)	1:1000	1:100
Nup62 antibody		1:100
Nup88 antibody (anti mouse)		1:100
Sumo antibody (anti mouse)	1:5000	
His6 antibody (anti mouse)	1:5000	
Mab414 antibody (anti mouse)	1:10,000 (for Nup62) and 1:2000 (for Nup153)	1:2000

Where not mentioned the antibodies have been generated in rabbit in the lab.

Expression and purification conditions for proteins used in this study.

Clone name	Temperature/expression mode	Ni-NTA beads (50% slurry: ml/L)	Elution volume (ml/L)	Yield obtained (mg/ml/L)	Expected weight (kDa)
pET28pNup93xl 1-820 (2203)	18°C / autoinduction	2	2+1	0.5	105
pET28sTEVNup93xl CO 1-579 (3774)	18°C / autoinduction	2	1+1	0.3	78
pET28sTEVNup93xl CO 605-820 (3775)	18°C / autoinduction	3	3+1.5	01.5	38
pET28sTEVNup93xl CO 183-820 (3776)	18°C / autoinduction	3	3+1.5	1	84
pET28sTEVNup93xl CO 183-579 (3777)	18°C / autoinduction	2	2+1	0.5	58
pET28sTEVNup93xl CO 1-820 (176-607 deleted) (4548)	18°C / autoinduction	2	2	0.3	60
pET28eNup53xlCO 1-320 (1219)	18°C / autoinduction	2	2+1	0.5	60
pET28eNup53xlCO 78-136 (3941)	18°C / autoinduction	4	4+2	6	31
pET28eNup53xlCO 52-166 (3927)	18°C / autoinduction	4	4+2	5	37
pET28eNup53xlCO 1-77 (3928)	18°C / autoinduction	4	4+2	4	33
pET28eNup53xlCO 130-267 (4170)	18°C / autoinduction	4	4+2	3	40
pET28eNup53xlCO 78-166 (3920)	18°C / autoinduction	4	4+2	3	35
pET28eNup53xlCO	18°C / autoinduction	4	4+2	4	36

162-267 (3830)					
pET28eNup53xlCO 1-166 (3930)	18°C / autoinduction	4	4+2	3	43
pET28eNup53xlCO 93-267 (4172)	18°C / autoinduction	4	4+2	2	44
pET28eNup53xlCO 52-136 (3926)	18°C / autoinduction	4	4+2	4	34
pET28eNup53xlCO 1-267 (4169)	18°C / autoinduction	4	4+2	1	55
pET28eNup53xlCO 162-312 (3843)	18°C / autoinduction	4	4+2	4	41
pET28e (1178)	18°C / autoinduction	2	2+1	1	25

Coomasie gels showing the protein yield for the above-mentioned constructs for GST Nup53
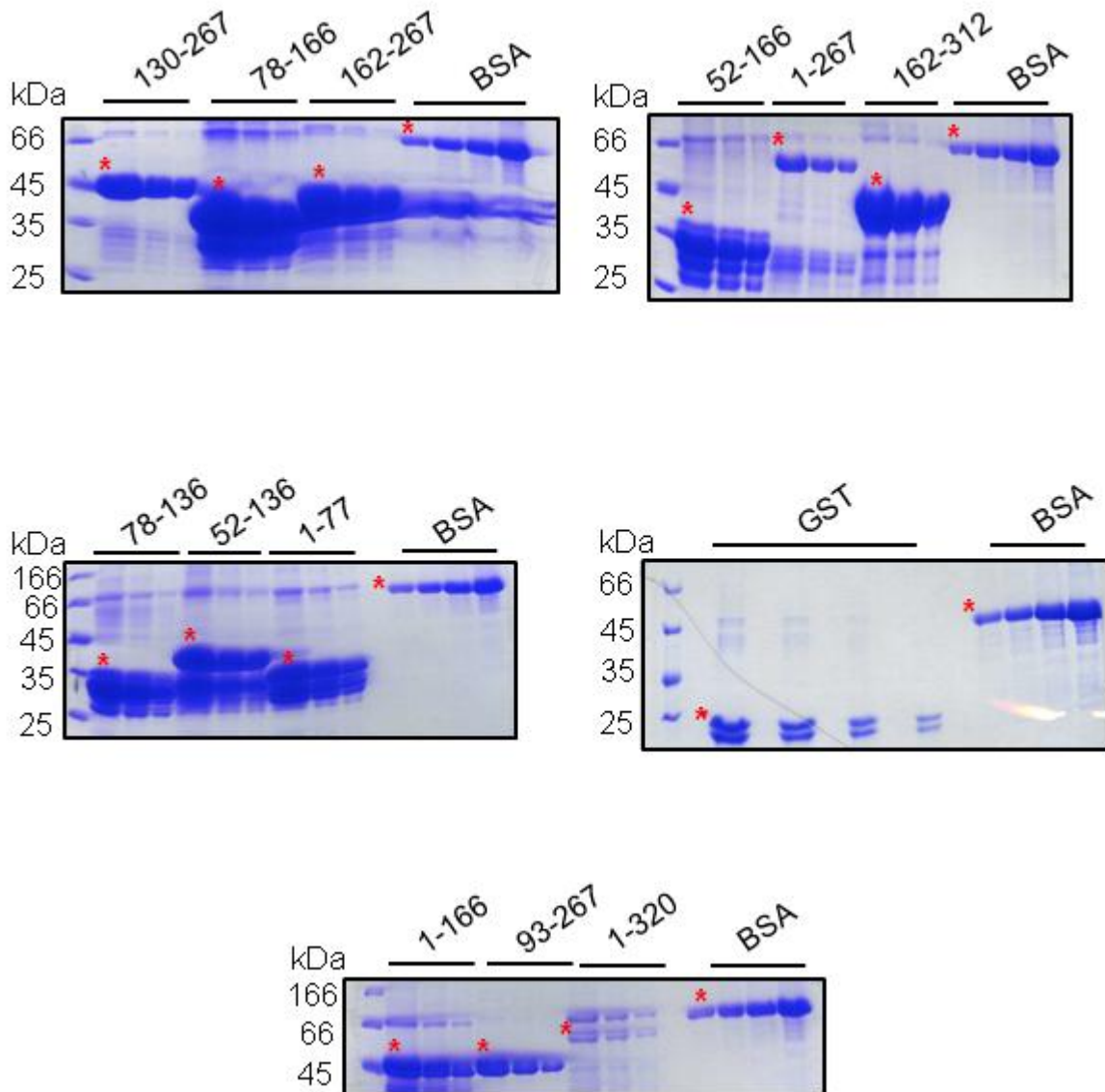
The numbers refer to the amino acids of the Nup53 constructs expressed as GST proteins. The * shows the desired protein band. Left hand side in each gel shows the molecular weight bands of the marker. Different dilutions of the proteins were loaded to calculate the protein concentration with respect to BSA as shown. Both protein and BSA were diluted 1:1 in SDS sample buffer and loaded on the 12% SDS PAGE gels. The dilutions of the protein are 10µl, 5µl and 2.5µl from left to right. BSA is 0.3, 0.5, 1 and 2 mg/ml from left to right. The final concentration is mentioned in the table above.

Coomasie gels showing the protein yield for the above-mentioned constructs for Nup93
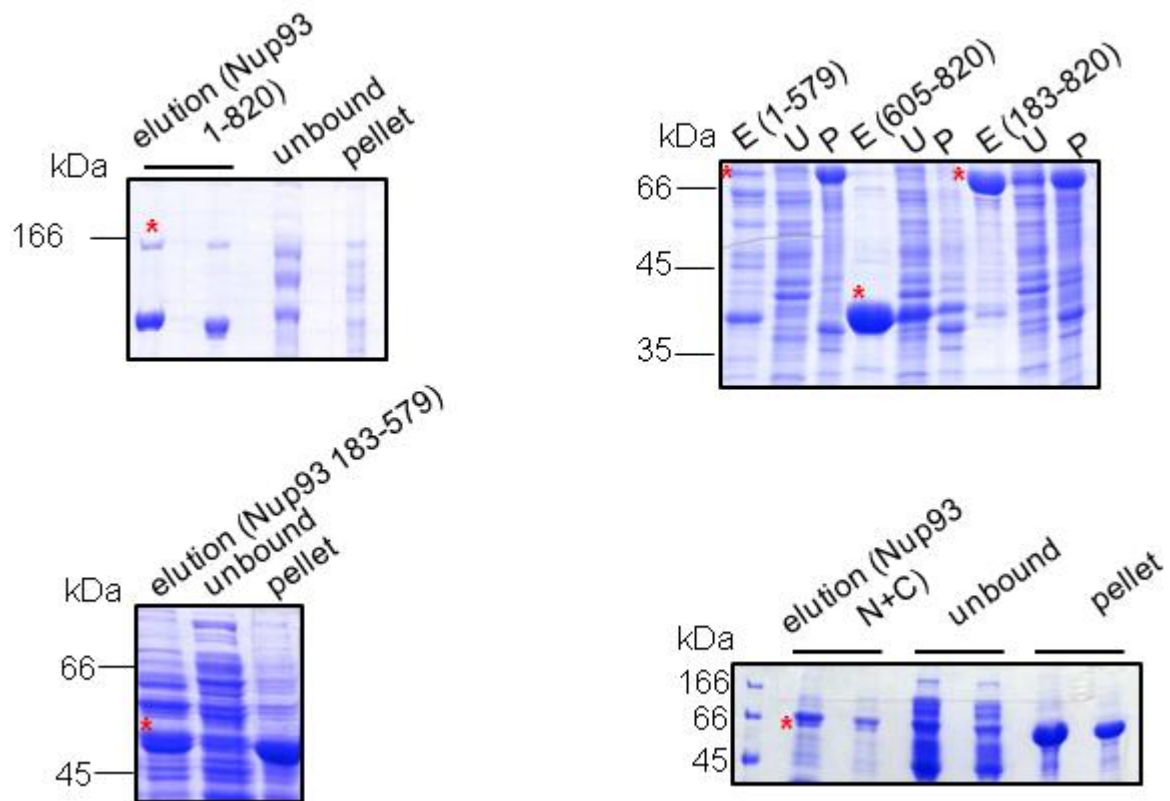
The numbers refer to the amino acids of the Nup93 constructs. The * shows the desired protein band. Left hand side in each gel shows the molecular weight bands of the marker. The final protein obtained (elution), unbound and pellet fractions were diluted 1:1 in SDS sample buffer and 10µl was loaded on the SDS PAGE gel. The final concentration as obtained by BCA method is mentioned in the table above. E: elution, U: unbound, P: pellet.

5. REFERENCES

1. Sorting out the nuclear envelope from the endoplasmic reticulum. Mattaj IW. Nat Rev Mol Cell Biol. 2004 Jan;5(1):65-9.

2. Integral membrane proteins specific to the inner nuclear membrane and associated with the nuclear lamina. Senior A, Gerace L. J Cell Biol. 1988 Dec;107(6 Pt 1):2029-36.

3. Nuclear pore complex assembly through the cell cycle: regulation and membrane organization. Antonin W, Ellenberg J, Dultz E. FEBS Lett. 2008 Jun 18;582(14):2004-16.

4. Structure and function in the nucleus. Lamond AI, Earnshaw WC. Science. 1998 Apr 24;280(5363):547-53.

5. Specific staining of human chromosomes in Chinese hamster x man hybrid cell lines demonstrates interphase chromosome territories. Schardin M, Cremer T, Hager HD, Lang M. Hum Genet. 1985;71(4):281-7.

6. The end adjusts the means: heterochromatin remodelling during terminal cell differentiation. Grigoryev SA, Bulynko YA, Popova EY. Chromosome Res. 2006;14(1):53-69.

7. Transcription and the territory: the ins and outs of gene positioning. Williams RR. Trends Genet. 2003 Jun;19(6):298-302.

8. Functional architecture in the cell nucleus. Dundr M, Misteli T. Biochem J. 2001 Jun 1;356(Pt 2):297-310.

9. Nucleolus: from structure to dynamics. Hernandez-Verdun D. Histochem Cell Biol. 2006 Jan;125(1-2):127-37.

10. Multiple roles of arginine/serine-rich splicing factors in RNA processing. Sanford JR, Ellis J, Cáceres JF. Biochem Soc Trans. 2005 Jun;33(Pt 3):443-6.

11. Cajal bodies: the first 100 years. Gall JG. Annu Rev Cell Dev Biol. 2000;16:273-300.

12. Inner nuclear membrane proteins: functions and targeting. Holmer L, Worman HJ. Cell Mol Life Sci. 2001 Nov;58(12-13):1741-7.

13. Inner nuclear membrane and signal transduction. Worman HJ. J Cell Biochem. 2005 Dec 15;96(6):1185-92.

14. Molecular biology and the diagnosis and treatment of liver diseases. Worman HJ, Feng L, Mamiya N. World J Gastroenterol. 1998 Jun;4(3):185-191.

15. Interaction between an integral protein of the nuclear envelope inner membrane and human chromodomain proteins homologous to Drosophila HP1. Ye Q, Worman HJ. J Biol Chem. 1996 Jun 21;271(25):14653-6.

16. LINC complexes form by binding of three KASH peptides to domain interfaces of trimeric SUN proteins. Sosa BA, Rothballer A, Kutay U, Schwartz TU. Cell. 2012 May 25;149(5):1035-47.

17. Mitosis in the hemoflagellate Trypanosoma cyclops. Heywood P, Weinman D. J Protozool. 1978 Aug;25(3 Pt 2):287-92.

18. Nucleus behavior during the closed mitosis of Tritrichomonas foetus. Ribeiro KC, Mariante RM, Coutinho LL, Benchimol M. Biol Cell. 2002 Sep;94(4-5):289-301.

19. Pushing the envelope: structure, function, and dynamics of the nuclear periphery. Hetzer MW, Walther TC, Mattaj IW. Annu Rev Cell Dev Biol. 2005;21:347-80.

20. Orchestrating nuclear envelope disassembly and reassembly during mitosis. Güttinger S, Laurell E, Kutay U. Nat Rev Mol Cell Biol. 2009 Mar;10(3):178-91.

21. Remodelling the walls of the nucleus. Burke B, Ellenberg J. Nat Rev Mol Cell Biol. 2002 Jul;3(7):487-97.

22. Endoplasmic reticulum remains continuous and undergoes sheet-to-tubule transformation during cell division in mammalian cells. Puhka M, Vihinen H, Joensuu M, Jokitalo E. J Cell Biol. 2007 Dec 3;179(5):895-909.

23. Reshaping of the endoplasmic reticulum limits the rate for nuclear envelope formation. Anderson DJ, Hetzer MW. J Cell Biol. 2008 Sep 8;182(5):911-24.

24. The nuclear envelope lamina is reversibly depolymerized during mitosis. Gerace L, Blobel G. Cell. 1980 Jan;19(1):277-87.

25. Phosphorylation of the nuclear lamins during interphase and mitosis. Ottaviano Y, Gerace L. J Biol Chem. 1985 Jan 10;260(1):624-32.

26. Nuclear membrane dynamics and reassembly in living cells: targeting of an inner nuclear membrane protein in interphase and mitosis. Ellenberg J, Siggia ED, Moreira JE, Smith CL, Presley JF, Worman HJ, Lippincott-Schwartz J. J Cell Biol. 1997 Sep 22;138(6):1193-206.

27. Nuclear envelope formation by chromatin-mediated reorganization of the endoplasmic reticulum. Anderson DJ, Hetzer MW. Nat Cell Biol. 2007 Oct;9(10):1160-6.

28. Endoplasmic reticulum remains continuous and undergoes sheet-to-tubule transformation during cell division in mammalian cells. Puhka M, Vihinen H, Joensuu M, Jokitalo E. J Cell Biol. 2007 Dec 3;179(5):895-909.

29. Reshaping of the endoplasmic reticulum limits the rate for nuclear envelope formation. Anderson DJ, Hetzer MW. J Cell Biol. 2008 Sep 8;182(5):911-24.

30. Systematic kinetic analysis of mitotic dis- and reassembly of the nuclear pore in living cells. Dultz E, Zanin E, Wurzenberger C, Braun M, Rabut G, Sironi L, Ellenberg J. J Cell Biol. 2008 Mar 10;180(5):857-65.

31. Nuclear pore complex number and distribution throughout the Saccharomyces cerevisiae cell cycle by three-dimensional reconstruction from electron micrographs of nuclear envelopes. Winey M, Yarar D, Giddings TH Jr, Mastronarde DN. Mol Biol Cell. 1997 Nov;8(11):2119-32.

32. Nuclear pores form de novo from both sides of the nuclear envelope. D'Angelo MA, Anderson DJ, Richard E, Hetzer MW. Science. 2006 Apr 21;312(5772):440-3.

33. Martin Hetzer: taking the nuclear membrane beyond the barrier. Hetzer M. J Cell Biol. 2010 Aug 23;190(4):484-5.

34. Proteomic analysis of the mammalian nuclear pore complex. Cronshaw JM, Krutchinsky AN, Zhang W, Chait BT, Matunis MJ. J Cell Biol. 2002 Sep 2;158(5):915-27.

35. Pore relations: nuclear pore complexes and nucleocytoplasmic exchange. Rout MP, Aitchison JD. Essays Biochem. 2000;36:75-88.

36. The nuclear pore complex: three-dimensional surface structure revealed by field emission, in-lens scanning electron microscopy, with underlying structure uncovered by proteolysis. Goldberg MW, Allen TD. J Cell Sci. 1993 Sep;106 (Pt 1):261-74.

37. The nuclear pore complex and lamina: three-dimensional structures and interactions determined by field emission in-lens scanning electron microscopy. Goldberg MW, Allen TD. J Mol Biol. 1996 Apr 12;257(4):848-65.

38. Toward a more complete 3-D structure of the nuclear pore complex. Jarnik M, Aebi U. J Struct Biol. 1991 Dec;107(3):291-308.

39. High-resolution field-emission scanning electron microscopy of nuclear pore complex. Ris H. Scanning. 1997 Aug;19(5):368-75.

40. High-resolution field emission scanning electron microscope imaging of internal cell structures after Epon extraction from sections: a new approach to correlative ultrastructural and immunocytochemical studies. Ris H, Malecki M. J Struct Biol. 1993 Sep-Oct;111(2):148-57.

41. ATP-Induced shape change of nuclear pores visualized with the atomic force microscope. Rakowska A, Danker T, Schneider SW, Oberleithner H. J Membr Biol. 1998 May 15;163(2):129-36.

42. The nuclear pore complex: from molecular architecture to functional dynamics. Stoffler D, Fahrenkrog B, Aebi U. Curr Opin Cell Biol. 1999 Jun;11(3):391-401.

43. Interactions and structure of the nuclear pore complex revealed by cryo-electron microscopy. Akey CW. J Cell Biol. 1989 Sep;109(3):955-70.

44. Architecture of the Xenopus nuclear pore complex revealed by three-dimensional cryo-electron microscopy. Akey CW, Radermacher M. J Cell Biol. 1993 Jul;122(1):1-19.

45. Three-dimensional architecture of the isolated yeast nuclear pore complex: functional and evolutionary implications. Yang Q, Rout MP, Akey CW. Mol Cell. 1998 Jan;1(2):223-34.

46. Nuclear pore complex structure and dynamics revealed by cryoelectron tomography. Beck M, Förster F, Ecke M, Plitzko JM, Melchior F, Gerisch G, Baumeister W, Medalia O. Science. 2004 Nov 19;306(5700):1387-90.

47. Snapshots of nuclear pore complexes in action captured by cryo-electron tomography. Beck M, Lucić V, Förster F, Baumeister W, Medalia O. Nature. 2007 Oct 4;449(7162):611-5.

48. Classification of cryo-electron sub-tomograms using constrained correlation. Förster F, Pruggnaller S, Seybert A, Frangakis AS. J Struct Biol. 2008 Mar;161(3):276-86.

49. Structural and functional analysis of Nup133 domains reveals modular building blocks of the nuclear pore complex. Berke IC, Boehmer T, Blobel G, Schwartz TU. J Cell Biol. 2004 Nov 22;167(4):591-7.

50. Components of coated vesicles and nuclear pore complexes share a common molecular architecture. Devos D, Dokudovskaya S, Alber F, Williams R, Chait BT, Sali A, Rout MP. PLoS Biol. 2004 Dec;2(12):e380.

51. Modularity within the architecture of the nuclear pore complex. Schwartz TU. Curr Opin Struct Biol. 2005 Apr;15(2):221-6.

52. The permeability of reconstituted nuclear pores provides direct evidence for the selective phase model. Hülsmann BB, Labokha AA, Görlich D. Cell. 2012 Aug 17;150(4):738-51.

53. Systematic analysis of barrier-forming FG hydrogels from Xenopus nuclear pore complexes. Labokha AA, Gradmann S, Frey S, Hülsmann BB, Urlaub H, Baldus M, Görlich D. EMBO J. 2012 Nov 30. doi: 10.1038/emboj.2012.302.

54. The nuclear pore complex: a jack of all trades? Fahrenkrog B, Köser J, Aebi U. Trends Biochem Sci. 2004 Apr;29(4):175-82.

55. Disorder in the nuclear pore complex: the FG repeat regions of nucleoporins are natively unfolded. Denning DP, Patel SS, Uversky V, Fink AL, Rexach M. Proc Natl Acad Sci U S A. 2003 Mar 4;100(5):2450-5.

56. Mapping the dynamic organization of the nuclear pore complex inside single living cells. Rabut G, Doye V, Ellenberg J. Nat Cell Biol. 2004 Nov;6(11):1114-21.

57. Dynamics of nuclear pore complex organization through the cell cycle. Rabut G, Lénárt P, Ellenberg J. Curr Opin Cell Biol. 2004 Jun;16(3):314-21.

58. Cell-cycle-dependent phosphorylation of the nuclear pore Nup107-160 subcomplex. Glavy JS, Krutchinsky AN, Cristea IM, Berke IC, Boehmer T, Blobel G, Chait BT. Proc Natl Acad Sci U S A. 2007 Mar 6;104(10):3811-6.

59. The entire Nup107-160 complex, including three new members, is targeted as one entity to kinetochores in mitosis. Loïodice I, Alves A, Rabut G, Van Overbeek M, Ellenberg J, Sibarita JB, Doye V. Mol Biol Cell. 2004 Jul;15(7):3333-44.

60. Dissection of the NUP107 nuclear pore subcomplex reveals a novel interaction with spindle assembly checkpoint protein MAD1 in Caenorhabditis elegans. Ródenas E, González-Aguilera C, Ayuso C, Askjaer P. Mol Biol Cell. 2012 Mar;23(5):930-44.

61. Caenorhabditis elegans nucleoporins Nup93 and Nup205 determine the limit of nuclear pore complex size exclusion in vivo. Galy V, Mattaj IW, Askjaer P. Mol Biol Cell. 2003 Dec;14(12):5104-15.

62. Role of the nuclear transport factor p10 in nuclear import. Nehrbass U, Blobel G. Science. 1996 Apr 5;272(5258):120-2.

63. The yeast nucleoporin Nup188p interacts genetically and physically with the core structures of the nuclear pore complex. Nehrbass U, Rout MP, Maguire S, Blobel G, Wozniak RW. J Cell Biol. 1996 Jun;133(6):1153-62.

64. Nic96p is required for nuclear pore formation and functionally interacts with a novel nucleoporin, Nup188p. Zabel U, Doye V, Tekotte H, Wepf R, Grandi P, Hurt EC. J Cell Biol. 1996 Jun;133(6):1141-52.

65. Insertional mutagenesis in zebrafish identifies two novel genes, pescadillo and dead eye, essential for embryonic development. Allende ML, Amsterdam A, Becker T, Kawakami K, Gaiano N, Hopkins N. Genes Dev. 1996 Dec 15;10(24):3141-55.

66. Systematic deletion and mitotic localization of the nuclear pore complex proteins of Aspergillus nidulans. Osmani AH, Davies J, Liu HL, Nile A, Osmani SA. Mol Biol Cell. 2006 Dec;17(12):4946-61.

67. Caenorhabditis elegans nucleoporins Nup93 and Nup205 determine the limit of nuclear pore complex size exclusion in vivo. Galy V, Mattaj IW, Askjaer P. Mol Biol Cell. 2003 Dec;14(12):5104-15.

68. A complex of nuclear pore proteins required for pore function. Finlay DR, Meier E, Bradley P, Horecka J, Forbes DJ. J Cell Biol. 1991 Jul;114(1):169-83.

69. The nuclear pore complex has entered the atomic age. Brohawn SG, Partridge JR, Whittle JR, Schwartz TU. Structure. 2009 Sep 9;17(9):1156-68.

70. Dynamics of nuclear pore complex organization through the cell cycle. Rabut G, Lénárt P, Ellenberg J. Curr Opin Cell Biol. 2004 Jun;16(3):314-21.

71. ELYS is a dual nucleoporin/kinetochore protein required for nuclear pore assembly and proper cell division. Rasala BA, Orjalo AV, Shen Z, Briggs S, Forbes DJ. Proc Natl Acad Sci U S A. 2006 Nov 21;103(47):17801-6.

72. MEL-28/ELYS is required for the recruitment of nucleoporins to chromatin and postmitotic nuclear pore complex assembly. Franz C, Walczak R, Yavuz S, Santarella R, Gentzel M, Askjaer P, Galy V, Hetzer M, Mattaj IW, Antonin W. EMBO Rep. 2007 Feb;8(2):165-72.

73. Steps in the assembly of replication-competent nuclei in a cell-free system from Xenopus eggs. Sheehan MA, Mills AD, Sleeman AM, Laskey RA, Blow JJ. J Cell Biol. 1988 Jan;106(1):1-12.

74. Distinct AAA-ATPase p97 complexes function in discrete steps of nuclear assembly. Hetzer M, Meyer HH, Walther TC, Bilbao-Cortes D, Warren G, Mattaj IW. Nat Cell Biol. 2001 Dec;3(12):1086-91.

75. Nuclear envelope formation by chromatin-mediated reorganization of the endoplasmic reticulum. Anderson DJ, Hetzer MW. Nat Cell Biol. 2007 Oct;9(10):1160-6.

76. Direct membrane protein-DNA interactions required early in nuclear envelope assembly. Ulbert S, Platani M, Boue S, Mattaj IW. J Cell Biol. 2006 May 22;173(4):469-76.

77. The integral membrane nucleoporin pom121 functionally links nuclear pore complex assembly and nuclear envelope formation. Antonin W, Franz C, Haselmann U, Antony C, Mattaj IW. Mol Cell. 2005 Jan 7;17(1):83-92.

78. Sequential recruitment of NPC proteins to the nuclear periphery at the end of mitosis. Bodoor K, Shaikh S, Salina D, Raharjo WH, Bastos R, Lohka M, Burke B. J Cell Sci. 1999 Jul;112 (Pt 13):2253-64.

79. Remodelling the walls of the nucleus. Burke B, Ellenberg J. Nat Rev Mol Cell Biol. 2002 Jul;3(7):487-97.

80. Direct interaction with nup153 mediates binding of Tpr to the periphery of the nuclear pore complex. Hase ME, Cordes VC. Mol Biol Cell. 2003 May;14(5):1923-40.

81. Cell cycle-dependent differences in nuclear pore complex assembly in metazoa. Doucet CM, Talamas JA, Hetzer MW. Cell. 2010 Jun 11;141(6):1030-41.

82. POM121 and Sun1 play a role in early steps of interphase NPC assembly. Talamas JA, Hetzer MW. J Cell Biol. 2011 Jul 11;194(1):27-37.

83. A new model for nuclear envelope breakdown. Terasaki M, Campagnola P, Rolls MM, Stein PA, Ellenberg J, Hinkle B, Slepchenko B. Mol Biol Cell. 2001 Feb;12(2):503-10.

84. Systematic kinetic analysis of mitotic dis- and reassembly of the nuclear pore in living cells. Dultz E, Zanin E, Wurzenberger C, Braun M, Rabut G, Sironi L, Ellenberg J. J Cell Biol. 2008 Mar 10;180(5):857-65.

85. In vivo dynamics of Drosophila nuclear envelope components. Katsani KR, Karess RE, Dostatni N, Doye V. Mol Biol Cell. 2008 Sep;19(9):3652-66.

86. Cytoplasmic dynein as a facilitator of nuclear envelope breakdown. Salina D, Bodoor K, Eckley DM, Schroer TA, Rattner JB, Burke B. Cell. 2002 Jan 11;108(1):97-107.

87. Nuclear envelope breakdown proceeds by microtubule-induced tearing of the lamina. Beaudouin J, Gerlich D, Daigle N, Eils R, Ellenberg J. Cell. 2002 Jan 11;108(1):83-96.

88. Cell cycle-dependent phosphorylation of nucleoporins and nuclear pore membrane protein Gp210. Favreau C, Worman HJ, Wozniak RW, Frappier T, Courvalin JC. Biochemistry. 1996 Jun 18;35(24):8035-44.

89. Differential mitotic phosphorylation of proteins of the nuclear pore complex. Macaulay C, Meier E, Forbes DJ. J Biol Chem. 1995 Jan 6;270(1):254-62.

90. Cell-cycle-dependent phosphorylation of the nuclear pore Nup107-160 subcomplex. Glavy JS, Krutchinsky AN, Cristea IM, Berke IC, Boehmer T, Blobel G, Chait BT. Proc Natl Acad Sci U S A. 2007 Mar 6;104(10):3811-6.

91. Detergent-salt resistance of LAP2alpha in interphase nuclei and phosphorylation-dependent association with chromosomes early in nuclear assembly implies functions in nuclear structure dynamics. Dechat T, Gotzmann J, Stockinger A, Harris CA, Talle MA, Siekierka JJ, Foisner R. EMBO J. 1998 Aug 17;17(16):4887-902.

92. The lamin B receptor of the inner nuclear membrane undergoes mitosis-specific phosphorylation and is a substrate for p34cdc2-type protein kinase. Courvalin JC, Segil N, Blobel G, Worman HJ. J Biol Chem. 1992 Sep 25;267(27):19035-8.

93. Phosphorylation of Nup98 by multiple kinases is crucial for NPC disassembly during mitotic entry. Laurell E, Beck K, Krupina K, Theerthagiri G, Bodenmiller B, Horvath P, Aebersold R, Antonin W, Kutay U. Cell. 2011 Feb 18;144(4):539-50.

94. Emerging roles of nuclear protein phosphatases. Moorhead GB, Trinkle-Mulcahy L, Ulke-Lemée A. Nat Rev Mol Cell Biol. 2007 Mar;8(3):234-44.

95. RCC1 isoforms differ in their affinity for chromatin, molecular interactions and regulation by phosphorylation. Hood FE, Clarke PR. J Cell Sci. 2007 Oct 1;120(Pt 19):3436-45.

96. Phosphorylation regulates the dynamic interaction of RCC1 with chromosomes during mitosis. Hutchins JR, Moore WJ, Hood FE, Wilson JS, Andrews PD, Swedlow JR, Clarke PR. Curr Biol. 2004 Jun 22;14(12):1099-104.

97. Phosphorylation of RCC1 in mitosis is essential for producing a high RanGTP concentration on chromosomes and for spindle assembly in mammalian cells. Li HY, Zheng Y. Genes Dev. 2004 Mar 1;18(5):512-27.

98. Cdc48/p97 promotes reformation of the nucleus by extracting the kinase Aurora B from chromatin. Ramadan K, Bruderer R, Spiga FM, Popp O, Baur T, Gotta M, Meyer HH. Nature. 2007 Dec 20;450(7173):1258-62.

99. A change in nuclear pore complex composition regulates cell differentiation. D'Angelo MA, Gomez-Cavazos JS, Mei A, Lackner DH, Hetzer MW. Dev Cell. 2012 Feb 14;22(2):446-58.

100. Chromatin-bound nuclear pore components regulate gene expression in higher eukaryotes. Capelson M, Liang Y, Schulte R, Mair W, Wagner U, Hetzer MW. Cell. 2010 Feb 5;140(3):372-83.

101. SUMO-1 targets RanGAP1 to kinetochores and mitotic spindles. Joseph J, Tan SH, Karpova TS, McNally JG, Dasso M. J Cell Biol. 2002 Feb 18;156(4):595-602.

102. Dissection of the NUP107 nuclear pore subcomplex reveals a novel interaction with spindle assembly checkpoint protein MAD1 in Caenorhabditis elegans. Ródenas E, González-Aguilera C, Ayuso C, Askjaer P. Mol Biol Cell. 2012 Mar;23(5):930-44.

103. Peering through the pore: nuclear pore complex structure, assembly, and function. Suntharalingam M, Wente SR. Dev Cell. 2003 Jun;4(6):775-89.

104. Nucleocytoplasmic transport: Ran, beta and beyond. Kuersten S, Ohno M, Mattaj IW. Trends Cell Biol. 2001 Dec;11(12):497-503.

105. Regulating access to the genome: nucleocytoplasmic transport throughout the cell cycle. Weis K. Cell. 2003 Feb 21;112(4):441-51.

106. Nucleocytoplasmic transport: taking an inventory. Fried H, Kutay U. Cell Mol Life Sci. 2003 Aug;60(8):1659-88.

107. NTF2 mediates nuclear import of Ran. Ribbeck K, Lipowsky G, Kent HM, Stewart M, Görlich D. EMBO J. 1998 Nov 16;17(22):6587-98.

108. Nuclear pore complex composition: a new regulator of tissue-specific and developmental functions. Raices M, D'Angelo MA. Nat Rev Mol Cell Biol. 2012 Nov;13(11):687-99.

109. Herpesvirus assembly: an update. Mettenleiter TC, Klupp BG, Granzow H. Virus Res. 2009 Aug;143(2):222-34.

110. A classical NLS and the SUN domain contribute to the targeting of SUN2 to the inner nuclear membrane. Turgay Y, Ungricht R, Rothballer A, Kiss A, Csucs G, Horvath P, Kutay U. EMBO J. 2010 Jul 21;29(14):2262-75.

111. Traversing the NPC along the pore membrane: targeting of membrane proteins to the INM. Antonin W, Ungricht R, Kutay U. Nucleus. 2011 Mar-Apr;2(2):87-91.

112. Formation in vitro of sperm pronuclei and mitotic chromosomes induced by amphibian ooplasmic components. Lohka MJ, Masui Y. Science. 1983 May 13;220(4598):719-21.

113. Induction of nuclear envelope breakdown, chromosome condensation, and spindle formation in cell-free extracts. Lohka MJ, Maller JL. J Cell Biol. 1985 Aug;101(2):518-23.

114. Different forms of soluble cytoplasmic mRNA binding proteins and particles in Xenopus laevis oocytes and embryos. Murray MT, Krohne G, Franke WW. J Cell Biol. 1991 Jan;112(1):1-11.

115. Initiation of DNA replication in nuclei and purified DNA by a cell-free extract of Xenopus eggs. Blow JJ, Laskey RA. Cell. 1986 Nov 21;47(4):577-87.

116. Assembly in vitro of nuclei active in nuclear protein transport: ATP is required for nucleoplasmin accumulation. Newmeyer DD, Lucocq JM, Bürglin TR, De Robertis EM. EMBO J. 1986 Mar;5(3):501-10.

117. Yeast genetics to dissect the nuclear pore complex and nucleocytoplasmic trafficking. Fabre E, Hurt E. Annu Rev Genet. 1997;31:277-313.

118. A novel mechanism of nuclear envelope break-down in a fungus: nuclear migration strips off the envelope. Straube A, Weber I, Steinberg G. EMBO J. 2005 May 4;24(9):1674-85.

119. Roles for 147 embryonic lethal genes on C.elegans chromosome I identified by RNA interference and video microscopy. Zipperlen P, Fraser AG, Kamath RS, Martinez-Campos M, Ahringer J. EMBO J. 2001 Aug 1;20(15):3984-92.

120. A targeted RNAi screen for genes involved in chromosome morphogenesis and nuclear organization in the Caenorhabditis elegans germline. Colaiácovo MP, Stanfield GM, Reddy KC, Reinke V, Kim SK, Villeneuve AM. Genetics. 2002 Sep;162(1):113-28.

121. Full-genome RNAi profiling of early embryogenesis in Caenorhabditis elegans. Sönnichsen B, Koski LB, Walsh A, Marschall P, Neumann B, Brehm M, Alleaume AM, Artelt J, Bettencourt P, Cassin E, Hewitson M, Holz C, Khan M, Lazik S, Martin C, Nitzsche B, Ruer M, Stamford J, Winzi M, Heinkel R, Röder M, Finell J, Häntsch H, Jones SJ, Jones M, Piano F, Gunsalus KC, Oegema K, Gönczy P, Coulson A, Hyman AA, Echeverri CJ. Nature. 2005 Mar 24;434(7032):462-9.

122. The nucleoporin Nup188 controls passage of membrane proteins across the nuclear pore complex. Theerthagiri G, Eisenhardt N, Schwarz H, Antonin W. J Cell Biol. 2010 Jun 28;189(7):1129-42.

123. Cell Cycle Extracts. Andrew W. Murray. Methods in Cell Biology. 1991 Vol. 36.

124. Egg Extracts for Nuclear Import and Nuclear Assembly Reactions. Donald D. Newmeyer. Methods in Cell Biology. 1991 Vol. 36.

125. Nup155 regulates nuclear envelope and nuclear pore complex formation in nematodes and vertebrates. Franz C, Askjaer P, Antonin W, Iglesias CL, Haselmann U, Schelder M, de Marco A, Wilm M, Antony C, Mattaj IW. EMBO J. 2005 Oct 19;24(20):3519-31.

126. Nup53 is required for nuclear envelope and nuclear pore complex assembly. Hawryluk-Gara LA, Platani M, Santarella R, Wozniak RW, Mattaj IW. Mol Biol Cell. 2008 Apr;19(4):1753-62.

127. Nucleoporins as components of the nuclear pore complex core structure and Tpr as the architectural element of the nuclear basket. Krull S, Thyberg J, Björkroth B, Rackwitz HR, Cordes VC. Mol Biol Cell. 2004 Sep;15(9):4261-77.

128. ELYS is a dual nucleoporin/kinetochore protein required for nuclear pore assembly and proper cell division. Rasala BA, Orjalo AV, Shen Z, Briggs S, Forbes DJ. Proc Natl Acad Sci U S A. 2006 Nov 21;103(47):17801-6.

129. MEL-28/ELYS is required for the recruitment of nucleoporins to chromatin and postmitotic nuclear pore complex assembly. Franz C, Walczak R, Yavuz S, Santarella R, Gentzel M, Askjaer P, Galy V, Hetzer M, Mattaj IW, Antonin W. EMBO Rep. 2007 Feb;8(2):165-72.

130. The conserved Nup107-160 complex is critical for nuclear pore complex assembly. Walther TC, Alves A, Pickersgill H, Loïodice I, Hetzer M, Galy V, Hülsmann BB, Köcher T, Wilm M, Allen T, Mattaj IW, Doye V. Cell. 2003 Apr 18;113(2):195-206.

131. Novel vertebrate nucleoporins Nup133 and Nup160 play a role in mRNA export. Vasu S, Shah S, Orjalo A, Park M, Fischer WH, Forbes DJ. J Cell Biol. 2001 Oct 29;155(3):339-54.

132. The integral membrane nucleoporin pom121 functionally links nuclear pore complex assembly and nuclear envelope formation. Antonin W, Franz C, Haselmann U, Antony C, Mattaj IW. Mol Cell. 2005 Jan 7;17(1):83-92.

133. Nup93, a vertebrate homologue of yeast Nic96p, forms a complex with a novel 205-kDa protein and is required for correct nuclear pore assembly. Grandi P, Dang T, Pané N, Shevchenko A, Mann M, Forbes D, Hurt E. Mol Biol Cell. 1997 Oct;8(10):2017-38.

134. Functional interaction of Nic96p with a core nucleoporin complex consisting of Nsp1p, Nup49p and a novel protein Nup57p. Grandi P, Schlaich N, Tekotte H, Hurt EC. EMBO J. 1995 Jan 3;14(1):76-87.

135. Crystal structure of nucleoporin Nic96 reveals a novel, intricate helical domain architecture. Jeudy S, Schwartz TU. J Biol Chem. 2007 Nov 30;282(48):34904-12.

136. Structural basis of the nic96 subcomplex organization in the nuclear pore channel. Schrader N, Stelter P, Flemming D, Kunze R, Hurt E, Vetter IR. Mol Cell. 2008 Jan 18;29(1):46-55.

137. Systematic kinetic analysis of mitotic dis- and reassembly of the nuclear pore in living cells. Dultz E, Zanin E, Wurzenberger C, Braun M, Rabut G, Sironi L, Ellenberg J. J Cell Biol. 2008 Mar 10;180(5):857-65.

138. Importin beta negatively regulates nuclear membrane fusion and nuclear pore complex assembly. Harel A, Chan RC, Lachish-Zalait A, Zimmerman E, Elbaum M, Forbes DJ. Mol Biol Cell. 2003 Nov;14(11):4387-96.

139. Removal of a single pore subcomplex results in vertebrate nuclei devoid of nuclear pores. Harel A, Orjalo AV, Vincent T, Lachish-Zalait A, Vasu S, Shah S, Zimmerman E, Elbaum M, Forbes DJ. Mol Cell. 2003 Apr;11(4):853-64.

140. Functional analysis of nuclear pore complex protein Nup62/p62 using monoclonal antibodies. Fukuhara T, Sakaguchi N, Katahira J, Yoneda Y, Ogino K, Tachibana T. Hybridoma (Larchmt). 2006 Apr;25(2):51-9.

141. Characterisation of the passive permeability barrier of nuclear pore complexes. Mohr D, Frey S, Fischer T, Güttler T, Görlich D. EMBO J. 2009 Sep 2;28(17):2541-53.

142. The molecular architecture of the nuclear pore complex. Alber F, Dokudovskaya S, Veenhoff LM, Zhang W, Kipper J, Devos D, Suprapto A, Karni-Schmidt O, Williams R, Chait BT, Sali A, Rout MP. Nature. 2007 Nov 29;450(7170):695-701.

143. Determining the architectures of macromolecular assemblies. Alber F, Dokudovskaya S, Veenhoff LM, Zhang W, Kipper J, Devos D, Suprapto A, Karni-Schmidt O, Williams R, Chait BT, Rout MP, Sali A. Nature. 2007 Nov 29;450(7170):683-94.

144. Tpr is localized within the nuclear basket of the pore complex and has a role in nuclear protein export. Frosst P, Guan T, Subauste C, Hahn K, Gerace L. J Cell Biol. 2002 Feb 18;156(4):617-30.

145. Analysis of the yeast nucleoporin Nup188 reveals a conserved S-like structure with similarity to karyopherins. Flemming D, Devos DP, Schwarz J, Amlacher S, Lutzmann M, Hurt E. J Struct Biol. 2012 Jan;177(1):99-105.

146. Dimerization and direct membrane interaction of Nup53 contribute to nuclear pore complex assembly. Vollmer B, Schooley A, Sachdev R, Eisenhardt N, Schneider AM, Sieverding C, Madlung J, Gerken U, Macek B, Antonin W. EMBO J. 2012 Oct 17;31(20):4072-84.

147. The yeast nucleoporin Nup53p specifically interacts with Nic96p and is directly involved in nuclear protein import. Fahrenkrog B, Hübner W, Mandinova A, Panté N, Keller W, Aebi U. Mol Biol Cell. 2000 Nov;11(11):3885-96.

148. Role of the Ndc1 interaction network in yeast nuclear pore complex assembly and maintenance. Onischenko E, Stanton LH, Madrid AS, Kieselbach T, Weis K. J Cell Biol. 2009 May 4;185(3):475-91.

149. Stepwise reassembly of the nuclear envelope at the end of mitosis. Chaudhary N, Courvalin JC. J Cell Biol. 1993 Jul;122(2):295-306.

150. Reorganization of the nuclear envelope during open mitosis. Kutay U, Hetzer MW. Curr Opin Cell Biol. 2008 Dec;20(6):669-77.

151. Nuclear pore complex assembly through the cell cycle: regulation and membrane organization. Antonin W, Ellenberg J, Dultz E. FEBS Lett. 2008 Jun 18;582(14):2004-16.

152. Dismantling the NPC permeability barrier at the onset of mitosis. Laurell E, Kutay U. Cell Cycle. 2011 Jul 15;10(14):2243-5.

153. Reshaping of the endoplasmic reticulum limits the rate for nuclear envelope formation. Anderson DJ, Hetzer MW. J Cell Biol. 2008 Sep 8;182(5):911-24.

154. Nup53p is a target of two mitotic kinases, Cdk1p and Hrr25p. Lusk CP, Waller DD, Makhnevych T, Dienemann A, Whiteway M, Thomas DY, Wozniak RW. Traffic. 2007 Jun;8(6):647-60.

155. Cell cycle-dependent phosphorylation of nucleoporins and nuclear pore membrane protein Gp210. Favreau C, Worman HJ, Wozniak RW, Frappier T, Courvalin JC. Biochemistry. 1996 Jun 18;35(24):8035-44.

156. Importin beta regulates the seeding of chromatin with initiation sites for nuclear pore assembly. Rotem A, Gruber R, Shorer H, Shaulov L, Klein E, Harel A. Mol Biol Cell. 2009 Sep;20(18):4031-42.

157. Transportin regulates major mitotic assembly events: from spindle to nuclear pore assembly. Lau CK, Delmar VA, Chan RC, Phung Q, Bernis C, Fichtman B, Rasala BA, Forbes DJ. Mol Biol Cell. 2009 Sep;20(18):4043-58.

158. Interaction of the nuclear GTP-binding protein Ran with its regulatory proteins RCC1 and RanGAP1. Klebe C, Bischoff FR, Ponstingl H, Wittinghofer A. Biochemistry. 1995 Jan 17;34(2):639-47.

159. The crystal structure of mouse Nup35 reveals atypical RNP motifs and novel homodimerization of the RRM domain. Handa N, Kukimoto-Niino M, Akasaka R, Kishishita S, Murayama K, Terada T, Inoue M, Kigawa T, Kose S, Imamoto N, Tanaka A, Hayashizaki Y, Shirouzu M, Yokoyama S. J Mol Biol. 2006 Oct 13;363(1):114-24.

160. Systematic identification of mitotic phosphoproteins. Stukenberg PT, Lustig KD, McGarry TJ, King RW, Kuang J, Kirschner MW. Curr Biol. 1997 May 1;7(5):338-48.

161. Separation and detection of large phosphoproteins using Phos-tag SDS-PAGE. Kinoshita E, Kinoshita-Kikuta E, Koike T. Nat Protoc. 2009;4(10):1513-21.

162. Covalent capture of kinase-specific phosphopeptides reveals Cdk1-cyclin B substrates.Blethrow JD, Glavy JS, Morgan DO, Shokat KM. Proc Natl Acad Sci U S A. 2008 Feb 5;105(5):1442-7.

163. Nic96p is required for nuclear pore formation and functionally interacts with a novel nucleoporin, Nup188p. Zabel U, Doye V, Tekotte H, Wepf R, Grandi P, Hurt EC. J Cell Biol. 1996 Jun;133(6):1141-52.

164. Purification of NSP1 reveals complex formation with 'GLFG' nucleoporins and a novel nuclear pore protein NIC96. Grandi P, Doye V, Hurt EC. EMBO J. 1993 Aug;12(8):3061-71.

165. Insertional mutagenesis in zebrafish identifies two novel genes, pescadillo and dead eye, essential for embryonic development.Allende ML, Amsterdam A, Becker T, Kawakami K, Gaiano N, Hopkins N. Genes Dev. 1996 Dec 15;10(24):3141-55.

166. Caenorhabditis elegans nucleoporins Nup93 and Nup205 determine the limit of nuclear pore complex size exclusion in vivo. Galy V, Mattaj IW, Askjaer P. Mol Biol Cell. 2003 Dec;14(12):5104-15.

167. Systematic deletion and mitotic localization of the nuclear pore complex proteins of Aspergillus nidulans. Osmani AH, Davies J, Liu HL, Nile A, Osmani SA. Mol Biol Cell. 2006 Dec;17(12):4946-61.

168. Nuclear pore complex assembly and maintenance in POM121- and gp210-deficient cells. Stavru F, Nautrup-Pedersen G, Cordes VC, Görlich D. J Cell Biol. 2006 May 22;173(4):477-83.

169. NDC1: a crucial membrane-integral nucleoporin of metazoan nuclear pore complexes. Stavru F, Hülsmann BB, Spang A, Hartmann E, Cordes VC, Görlich D. J Cell Biol. 2006 May 22;173(4):509-19.

170. Traversing the NPC along the pore membrane: targeting of membrane proteins to the INM. Antonin W, Ungricht R, Kutay U. Nucleus. 2011 Mar-Apr;2(2):87-91.

171. The permeability of reconstituted nuclear pores provides direct evidence for the selective phase model. Hülsmann BB, Labokha AA, Görlich D. Cell. 2012 Aug 17;150(4):738-51.

172. Phosphorylation of Nup98 by multiple kinases is crucial for NPC disassembly during mitotic entry. Laurell E, Beck K, Krupina K, Theerthagiri G, Bodenmiller B, Horvath P, Aebersold R, Antonin W, Kutay U. Cell. 2011 Feb 18;144(4):539-50.

173. Systematic analysis of barrier-forming FG hydrogels from Xenopus nuclear pore complexes. Labokha AA, Gradmann S, Frey S, Hülsmann BB, Urlaub H, Baldus M, Görlich D. EMBO J. 2012 Nov 30. doi: 10.1038/emboj.2012.302.

174. Nuclear pore complex assembly through the cell cycle: regulation and membrane organization. Antonin W, Ellenberg J, Dultz E. FEBS Lett. 2008 Jun 18;582(14):2004 16.

175. Reorganization of the nuclear envelope during open mitosis. Kutay U, Hetzer MW. Curr Opin Cell Biol. 2008 Dec;20(6):669-77.

176. Nup53 is required for nuclear envelope and nuclear pore complex assembly. Hawryluk-Gara LA, Platani M, Santarella R, Wozniak RW, Mattaj IW. Mol Biol Cell. 2008 Apr;19(4):1753-62.

177. Nup155 regulates nuclear envelope and nuclear pore complex formation in nematodes and vertebrates. Franz C, Askjaer P, Antonin W, Iglesias CL, Haselmann U, Schelder M, de Marco A, Wilm M, Antony C, Mattaj IW. EMBO J. 2005 Oct 19;24(20):3519-31.

178. Pom121 links two essential subcomplexes of the nuclear pore complex core to the membrane. Mitchell JM, Mansfeld J, Capitanio J, Kutay U, Wozniak RW. J Cell Biol. 2010 Nov 1;191(3):505-21.

179. The Nup155-mediated organisation of inner nuclear membrane proteins is independent of Nup155 anchoring to the metazoan nuclear pore complex. Busayavalasa K, Chen X, Farrants AK, Wagner N, Sabri N. J Cell Sci. 2012 Sep 15;125(Pt 18):4214-8.

180. Live imaging of single nuclear pores reveals unique assembly kinetics and mechanism in interphase. Dultz E, Ellenberg J. J Cell Biol. 2010 Oct 4;191(1):15-22.

181. Piecing together nuclear pore complex assembly during interphase. Rexach M. J Cell Biol. 2009 May 4;185(3):377-9.

182. Nuclear assembly with lambda DNA in fractionated Xenopus egg extracts: an unexpected role for glycogen in formation of a higher order chromatin intermediate. Hartl P, Olson E, Dang T, Forbes DJ. J Cell Biol. 1994 Feb;124(3):235-48.

183. Proteogenomics of Pristionchus pacificus reveals distinct proteome structure of nematode models. Borchert N, Dieterich C, Krug K, Schütz W, Jung S, Nordheim A, Sommer RJ, Macek B. Genome Res. 2010 Jun;20(6):837-46.

184. Systematic identification of mitotic phosphoproteins. Stukenberg PT, Lustig KD, McGarry TJ, King RW, Kuang J, Kirschner MW. Curr Biol. 1997 May 1;7(5):338-48.

185. Cell cycle-dependent phosphorylation of nucleoporins and nuclear pore membrane protein Gp210. Favreau C, Worman HJ, Wozniak RW, Frappier T, Courvalin JC. Biochemistry. 1996 Jun 18;35(24):8035-44.

186. Domain topology of the p62 complex within the 3-D architecture of the nuclear pore complex. Schwarz-Herion K, Maco B, Sauder U, Fahrenkrog B. J Mol Biol. 2007 Jul 20;370(4):796-806.

187. The nucleoporin Nup153 is required for nuclear pore basket formation, nuclear pore complex anchoring and import of a subset of nuclear proteins. Walther TC, Fornerod M, Pickersgill H, Goldberg M, Allen TD, Mattaj IW. EMBO J. 2001 Oct 15;20(20):5703-14.

6. PUBLICATION

The C-terminal domain of Nup93 is essential for assembly of the structural backbone of nuclear pore complexes

Ruchika Sachdev[a], Cornelia Sieverding[a], Matthias Flötenmeyer[b], and Wolfram Antonin[a]
[a]Friedrich Miescher Laboratory of the Max Planck Society and [b]Max Planck Institute for Developmental Biology, 72076 Tuebingen, Germany

ABSTRACT Nuclear pore complexes (NPCs) are large macromolecular assemblies that control all transport across the nuclear envelope. They are formed by about 30 nucleoporins (Nups), which can be roughly categorized into those forming the structural skeleton of the pore and those creating the central channel and thus providing the transport and gating properties of the NPC. Here we show that the conserved nucleoporin Nup93 is essential for NPC assembly and connects both portions of the NPC. Although the C-terminal domain of the protein is necessary and sufficient for the assembly of a minimal structural backbone, full-length Nup93 is required for the additional recruitment of the Nup62 complex and the establishment of transport-competent NPCs.

INTRODUCTION

Nuclear pore complexes (NPCs) are the gatekeepers of the nuclear envelope. They mediate all transport of proteins and nucleic acids between the cytoplasm and the nucleoplasm (for review see Brohawn et al., 2009; Hetzer and Wente, 2009). At the same time, they restrict access to the nucleus by forming a permeability barrier. NPCs are among the largest cellular complexes. Despite their enormous size—60 MDa in vertebrates and 40 MDa in yeast—they are composed of only ~30 distinct proteins named nucleoporins (Nups), which, because of the eightfold symmetry of NPCs, are present in 8, 16, or 32 copies per NPC (Rout et al., 2000; Cronshaw et al., 2002; Alber et al., 2007).

The majority of nucleoporins are organized in discrete subcomplexes both in yeast and metazoa. These subcomplexes are defined biochemically and reflect a stable interaction among nucleoporins. During the open mitosis used by metazoans the nuclear envelope and NPCs break down, but several nucleoporin subcomplexes remain intact. At the end of mitosis NPCs assemble from these subcomplexes in a defined order (Dultz et al., 2008). First, the Nup107–160 complex binds to chromatin, acting as a seeding point for NPC assembly (Harel et al., 2003; Walther et al., 2003). Membranes subsequently associate with chromatin causing enrichment of nuclear envelope/NPC–specific membrane proteins (Antonin et al., 2005; Anderson et al., 2009). Once nuclear envelope membranes have been recruited, the Nup93 complex, followed closely by the Nup62 complex, which is largely made up of phenylglycine (FG) repeat–containing nucleoporins, associates with the assembling pore to form its central channel. Finally, peripheral nucleoporins, including Nup214, TPR (translocated promoter region), and the largest pools of Nup153 and Nup50 associate with the NPC (Dultz et al., 2008).

The Nup93 complex—the second major subcomplex recruited to the assembling NPC—has been implicated in several structural aspects of the pore. Nup53—one member of this complex—as well as the corresponding yeast homologues Nup53p and Nup59p, interacts with the transmembrane nucleoporin Ndc1, potentially linking the NPC to the pore membrane (Mansfeld et al., 2006; Onischenko et al., 2009). Nup53 interacts with two other members of the complex—Nup155 and Nup93—in vertebrates (Hawryluk-Gara et al., 2008) and the corresponding proteins in yeast (Fahrenkrog et al., 2000; Onischenko et al., 2009). Nup93 in turn tightly interacts with the remaining two members of the subcomplex—Nup188 and Nup205 (Grandi et al., 1997; Miller et al., 2000; Theerthagiri et al., 2010). Of interest, a subfraction of Nup93 interacts with the FG-repeat nucleoporin Nup62, as does the yeast homologue Nic96p with Nsp1p (Grandi et al., 1997; Grandi et al., 1993), thus potentially linking the structured part of the NPC to the unstructured FG repeat–containing nucleoporin complexes that form the central channel.

In vertebrates, Nup53 and Nup155 are indispensable for NPC formation (Franz *et al.*, 2005; Hawryluk-Gara *et al.*, 2008; Mitchell *et al.*, 2010). Of interest, Nup93 is an essential gene in most organisms tested, including *Caenorhabditis elegans*, *Danio rerio*, *Saccharomyces cerevisiae*, and *Aspergillus nidulans* (Grandi *et al.*, 1993; Allende *et al.*, 1996; Galy *et al.*, 2003; Osmani *et al.*, 2006), but, surprisingly, not in *Schizosaccharomyces pombe* (Yoon *et al.*, 1997). Quantification of the Nup93 in the NPCs of rat liver cells and the corresponding Nic96p in *S. cerevisiae* suggests that it is present in 32–48 or more copies per NPC and is thus one of the most abundant nucleoporins (Rout *et al.*, 2000; Cronshaw *et al.*, 2002; Alber *et al.*, 2007). Immunodepletion of Nup93 from *Xenopus laevis* extracts followed by in vitro nuclear assembly reactions results in nuclei with reduced NPC staining (Grandi *et al.*, 1997). This suggests that Nup93 has an important function in NPC assembly and function. However, because Nup93 tightly associates with Nup205 and Nup188 (Theerthagiri *et al.*, 2010; Amlacher *et al.*, 2011), it is not clear whether the effect of Nup93 depletion is due to the loss of the protein itself or a codepletion of both Nup205 and Nup188. When depleted individually, neither Nup188 nor Nup205 is essential for NPC formation (Theerthagiri *et al.*, 2010). However, these proteins may have partially redundant functions in NPC assembly, and it has indeed been suggested that they arose, like many other nucleoporins, from duplication and diversification events during evolution (Alber *et al.*, 2007).

To dissect the importance of Nup93, Nup188, and Nup205 in NPC assembly and function, we depleted all three proteins from *Xenopus* egg extracts. We performed add-back experiments using recombinant Nup93, and here we show that Nup93 by itself is essential for NPC formation. Functional NPCs can be assembled in the absence of both Nup205 and Nup188. Although the N-terminal part of Nup93 is important for the recruitment of the Nup62 complex and establishment of the permeability barrier and transport competency of the NPC, the C-terminal region of the protein is sufficient for the assembly of the NPC's structural backbone.

RESULTS

Nup93 is essential for nuclear pore complex assembly

We previously showed that two components of the Nup93 complex—Nup188 and Nup205—both interact separately with Nup93, forming Nup205–Nup93 and Nup188–Nup93 complexes (Theerthagiri *et al.*, 2010). Neither complex is individually essential for NPC formation. However, we could not rule out that these complexes have at least partially redundant functions in NPC formation, as depletion of both complexes together using a combination of antibodies against Nup188 and Nup205 was not technically feasible (Theerthagiri *et al.*, 2010). To overcome this limitation, we raised antibodies against the common protein of both complexes, Nup93. We were able to efficiently immunodeplete cellular extracts derived from *X. laevis* eggs of Nup93 (Figure 1A; note that a slightly slower migrating cross-reactivity detected by the Nup93 antibody by Western blotting (asterisk) is not immunoprecipitated or depleted). Because Nup188 and Nup205 interact tightly with Nup93 (Grandi *et al.*, 1997; Miller *et al.*, 2000; Theerthagiri *et al.*, 2010; Amlacher *et al.*, 2011), both proteins were efficiently codepleted. The levels of other nucleoporins, including Nup155 and Nup53 from the same Nup93 subcomplex, as well as Nup62, Nup98, and Nup160, were not affected by this treatment (Figure 1A).

We analyzed the effect of Nup93 depletion on NPC assembly. In fractionated *Xenopus* egg extracts nuclei are able to form in vitro upon incubation of DNA with cytosolic and membrane components. When sperm chromatin was incubated for 90 min in Nup93-depleted extracts, membrane vesicles bound to the chromatin surface but did not fuse to form a closed nuclear envelope (Figure 1B; see also Grandi *et al.*, 1997). This phenotype was previously observed when depleting nucleoporins that are essential for NPC formation (Franz *et al.*, 2005; Hawryluk-Gara *et al.*, 2008). Consistent with this idea, immunofluorescence staining for mAB414, an antibody that recognizes several FG repeat–containing nucleoporins that localize to different substructures of the NPC, was largely absent from Nup93-depleted nuclei (Figure 2). This observation suggests that NPCs are not properly formed. A similar reduction in mAB414 staining was also observed in HeLa cells, where levels of Nup93 were decreased by RNA interference treatment (Krull *et al.*, 2004). As expected, when Nup93 was depleted, neither Nup188 nor Nup205 was detected on the chromatin (Figure 2), as both proteins were codepleted with Nup93 (Figure 1A).

However, the other members of the Nup93 complex—Nup155 and Nup53—as well as the transmembrane nucleoporins pom121 and gp210, were present, albeit at reduced levels, on the chromatin (Figure 3). In contrast, Nup107, as well as MEL-28, which recruits the Nup107–160 complex to chromatin, could be detected on chromatin. With the exception of gp210, all of these nucleoporins have been implicated in early steps of NPC assembly (Harel *et al.*, 2003; Walther *et al.*, 2003; Antonin *et al.*, 2005; Rasala *et al.*, 2006; Franz *et al.*, 2007). Nup153 and Nup98, both of which interact with the Nup107–160 complex (Vasu *et al.*, 2001), could also be detected. Their presence on chromatin probably reflects recruitment via the Nup107–160 complex, which proceeds in vitro in the absence of Nup93.

These data indicate that Nup93 crucially contributes to nuclear envelope and NPC formation subsequent to chromatin binding of the Nup107–160 complex and the initial recruitment of pom121, Nup53, and Nup155. However, the phenotype observed could be either a direct consequence of Nup93 depletion or the result of codepleting its two interacting partners, Nup205 and Nup188. To distinguish between these two scenarios, we added recombinant Nup93 protein, which was expressed and purified from *Escherichia coli*, to the Nup93-depleted extracts at approximately endogenous levels as detected by Western blotting (Figure 1A). The readdition of Nup93 resulted in the formation of a closed nuclear envelope, as visualized by the membrane stain DiIC18 and electron microscopy (Figure 1, B–D). Recombinant Nup93 was detected at the nuclear rim by immunofluorescence and costained with mAB414 (Figure 2), suggesting that NPC formation is restored and that the recombinant protein integrates into assembling NPCs.

Despite the fact that a closed nuclear envelope formed, Nup188 and Nup205 could not be detected by immunofluorescence when recombinant Nup93 was added back to the depleted extracts (Figure 2). Thus the rescue of the depletion phenotype in the add-back experiment cannot be attributed to residual levels of Nup188 and/or Nup205 in the depleted extracts acting with the recombinant Nup93. Of interest, the nuclei in the add-back experiment were larger in diameter than mock-treated nuclei, a phenotype that was previously observed upon depletion of Nup188 (Theerthagiri *et al.*, 2010). Most likely, this effect is due to the codepletion of Nup188. Structural nucleoporins such as Nup155, Nup53, and Nup107, as well as the transmembrane nucleoporins pom121 and gp210, showed normal recruitment in the add-back experiments (Figure 3). In addition, peripheral nucleoplasmic or cytoplasmic nucleoporins Nup153 and Nup88, respectively, could be detected on these nuclei.

Taken together, these data indicate that Nup205 and Nup188 are not essential for nuclear envelope and NPC assembly. Thus NPCs can form even in the absence of two major components of the
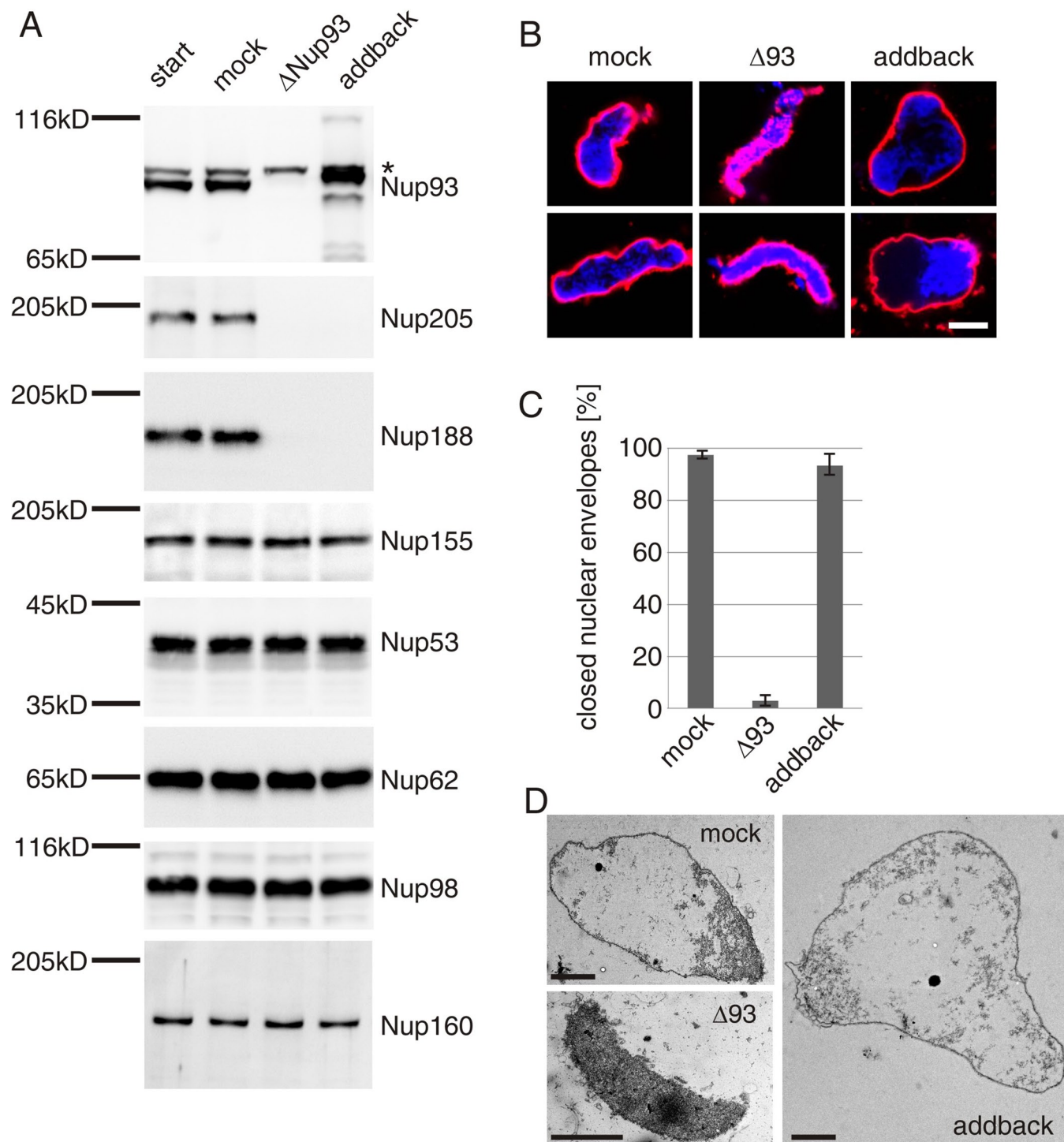
FIGURE 1: Nup93 is essential for NPC formation. (A) Western blot analysis of untreated, mock, Nup93-depleted (Δ93) and Nup93-depleted extracts with full-length recombinant Nup93 (addback), respectively. The Nup93 antibody recognizes a slightly slower migrating cross-reactivity by Western blotting (asterisk), which is neither immunoprecipitated nor depleted. The recombinant Nup93 migrates slightly more slowly than the endogenous protein probably due to absence of eukaryotic posttranslational modifications. (B) Nuclei were assembled in mock, Nup93-depleted extracts (Δ93) or Nup93-depleted extracts supplemented with full-length recombinant Nup93 (addback) for 90 min, respectively, fixed with 2% paraformaldehyde (PFA) and 0.5% glutaraldehyde, and analyzed for chromatin and membrane staining (blue, 4′,6-diamidino-2-phenylindole [DAPI]; red, DiIC18; bar, 10 μm). (C) Quantitation of chromatin substrates with a closed nuclear envelope of reactions done as in B. More than 100 randomly chosen chromatin substrates were counted per reaction. The average of three independent experiments are shown; error bars represent the total variation. (D) Transmission electron micrography of a nucleus assembled in mock, Nup93-depleted extracts or depleted extracts supplemented with full-length Nup93 as in B. Bar is 2 μm.
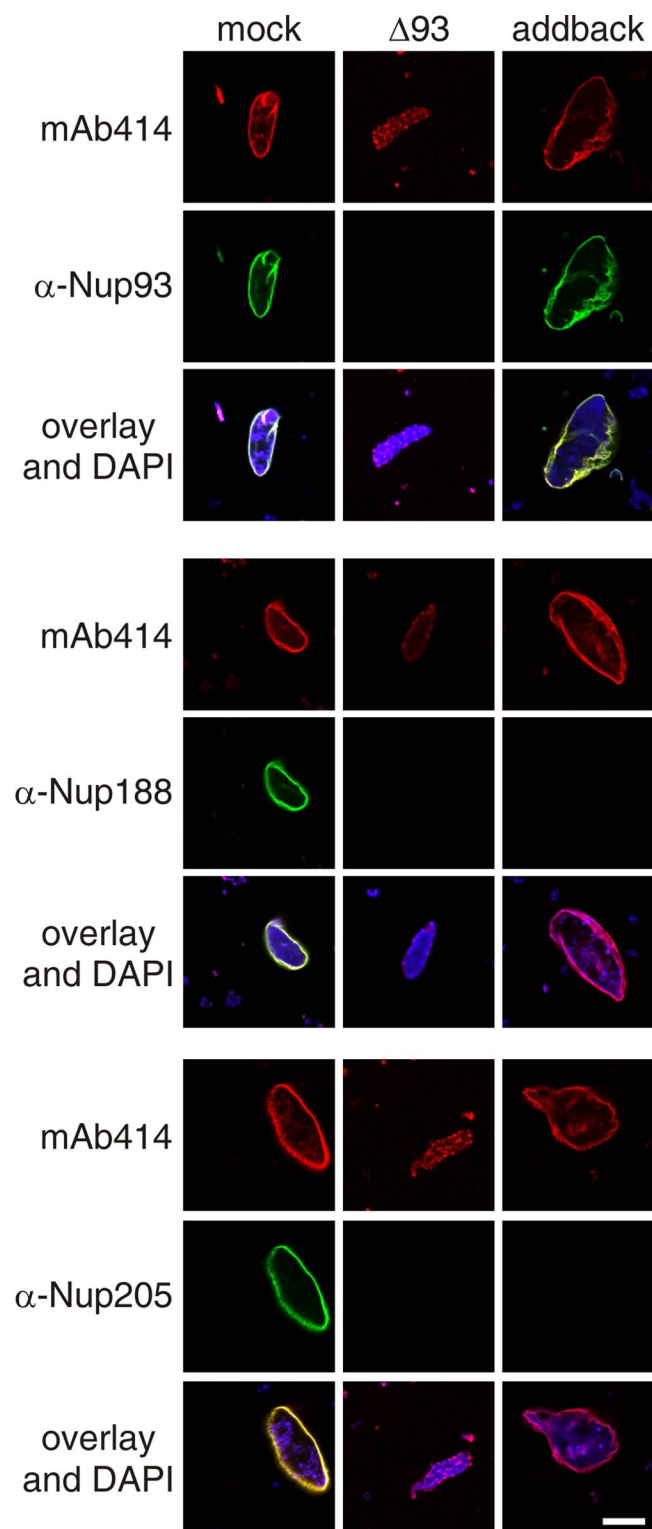
FIGURE 2: Nup188 and Nup205 together are not essential for NPC formation. Nuclei were assembled in mock, Nup93-depleted extracts (Δ93) or Nup93-depleted extracts supplemented with full-length Nup93 (addback) for 90 min, fixed with 4% PFA, and analyzed with Nup93-, Nup188-, or Nup205-specific antibodies, respectively (green), and the monoclonal antibody mAb414, which recognizes FG repeat nucleoporins (red). Chromatin is stained with DAPI; scale bar, 10 μm.

Nup93 subcomplex. However, Nup93 is essential for NPC formation, and addition of Nup93 alone is sufficient to compensate for the loss of the Nup188–Nup93 and Nup205–Nup93 complexes.
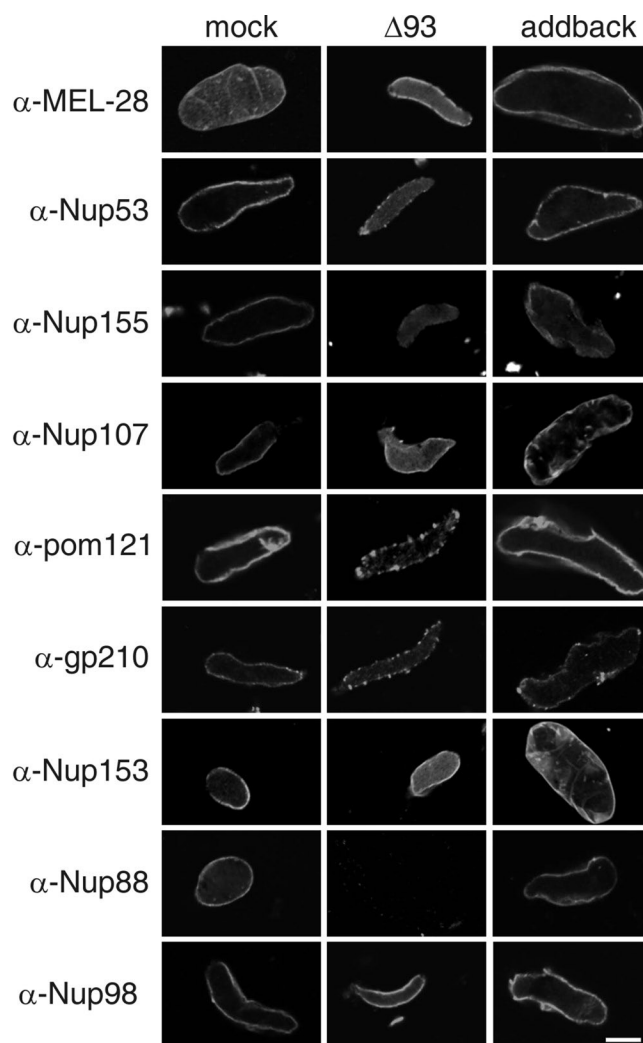

FIGURE 3: Nuclei lacking Nup188 and Nup205 have a normal NPC composition. Nuclei were assembled in mock, Nup93-depleted extracts (Δ93) or Nup93-depleted extracts supplemented with full-length Nup93 (addback) for 90 min, fixed with 4% PFA, and stained with the respective antibodies. Scale bar, 10 μm.

The C-terminal domain of Nup93 is sufficient for assembly of a minimal pore

Because Nup93 is essential for NPC formation but neither its interaction with Nup188 nor Nup205 is necessary in this regard, we sought to determine which regions of the protein contribute to NPC assembly and function. The amino terminus of Nup93 and its yeast homologue Nic96p is predicted to form a coiled-coil domain (Grandi *et al.*, 1995, 1997). In yeast, this region is important for the interaction to Nsp1p, the Nup62 homologue (Grandi *et al.*, 1995). The remainder of the protein consists of an elongated, mostly α-helical structure (Jeudy and Schwartz, 2007; Schrader *et al.*, 2008) that can be subdivided into a middle part (amino acids [aa] 197–583 in *S. cerevisiae*, corresponding to aa 183–579 in *Xenopus*) and C-terminal part (aa 617–839, corresponding to aa 608–820 in *Xenopus*). To analyze the function of the different regions of Nup93, we generated fragments of the protein comprising the N-terminal (aa 1–175), middle (aa 183–579), and C-terminal (aa 608–820) portions, as well as fragments lacking either the N-terminal or C-terminal domain (aa 183–820 or 1–579, respectively) and expressed and purified them in *E. coli* (see Figure 4A for a schematic representation of
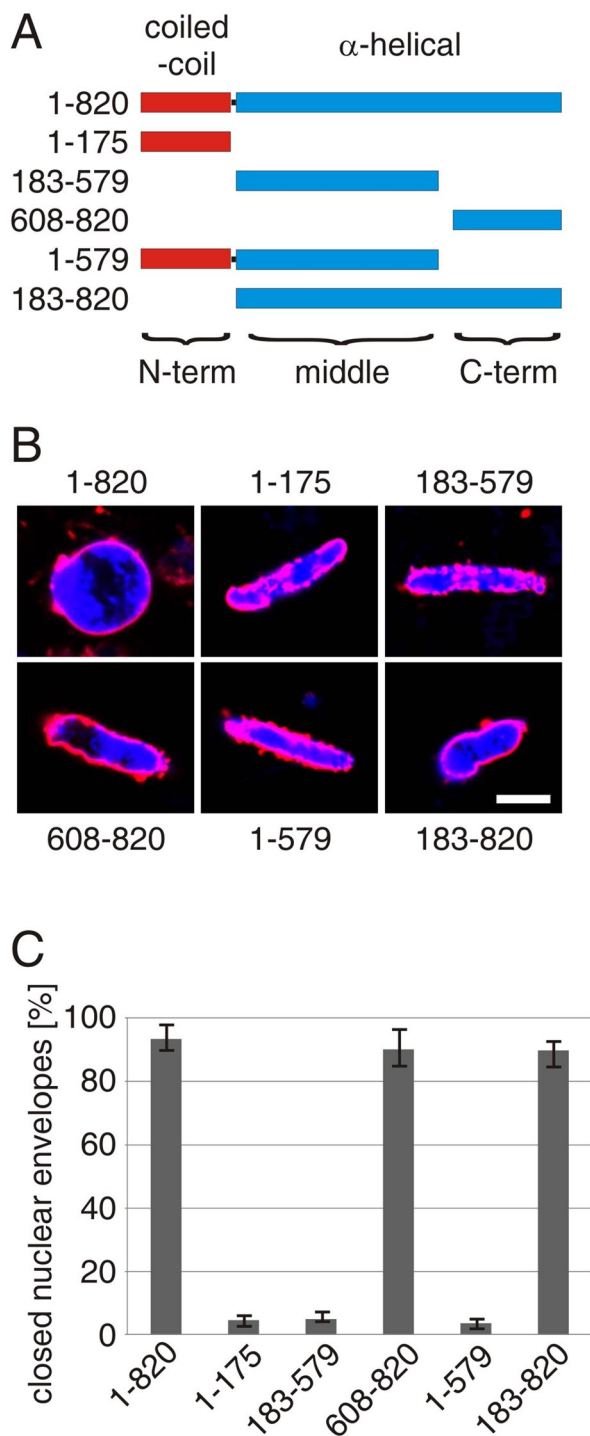
FIGURE 4: The C-terminal Nup93 fragment supports formation of a closed nuclear envelope. (A) Schematic representation of the domain structure of *Xenopus* Nup93 and the fragments used. The N-terminal coiled-coil region is marked in red, the α-helical region in blue. Numbers indicate the amino acids of the respective constructs. (B) Nuclei were assembled in Nup93-depleted extracts supplemented as indicated either with full-length recombinant Nup93 (1–820) or the respective fragments for 90 min, fixed with 2% PFA and 0.5% glutaraldehyde, and analyzed for chromatin and membrane staining (blue, DAPI; red, DiIC18; bar, 20 μm). (C) Quantitation of chromatin substrates with a closed nuclear envelope of reactions done as in B. More than 100 randomly chosen chromatin substrates were counted per reaction. The average of three independent experiments is shown; error bars represent the total variation.
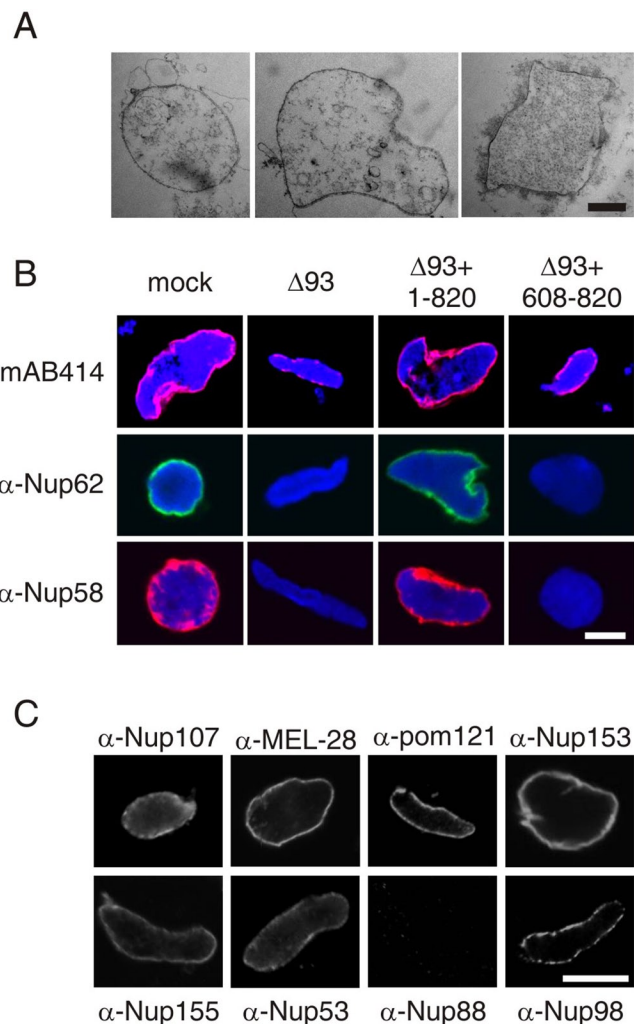

FIGURE 5: The C-terminal Nup93 fragment supports formation of the structural part of the NPC but not incorporation of the Nup62 complex. (A) Transmission electron micrographs of nuclei assembled in Nup93-depleted extracts supplemented with the C-terminal Nup93 fragment containing aa 608–820. Note the presence of a closed nuclear envelope. Bar, 2 μm. (B) Nuclei were assembled in mock, Nup93-depleted extracts (Δ93) or Nup93-depleted extracts supplemented with either full-length recombinant Nup93 (1–820) or the C-terminal fragment (608–820) for 90 min, fixed with 4% PFA, and analyzed with the antibody mAB414 (top), an antibody against Nup62 (middle), or one against Nup58 (bottom). Overlays with DAPI staining (blue) are shown. Scale bar, 10 μm. (C) Nuclei were assembled in Nup93-depleted extracts supplemented with the C-terminal fragment (aa 608–820) for 90 min, fixed with 4% PFA, and stained with the respective antibodies. Scale bar, 10 μm.

the generated fragments). When added to extracts depleted of endogenous Nup93, all fragments lacking the C-terminal region of Nup93 did not support formation of a closed nuclear envelope (Figure 4, B and C). In contrast, fragments containing the middle and C-terminal regions (183–820) or, surprisingly, only the C-terminal region of Nup93 (608–820) formed small nuclei with closed nuclear envelopes as visualized by membrane staining.

Thus an astonishingly small part of Nup93 of ~200 amino acids is sufficient to seemingly compensate for the loss of the endogenous protein in nuclear assembly. It allows for formation of a closed nuclear envelope, as confirmed by electron microscopy (Figure 5A). We therefore analyzed these nuclei in detail. First, we checked for

the presence or absence of nucleoporins. Immunofluorescence using the antibody mAB414 as a marker for FG-containing nucleoporins revealed a weaker nuclear rim staining after readdition of the C-terminal fragment (608–820) compared with control nuclei or nuclei formed when full-length Nup93 (1–820) was added back to the depleted extracts (Figure 5B).

The antibody mAB414 recognizes a subset of nucleoporins, including Nup62. Because Nup62 is known to interact with the N-terminal region of Nup93, we tested for the presence of Nup62 on nuclei formed in the presence of the extreme C-terminal Nup93 fragment (Figure 5B). The antigen was absent, indicating that the Nup62 complex, a major constituent of the NPC, is missing. The absence of Nup62 is not due to a codepletion of the protein with Nup93 from the egg extracts (Figure 1A). Consistent with this, the readdition of full-length Nup93 results in detectable Nup62 at the nuclear rim (Figure 5B). Similarly, Nup58, which is also part of the Nup62 subcomplex, was only detected in the presence of full-length Nup93 and not in nuclei formed in the presence of the C-terminal Nup93 fragment (Figure 5B).

Of interest, structural nucleoporins such as Nup107, Nup53, Nup155, and MEL-28 could be detected in nuclei formed in the presence of the C-terminal Nup93 fragment (Figure 5C). Nup153, which is a part of the nuclear basket of the NPC and interacts with the Nup107–160 subcomplex (Vasu et al., 2001), was also detected at the NPCs of these nuclei. The weak mAB414 staining observed might therefore be Nup153, which is also recognized by this antibody. Furthermore, the FG-repeat containing nucleoporin Nup98 was detected on these nuclei, albeit at reduced levels. At least a subfraction of this protein interacts with the Nup107–160 complex (Vasu et al., 2001), and its recruitment to the chromatin probably reflects this feature. Together, these data suggest that nuclei in which endogenous Nup93 is replaced by the C-terminal fragment form a closed nuclear envelope and the structural part of NPCs but lack Nup62 complexes—a substantial portion of the unstructured FG repeat–containing nucleoporins.

Because the Nup62 subcomplex is implicated in nuclear transport and establishment of the permeability barrier of the NPC, we tested whether either function was impaired in nuclei that had been assembled with the C-terminal Nup93 fragment instead of the endogenous protein. When an enhanced green fluorescent protein–fused nuclear import substrate was added to in vitro assembly reactions it was quickly imported and enriched in the nucleoplasm in the mock control as well as when full-length Nup93 was added back to depleted extracts (Figure 6). In contrast, only faint or no nuclear staining could be detected in nuclei assembled in the presence of the C-terminal Nup93 fragment only. The same results were obtained when a fragment comprising the middle and C-terminal regions of Nup93 and thus missing the N-terminus was used. Thus the NPCs in the nuclei assembled in the presence of Nup93 fragments lacking the N-terminus were not competent for nuclear import. This defect could explain why these nuclei are small (Figure 4B), as nuclear growth requires nuclear import after initial nuclear envelope enclosure.

A second major function of FG-nucleoporins is the establishment of a diffusion barrier within the NPC. Small molecules are able to diffuse between cytoplasm and nucleoplasm, but substances larger 2.5 nm in radius are excluded from the nucleus (Mohr et al., 2009) and are translocated only by signal-mediated transport. The exclusion of nonnuclear factors larger than 30 kDa from the nucleoplasm is important for the establishment of the distinct environments of the cytosol and nuclear compartments. We assayed the integrity of the nuclear envelope barrier by adding fluorescently labeled dex-
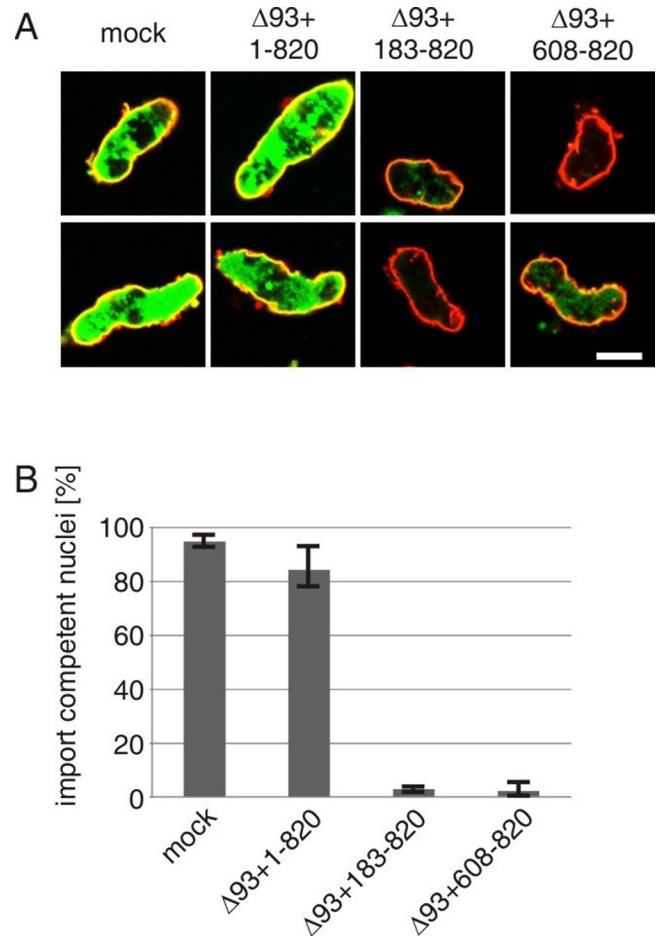

FIGURE 6: The N-terminal coiled-coil region of Nup93 is required to assemble import-competent nuclei. (A) Nuclei were assembled in mock or Nup93-depleted extracts supplemented with the either full-length Nup93 (1–820), a fragment lacking the N-terminal coiled-coil region (183–820), or the C-terminal fragment (608–820). After 50 min an enhanced green fluorescent protein–fused nuclear import substrate was added. After 120 min nuclei were isolated and analyzed by confocal microscopy. Membranes are stained with DiIC18 (red). Bars, 20 μm. (B) Quantitation of import reactions performed as in A. More than 100 randomly chosen chromatin substrates were counted per reaction. The average of three independent experiments is shown; error bars represent the total variation.

trans to the in vitro–reconstituted nuclei (Figure 7). Control nuclei, as well as nuclei assembled in the presence of full-length Nup93, excluded 70-kDa dextrans. However, nuclei assembled in the presence of the C-terminal Nup93 fragment (608–820) did not exclude dextrans of this size. These nuclei form an apparently closed nuclear envelope (Figure 5A), indicating that the loss of permeability barrier function is not due to a block in nuclear envelope formation.

Together these data indicate that Nup93 is important for the assembly of import- and exclusion-competent nuclei. Our data support the view that in vertebrates, similar to yeast (Grandi et al., 1995), the N-terminal coiled-coil region is important for recruiting the Nup62 complex and thus establishing the barrier function of NPCs. The C-terminal Nup93 fragment (608–820) does not support recruitment of the Nup62 complex or assembly of import- and exclusion-competent nuclei. However, this fragment is sufficient for formation of a closed nuclear envelope and at least partially assembled NPCs. These NPCs contain structural nucleoporins (Figure 5), including Nup53 and Nup155.
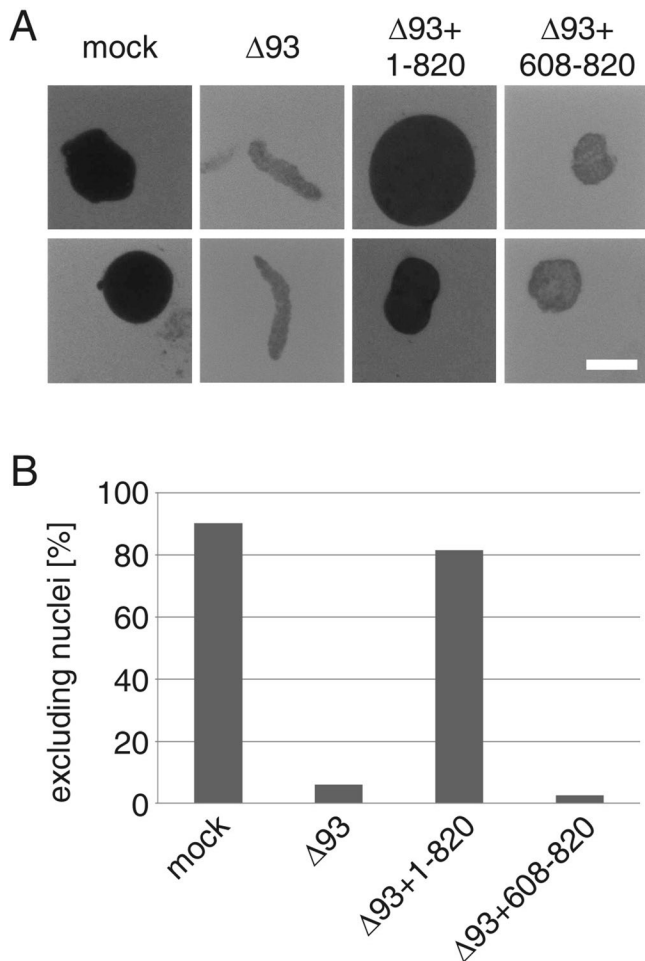
FIGURE 7: The N-terminal-coiled coil region of Nup93 is required to assemble exclusion-competent nuclei. (a) Nuclei were assembled in mock or Nup93-depleted extracts supplemented with the either full-length Nup93 (1–820) or the C-terminal fragment (608–820). After 120 min fluorescein-labeled, 70-kDa dextran was added. DNA was stained with DAPI to identify nuclei. Samples were analyzed by confocal microscopy. Representative images of the dextran staining are shown. Scale bar, 10 μm. (B) Quantitation of the size exclusion assays with 70-kDa dextran performed as in A. For each condition more than 40 nuclei from at least two independent experiments were analyzed.

The C-terminal domain of Nup93 promotes the Nup155–Nup53 interaction

Nup53 is known to interact with Nup93 and Nup155 via its N- and C-terminal regions, respectively (Fahrenkrog et al., 2000; Hawryluk-Gara et al., 2008; Amlacher et al., 2011), linking these two protein in an interaction network (Onischenko et al., 2009; Amlacher et al., 2011). We wondered how the C-terminal region of Nup93 could contribute to this interaction. Previous immunoprecipitation experiments in Xenopus egg extracts did not reveal detectable interactions between Nup93, Nup53, or Nup155 (data not shown, but see Figure 1A in Theerthagiri et al., 2010). However, using glutathione S-transferase (GST) pulldowns with recombinant Nup53 that was incubated with Xenopus egg extracts, we could detect its interaction with Nup155 (Figure 8A). This interaction was strengthened in the presence of the C-terminal Nup93 fragment (aa 608–820, expressed as a SUMO fusion to facilitate detection) but not the middle part of Nup93 (aa 183–579). Of note, when we performed GST pulldowns

using the C-terminal Nup93 fragment, its interaction with Nup155 could not be detected (data not shown). This result is consistent with the fact that Nup53 is necessary for the formation of a trimeric complex, as detected with recombinant proteins from the fungus *Chaetomium thermophilum* (Amlacher et al., 2011). Indeed, if we replace Xenopus egg extracts in our GST-pulldown experiments by bacterial lysates containing recombinant Xenopus Nup155, we detect an interaction with Nup53 that is strengthened in the presence of the C-terminal Nup93 fragment (aa 608–820), supporting the existence of direct interactions between these proteins. Thus our data indicate that the C-terminus of Nup93 is sufficient for its binding to Nup53, which in turn promotes the interaction between Nup53 and Nup155.

Taken together with the nuclear assembly experiments, these data suggest that the C-terminal region of Nup93 induces or stabilizes an interaction between Nup155 and Nup53 as central components of the structural part of the NPC and that this region is sufficient for formation of the structural backbone of the NPC.

DISCUSSION

In summary, we found that Nup93 is essential for NPC formation and function in Xenopus egg extracts, whereas both Nup188 and Nup205 are dispensable. Unexpectedly, the C-terminal domain of Nup93 is able to replace the full-length protein for the assembly of the structural part of the NPC. Our data indicate that it does so by strengthening the interaction between Nup155 and Nup53, which are core components of the structural part of NPCs.

We previously showed that two large vertebrate nucleoporins—Nup205 and Nup188—can be individually depleted without compromising NPC assembly. This is surprising when considering that both proteins are localized to the structural part of the pore and believed to participate in central ring formation (Alber et al., 2007; Amlacher et al., 2011). It was proposed that both proteins arose during evolution from a common ancestor (Alber et al., 2007). Such duplication and diversification of nucleoporins could well explain the redundancies observed among other NPC components (Stavru et al., 2006). However, here we demonstrate that NPCs, which are functional with regard to nuclear transport and exclusion properties, can form in vitro in the absence of both proteins. These experiments rule out the possibility that each protein compensates for the loss of the other when nuclei are assembled in vitro. Of course, we cannot exclude that other nuclear functions are affected in vitro or in vivo by the codepletion of Nup188 and Nup205. Indeed, in vitro–assembled nuclei lacking both proteins grow larger. This phenotype was previously observed upon depletion of Nup188 and was found to be caused by an enhanced passage of integral membrane proteins through NPCs (Theerthagiri et al., 2010; Antonin et al., 2011).

In contrast to Nup188 and Nup205, the nucleoporin Nup93 is essential for the formation of in vitro functional NPCs. In the absence of Nup93, NPC assembly and nuclear envelope closure are blocked. Our add-back experiments unambiguously demonstrate that this phenotype is caused by the absence of Nup93 and not by the codepletion of Nup205 and/or Nup188. Nic96, the yeast Nup93 homologue, is essential, and a thermosensitive Nic96p protein leads to a decrease in NPC density at restrictive temperature (Grandi et al., 1993; Zabel et al., 1996) suggesting that its function in NPC assembly is conserved during evolution.

Fragments lacking the N-terminal domain of Nup93 can substitute for the endogenous protein in NPC assembly. However, these NPCs lack the Nup62 complex and are not functional for nuclear import or exclusion of nonnuclear factors. The amino-terminal coiled-coil region of yeast Nic96p is known to interact with the
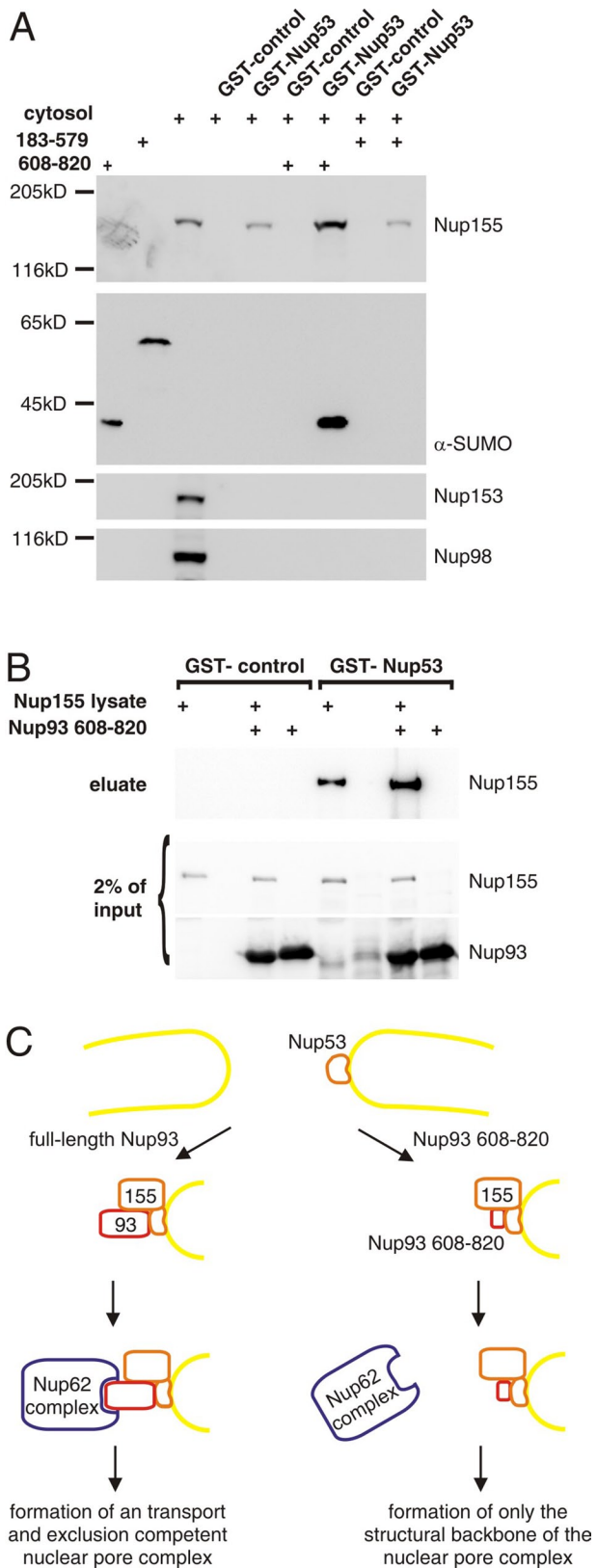
FIGURE 8: The C-terminus of Nup93 stabilizes the Nup53–Nup155 interaction. (A) GST fusions of the nucleoplasmic domain of gp210 (control) or Nup53 were incubated with cytosol from *Xenopus* egg extracts alone or, where indicated, in the presence of SUMO fusions of the Nup93 middle fragment (183–582) or Nup93 C-terminal fragment (608–820), respectively. Eluates were analyzed by Western blotting with antibodies against SUMO to detect the Nup93

Nup62 complex (Grandi *et al.*, 1995). Recent data from the Hurt lab suggest that the Nup62 complex is synergistically recruited by this region and interactions with Nup188 and Nup192—the yeast homologues of vertebrate Nup188 and Nup205, respectively (Amlacher *et al.*, 2011). Deletion of an α-helix in Nic96p, which is known to be important for its interaction with Nup188 and Nup192 and probably its recruitment to NPCs, showed a mild growth defect. In contrast, deletion of the coiled-coil region important for the interaction of Nic96p with the Nup62 complex retarded cell growth more severely. If both interacting regions were lacking, an extremely slow growth phenotype was observed. This could indicate that the Nup62 complex is recruited to NPCs by a direct and more important interaction to Nic96p and an indirect interaction via Nup188p and/ or Nup192p. In support of this view, our add-back experiments with full-length Nup93 and fragments show that in vertebrates the N-terminus of Nup93 is sufficient to recruit the Nup62 complex in the absence of Nup188 and Nup205.

A small portion of Nup93 in the extreme C-terminus, ~200 amino acids, is sufficient for the assembly of a minimal pore. This finding is surprising in light of results in *S. cerevisiae*, where the C-terminus was regarded as of minor importance (Grandi *et al.*, 1995; Schrader *et al.*, 2008). However, one of two highly conserved surface patches identified in Nic96p is located in this C-terminal region and likely represents an important site for protein–protein interactions (Jeudy and Schwartz, 2007). Our data suggest that this region interacts with Nup53, but we cannot exclude that a different region is involved in the Nic96p–Nup53p interaction in yeast. Although it has been suggested that yeast Nic96p and vertebrate Nup93 are likely to exhibit the same overall structure (Jeudy and Schwartz, 2007; Schrader *et al.*, 2008), Nup93 is predicted to have a much smaller dipole moment than Nic96p, which might hint at a yeast-specific particularity (Schrader *et al.*, 2008). Certainly, we cannot exclude that the discrepancy observed in the importance of the Nic96p and Nup93 C-terminal domains reflects differences in the assembly of NPC between yeast and vertebrates. In yeast, where closed mitosis is used, NPCs assemble only into the intact nuclear envelope. In metazoa, NPC assembly also occurs postmitotically on the chromatin surface concomitantly with formation of a closed nuclear envelope (for review see Antonin *et al.*, 2008; Kutay and Hetzer, 2008). This process is particularly emphasized in the *Xenopus* egg extract nuclear assembly system and probably has distinct requirements of

---

fragments or antibodies against Nup155, Nup153, and Nup98 to detect the respective protein. In the left three lanes 5% of the input of the Nup93 fragments and 2% of the cytosol were loaded. (B) Purified recombinant GST or GST-Nup53 fusion protein was incubated with lysates from bacteria expressing recombinant *Xenopus* Nup155 and supplemented with the C-terminal fragment Nup93 (608–820) where indicated. Eluates and 2% of the input were analyzed by Western blotting using antibodies against the His6 tag. Because of the removal of the His6 tag from the Nup93 fragment during TEV protease elution, it is not possible to detect this protein in the eluate. (C) Model for Nup93 function in postmitotic NPC assembly. The C-terminal region of Nup93 stabilizes the Nup155–Nup53 interaction, allowing the assembly of the structural part of the NPC. This function of Nup93 can be substituted by a fragment comprising amino acids 608–820 (right). The N-terminal coiled-coil region of Nup93 recruits the Nup62 complex to the structural part of the NPC. This requires in the assembly reaction full-length Nup93 and leads to the association of the central channel and formation of functional NPCs (left). Note that for the sake of simplicity, transmembrane nucleoporins and the Nup107–160 complex are not shown, although our data indicate that they are present in both assembly lines.

nucleoporin interactions. The fact that the N-terminal domain of Nic96p is sufficient to substitute for the loss of the endogenous protein in yeast (Jeudy and Schwartz, 2007) but not in our system might reflect such a differences in NPC assembly pathways and mechanisms.

Our pulldown data suggest not only that the C-terminal region of Nup93 is interacting with Nup53, but also that this interaction stabilizes the Nup155–Nup53 interaction, probably by inducing a conformational change in Nup53. Both Nup155 and Nup53 are essential for NPC formation in vertebrates (Franz *et al.*, 2005; Hawryluk-Gara *et al.*, 2008; Mitchell *et al.*, 2010) and are most likely central components of the structural backbone of the NPC (Alber *et al.*, 2007). Establishing and/or stabilizing the Nup53–Nup155 interaction might be a key event in assembling the structural backbone of the NPC (Onischenko *et al.*, 2009). Of interest, depletion of Nup53 blocks Nup93 recruitment to chromatin substrates (Hawryluk-Gara *et al.*, 2008), whereas depletion of Nup93 reduces but does not abolish Nup53 staining on chromatin (Figure 3). This could indicate that Nup53 recruitment not only precedes but is also required for Nup93 binding to the assembling NPC at the end of mitosis, a hypothesis consistent with models for yeast nuclear pore complex assembly (Rexach, 2009).

On the basis of our findings, we propose a model (Figure 8B) in which Nup53 and Nup155 are recruited to the assembling NPC, probably via their interactions with the transmembrane nucleoporins ndc1 and pom121 (Mansfeld *et al.*, 2006; Onischenko *et al.*, 2009; Mitchell *et al.*, 2010). The Nup53–Nup155 interaction is stabilized by the C-terminal region of Nup93 interacting with Nup53. This leads to the assembly of the structural part of the NPC (Figure 8C, right). Neither Nup188 nor Nup205 is required for the stabilization of Nup53 at the pore. In the presence of full-length Nup93 the N-terminus of the protein recruits the Nup62 complex (Figure 8C, left). This recruitments allows for formation of import- and exclusion-competent NPCs. Our data suggest that Nup93 is a key factor in the ordered assembly of NPCs during postmitotic nuclear envelope reassembly, completing the formation of the structural part of the NPC via its C-terminal domain and recruiting, via its N-terminus, the Nup62 complex and thus the central channel to the pore.

MATERIALS AND METHODS
Materials
1,1′-Dioctadecyl-3,3,3′,3′-tetramethylindocarbocyanine perchlorate (DiIC18), fluorescein-labeled dextran, and secondary antibodies (Alexa Fluor 488 goat α-rabbit immunoglobulin G [IgG] and Cy3 goat α-mouse IgG) were obtained from Invitrogen (Carlsbad, CA).

Antibodies
For the generation of antibodies, an amino-terminal fragment of *Xenopus* Nup93 (aa 1–230) or full-length Nup58, respectively, was cloned into a pET28a vector (EMD, San Diego, CA) and purified using Ni-nitrilotriacetic acid agarose (Qiagen, Valencia, CA), dialyzed to phosphate-buffered saline (PBS), and injected into rabbits.

Antibodies against pom121 and gp210 (Antonin *et al.*, 2005), Nup155 (Franz *et al.*, 2005), Nup160 and MEL-28 (Franz *et al.*, 2007), and Nup153 and Nup107 (Walther *et al.*, 2003), as well as Nup188, Nup205, Nup98, and Nup53 (Theerthagiri *et al.*, 2010), were as described. mAB414 was obtained from BAbCO (Richmond, CA), antibodies against yeast SUMO (SMT3) are from Acris (Herford, Germany), Nup88 is from BD Biosciences (San Diego, CA), 6-histidine (His6) antibody is from Roche (Indianapolis, IN), and Nup62 is from

Birthe Fahrenkrog (Université Libre de Bruxelles, Belgium; Schwarz-Herion *et al.*, 2007).

Nuclear assembly
Nuclear assembly reactions, dextran exclusion, nuclear transport assays, and transmission electron microscopy were performed as described (Theerthagiri *et al.*, 2010). Generation of affinity resins for protein depletion and preparation of sperm heads and floated membranes were described previously (Franz *et al.*, 2005). For depletions, high-speed extracts were incubated twice with a 1:1.2 bead-to-cytosol ratio for 20 min (Franz *et al.*, 2007). Prelabeled membranes were prepared as in Antonin *et al.* (2005) using DiIC18.

All fluorescence microscopy images were recorded on the confocal microscope (FV1000 [Olympus, Center Valley, PA] equipped with a photomultiplier [model R7862; Hamamatsu, Hamamatsu, Japan]) with 405-, 488-, and 559-nm laser lines and a 60× numerical aperture 1.35 oil immersion objective lens using the FluoView software (Olympus) at room temperature with Vectashield (Vector Laboratories, Burlingame, CA) as a mounting medium.

Generation of Nup93 and fragments
Expression constructs for full-length *Xenopus* Nup93 and fragments were generated from a synthetic DNA optimized for codon usage and expression in *E. coli* (Geneart, Regensburg, Germany; see Supplemental Information for DNA sequence) and cloned into a modified pET28a vector (EMD) with a yeast SUMO (SMT3) as solubility tag, followed by a recognition site for the tobacco etch virus (TEV) protease upstream of the Nup93 fragments. The proteins were expressed in *E. coli*, purified using Ni-nitrilotriacetic acid agarose (Qiagen) via N-terminal His6 tag, and dialyzed to sucrose buffer (10 mM 4-(2-hydroxyethyl)-1-piperazineethanesulfonic acid [HEPES], 50 mM KCl, 2.5 mM $MgCl_2$, 250 mM sucrose, pH 7.5) and the His6 and SUMO tag was cleaved using TEV protease.

Pulldown experiments
Full-length *Xenopus* Nup53 or the nucleoplasmic domain of gp210 (Antonin *et al.*, 2005) was cloned into a modified pET28a vector (EMD) with GST tag, followed by a recognition site for thrombin protease and purified via an N-terminal His6 tag as described. In a 800-μl volume, 2 μM of the respective proteins was incubated with *Xenopus* egg extracts (diluted 1:1 with 10 mM HEPES, 50 mM KCl, 2.5 mM $MgCl_2$, pH 7.5, and cleared by centrifugation for 10 min at 100,000 rpm in a TLA110 rotor [Beckman Coulter, Brea, CA]) and 5 μM SUMO-tagged Nup93 (aa 183–582) or Nup93 (aa 608–820), respectively (except for the TEV cleavage generated and purified as in the preceding section). After 2 h, 50 μl of GSH–Sepharose (GE Healthcare, Piscataway, NJ) was added and the sample incubated for another 90 min. After six washes with PBS the samples were eluted by cleavage with thrombin (0.1 mg/ml) for 1 h and analyzed by SDS–PAGE and Western blotting.

For bacterial lysate pulldown experiments, full-length *Xenopus* Nup155 was cloned into a modified pET28a vector containing an N-terminal NusA solubility tag and a C-terminal His6 tag. In a volume of 800 μl, 2 μM GST or GST-Nup53 was incubated with 500 μl of lysates from bacteria expressing Nup155 or from untransformed bacteria and 10 μM recombinant Nup93 (608–820), After 1 h, 50 μl of GSH–Sepharose (GE Healthcare) was added, and the sample was further incubated for 1 h. After six washes with 20 mM Tris and 50 mM NaCl, pH 7.4, the samples were eluted by cleavage using 30 μl of TEV protease (0.5 mg/ml) for 1 h and analyzed by SDS–PAGE and Western blotting.

REFERENCES

Alber F *et al.* (2007). The molecular architecture of the nuclear pore complex. Nature 450, 695–701.

Allende ML, Amsterdam A, Becker T, Kawakami K, Gaiano N, Hopkins N (1996). Insertional mutagenesis in zebrafish identifies two novel genes, pescadillo and dead eye, essential for embryonic development. Genes Dev 10, 3141–3155.

Amlacher S, Sarges P, Flemming D, van Noort V, Kunze R, Devos DP, Arumugam M, Bork P, Hurt E (2011). Insight into structure and assembly of the nuclear pore complex by utilizing the genome of a eukaryotic thermophile. Cell 146, 277–289.

Anderson DJ, Vargas JD, Hsiao JP, Hetzer MW (2009). Recruitment of functionally distinct membrane proteins to chromatin mediates nuclear envelope formation in vivo. J Cell Biol 186, 183–191.

Antonin W, Ellenberg J, Dultz E (2008). Nuclear pore complex assembly through the cell cycle: regulation and membrane organization. FEBS Lett 582, 2004–2016.

Antonin W, Franz C, Haselmann U, Antony C, Mattaj IW (2005). The integral membrane nucleoporin pom121 functionally links nuclear pore complex assembly and nuclear envelope formation. Mol Cell 17, 83–92.

Antonin W, Ungricht R, Kutay U (2011). Traversing the NPC along the pore membrane: targeting of membrane proteins to the INM. Nucleus 2, 87–91.

Brohawn SG, Partridge JR, Whittle JR, Schwartz TU (2009). The nuclear pore complex has entered the atomic age. Structure 17, 1156–1168.

Cronshaw JM, Krutchinsky AN, Zhang W, Chait BT, Matunis MJ (2002). Proteomic analysis of the mammalian nuclear pore complex. J Cell Biol 158, 915–927.

Dultz E, Zanin E, Wurzenberger C, Braun M, Rabut G, Sironi L, Ellenberg J (2008). Systematic kinetic analysis of mitotic dis- and reassembly of the nuclear pore in living cells. J Cell Biol 180, 857–865.

Fahrenkrog B, Hubner W, Mandinova A, Pante N, Keller W, Aebi U (2000). The yeast nucleoporin Nup53p specifically interacts with Nic96p and is directly involved in nuclear protein import. Mol Biol Cell 11, 3885–3896.

Franz C, Askjaer P, Antonin W, Iglesias CL, Haselmann U, Schelder M, de Marco A, Wilm M, Antony C, Mattaj IW (2005). Nup155 regulates nuclear envelope and nuclear pore complex formation in nematodes and vertebrates. EMBO J 24, 3519–3531.

Franz C, Walczak R, Yavuz S, Santarella R, Gentzel M, Askjaer P, Galy V, Hetzer M, Mattaj IW, Antonin W (2007). MEL-28/ELYS is required for the recruitment of nucleoporins to chromatin and postmitotic nuclear pore complex assembly. EMBO Rep 8, 165–172.

Galy V, Mattaj IW, Askjaer P (2003). *Caenorhabditis elegans* nucleoporins Nup93 and Nup205 determine the limit of nuclear pore complex size exclusion in vivo. Mol Biol Cell 14, 5104–5115.

Grandi P, Dang T, Pane N, Shevchenko A, Mann M, Forbes D, Hurt E (1997). Nup93, a vertebrate homologue of yeast Nic96p, forms a complex with a novel 205-kDa protein and is required for correct nuclear pore assembly. Mol Biol Cell 8, 2017–2038.

Grandi P, Doye V, Hurt EC (1993). Purification of NSP1 reveals complex formation with "GLFG" nucleoporins and a novel nuclear pore protein NIC96. EMBO J 12, 3061–3071.

Grandi P, Schlaich N, Tekotte H, Hurt EC (1995). Functional interaction of Nic96p with a core nucleoporin complex consisting of Nsp1p, Nup49p and a novel protein Nup57p. EMBO J 14, 76–87.

Harel A, Orjalo AV, Vincent T, Lachish-Zalait A, Vasu S, Shah S, Zimmerman E, Elbaum M, Forbes DJ (2003). Removal of a single pore subcomplex results in vertebrate nuclei devoid of nuclear pores. Mol Cell 11, 853–864.

Hawryluk-Gara LA, Platani M, Santarella R, Wozniak RW, Mattaj IW (2008). Nup53 is required for nuclear envelope and nuclear pore complex assembly. Mol Biol Cell 19, 1753–1762.

Hetzer MW, Wente SR (2009). Border control at the nucleus: biogenesis and organization of the nuclear membrane and pore complexes. Dev Cell 17, 606–616.

Jeudy S, Schwartz TU (2007). Crystal structure of nucleoporin nic96 reveals a novel, intricate helical domain architecture. J Biol Chem 282, 34904–34912.

Krull S, Thyberg J, Bjorkroth B, Rackwitz HR, Cordes VC (2004). Nucleoporins as components of the nuclear pore complex core structure and Tpr as the architectural element of the nuclear basket. Mol Biol Cell 15, 4261–4277.

Kutay U, Hetzer MW (2008). Reorganization of the nuclear envelope during open mitosis. Curr Opin Cell Biol 20, 669–677.

Mansfeld J *et al.* (2006). The conserved transmembrane nucleoporin NDC1 is required for nuclear pore complex assembly in vertebrate cells. Mol Cell 22, 93–103.

Miller BR, Powers M, Park M, Fischer W, Forbes DJ (2000). Identification of a new vertebrate nucleoporin, Nup188, with the use of a novel organelle trap assay. Mol Biol Cell 11, 3381–3396.

Mitchell JM, Mansfeld J, Capitanio J, Kutay U, Wozniak RW (2010). Pom121 links two essential subcomplexes of the nuclear pore complex core to the membrane. J Cell Biol 191, 505–521.

Mohr D, Frey S, Fischer T, Guttler T, Gorlich D (2009). Characterisation of the passive permeability barrier of nuclear pore complexes. EMBO J 28, 2541–2553.

Onischenko E, Stanton LH, Madrid AS, Kieselbach T, Weis K (2009). Role of the Ndc1 interaction network in yeast nuclear pore complex assembly and maintenance. J Cell Biol 185, 75–491.

Osmani AH, Davies J, Liu HL, Nile A, Osmani SA (2006). Systematic deletion and mitotic localization of the nuclear pore complex proteins of *Aspergillus nidulans*. Mol Biol Cell 17, 4946–4961.

Rasala BA, Orjalo AV, Shen Z, Briggs S, Forbes DJ (2006). ELYS is a dual nucleoporin/kinetochore protein required for nuclear pore assembly and proper cell division. Proc Natl Acad Sci USA 103, 17801–17806.

Rexach M (2009). Piecing together nuclear pore complex assembly during interphase. J Cell Biol 185, 377–379.

Rout MP, Aitchison JD, Suprapto A, Hjertaas K, Zhao Y, Chait BT (2000). The yeast nuclear pore complex: composition, architecture, and transport mechanism. J Cell Biol 148, 635–651.

Schrader N, Stelter P, Flemming D, Kunze R, Hurt E, Vetter IR (2008). Structural basis of the nic96 subcomplex organization in the nuclear pore channel. Mol Cell 29, 46–55.

Schwarz-Herion K, Maco B, Sauder U, Fahrenkrog B (2007). Domain topology of the p62 complex within the 3-D architecture of the nuclear pore complex. J Mol Biol 370, 96–806.

Stavru F, Nautrup-Pedersen G, Cordes VC, Gorlich D (2006). Nuclear pore complex assembly and maintenance in POM121- and gp210-deficient cells. J Cell Biol 173, 477–483.

Theerthagiri G, Eisenhardt N, Schwarz H, Antonin W (2010). The nucleoporin Nup188 controls passage of membrane proteins across the nuclear pore complex. J Cell Biol 189, 1129–1142.

Vasu S, Shah S, Orjalo A, Park M, Fischer WH, Forbes DJ (2001). Novel vertebrate nucleoporins Nup133 and Nup160 play a role in mRNA export. J Cell Biol 155, 339–354.

Walther TC *et al.* (2003). The conserved Nup107–160 complex is critical for nuclear pore complex assembly. Cell 113, 195–206.

Yoon JH, Whalen WA, Bharathi A, Shen R, Dhar R (1997). Npp106p, a Schizosaccharomyces *pombe* nucleoporin similar to *Saccharomyces cerevisiae* Nic96p, functionally interacts with Rae1p in mRNA export. Mol Cell Biol 17, 7047–7060.

Zabel U, Doye V, Tekotte H, Wepf R, Grandi P, Hurt EC (1996). Nic96p is required for nuclear pore formation and functionally interacts with a novel nucleoporin, Nup188p. J Cell Biol 133, 1141–1152.

Supplementary information

DNA sequence of Xenopus Nup93 optimized for expression in *E. coli*

```
ATGGATGGTGAAGGTTTTGGTGAACTGCTGCAGCAAGCAGAACAGCTGGCAGCAGAAA
CCGAAGGTGTTACCGAACTGCCGCATGTTGAACGTAATCTGCAAGAAATTCAGCAGGCA
GGCGAACGTCTGCGTAGCAAAACCATGACCCGTACCAGCCAAGAAAGCGCAAATGTTA
AAGCAAGCGTTCTGCTGGGTAGCCGTGGTCTGGATATTAGCCATATTAGTCAGCGTCTG
GAAAGCCTGAGCGCAGCAACCACCTTTGAACCGCTGGAACCGGTTAAAGATACCGATAT
TCAGGGCTTTCTGAAAAACGAAAAGATAATGCACTGCTGAGCGCAATTGAAGAAAGCC
GTAAACGTACCTTTGTTATGGCCGAAGAATATCATCGTGAAAGCATGCTGGTTGAATGG
GAACAGGTTAAACAGCGTGTTCTGCATACCCTGCTGGCAAGCGGTGAAGATGCACTGG
ATTTTACCCAAGAAAGCGAAACCAGCTATATCAGCGAAAGCGGTGCACCTGGTCGTAGC
AGCCTGGATAATGTTGAAATGGCCTATGCACGTCAGATGTATATGTATAACGAGAAAGTT
GTGAGCGGTCATCTGCAGCCGAGCCTGGTTGATCTGTGTACCGAAGCAGCAGAACGTC
TGGATGATAAAAATGTTAGCGATCTGTGGGTGATGGTGAAACAAATGACCGATGTTCCG
CTGATTCCGGCAAGCGATACCCTGAAAAGCCGTTGTAGCGGTCAGATGCAGATGGCAT
TTGTTCGTCAGGCACTGAATTATCTGGAACAGAGCTATAAAAATTATACCCTGATCAGCG
TGTTTGCAAATCTGCAGCAGGCACAGTTAGGTGGTGTTCCGGGTACATATAATCTGGTT
CGTAGCTTTCTGAATATTCGTCTGCCGACCCCGATTCCGGGTCTGCAGGATGGTGAAAT
TGAAGGTTATCCGGTTTGGGCACTGATCTATTATTGTATGCGTTGTGGTGATCTGATGG
CAGCACAGCAGGTTGTTAATCGTGCACAGCATCAGCTGGGCGATTTTAAAAATTGCTTC
CAAGAGTACATTCATAATAAAGATCGTCGTCTGAGCCCGACCACCGAAAATAAACTGCG
TCTGCATTATCGTCGTGCAGTTCGTGCAAGCACCGATCCGTATAAACGTGCAGTTTATT
GCATTATTGGTCGTTGTGATGTGAGCGATAATCATAGCGAAGTTGCAGATAAAACCGAG
GATTATCTGTGGCTGAAACTGAGCCAGGTTTGTTTTGAAGATGAAGCAAATAGCAGTCC
GCAGGATCGTCTGACCCTGCCGCAGTTTCAGAAACAGCTGTTCGAAGATTATGGCGAAA
GCCATTTTGCAGTTAATCAGCAGCCGTATCTGTATTTTCAGGTTCTGTTTCTGACCGCAC
AGTTTGAAGCAGCAATTGCATTTCTGTTTCGTCTGGAACGTACCCGTTGTCATGCAGTTC
ATGTTGCACTGGCACTGTTTGAACTGAAACTGCTGCTGAAAAGCACCGGTCAGAGCGCA
CAGCTGCTGAGCCAAGAACCGGGTGAACCGCAGGGTGTTCGTCGTCTGAATTTTATTC
GTCTGCTGATGCTGTATACCCGTAAATTTGAACCGACCGATCCGCGTGAAGCACTGCAG
TATTTTATTTTCTGCGCAACGAGAAAGATAATCAGGGTGAAAGCATGTTTCTGCGTTGT
GTTAGCGAACTGGTTATTGAAAGCCGTGAATTTGATATGCTGCTGGGTAAACTGGAAAA
AGATGGTAGCCGTAAACCGGGTGCCATTGATAAATTTACCCGTGATACCAAAACCATTAT
TAACAAAGTTGCCAGCGTGGCCGAAAATAAAGGTCTGTTTGAAGAGGCAGCCAAACTGT
ATGATCTGGCAAAAAATCCGGACAAAGTTCTGGAACTGACCAATAAACTGCTGAGTCCG
GTTGTTAGCCAGATTAGCGCACCGCAGAGCAATCGTGAACGTCTGAAAAATATGGCACT
GGCAATTGCCGAACGTTATAAAGCCAGGGTGTTAGCGCAGAAAAAGCATTAACAGCA
CCTTTTATCTGCTGCTGGATCTGATCACCTTCTTTGATGAATATCATGCCGGTCATATCG
ATCTGAGCTTTGATGTTATTGAACGCCTGAAACTGGTTCCGCTGAGCCAGGATAGCGTT
GAAGAACGTGTTGCAGCATTTCGCAATTTTAGTGATGAAATTCGCCACAACCTGAGCGA
AATTCTGCTGGCAACCATGAATATTCTGTTCACCCAGTATAAACGCCTGAAAGGTAGCG
GTCCGACCACCCTGGGTCGTCCGCAGCGTGTTCAAGAAGATAAAGATAGCGTTCTGCG
TAGCCAGGCACGTGCACTGATTACCTTTGCAGGTATGATTCCGTATCGTATGAGCGGTG
ATACCAATGCACGTCTGGTTCAGATGGAAGTTCTGATGAATTAGTGA
```

7. CURRICULUM VITAE

Curriculum Vitae

Ruchika Sachdev

Friedrich Miescher Laboratory of the Max Planck Society
Spemannstrasse 39, D-72076, Tubingen, Germany
Tel: +4917670663957
ruchika.sachdev@tuebingen.mpg.de, ruchikasach@gmail.com
http://www.fml.tuebingen.mpg.de/antonin-group.html

Education

2009-Present: PhD student at the Friedrich Miescher Laboratory (FML) of the Max Planck Society, Tubingen, Germany.

Dissertation title: Functional characterization of the Nup93 complex in nuclear pore complex assembly.

PhD supervisor: Dr. Wolfram Antonin, FML of the Max Planck Society.

PhD committee: Professor Andrei Lupas, Max Planck Institute of Developmental Biology, Tubingen, Germany.

Professor Ralf Peter Jansen, IFIB (Inter Faculty Institute of Biochemistry) Tubingen, Germany.

Dr. Oliver Weichenrieder, Max Planck Institute of Developmental Biology, Tubingen, Germany.

Project Synopsis: During my PhD I studied the molecular mechanisms of nuclear pore complex (NPC) assembly. NPCs are large macromolecular assemblies that are involved in nucleocytoplasmic transport. NPCs are composed of approx. 30 proteins called as nucleoporins, which are organized into discrete sub complexes. During open mitosis employed by the metazoans, the nuclear envelope (NE) and the NPCs breakdown and at the end of mitosis the NE and the NPC have to reform in a defined order from these sub complexes. I used Xenopus *laevis* egg extract system and various cell biological and biochemical assays to elucidate the role of one of the structural complex i.e. the Nup93 complex in NPC assembly. I found out that the conserved nucleoporin Nup93 is essential for the NPC formation. I also showed that Nup93 forms a link between the structural backbone and the functional central channel of the NPC.

2007-2009:   Masters of Science in Biochemistry (aggregate marks: 78% / Rank II) Department of Biochemistry, University of Delhi, India.

Dissertation title: Characterization of a novel algal globin from *Chlamydomonas reinhardtii.*

Supervisor: Dr. Suneel Kateriya, Department of Biochemistry, University of Delhi, South Campus, New Delhi, India.

Project synopsis: Identified a novel two domain algal globin from *C. reinhardtii.* Spectroscopic, biochemical and biophysical characterization was done to elucidate the structure- function relationship of the full-length protein in comparison to its domains.

<u>2004-2007</u>:   Bachelors of Science in Biochemistry (Hons) (aggregate marks: 85%/ Rank I), Daulat Ram College, University of Delhi, India.

<u>2002-2004</u>:   High school (aggregate marks: 88%) Springdales School, Pusa Road, New Delhi, India.

Publications

- **Ruchika Sachdev**, Cornelia Sieverding, Matthias Flötenmeyer and   Wolfram Antonin. The C –terminal domain of Nup93 is essential for assembly of the structural backbone of nuclear pore complexes. **Molecular Biology of the Cell** (2012) 23 (4): 740-9.

- Benjamin Vollmer, Allana Schooley, **Ruchika Sachdev**, Nathalie Eisenhardt, Anna Schneider, Johannes Madlung, Boris Macek, Uwe Gurken and Wolfram Antonin. Nuclear pore complex assembly depends on a direct interaction of Nup53 with nuclear membranes. **EMBO J.** (2012) 31 (20) 4072-84.

- Adriana Magalaska, Amalie Dick, Fabio Zanini, Allana Schooley, **Ruchika Sachdev**, Christorph Markus Sommer, Heinz Schwarz, Daniel Gerlich and Wolfram Antonin. The ATPases pontin and reptin function in post mitotic chromatin decondensation. **(*Submitted*)**

- **Ruchika Sachdev** / Anil Kumar Tyagi: Gerty Theresa Cori: Nobel Laureate Women Scientists Pp: 17-22. (2008) Book chapter, published by the National Academy of Sciences.

Research Experience and Technical skills

<u>Technical skills</u>

Proficient in various practical and theoretical aspects of molecular cloning, protein expression and purification, pull down assays, immune precipitation and co immune precipitation, cross linking coupled to mass spectrometry, FPLC, florescent microscopy, electron microscopy, *Xenopus laevis* egg extract system, in vitro nuclear assembly reactions, NMR, CD, SPR, ELISA, immunofluorescence, FTIR spectroscopy, cell culture, MTT assays and live imaging of cells. I also attended courses offered by the Max Planck Institute such as image J, statistics, Mathematical modeling, Imaris, soft skill and scientific writing.

Software skills

Linux, Mac OS X, Windows, Adobe Illustrator, Photoshop, Image J, Imaris, MATLAB, Python, MS/ open-office.

Summer trainings

- 2007: Summer trainee at Ranbaxy Limited, pharmaceutical company, India.

  Supervisor: Dr. Deepika Singh, Lab Head of the Biotechnology Department Ranbaxy Limited, India.

  Project: Cloning, expression and purification of PI3 kinase (gamma and delta subunit) and screening for its inhibitors from the chemical library.

- 2006: Summer trainee at Dr. B.R. Ambedkar Centre for Biomedical Research (ACBR) University of Delhi, New Delhi, India.

  Supervisor: Dr. Madhu Chopra, ACBR, India.

  Project: Screening of anti cancer metabolites from *Hibiscus rosa sinesis*.

Posters, Presentations and Conferences

- Poster presentation at the American Society of Cell Biology (ASCB) 51st Annual Meeting, 2012, in Denver, Colorado, USA. The C terminal domain of Nup93 is essential for assembly of the structural backbone of nuclear pore complexes.

- Oral presentation at the PhD symposium in Max Planck Institute of Developmental Biology/ Friedrich Miescher Laboratory, 2011, Germany. The Nup93 complex in nuclear pore complex assembly.

- Oral presentation at the Annual PhD Retreat (TIPP) organized by the Max Planck Institute of Developmental Biology/FML, 2011,Germany. Role of Nup93 complex in NPC assembly.

- Poster presentation at the PhD symposium in Max Planck Institute of Developmental Biology/ FML, Germany. (2010) Functional characterization of the Nup93 complex in NPC assembly.

- Poster presentation at Photoreceptor Conference in Banaras Hindu University, India. (2009) Characterization of animal homologue eye absent gene *eya* from *C.reinhardtii.*

Teaching Experience

- Teaching assistant at the IFIB (Interfaculty Institute of Biochemistry), Tubingen, Germany. Successfully guided a group of master students for practical training in molecular biology and biochemistry.

- Qualified the UTA (University Teaching Assistantship) scholarship, granted by the University of Delhi, India. (Declined as I pursued my PhD in Germany)

Academic Achievements (Scholarships and Awards)

- Max Planck Scholarship for PhD (2009-Present)
- Selected for (CSIR-UGC)-NET and JFR (junior research fellowship). The exam is written by all master's students for obtaining scholarship to conduct research or teaching in Indian universities. Additionally, I was placed among the top 50 of all candidates who cleared the exam and was selected for prestigious Shyama Prasad Mukherjee scholarship (SPM), 2008.
- Qualified All India Graduate Aptitude Test in Engineering (GATE), 2009.
- GRE: Graduate Record Examination: 1200/1600.
- Monsanto Scholarship in Masters of Science in Biochemistry (2008-09) for excellent academic performance in both years.
- Instituted Prize for securing rank I in Delhi University for Bachelors of Science (Hons) in Biochemistry. (2004-07)
- Monetary Award for securing highest aggregate marks in Bachelors of Science (Hons) Biochemistry. (2006)
- Silver Jubilee Merit Scholarship for securing 1st position in Bachelors of Science (Hons) Biochemistry. (2006)
- Silver Jubilee Merit Scholarship for securing 2nd position in Bachelors of Science (Hons) Biochemistry. (2005)
- Teachers Memorial Prize for securing 1st position in Bachelors of Science (Hons) Biochemistry. (2004)
- Diploma in Biotechnology from Bioinformatics Institute of India. (2005-06)

Referees

- Dr. Wolfram Antonin: PhD supervisor
  Friedrich Miescher Laboratory of the Max Planck Society
  Tubingen, D-72076, Germany.
  Email: wolfram.antonin@tuebingen.mpg.de
  Phone: +49-7071-601 836

- Professor Andrei Lupas: Director of the Department of Protein Evolution.
  Max Planck Institute of Developmental Biology
  Tubingen, D-72076, Germany.
  Email: andrei.lupas@tuebingen.mpg.de

Phone: +49 7071 601-340

- Professor Anil Kumar Tyagi: Head of the Department of Biochemistry.
  University of Delhi, South campus
  New Delhi, 110021, India.
  Email: akt1003@rediffmail.com, aniltyagi@south.du.ac.in
  Phone: 0091-9312266218, 0091-11-24110970, and 0091-11-24118434